Antibiotic-free antibacterial hydrogels for wound healing applications

Orlando, I.

Antibiotic-free antibacterial hydrogels for wound healing applications

Isabel Orlando

A thesis submitted to the University of Westminster
in candidature for the award of the degree of Doctor of Philosophy

July 2019

Author's declaration

I declare that the present work was carried out in accordance with the Guidelines and Regulations of the University of Westminster. The work is original except where indicated by special reference in the text.

The submission as a whole or part is not substantially the same as any that I previously or am currently making, whether in published or unpublished form, for a degree, diploma or similar qualification at any university or similar institution.

Until the outcome of the current application to the University of Westminster is known, the work will not be submitted for any such qualification at another university or similar institution.

Any views expressed in this work are those of the author and in no way represent those of the University of Westminster.

Signed: Isabel Orlando Date: July, 2019

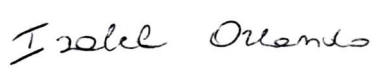

Acknowledgements

I would first like to thank my supervisor, Prof. Ipsita Roy, for giving me the opportunity to join the HyMedPoly project and work in her lab, and for the availability, motivation and support even during and after my secondment period. I would also like to express my gratitude to Dr Pooja Basnett for her precious welcoming, training and guidance, and Dr Rinat Nigmatullin for the inspiring suggestions. I would like to thank my lab at the University of Westminster, Barbara, Hima, Moyin, Sheila, Alex, and Elena, for the time spent together and their company throughout this journey.

I am also sincerely thankful to the whole HyMedPoly group for all the exciting discussions both with supervisors and students. In particular, I would like to thank Prof. Aldo Boccaccini and Dr Lukas Gritsch for providing me with copper(II)-chitosan for my work. Also, I wish to thank Dr Jochen Salber for the useful advices on the biological characterisation.

I am extremely grateful to Dr Marguerite Clyde and her group from University College Dublin for the possibility to perform the microbiological assays in her lab.

I would also like to thank all my friends, from University and before, who kept me company and gave me strength during these years.
Finally, a big thank you to my family, who supported me and remained by my side every single day.

Abstract

Over the past decades, bacterial cellulose (BC) has attracted great interest as a wound dressing thanks to its innate hydrogel-like structure and high biocompatibility. However, the lack of antibacterial features of cellulose poses some limitations to its use, especially in the context of increasing antimicrobial resistance. In this work, various strategies were explored for the development of novel BC-based wound healing devices that can efficiently inhibit bacterial proliferation. First, the production of BC by fermentation of *Gluconacetobacter xylinus* and its purification from the biomass were optimised. The material was characterised with respect to its morphological, chemical and mechanical properties. The introduction of antibacterial functional groups was then investigated by ring-opening reaction of two epoxides with the hydroxyl groups of glucose in wet basic conditions. Biological tests evidenced that the functionalisation caused a decrease in the bacterial cell count of about 50% for *Staphylococcus aureus* and *Escherichia coli* in the first 24 hours, whereas cell viability of over 90% was observed for keratinocytes for up to 6 days. An alternative method for the modification of bacterial cellulose was also studied to improve the antibacterial efficiency. The functionalisation was carried out in anhydrous conditions in two steps, i.e. acrylation by Schotten-Baumann reaction and thiol-ene Michael type addition. Once again, the material was chemically and mechanically characterised, and biological studies were carried out: >99% reduction in the bacterial cell count was observed for both *S. aureus* and *E. coli*, with high cytocompatibility towards keratinocytes at all time-points. Finally, the fabrication of Cu-chitosan/BC composites was investigated. SEM images showed no evident phase separation between the polymers, whereas mechanical assays evidenced an increase in the tensile strength and elastic modulus as compared to plain chitosan. An optimal copper concentration threshold was then identified that ensures low cytotoxicity towards keratinocytes and antibacterial activity upon direct contact of over 90% for both *S. aureus* and *E. coli*. Overall, the materials developed showed promising results in terms of biological performance to tackle the ever-growing problem of antimicrobial resistance.

Table of contents

List of Figures

Chapter I - *Introduction*

Chapter III – *Production and characterisation of bacterial cellulose*

Chapter IV – *Bacterial cellulose modification in aqueous conditions*

Chapter V – *Bacterial cellulose modification in anhydrous conditions*

Chapter VI – *Production of bacterial cellulose/copper-chitosan composites*

List of Tables

List of abbreviations

A	Absorbance
AMPs	Antimicrobial peptides
AMR	Antimicrobial resistance
BC	Bacterial cellulose
CFU	Colony forming units
CuChiX	Copper(II)-chitosan complex, with X=% ratio between Cu(II) ions and non-acetylated amino groups
DAPI	4',6-Diamino-2-phenylindole, dilactate
DD	Degree of deacetylation
DMAP	4-(Dimethylamino) pyridine
DMEM	Dulbecco's modified Eagle medium
DMSO	Dimethyl sulfoxide
E	Young's modulus
EDX	Energy Dispersive X-ray
FBS	Fetal bovine serum
FT-IR	Fourier-transform infrared
G'	Storage modulus
G''	Loss modulus
GHDE	Glycidyl hexadecyl ether
GTMAC	Glycidyl trimethylammonium chloride
HS	Hestrin and Schramm
ISO	International organisation for standardisation
LVR	Linear viscoelastic region
MCC	Microcrystalline cellulose
MRSA	Methycillin resistant *Staphylococcus aureus*
MW	Molecular weight
NFC	Nanofibrillated cellulose
NP	Nanoparticles
OD	Optical density
PBS	Phosphate-buffered saline
PEC	Polyelectrolyte complex
PET	Polyethylene terephthalate
PHAs	Polyhydroxyalkanoates
PI	Propidium iodide
R	Antibacterial activity
SEM	Scanning electron microscopy
SOAS	Small amplitude oscillatory shear
SSIs	Surgical site infections

STD	Standard deviation
TEA	Triethylamine
THF	Tetrahydrofuran
WU	Water uptake
XPS	X-ray Photoelectron Spectroscopy
ΔW	Weight variation
ε_u	Elongation at break
σ_u	Ultimate tensile strength

Chapter I

Introduction

1.1 Background

1.1.1 Statement of purpose

The unregulated prescription and overuse of antibiotics that characterised the past decades has triggered bacteria to develop antimicrobial resistance (AMR) towards an increasing number of different drugs (Walsh, 2000; Tenover, 2006). Nowadays, antibiotics are widely available at low prices, and in developing countries they can even be purchased over the counter, with the result that many people are likely to consume them in wrong dosages or when they are not required (Reardon, 2014). As a consequence, the 20th century has seen the rise of bacterial resistance towards antibiotic treatments, leading the scientific community to explore diverse strategies to address what is now one of the major issues of concern both inside healthcare institutions and in the community. The 2018 O'Neill report on antimicrobial resistance estimated that 700,000 people die every year because of infectious diseases such as bacterial infections and malaria (O'Neill, 2018). In addition to this, a void in the discovery of new classes of antibiotics has been witnessed in the last 30 years (The PEW charitable trust, 2016). In this scenario, a great increase in the mortality rate is expected in the next years.

One of the main medical issues affected by the development of bacterial resistance is wound healing. A wound is an injury of the skin that provides an open access for bacteria to the inner layers of the human body, resulting in high risk of bloodstream infections. It has been reported that of 100,000 healthcare-associated infections, 8,000 deaths resulted from surgical site infections (SSIs), i.e. infections contracted within the first 30 days from surgery (Anderson *et al.*, 2014). Furthermore, SSIs are one of the main factors that cause prolonged hospitalisation time. In the US, it is believed that hospitalisation is increased by an average of 6.5 days in case of SSIs, with a total cost of 10 billion USD every year, whereas an average increase of 9.8 days of hospitalisation is registered in Europe at a cost of 325 € per day (Owens and Stoessel, 2008; Leaper and Edmiston, 2017). In this context, the development of novel biomaterials with

effective antibacterial properties for wound healing applications is an urgent need in the medical field.

Polymers constitute one of the main classes of materials used in the biomedical field thanks to their availability, low price and tailorable properties. In particular, increasing attention has been recently focused on the development of polymeric hydrogels, especially in the context of wound healing. Hydrogels, generally known as hydrophilic three-dimensional networks interconnected by chemical or physical cross-links, present in fact attractive properties that make them suitable for applications as wound dressings. Thanks to their unique structure, they are able to trap and immobilise water molecules in their interstitial spaces, providing moisture to the application area. As confirmed by literature reports, maintaining optimal levels of hydration is a fundamental requirement for a wound dressing, as it is widely acknowledged that continuous hydration is necessary for new tissues to regenerate (Ousey *et al.*, 2016). Antibacterial activity of hydrogels can be achieved by loading leachable antibacterial agents or by using a polymer that possesses inherent antibacterial activity related to its chemical structure. Inherently active hydrogels can ensure a long-term action against bacteria as they do not involve diffusion of molecules. In addition to this, they are unlikely to contaminate the environment by releasing active molecules during the degradation process (Li *et al.*, 2018). Furthermore, it has been observed that these polymers are less likely to generate bacterial resistance thanks to their mechanism of action. Intrinsically antibacterial polymers are in fact usually polycationic, meaning that they deactivate bacteria on contact through disruption of their anionic cell membrane and alteration of their physiological equilibrium. This non-selective approach has been proven to be more efficient as it does not involve interfering with metabolic pathways, which can be easily rearranged by bacteria (Du *et al.*, 2016).

1.1.2 Bacterial resistance

Since the discovery of penicillin by Alexander Fleming in 1928, the 20th century has witnessed a huge rise in the number of antibiotics, with a great amount being

discovered or synthesised besides penicillins. Antibiotics are usually classified depending on their mode of action or, more specifically, on their biological target. The main targets of antibiotics are in fact cell-wall biosynthesis (e.g. β-lactams and cephalosporins), protein synthesis (e.g. erythromycin, aminoglycosides and tetracyclines) and DNA replication and repair (fluoroquinolones). Other (less common) mechanisms of action of antibiotics rely on the inhibition of a metabolic pathway (e.g. sulphonamides) and disruption of the bacterial membrane (Kapoor, Saigal and Elongavan, 2017).

Unfortunately, as soon as antibiotics became clinically available, bacteria began to develop antibiotic resistance. The main mechanisms put in place by bacteria to counteract the action of antibiotics involve expulsion of the drug, deactivation of the active site and reprogramming of the bacterial structure (**Figure 1.1**).

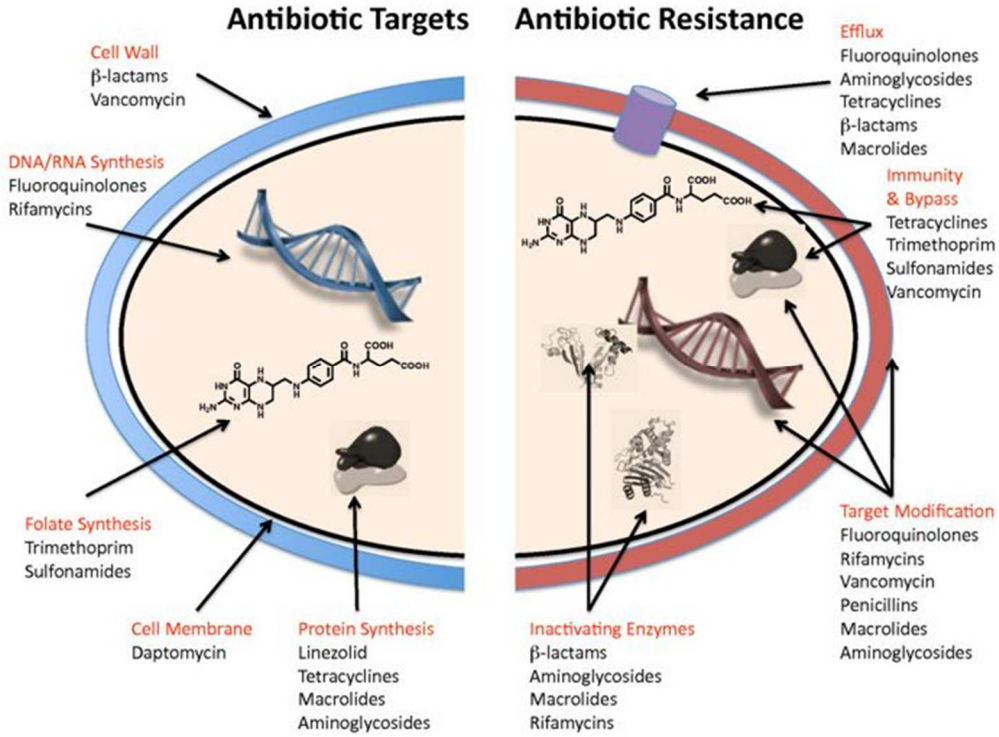

Figure 1.1 Antibiotic targets and resistance mechanisms (Wright, 2010).
Image reproduced under Creative Commons (CC) license.

The expulsion of the drug from the cell consists in the overproduction of proteins that are able to act as efflux pumps and exclude the agent. One example of

resistant bacterium adopting this strategy is the erythromycin-resistant strain of *Staphylococci*. The destruction of the active site, on the other hand, can be performed in different ways, depending on the chemical structure of the antibiotic. The most known example of this mechanism is the hydrolysis of the four-membered β-lactam ring of penicillins by the hydrolytic enzyme β-lactamase. Finally, bacteria can develop resistance through reprogramming of their own structure in order to become unaffectable by the drug. Vancomycin-resistant *Enterococci*, for instance, are capable of modifying the structure of a peptide, thus lowering the binding affinity of vancomycin by 1,000-fold. All these mechanisms take place as a result of chromosomal mutation and selection that generate acquired resistance, and are referred to as *vertical evolution*. A different mechanism of resistance is based on the exchange of genetic information between different strains of the same species or between different species. This approach is known as *horizontal evolution* and can occur through conjugation, transduction and transformation of new genetic material from resistant organisms (Walsh, 2000).

Various strategies have been explored by the scientific community to address the drug resistance issue. Bacterial genomics has been investigated in depth in an attempt to isolate virulent genes and find suitable inhibitors. The utilisation of combinations of different antibiotics has also been suggested as an option to prolong the useful life of new generation antibiotics. Furthermore, indications for both patients and physicians have been spread to raise awareness and promote a more responsible prescription of antibiotics, especially in developed countries. Finally, guidelines to prevent infections after surgical operations have been published and kept updated by national health societies and associations dealing with infection prevention and control such as the Infectious Diseases Society of America (IDSA) (Anderson *et al.*, 2014).

1.1.3 Biofilm formation

In the human body, bacterial resistance is strictly related to the formation of biofilms, both on tissues or medical devices. A biofilm is defined as an

aggregation of microorganisms that adhere on a surface and produce a hydrated self-secreted matrix consisting of extracellular polysaccharides and proteins (**Figure 1.2**). This particular state allows bacteria to create a protected environment and develop resistance to antibiotics. The formation of a biofilm can lead to the development of chronic infections due to the bacterial ability of developing different mechanisms of resistance against commonly used drugs. In most cases, surgical removal of the contaminated site or medical implant is necessary (Stewart and William Costerton, 2001; Høiby *et al.*, 2010).

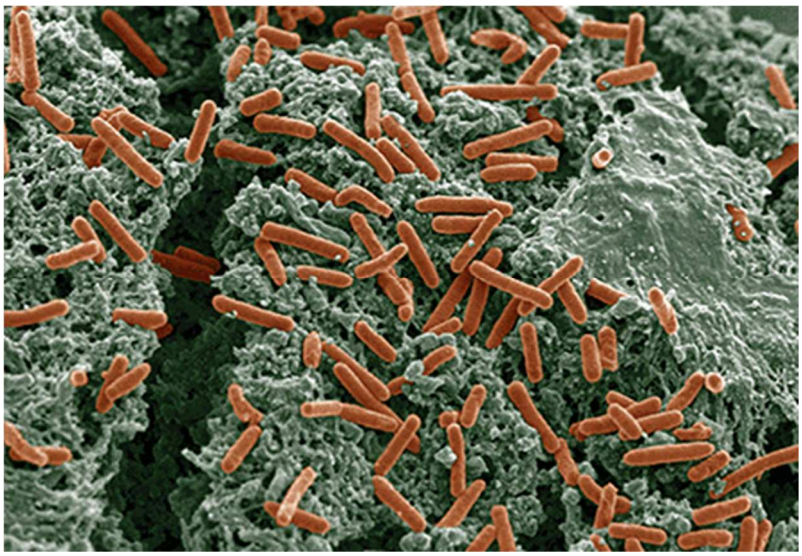

Figure 1.2 SEM image of *Pseudomonas aeruginosa* biofilm on intravenous catheter (Chauhan, Ghigo and Beloin, 2016). Image adapted with permission of Springer Nature.

The first stage of biofilm formation is the adhesion of planktonic cells to a substrate. At this point, the nature of the material on which they attach as well as the cell surface structure play a central role. For instance, the presence of flagella or pili on the cell membrane can facilitate the cell adhesion at early stages, when relevant adhesion mechanisms are not yet in place. As regards the characteristics of the substrate, it has been shown that higher roughness and hydrophobicity promote faster biofilm formation, whereas slippery surfaces display anti-fouling properties (Donlan, 2001; Kratochvil *et al.*, 2016).

As previously mentioned, the most concerning feature of these aggregated communities is their antibiotic resistance, which follows different rules as

compared to the usual mechanisms adopted by planktonic bacterial cells. It has been observed, in fact, that bacteria that are usually susceptible to drugs exhibit resistance in mature biofilms. On the other hand, cells isolated from a biofilm re-acquire responsiveness when dispersed in a solution. This evidence suggests that bacteria do not acquire resistance after attachment on a substrate through permanent mutation of their own structure. Different mechanisms have been proposed to explain resistance in biofilms (**Figure 1.3**). The first hypothesis refers to the reduced ability of the drug to reach the bacteria due to slow penetration through the extracellular polymeric matrix. In addition to this, it has been observed that antibiotics can be deactivated before reaching the inner communities. One example is represented by a particular strain of *Klebsiella pneumoniae*, which forms a biofilm able to deactivate ampicillin either by functioning as a physical barrier that limits the transportation of the antibiotic to the inner layers of the biofilm or by synthesis of an enzyme that chemically degrades the drug (Anderl, Franklin and Stewart, 2000). Another explanation for the generation of biofilm resistance could be the altered environment inside the biofilm. Gradients of concentrations of acidic products, for instance, can result in more acidic waste products, which can affect the chemical stability of the antibiotics. Furthermore, some of the cells can enter a slow-growing or starving state because of limiting nutrient conditions. This effect can cause lower efficiency of drugs that interfere with metabolic pathways, as their principal target are fast-growing cells. Finally, the studies conducted on early stage biofilms have led to the formulation of another hypothesis, as these communities have proved to be resistant despite their thin protective barrier. It has been observed that although more than 99% of bacteria in early stage biofilms are killed by antibiotic treatments, the remaining colonies are able to persist. A still speculative explanation for this is the existence of a specific phenotype adopted by bacteria growing on surfaces. This phenotype is supposed to consist in a spore-like state that provides a high degree of protection against drugs and chemicals (Costerton, 1999).

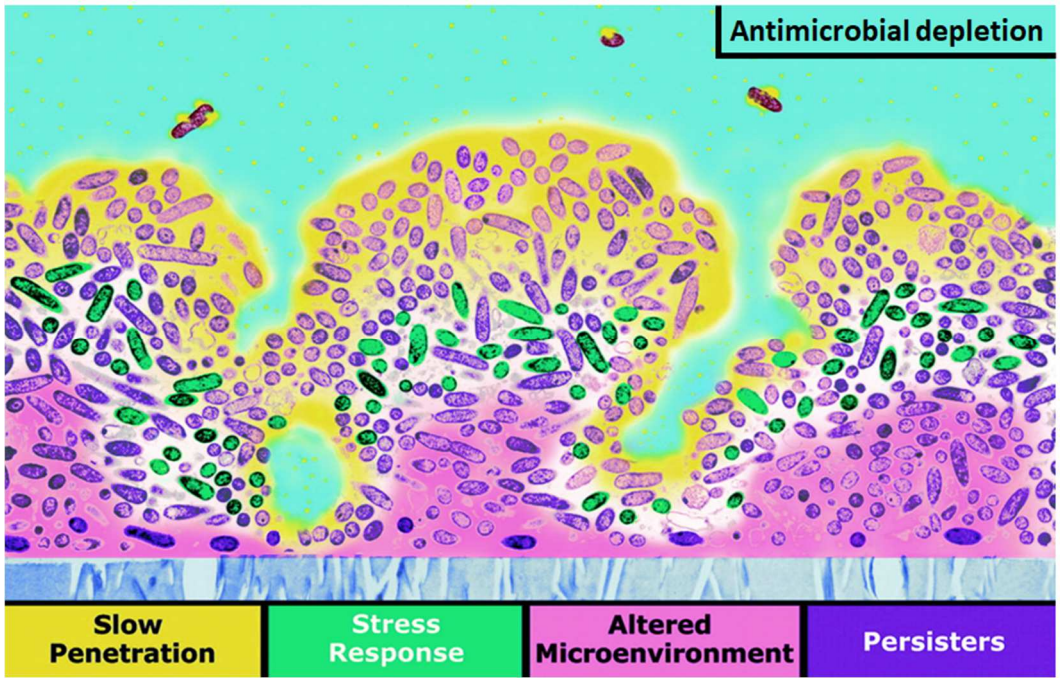

Figure 1.3 Proposed mechanisms of resistance in biofilms. Yellow: external aqueous phase containing the antibiotic, purple: internal section with cells attached to the surface (Chambless, Hunt and Stewart, 2006). Image adapted as courtesy of American Society for Microbiology © 2006.

Overall, it is generally acknowledged that resistance in biofilms is a phenomenon related to their multicellular nature. All the mechanisms described to explain antibiotic inefficiency are in fact linked to the aggregation status of bacteria. Higher cell density is usually observed in biofilms as compared to planktonic bacteria. It has been proven that for planktonic populations at cell density comparable to those found in biofilms, a decrease in the antibiotic efficiency is displayed. However, a still higher biocidal effect was registered as compared to the action of the same dosage on an equal number of biofilm cells (Davies, 2003).

1.1.4 Wound types and healing process

The primary function of the skin in the human body is to serve as a protective barrier for the internal organs. However, being it the first layer in contact with the external environment, it is subjected to injuries of various type such as surgical incision, contact with a penetrating body or any accident. All of these can result in the development of a wound.

The wound healing process (**Figure 1.4**) starts at the moment of the injury, when several cellular mechanisms are activated in order to restore the damaged area. Three main overlapping stages are usually identified, i.e. inflammation, proliferation and remodelling. Along with these, sub-phases can be observed for a more comprehensive understanding. The disruption of blood vessels upon injury causes extravasation of their constituents. To restore the haemostasis, clotting factors intervene that form a platelet plug followed by generation of a fibrin matrix. After 2-3 days, monocytes start to differentiate into inflammatory or reparatory macrophages, which, together with neutrophils recruited at the site, remove any foreign product such as dead tissue cells and bacterial degradation products. After 48 hours, the inflammation phase is usually over and the formation of new tissue starts to take place. Keratinocytes begin to migrate to the wound and angiogenesis (i.e. formation of new blood vessels) occurs. Granulation tissue is generated upon sprouting of capillaries and proliferation of fibroblasts, and replaces the fibrin matrix. At this stage, the epidermal cells at the margins of the wound start to replicate, probably as a result of the absence of neighbouring cells. Finally, fibroblasts migrate to the wound and start to differentiate into myofibroblasts. This type of contractile cells works to bring the wound edges closer and, together with fibroblasts, cooperates to produce the extracellular matrix (mostly collagen) that constitute the mature scar. Finally, the remodelling stage begins, generally after 2-3 weeks from the injury, and can be prolonged for one year or even longer. The cells activated in the first phases undergo apoptosis, leaving behind an extracellular matrix mass containing only a few cells. Remodelling of collagen from type III to mainly type I is observed, which is controlled by matrix metalloproteinases secreted by fibroblasts, macrophages and endothelial cells. Although this process is aimed at restoring the skin strength, it is not possible to regain the same properties of uninjured skin, with only 70% recovery when maximum strength is achieved (Singer and Clark, 1999; Gurtner *et al.*, 2008).

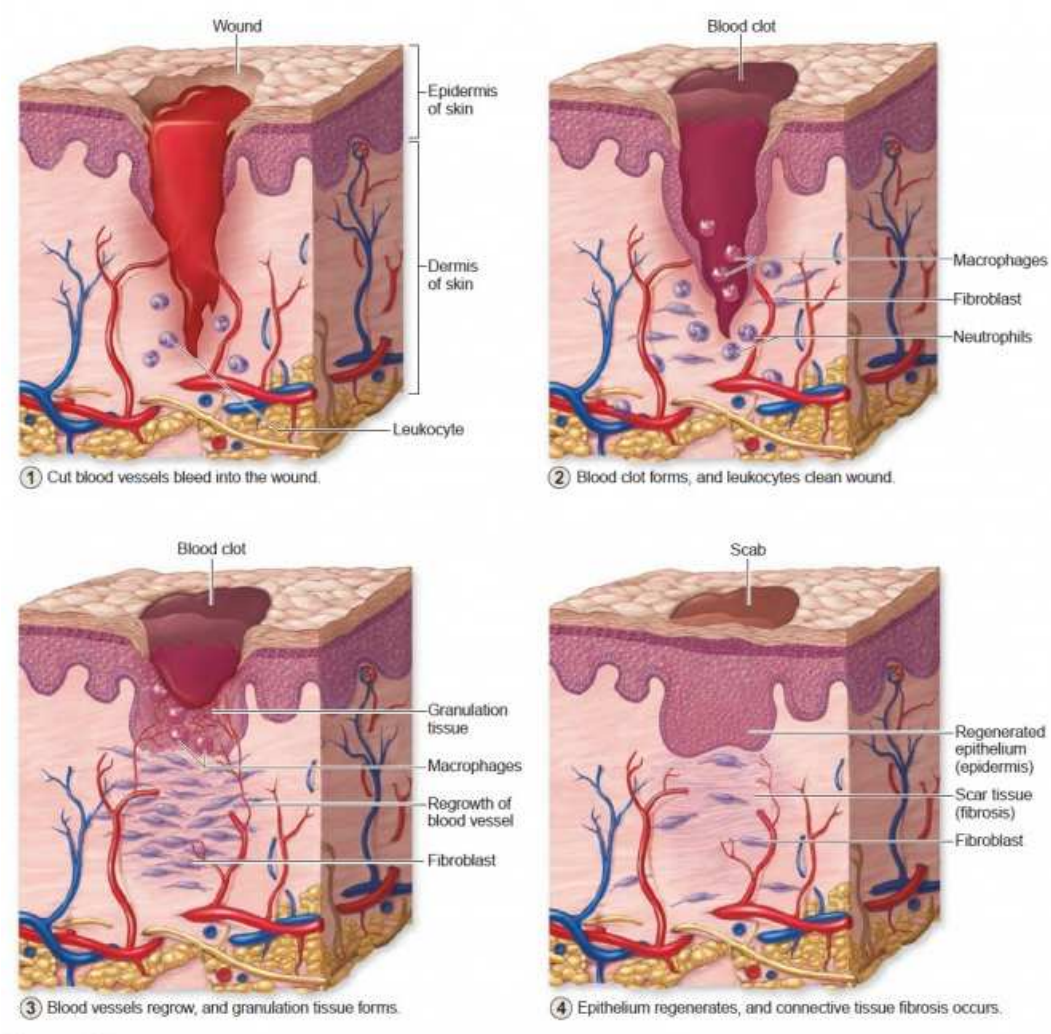

Figure 1.4 Wound healing stages. From top-left: injury, haemostasis, granulation, regeneration (Jeschke and Rogers, 2016). Image reproduced under Creative Commons (CC) license.

The process of wound healing is affected by several factors, which can be distinguished between systemic and local. Systemic factors are the health or disease conditions of the individual that can have an adverse effect on the healing process. Examples are advanced age, stress, presence of physiological diseases, obesity, malnutrition, smoking, use of drugs such as anticoagulants and corticosteroids. Local factors, on the other hand, are considered as the ones that directly influence the characteristics and progression of the wound. Among these, some of the most important are low oxygenation, inadequate blood supply, presence of foreign body/foreign body reaction and infection. In particular, the contamination of a wound site is one of the main causes leading to the development of chronic wounds. The evaluation of the replication state of the

microorganisms involved determines the stage of the infection. If no proliferation is observed, the wound is considered as contaminated, whereas if replication takes place without damage of the tissue, the site is said to be colonised. After this, critical colonisation can occur, with increasing number of bacteria and delayed wound healing. Finally, the most severe stages are infections, in particular, local and systemic. Local infection shows the typical signs of infection such as redness, swelling and pain, whereas systemic/invasive infection sees an increase in the bacterial burden and can result in sepsis and, ultimately, organ failure and death (Robson, Stenberg and Heggers, 1990; Grey, Enoch and Harding, 2006; Guo and DiPietro, 2010).

Wounds can be classified considering important parameters such as depth/layers involved, nature of the injury and healing time, which allow to carefully choose the best management path. As regards the classification based on the time required for healing, wounds can be divided into acute and chronic (**Figure 1.5**). Acute wounds, which are usually the result of a mechanical or chemical trauma, show complete healing after 8-12 weeks ("right" timeframe). On the other hand, in the case of chronic wounds, the continuous exposure to the cause of the injury or the presence of a physiological disease such as diabetes or anaemia prevents the healing process, with no progression observed in the first 12 weeks (Percival, 2002).

Figure 1.5 a) Acute granulating leg ulcer (Jones, Grey and Harding, 2006) and b) chronic leg ulcer (Han and Ceilley, 2017). Images reproduced, respectively, under permission of BMJ Publishing Group Ltd. (a) and Creative Commons (CC) license (b).

In addition to this, wounds can be classified depending on their appearance. A wound can in fact be described as necrotic, sloughy, granulating or epithelialising. Necrotic wounds present non-viable tissue usually dark coloured because of lack of hydration. In case of sloughy wounds, on the other hand, a yellowish layer is observed due to the presence of slough, which is composed of serum proteins such as fibrin. Pink or red coloured wounds are referred to as granulating, and are characterised by a high degree of vascularisation. Finally, wounds that are in the last stage of the healing process are said to be epithelialising (Grey, Enoch and Harding, 2006; Abdelrahman and Newton, 2011).

1.1.5 Wound dressings

Since ancient times, humans have been covering wounds with a variety of materials to protect the damaged area from the external environment. Depending on the nature of the wound, a suitable dressing can be chosen to promote fast and healthy healing. The evaluation of the characteristics of a wound is in fact crucial in determining the type of dressing to be applied. Several parameters should be taken into account, as an optimal dressing needs to ensure thermal insulation, control the hydration level by providing moisture or absorbing the excess exudate, constitute a barrier against bacterial contamination, minimise the pain related to its change and the formation of necrotic tissue and allow gas exchange (Abdelrahman and Newton, 2011).

Among these, maintaining an optimal moisture level throughout the wound healing stages is of crucial importance, as confirmed by numerous studies focused on the evaluation of wound management. The work conducted in 1962 by Winter is in fact the starting point of the so-called dressing revolution (Winter, 1962). Before that time, it was commonly agreed that wounds needed to be kept dry to improve the healing process. However, since then it has been extensively demonstrated that adequate hydration can enhance and accelerate wound closure. In particular, it has been shown that a moist environment can minimise the pain during dressing change and the generation of necrotic tissue by

preventing dehydration as well as facilitate cell growth and proliferation. This is generally achieved through enhanced expression of growth factors and promotion of angiogenesis, resulting in an overall accelerated healing rate as compared to dry wounds (Field and Kerstein, 1994).

In light of this, an appropriate dressing needs to be carefully chosen also by keeping in mind the hydration level of the wound. Dressings can in fact be classified depending on their ability to provide, maintain or absorb moisture (**Figure 1.6**). In the case of moderate to highly exuding wounds, the dressing needs to possess absorbent capacity in order to capture the fluids secreted and to avoid maceration of the tissues. The most common absorbent dressings are based on alginate, which is able to hold the exudates by forming a hydrophilic gel easy to remove. In addition to this, polyurethane or silicone foams that swell upon contact with liquids can be used. When the level of fluid secretion decreases, excessive absorbent capacity can result in dehydration of the wound. For this reason, dressings that are able to maintain the physiological moisture need to be applied. Examples of this are hydrocolloid dressings, which consist of gel forming materials such as cellulose and gelatine. Finally, additional moisture might be required for particularly dry wounds that present increased formation of dry and dead tissue. The necrotic tissue can be removed through surgical debridement, however, if the amount is too low or there are impeding circumstances (for instance related to the patient's health conditions), it is possible to proceed via autolytic debridement, a mechanism consisting in the digestion of dead cells by endogenous phagocytes and enzymes. In this case, moist dressings can be applied to the wound as they have been proven to facilitate this process. The most common type of moist dressings are hydrogels, which consist of a hydrophilic network characterised by high water content, up to 70-90% of the total mass (Ovington, 2007; Abdelrahman and Newton, 2011; Dhivya, Padma and Santhini, 2015).

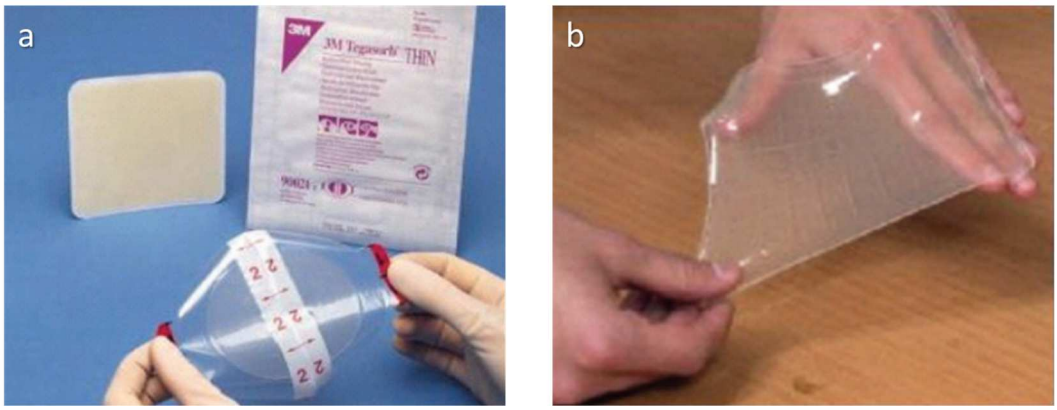

Figure 1.6 a) 3M Tegasorb™ hydrocolloid dressing and b) hydrogel sheet wound dressing (Boateng *et al.*, 2008). Images reproduced with permission of Elsevier.

Along with the classification based on the moisturising ability, an important method for categorising dressings is based on the application mode. If the dressing is in direct contact with the wound, it is referred to as primary, whereas if there is another external layer on top of the primary dressing, this is called secondary dressing. In addition to this, island dressings can be used that present a central absorbent region that is surrounded by an adhesive area. Furthermore, depending on the evaluation of specific parameters, a huge variety of dressings can be developed and is already available on the market, including antibacterial dressings, bioactive dressings (i.e. dressings that are able to actively participate in the healing process) and drug delivery platforms (Boateng *et al.*, 2008).

1.1.6 Hydrogels

As mentioned in the previous section, hydrogels are 3D hydrophilic networks characterised by great water content. More specifically, a hydrogel consists of a cross-linked network of polymeric chains that is able to absorb water in liquid medium and swell without dissolving. This feature is related to the cross-linked nature of the system, as the water molecules can be easily trapped in the interstitial spaces between the chains. Depending on the type of cross-linking, hydrogels can be divided into chemical (or permanent) and physical (or reversible) (**Figure 1.7**). Chemical hydrogels present covalent bonds between the chains, and can be obtained through the use of cross-linking agents such as

ethylene glycol dimethacrylate (EGDMA). In addition to this, photo-initiated polymerisation can be performed to achieve hydrogel formation upon light irradiation. Physical cross-links, on the other hand, usually rely on electrostatic/ionic attractions (in which case the resulting hydrogel is referred to as a polyelectrolyte complex, PEC), hydrogen bonds, metal coordination and hydrophobic/hydrophilic interactions, among others. One famous example of PEC obtained using multivalent ions of opposite charge is calcium alginate (Hoffman, 2002; Hu *et al.*, 2019).

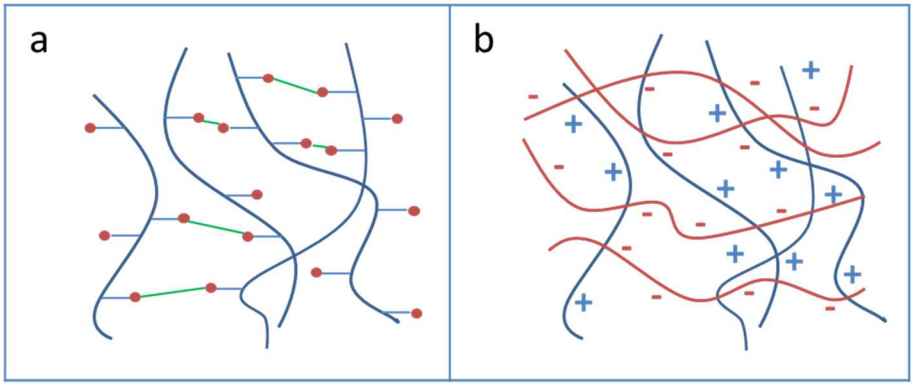

Figure 1.7 Schematic representation of a) chemical/UV cross-linked hydrogels and b) physically cross-linked hydrogels

Thanks to their unique features, hydrogels have been attracting increasing interest in the last few decades, and have become the subject of extensive research in a wide range of fields. In particular, these materials play a central role in the biomedical world, with application in areas such as ophthalmology (i.e. for the development of contact lenses), soft tissue engineering, drug delivery and wound healing (Drury and Mooney, 2003; Caló and Khutoryanskiy, 2015). Moreover, numerous studies have been directed towards the development of hydrogel-based smart materials, for instance, through incorporation of thermo-responsive compounds such as carbon nanotubes or light sensitive molecules that are activated by external stimuli. This approach allows remote control of various properties, i.e. the possibility to trigger some specific responses, in this case the generation of heat, only by controlling the surrounding environment, as a result of external inputs (Satarkar, Biswal and Hilt, 2010).

Numerous polymers have been used as substrates to develop hydrogels with a broad spectrum of properties, both of natural and synthetic origin. The most common natural polymers used for the fabrication of hydrogels are polysaccharides (e.g. chitosan, alginate), polypeptides (e.g. gelatine) and polynucleotides. Among the synthetic ones, cationic polymers have been extensively studied such as polyacrylates, poly(ethylene imine) and polycarbonates, together with non-cationic polymers like poly(ethylene oxide) and poly(vinyl alcohol) (Veiga and Schneider, 2013).

Because of the widespread of infections in the biomedical world, and especially in the context of wound healing, the development of antibacterial hydrogels has been deeply explored. Antibacterial activity can be achieved both by using an inherently active polymer or by incorporating a leachable active agent. In the first case, cationic substrates or polymers containing amino groups such as chitosan can be utilised. In the second example, compounds like antimicrobial peptides (AMPs), antibiotics and metal ions can be loaded into the matrix and released over time. These substances can be transferred to the surrounding environment with a controlled rate by monitoring parameters such as pH, temperature and degree of cross-linking (Ng *et al.*, 2014).

1.1.7 Polymers of natural origin

As a general assumption, every material that is designed to be in contact with biological systems can be referred to as a biomaterial. In particular, great attention has been directed to a class of biomaterials, i.e. biopolymers. The medical and pharmaceutical applications of biomaterials, and in particular biopolymers, are wide and include tissue engineering, wound healing, drug delivery and development of medical devices such as stents and orthopaedic implants (Tian *et al.*, 2012; Augustine *et al.*, 2013). In addition to this, the definition of biopolymers includes all polymers of natural origin, such as the ones derived from microorganisms or plants. According to their structure, natural polymers can be distinguished between polynucleotides, polypeptides (e.g. collagen and gelatine), polyesters (polyhydroxyalkanoates) and polysaccharides (for instance,

cellulose, chitosan and alginate). Further classifications can be also used that are based on their origin (Yadav, 2015).

The production of biopolymers in living organisms can be related to a variety of different cellular functions, including nutrient storage, adhesion to surfaces, reaction catalysis, inter-species communication/communication with the extracellular environment and structural roles. Thanks to their unique features, the relevance of these biopolymers has greatly increased in the recent decades. These materials, in fact, are characterised by excellent biocompatibility, which is related to their complex structure mirroring components of the human body such as proteins and extracellular matrix constituents (Aravamudhan *et al.*, 2014). A particularly relevant class of biopolymers produced by living organisms is represented by the ones biosynthesised by bacteria upon fermentation. The major classes of bacteria derived polymers are polysaccharides, polyesters, polyamides and polyphosphates. In most cases, these structures cannot be achieved through synthetic pathways, turning these materials into unique platforms for the development of biomedical products. Furthermore, they usually degrade into non-toxic compounds, making them safe for long-term applications. However, there is a major limitation to their large-scale production and commercialisation, which is associated with their high production costs. For this reason, a lot of effort is being directed towards the study and optimisation of their biotechnological production.

The metabolic synthesis of biopolymers occurs through enzymatic pathways and can take place in various cellular regions such as cytoplasm or cytoplasmic membrane, cell wall, organelles. The polymer can then be transported to other compartments and can be stored inside the cell or secreted into the environment (**Figure 1.8**). Examples of intracellularly accumulated polymers are polyhydroxyalkanoates (PHAs), polyphosphates and starch. In this case, the yield of the production is limited by the maximum quantity that can be stored. Furthermore, cell lysis is required for the extraction, hence prolonging the time and increasing the costs of the process. On the other hand, if the polymer is secreted by the cell in the surrounding environment, there are no restrictions to

the volume that can be occupied. However, the solubility of these biopolymers can result in increased viscosity, which can make the handling of the culture medium more difficult (Steinbüchel, 2001).

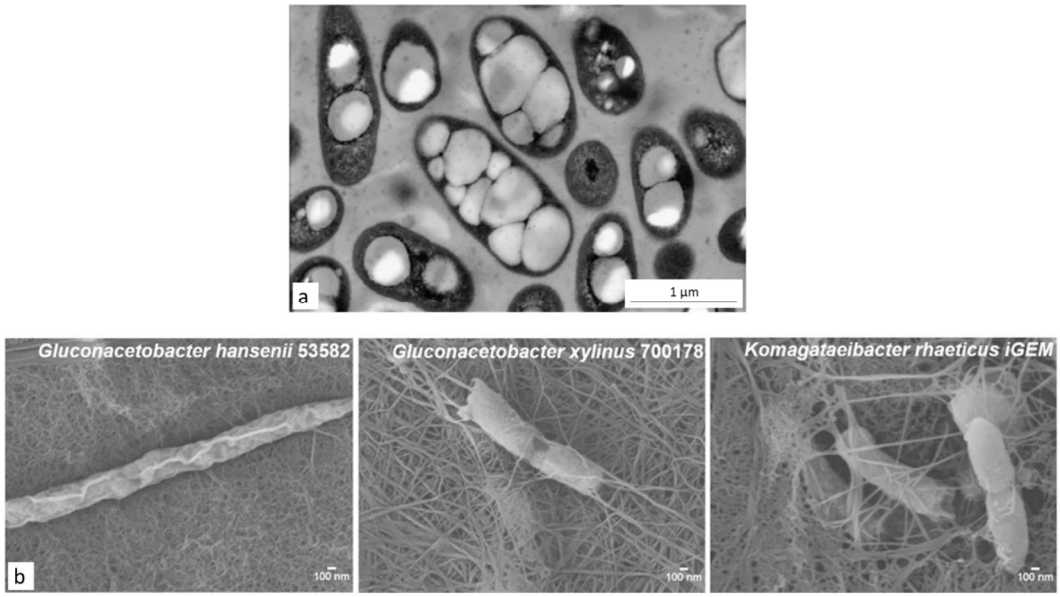

Figure 1.8 a) Intracellular production of polyhydroxyalkanoates by *Cupriavidus necator* DSM 545 (Koller *et al.*, 2011) and b) extracellular production of bacterial cellulose by various strains (Basu, Vadanan and Lim, 2018). Images reproduced, respectively, with permission of John Wiley and Sons and under Creative Commons (CC) license.

As regards the production costs of biopolymers, the main parameter to consider is the ratio between the polymer yield and the price of the carbon sources, which usually consist of sugars, vegetable oils, yeast extract and glycerol. In addition to this, if the product is intended for biomedical applications, it is crucial to obtain a highly pure material, hence the purification phase can greatly affect the final affordability of the entire process (Rehm, 2010).

1.1.8 Metabolic synthesis of bacterial cellulose

Bacterial cellulose (BC), a polysaccharide having the same chemical structure of plant-cellulose but different supramolecular arrangement and, therefore, mechanical properties, is produced by several microorganisms such as fungi and algae, where it is mainly involved in structural functions. Moreover, BC is extracellularly secreted by several types of bacteria in the presence of a suitable

carbon source. Several Gram negative strains have been reported to produce cellulose, i.e. *Gluconacetobacter* (formerly *Acetobacter*), *Agrobacterium*, *Achromobacter*, *Aerobacter*, *Sarcina*, *Azotobacter*, *Rhizobium*, *Pseudomonas*, *Salmonella* and *Alcaligenes*, as well as one type of Gram positive bacterium, *Sarcina ventriculi*. Among these, *Gluconacetobacter* has been extensively studied as a model cellulose-producing strain thanks to its ability to produce high amounts of polymer starting from a wide range of carbon and nitrogen sources. It has been observed that one *Gluconacetobacter xylinus* cell can polymerise up to 200,000 glucose molecules per second into glucan chains, which are then assembled into the typical ribbon-like structure. *Gluconacetobacter xylinus* is a rod-shaped bacterium able to produce cellulose as self-assembled microfibrils forming a porous hydrogel-like structure. The fibrils are composed of glucan chains interconnected by hydrogen bonds, thus resulting in a crystalline structure that is responsible for the mechanical properties of BC, such as higher tensile strength and Young's modulus compared to plant cellulose. Moreover, such fibrils are very thin, with a width of one-hundredth the ribbons of plant cellulose, making this material highly porous. Cellulose is synthesised by *Gluconacetobacter* as two different crystalline forms: cellulose I, which consists of a parallel arrangement, and cellulose II, the thermodynamically more stable and amorphous form of cellulose. The predominant form is cellulose I, however the chains usually rearrange into the more stable cellulose II structure.

The metabolic synthesis of bacterial cellulose is a complex process involving several highly regulated steps. The biochemical production pathway starts with the conversion of glucose into glucose-6-phosphate (Glc-6-P) catalysed by glucose hexokinase. If fructose is used as the carbon source, a previous step consisting in the phosphorylation of fructose by fructose hexokinase and isomerisation of fructose-6-phosphate to Glc-6-P by phosphoglucose isomerase takes place. Glc-6-P is then isomerised to glucose-α-1-phosphate by phosphoglucomutase, and after this the metabolite is converted into uridine diphosphoglucose (UDP-GIc) by pyrophosphorylase uridine diphosphoglucose

(UGP). UDP-Glc is the precursor of cellulose, which can be finally polymerised by cellulose synthase (**Figure 1.9**).

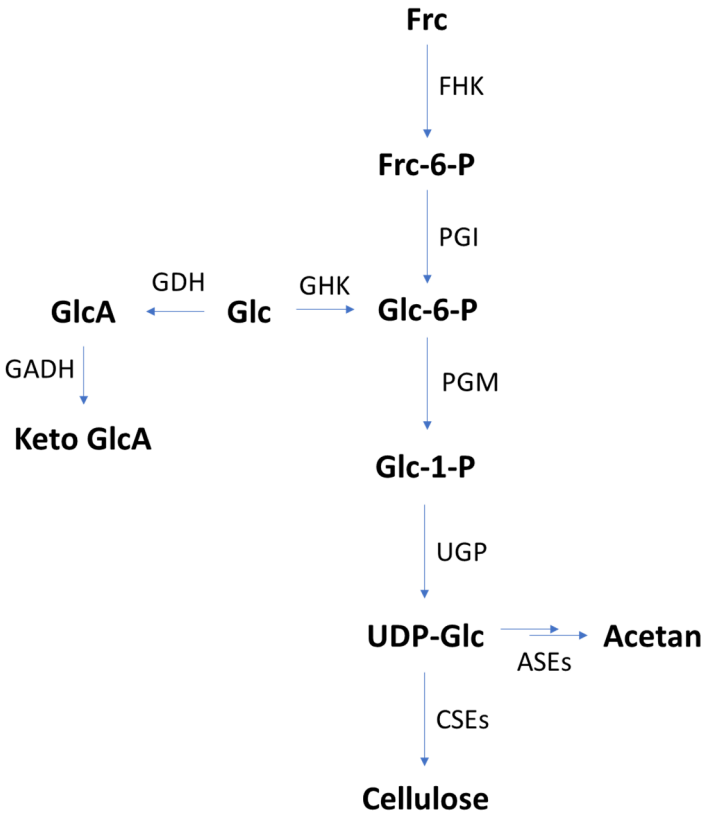

Figure 1.9 A simplified scheme of metabolic synthesis of bacterial cellulose starting from glucose or fructose. Frc: fructose; FHK: fructose hexokinase; Frc-6-P: fructose-6-phosphate; PGI: phosphoglucose isomerase; Glc-6-P: glucose-6-phosphate; Glc: glucose; GHK: glucose hexokinase; GDH: glucose dehydrogenase; GlcA: gluconate; GADH: gluconate dehydrogenase; keto GlcA: keto-gluconate; PGM: phosphoglucomutase; Glc-1-P: glucose-1-phosphate; UGP: pyrophosphorylase uridine diphosphoglucose; UDP-GIc: uridine diphosphoglucose; ASEs: acetan synthesis enzymes; CSEs: cellulose synthesis enzymes (Shoda and Sugano, 2005). Image adapted with permission of Springer Nature.

The most important enzymes involved in the biosynthesis process are UGP and CS. It has been shown that bacteria lacking UGP activity are not able to secrete cellulose even in the presence of cellulose synthase, proving its crucial importance for the polymer production. On the other hand, cellulose synthase, a highly unstable protein of 400-500 kDa anchored to the cytoplasmic membrane, is responsible for the polymerisation of UDP-Glc into the β(1→4) glucan chains. As soon as the glucan chains are formed, the assembling and crystallisation of

the chains takes place immediately outside the cell membrane. This phase represents the rate limiting step in the rate of polymerisation. A pre-cellulosic polymer is synthesised inside the cell and then extruded in groups of 10 to 15 chains called tactoidal aggregates consisting of left-handed triple helices. The extrusion sites are 50-80 pore-like sites organised in a long row alongside the long axis of the cell; although the assembly of the chains in microfibrils and ribbons occurs extracellularly, the process is cell directed as it is governed by the orientation of the extrusion sites (Chawla *et al.*, 2009).

Although the role of cellulose in plants as well as in algae is mainly structural, its biological function in bacteria is to provide mechanical, chemical and biological protection and/or facilitate cell adhesion processes. The pellicle constitutes in fact a stable matrix in which cells are embedded. Moreover, it acts as a flotation device for bacteria, as they are produced at the interface between liquid and air, enhancing contact with the atmosphere and providing oxygen for the aerobic species. Finally, BC promotes the colonisation of surfaces by protecting cells from competitors and provides chemical protection from UV light (Ross, Mayer and Benziman, 1991).

1.1.9 Antibacterial polymers

As the need of antibacterial materials has become more stringent due to the antibiotic crisis, extensive research has been focused on the development of polymers active against bacteria. One of the principal strategies to achieve antibacterial activity consists in the modification of biopolymers by loading the matrix with small active molecules. For this purpose, a wide range of different compounds has been investigated. However, there are some disadvantages related to this approach, which have brought the scientific community to look into different strategies. The use of inherently antibacterial polymers represents a valid alternative for the development of bactericidal biomaterials. Such materials allow us to overcome the limitations related to the use of low molecular weight compounds, e.g. the maximum concentration that can be loaded in the system or environmental issues due to the generally high volatility caused by

their low molecular weight. In addition to this, a small molecule is more likely to be unstable and reactive as compared to a high molecular weight compound. Finally, using an inherently active polymer can ensure a long-term activity as the antibacterial action it is not exhausted when the release of external molecules is complete (Deka, Sharma and Kumar, 2015).

A huge number of polymers with structure-dependent antibacterial properties has been developed and studied for applications in the biomedical field. The most common type of inherently active polymers is polycations, which contain ionic groups (generally quaternary ammonium or phosphonium groups) in the backbone or as pendant chains (Timofeeva and Kleshcheva, 2011). The generally acknowledged hypothesis for the explanation of the mechanism of action of such materials involves a first contact between bacteria and their cationic group based on electrostatic interactions. As confirmed by electrophoretic studies, the outer bacterial membrane of both Gram positive and Gram negative bacteria exhibits a net negative charge due to the presence of anionic species. In the case of Gram positive strains, the cell wall consists of a thick peptidoglycan layer interweaved with negatively charged polymers, i.e. teichoic acids, which can be covalently attached to the membrane (wall teichoic acids) or anchored to groups of the membrane lipids (lipoteichoic acids). These anionic compounds, which mostly include glycerol phosphate and glucosyl phosphate units, are stabilised by positive counter-ions such as calcium or magnesium. In the presence of an external cationic group, a competition can occur for the anionic sites. Cationic polymers can in fact interact with these groups, resulting in penetration and disruption of the membrane and cell lysis followed by leakage of intracellular components. Gram negative bacteria, on the other hand, present a thinner peptidoglycan wall and an additional outer membrane composed of lipid bilayer. In particular, the inner section contains phospholipids whereas the external one is composed of glycolipids, mainly lipopolysaccharides. Once again, a negative charge is observed due to the presence of phosphate groups, however, the presence of a permeability barrier makes Gram negative less susceptible to the attack of biocidal substances by preventing their penetration through the cell

(**Figure 1.10**) (Silhavy, Kahne and Walker, 2010; Malanovic and Lohner, 2016; Exner, 2017).

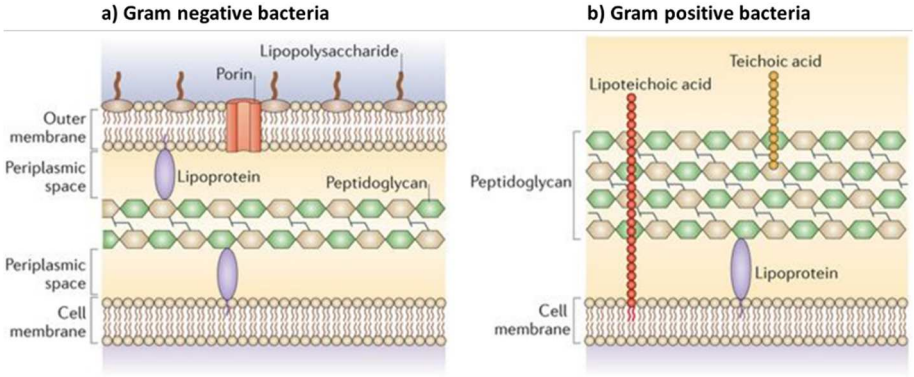

Figure 1.10 Cell wall structure of a) Gram negative and b) Gram positive bacteria (Brown *et al.*, 2015). Image adapted with permission of Springer Nature.

A well-known class of polymers containing cationic ammonium groups is represented by polyguanidines. Thanks to their high antimicrobial efficiency, these guanidine-derived polymers have been widely studied for applications in the biomedical field. As previously explained, the most accredited hypothesis to elucidate the mechanism of action of polyguanidines consists in their binding of the membrane phospholipids, followed by penetration through the damaged outer membrane and bacteriolysis (**Figure 1.11**).

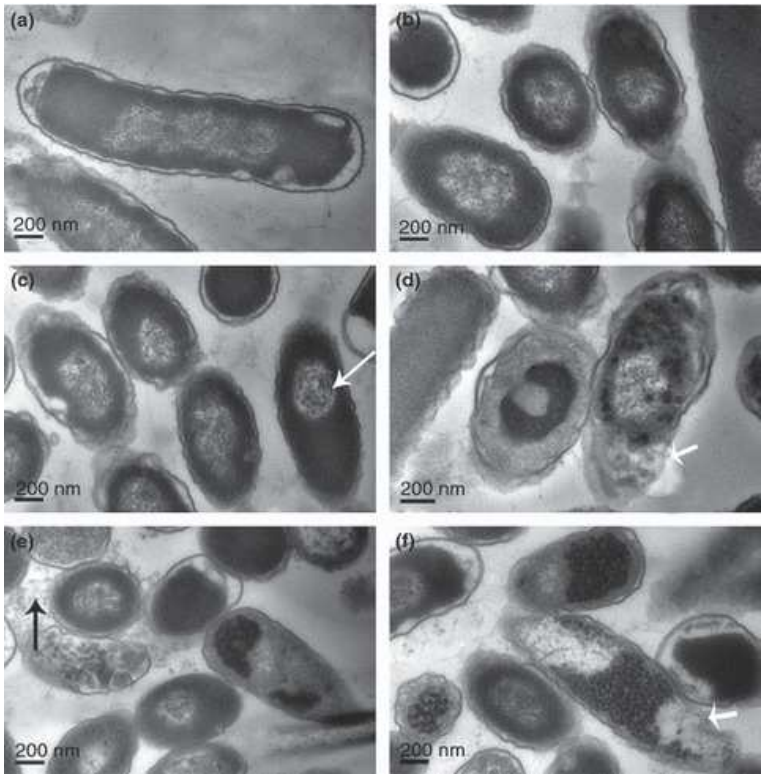

Figure 1.11 Membrane damage of *Escherichia coli* 8099: a) control cell, b) and c) cells after treatment for 60 minutes with 13 µg/mL of polyhexamethylene guanidine hydrochloride (PHMG) and d), e) and f) cells after treatment for 60 minutes with 23 µg/mL of PHMG (Zhou *et al.*, 2010). Image reproduced with permission of John Wiley and Sons.

Another important group of inherently active polymers consists of *N*-halamine-based polymers. An *N*-halamine group is defined as a covalent bond between nitrogen and a halogen, typically chlorine but also bromine and iodine. Such molecules can be organic or inorganic (depending on the substituent linked to the nitrogen atom) and are usually obtained by halogenation of imide, amide or amino functionalities, yielding the corresponding halamines. The stability of these compounds depends on the presence of α-hydrogens, i.e. hydrogens in position α to the nitrogen atom. When α-hydrogens are present, a dehydrohalogenation reaction can be observed, with release of hydrogen halides. It has been observed that the order of stability for organic *N*-halamines follows the trend imide < amide < amine, which is the inverse of their biocidal activity. Depending on the application, the most suitable *N*-halamine polymer can be used to achieve fast activity or long-term action against bacteria. The antimicrobial efficiency of these compounds is ascribed to the presence of halides

with oxidation state +1, which turns them into potent oxidative agents for biological receptors such as amino or thio groups of proteins, leading to cell inactivation. (Muñoz-Bonilla and Fernández-García, 2012; Hui and Debiemme-Chouvy, 2013).

A third class of antibacterial polymers is represented by polymers containing alkyl chains. It has been proven, in fact, that alkyl chains are effective in bacterial inhibition, with activity directly proportional to the number of carbon atoms. Moreover, their haemolytic activity and cytotoxicity have been investigated, showing that these compounds possess low or no cytotoxicity to mammalian cells (Tiller *et al.*, 2001; Roy and Das, 2008; Lu *et al.*, 2015). The mechanism of action of such polymers is believed to be related to the efficient penetration of the carbon chains through the bacterial cell membrane. This effect can be explained by the high degree of hydrophobicity of these moieties, which allows stronger interactions with the phospholipid layer of the bacterial cell membrane (Altay *et al.*, 2015).

An important factor that must be taken into consideration when evaluating the antimicrobial activity of a polymer is its molecular weight (MW). It has been observed that the correlation between MW and bacterial inhibition follows a bell-like trend, with an optimal range of molecular weight that shows the highest bactericidal efficiency. This behaviour can be interpreted as a consequence of the ease of permeability through the cell membrane. In case of high molecular weight molecules, a high content of cationic or hydrophobic groups are available, ensuring a stronger binding ability to the cell surface. On the other hand, a MW higher than a "critical value" (which is typical for each polymer) prevents the polymer from penetrating. This effect is particularly important in the case of Gram negative bacteria because of the presence of the outer membrane (Kenawy, Worley and Broughton, 2007; Badawy and Rabea, 2011).

1.2 State-of-the-art

1.2.1 Plant cellulose-based hydrogels

Cellulose is an inexpensive, readily available polysaccharide characterised by a great degree of biocompatibility and biodegradability. Thanks to these features, this versatile polymer represents one of the most used materials in several fields, including the biomedical area (Kalia *et al.*, 2014; Lin and Dufresne, 2014; Nechyporchuk, Belgacem and Bras, 2016). Cellulose is a fibrous polymer insoluble in water that can be mainly found in the cell wall of plants. Six different interconvertible crystalline structures of cellulose have been isolated, namely I, II, III_1, III_{11}, IV_1 and IV_{11}. Cellulose II can be obtained from I through regeneration (i.e. solubilisation in a suitable solvent followed by reprecipitation in water) or mercerisation (i.e. swelling of the fibres in the presence of sodium hydroxide). Cellulose III_1 and III_{11} can be produced, respectively, by treating in liquid ammonia the polymorphs I and II, whereas structures IV_1 and IV_{11} are formed upon heating of celluloses III_1 and III_{11}. Cellulose I is the most stable form, and the one characterising native cellulose; more specifically, this polymorph has been found to contain two structures, i.e. I_α and I_β, which present different cell unit organisation. As regards the chemical composition, cellulose presents a linear backbone consisting of β-D-glucopyranose units linked by β(1→4) glycosidic bonds. It has been observed that glucopyranose units present hydroxyl groups in equatorial positions and a $^4C_1$ chair conformation, which means that the C_4 is located above the reference plane of the chair whereas the C_1 is located below it. This structure is the most stable as it allows to minimise the electrostatic repulsion of the ring substituents. Thanks to the presence of three hydroxyl groups on each monomer, the supramolecular structure of cellulose presents an extensive hydrogen bonding network, which is believed to be responsible for its crystallisation. Moreover, these moieties facilitate further chemical modifications, turning cellulose into a polymer with tunable properties for a wide number of applications. Among its several other application, cellulose has been largely used to develop hydrogels for application as wound dressings, as

its biocompatibility makes it an excellent substrate for contact with both burnt or wounded skin (O'Sullivan, 1997; Klemm *et al.*, 2005).

Due to its natural sourcing, optimal purification of the raw material before its application in contact with body tissues must be ensured. In this respect, a recent report by Nordli *et al*. proposed an optimised method for the purification of nano-fibrillated cellulose (NFC) derived from natural wood cellulose with the intent of obtaining a material for wound healing applications. The protocol proposed consisted of an initial treatment involving a combination of high temperature and sodium hydroxide, followed by TEMPO-mediated oxidation in the presence of NaClO. After this, the cellulose fibres were homogenised in an ultra-turrax. The final product was characterised in terms of endotoxin content, cytotoxicity towards fibroblasts and keratinocytes and cytokine production. The tests showed that the process yielded a material with a remarkably low endotoxin level of 45 EU/g, significantly lower than traditional treatments that usually result in endotoxin contents above the acceptable limit (i.e. 100 EU/g). Furthermore, no variation in cytotoxicity or cytokine stimulation was observed when compared to the control (i.e. a commercial dressing based on carboxymethyl cellulose). However, a mild decrease in metabolic activity was observed in high-purity NFC compared to the positive control. Authors suggest that this could be due to a mechanical stress exerted by cellulose fibres on the cells, and further studies should be performed to clarify the matter (Nordli *et al.*, 2016).

The development of cellulose-based hydrogels using oxidised cellulose was investigated through combination of anionic NFC (a-NFC) and cationic NFC (c-NFC) to produce a potential structural material for wound healing devices. Initially, carboxylated cellulose was obtained by TEMPO-mediated oxidation. Then, a-NFC and c-NFC were cross-linked using calcium nitrate as a source of Ca^{2+} ions in order to obtain two formulations of ionically cross-linked hydrogels, namely a-NFC and ac-NFC. The hydrogels were biologically tested using two cell lines, human dermal fibroblasts and monocyte-like. Cell viability was above 70% in all cases as compared to the control, confirming the high biocompatibility of wood cellulose-based materials. The effect of a-NFC and ac-NFC on the

inflammatory response was also evaluated. Results showed that these materials have a rather inert behaviour, neither promoting inflammatory onsets nor fostering already occurring phlogoses (Basu *et al.*, 2017). A superabsorbent cellulose-based hydrogel was developed using an approach similar to the one proposed by Basu *et al*. Briefly, anionic carboxymethyl and hydroxyethyl cellulose were produced and combined into a polyelectrolyte complex (PEC) by means of aluminium ions (Al^{3+}) as cross-linking agents. The process yielded a sponge-like structure with high swelling potential. In particular, absorption was dose-dependent and it was correlated with the amount of cross-linking agent, a phenomenon that is most probably due to an increase in the degree of cross-linking of the structure (Liu *et al.*, 2015).

Along with chemical treatments, a plethora of different approaches has been investigated in the attempt to modify and optimise the properties of native cellulose. A very interesting strategy, for instance, relies on seeding cells on the surface of the material to increase its biological performance. In this respect, Mertaniemi *et al*. studied the use of NFC as a delivery carrier for human adipose mesenchymal stem cells (hASC) into wounds to promote healing. NFC was first moulded into a three-dimensional structure by 3D printing, and the resulting filaments were cross-linked with glutaraldehyde to ensure ideal wet strength of the construct. hASC showed good adhesion to the scaffold and proliferation to confluence within 7 days. Cell attachment and viability were also assessed by an *ex vivo* suturing assay, showing that the cellulose-based hydrogel performed comparably to a positive control (Mertaniemi *et al.*, 2015). Thanks to the high versatility of this technique, the use of cellulose in 3D printing is a promising approach for the fabrication of scaffolds. Apart from the aforementioned example, several other types of nanocellulose were confirmed suitable for 3D printing, including TEMPO-oxidised and carboxymethylated/periodate (C-periodate) oxidised nanocellulose. In particular, it was demonstrated that C-periodate oxidised nanocellulose can be used as a bio-ink to print self-standing 3D constructs with porous structure. As in the previous example, a subsequent

cross-linking step consisting of $CaCl_2$ injection was performed to obtain a more compact and solid structure (Powell *et al.*, 2015).

Efforts were also made towards the optimisation of the mechanical properties of native cellulose. For instance, hydrogel sheets (HGS) and glycerol-impregnated hydrogels (G-HGS) were developed using low-substituted hydroxypropyl cellulose (L-HPC). G-HGS displayed increased values of both Young's modulus and tensile strength without any significant reduction in the elongation rate. The authors suggested that the explanation for this interesting behaviour should be sought in an increase in the rate of intermolecular hydrogen bonding of L-HPC chains as a result of the incorporation of glycerol. In addition to this, when compared to both silicone-based commercial dressings and hydrogel dressings, L-HPC-based hydrogels showed lower adhesiveness, indicating that they could be optimal candidates for wound healing applications, where a bond between material and tissue must be avoided (Ogawa *et al.*, 2014). Liu *et al*. prepared hemicellulose-reinforced hydrogels by modifying TEMPO-oxidised NFC. Differently sourced hemicelluloses were incorporated into NFC using two sorption methods. *O*-acetyl-galactoglucomannan (GGM), xyloglucan (XG) and xylan were incorporated either via pre-sorption (i.e. adsorption of hemicellulose prior to hydrogel swelling) or via *in situ* sorption (i.e. hemicellulose adsorption and hydrogel swelling happening at the same time through the water uptake procedure). Regardless of the method, it was possible to load a higher amount of hemicelluloses within nano-cellulose with high charge density due to greater water uptake ability. Following fabrication, the biological performance of the hydrogels was evaluated: fibroblasts were found to adhere and proliferate better on XG-containing low-charged NFC prepared by pre-sorption, probably thanks to its higher mechanical strength (J. Liu *et al.*, 2016). In addition to these, composite-development approaches were explored as a strategy to optimise the mechanical properties of plain cellulose. In an article by Huang *et al*. cellulose was combined with halloysite nanotubes (HNTs), resulting in successful enhancement of the mechanical properties of the material. The filler was introduced in the structure by means of continuous ultrasonication and,

subsequently, the hydrogels were cross-linked using epichlorohydrine. The HNTs-loaded hydrogels exhibited outstanding mechanical properties both in terms of higher compressive modulus and higher resistance to deformation. In parallel, cell viability was assessed using mouse embryo osteoblast precursor cells (MC3T3-E1) and human breast adenocarcinoma cells (MCF-7). Increased viability was observed for both cells up to a limit cellulose to HNT weight ratio of 1:2. Above this threshold the metabolic activity of cells starts to decrease, probably as a consequence of an excessive loading of halloysite above cytotoxic levels (Huang, Liu and Zhou, 2017).

Along with the modification of cellulose by chemical alteration of its structure and doping with active agents, blending with other polymers was also investigated to tailor the properties of the product towards specific biomedical applications. For example, pullulan was incorporated into carboxymethyl cellulose (CMC) to develop an injectable post-operative barrier hydrogel. Pullulan is a polysaccharide obtained from starch and used as food additive thanks to its adhesive properties. First, the side-chains of CMC were functionalised with tyramine by EDC/NHS coupling chemistry (1-ethyl-3-(3-dimethylaminopropyl) carbodiimide and *N*-hydroxysuccinimide). The phenol groups of tyramine, grafted onto cellulose, were then used to perform enzymatic cross-linking. This procedure increases the structural integrity of cellulose and allows for more reproducible *in vivo* experiments. After this, pullulan was incorporated into cross-linked hydrogels by adsorption. The material developed following this protocol was characterised by good cytocompatibility towards embryonic fibroblasts, with cell viability in the range of 80-82% as compared to a positive control. CMC/pullulan hydrogels were also found to be antifouling, meaning that they successfully inhibit cell attachment and avoid the formation of new tissue, a key property of post-operative barrier materials. Furthermore, an *in vivo* animal model with male Sprague Dawley rats was also used. The assay showed that the control group displayed 100% cell adhesion on the material, whereas the CMC/pullulan hydrogel resulted in only 27% abdominal adhesion (Bang *et al.*, 2017).

CMC was also blended with a hydrophilic silk-derived polypeptide, i.e. sericin. Sericin is considered a waste product of the silk industry due to its mechanical weakness and, as such, is readily available at low cost, making it a very promising agent for commercially competitive wound healing platforms. Furthermore, it is also known for its anticoagulant and antityrosinase properties. Thanks to its great hydrophilicity, sericin was used in combination with cellulose to grant high water content in the dressing and thus ideal moisture during healing. Porous CMC/sericin hydrogels were prepared using a dual cross-linking approach. Briefly, glutaraldehyde and $AlCl_3$ were used, respectively, to improve the mechanical properties of sericin and CMC ($AlCl_3$ reacts with the carboxyl groups of CMC). The biological assessment, carried out using a human cell line of keratinocytes (HaCaT), proved that the addition of sericin enhanced cell attachment and proliferation. However, a decrease in mechanical strength was observed at increasing sericin content, owing to the low properties of the polypeptide. According to the authors, the ideal ratio to optimise both the biological and mechanical properties of the construct was found to be 1:1 CMC to sericin (Nayak and Kundu, 2014). In a follow up study on the same type of material, the role of the molecular weight (MW) of CMC in determining the overall properties of CMC/sericin hydrogel was examined. Carboxymethyl cellulose with three different molecular weights (namely low, L-CMC, medium, M-CMC and high, H-CMC) were combined with sericin and used to prepare an array of different hydrogels. A porous structure was obtained regardless of the MW of CMC. Smaller pores were obtained for specimens containing sericin as compared to the corresponding sericin-free samples. Indirect cytotoxicity did not highlight any major concern regarding the biological safety of these materials for any of the tested formulations. In addition, enzymatic degradation assays performed on CMC/sericin hydrogels revealed that L-CMC and M-CMC based hydrogels were characterised by faster degradation kinetics, possibly as a consequence of the higher number of glycosidic linkages serving as cleavage sites for the enzyme amylose, which in turn allow for faster sericin dissolution. As a result, L929 fibroblasts cultured on these materials were stimulated by the sericin

available in the medium and increased their collagen production, ultimately promoting wound healing (Siritientong and Aramwit, 2015).

1.2.2 Bacterial cellulose-based hydrogels

In recent years, the use of bacterial cellulose (BC) in biomedical applications gained increasing interest among the scientific community. As previously mentioned, BC is an external secretion produced by several genera such as *Gluconacetobacter*, *Sarcina*, *Acetobacter*, *Agrobacterium* and *Rhizobium*. Among these, *Gluconacetobacter xylinus* is probably the most studied and extensively used thanks to the high polymer yield and ability to metabolise a wide array of carbon and nitrogen sources (Römling, 2002; Nguyen *et al.*, 2008). Bacterial cellulose is naturally produced in a nanofibrous, hydrogel-like structure with high water content ideal for wound healing applications, in which a highly moisturised environment is key. Compared to plant cellulose, this biopolymer is characterised by a higher degree of crystallinity that results in increased tensile strength, Young's modulus and water-holding capacity. Moreover, BC is an intrinsically pure product that does not need harsh purification processes (such as separation from hemicellulose and lignin) and, as a consequence, is inherently biocompatible (Helenius *et al.*, 2006). Due to its promising properties, this material has been widely studied for applications in numerous biomedical fields (Huang *et al.*, 2014), with a particular focus on its application for skin regeneration and development of wound healing devices (Fu, Zhang and Yang, 2013; Kucińska-Lipka, Gubanska and Janik, 2015).

Thanks to its high mechanical properties, the use of bacterial cellulose-derived fibres as a reinforcing agent for weak materials has been extensively researched. One example is the work proposed by Awadhiya *et al.* based on the incorporation of BC into an agarose matrix. Agarose is in fact a polysaccharide characterised by exceptionally high water uptake but low mechanical properties. For this reason, a composite based on the two polymers was developed through solvent casting technique. Prior to this, BC was finely homogenised and mixed with a solution of agarose and glycerol. Various concentrations of cellulose fibres were tested,

and the optimal ratio was found to be 20% w/w. This composition resulted in fact in an increase of 140% in the tensile strength as compared to pure agarose, and a decrease in the water uptake of 250% at physiological temperature and 350% at 4 °C, probably because of the denser structure of the fibres as compared to the unmodified membranes. A decrease in the tensile strength was observed, however, for higher BC content, probably because of the inability of the agarose matrix to incorporate and homogeneously disperse excessive amounts of fibres and, therefore, to hold the stress applied (Awadhiya *et al.*, 2017).

As regards the biological performance of cellulose, several studies have been focusing on the enhancement of its native properties in order to produce materials with high biocompatibility. As previously mentioned, sericin is an optimal candidate for the development of biomedical substrates thanks to its innate features. Lamboni *et al*. reported the coupling of this polypeptide with BC to produce a wound healing platform. To achieve this, the cellulose membranes were impregnated with sericin by immersion in solutions at increasing sericin concentration (1, 2 and 3% w/v). A high degree of incorporation was achieved, with uniform dispersion of the fibres and smooth surface as a result of sericin addition. Furthermore, the fibrillar network of cellulose was retained after the blending process. The biological assessment of the composites showed increased cell viability for higher sericin content both for fibroblasts and keratinocytes. Similar adhesion degree was observed for the two samples and the control, although lower cell proliferation rate was detected. The authors suggested that this behaviour could be ascribed to the stiffness of cellulose (Lamboni *et al.*, 2016). A similar approach was investigated by Lin *et al.*, with introduction of bioactive substances in a BC matrix. First, a porous scaffold was fabricated through physical punching of cellulose and subsequently coated with an alginate solution cross-linked with $CaCl_2$. After this, a variety of extracellular matrix components was incorporated (i.e. collagen, elastin and hyaluronic acid), as well as three different growth factors (namely B-FGF, H-EGF and KGF). Good release rate was observed for both collagen and hyaluronic acid under physiological conditions, as well as controlled diffusion of the growth factors. Furthermore, the scaffolds

loaded with collagen and H-EGF exhibited significantly improved biocompatibility towards fibroblasts, although a dose-dependent cytotoxic response was detected with increasing amount of $CaCl_2$ (Lin *et al.*, 2011). Another recent study proposed the combination of cellulose and collagen to obtain a hydrogel with enhanced wound healing ability. In this work, the composite gel (BC/COL) was produced by mixing collagen and homogenised BC pulp. The material was then tested *in vivo* on adult male rats to compare the biological behaviour with a commercial collagenase ointment. Overall, the group treated with the BC/COL hydrogel exhibited enhanced re-epithelialisation and adhesiveness as compared to the control groups. Furthermore, macroscopic evaluation evidenced improved tissue repair, probably thanks to the biological properties of BC (Moraes *et al.*, 2016).

The porosity of a substrate is a crucial parameter as it plays a central role in the determination of cell attachment, growth and proliferation. An optimal degree of porosity, size and interconnection of the pores must be therefore ensured when developing a tissue engineering scaffold. In the case of BC-based structures, achieving porosity might be challenging due to the innate hydrogel-like form in which it is biosynthesised. However, a few strategies to overcome this issue have been investigated and reported in recent years. In this context, an interesting strategy has been proposed by Yu *et al*. involving the use of microfluidics to produce hollow microspheres. This was achieved by culturing *Gluconacetobacter xylinus* in a double-layer hydrogel template. The core-shell structure was in fact obtained through encapsulation of alginate microparticles into a droplet of agarose precursor solution containing culture medium and bacteria. The formation of the agarose microspheres with alginate core was carried out using a microfluidics device consisting of a two-cross channel junction. After collection, the agarose microspheres were cooled down to allow agarose gelation and then stored at 25 °C for BC cellulose production. Thanks to the density difference of the two polymers, the biosynthesis was confined to the agarose layer. Afterwards, the agarose and the bacteria were removed by high-temperature treatment, whereas the alginate core was dissolved using a sodium citrate

solution. The hollow BC microspheres thus generated were assembled to form a 3D porous scaffold and biologically characterised *in vitro* (using lung adenocarcinoma cells) and *in vivo* with respect to cellulose membranes. In both cases, enhanced performance was observed for the microspheres. In particular, the *in vivo* study on male Sprague Dawley rats showed improved wound healing rate for the group treated with the injectable BC scaffold, probably as a result of the increased contact area of the microspheres (Yu *et al.*, 2016). A similar strategy was adopted for the production of a 3D scaffold based on micro-stranded cellulose. Once again, the structures were obtained by growing bacteria in an alginate template consisting of a hollow hydrogel tube. The alginate shell was then dissolved and fibroblasts were seeded onto the strands. The scaffolds were then used as building blocks to fabricate cellular constructs of different shape, namely coiled and barn-of-yard. In both cases, the structure was maintained, indicating good stability and stiffness. Furthermore, the cells were found to be alive up to 6 days within the barn-of-yard construct, suggesting that it is able to provide adequate nutrition and oxygenation (Hirayama *et al.*, 2013).

As previously mentioned, bacterial cellulose is an optimal substrate for various types of wounds including burn wounds, demonstrating excellent healing ability thanks to the high level of hydration provided. Several studies have been carried out investigating the development of hydrogel dressings for burnt skin, often involving coupling with other polymers to improve the properties of the material. One example is the work proposed by Mohamad *et al*. on the fabrication of a composite based on BC and acrylic acid. The polymers were homogenised and cross-linked through accelerated electron beam irradiation using two different ionising doses, i.e. 35 and 50 kGy, yielding two hydrogels, respectively, H_{35} and H_{50}. Both specimens demonstrated good biocompatibility *in vitro* towards fibroblasts up to 48 hours after incubation. However, H_{35} was found to perform better, probably because of its higher mechanical strength, water uptake and elasticity. The *in vivo* evaluation was therefore carried out on the H_{35} sample using Sprague Dawley rats. The group treated with the hydrogel did not evidence any dermal irritation, and faster wound closure rate was observed as

compared to the control group (i.e. a commercial wound healing hydrogel) and the untreated group after 7 days. The results were confirmed by histological studies, which showed enhanced re-epithelialisation for the test group as compared to the other two (Mohamad *et al.*, 2014). A similar approach was proposed by the same group for the development of BC/polyacrylamide microparticles. In this case, the two polymers were cross-linked using both a chemical agent (i.e. *N*,*N*'-methylenebisacrylamide) and microwave irradiation. The hydrogel was then micronised and sieved in order to isolate microparticles with size of 50-150 μm. Once again, the cell viability of fibroblasts was evaluated after contact with the sample as well as the *in vivo* performance on burn wounds using female Sprague Dawley rats. The group treated with the hydrogel did not show any sign of irritation or haemorrhage, and slightly superior wound closure rate was noted even as compared to the positive control. Moreover, the histological tests evidenced increased epithelialisation, with higher number of hair follicles and blood vessels and increased keratin secretion with respect to the control (Pandey *et al.*, 2017).

1.2.3 Cellulose-based antibacterial hydrogels

As mentioned in the previous sections of this chapter, one of the main issues faced by the scientific community in the biomedical field is the spread of infections due to the rise of antibiotic resistance. In this context, a particular focus is directed towards the infection of wounds, as it is one of the most common targets of bacterial contamination, with consequences both for the patient and for the healthcare system. As cellulose (both plant-derived and bacterial) has become one of the principal polymers used for wound dressings, a lot of effort has been spent on its modification to introduce antibacterial features. To achieve this, various strategies have been investigated, involving both chemical/physical modification as well as loading of active agents.

In this respect, several studies have been proposed that rely on the combination with polymers that present antibacterial activity. The most common example of such materials is chitosan, thanks to the high biocompatibility, low cost and

easily tailorable structure. For instance, the work reported by Fan *et al*. utilised carboxymethylated cellulose (OCMC) and carboxymethyl chitosan (CMCS) as substrates to fabricate antibacterial hydrogels. The two polysaccharides were chemically cross-linked through reaction between the aldehydic groups of the modified cellulose and the amino groups of chitosan. An array of hydrogels was prepared with increasing concentration of chitosan (which resulted in lower gelation time thanks to the higher availability of cross-linking sites). One formulation, namely CSOC-5, was tested *in vivo* on adult male Wistar rats in order to assess the wound healing and antibacterial capacity of the material, showing effective bacterial inhibition. Furthermore, the hydration potential of the hydrogel prevented the formation of a dry scab, enhancing wound closure. Finally, lower inflammatory response was observed for the hydrogel-treated group as compared to the positive control, probably thanks to the biological properties of both cellulose and chitosan (Fan *et al.*, 2013).

Along with active polymers, extensive research has been carried out on the incorporation of active metal ions into a cellulose matrix to impart antibacterial properties. The most common therapeutic metal is silver, which is widely available on the market in numerous forms and compositions. An interesting approach was proposed by Singla *et al*. for the production of hydrogels based on bamboo-derived cellulose for application on diabetic wounds. In particular, two different cellulose sources were used to extract the cellulose nanocrystals (CNC), i.e. DH-CNCs and BB-CNCs. AgNPs were then introduced by *in situ* reduction of silver nitrate through a green process involving the use of a leaf extract. The material was then mixed with Vaseline in order to form an ointment for topical application. The Ag-containing hydrogel was tested *in vivo* using swiss albino mice, and good inhibitory effect was observed as compared to the control group. The test group, in fact, did not present any sign of infection, whereas the untreated one manifested the formation of pus. Furthermore, the presence of AgNPs resulted in lower inflammation, probably thanks to the protease inactivation effect of silver, as well as higher collagen deposition and vasculogenesis (Singla *et al.*, 2017). A similar study reported a method for the

formation of AgNPs through reduction of silver nitrate using a fungal extract. The nanoparticles thus produced were then coated with various agents including polyethylene glycol (PEG) 6000, sodium dodecyl sulphate and β-cyclodextrin, to improve their stability and control the size. After this, hydrogels were developed by combination of the particles with swelling agents such as carboxymethyl cellulose (Na-CMC) and hydroxypropylmethyl cellulose (HPMC). Thanks to the higher *in vitro* performance of the PEG/Na-CMC formulation against bacteria and lower release rate of AgNPs, this hydrogel was selected for further *in vivo* characterisation using an MRSA-infected wound model on adult female mice. The study evidenced higher bacterial inhibition for the material as compared to the control (commercial sulfadiazine cream) and untreated groups. Furthermore, enhanced wound closure rate and cosmesis was observed, with good epithelialisation and hair growth (Mekkawy *et al.*, 2017).

A research of 2015 reported the fabrication of an occlusive dressing containing a silver-based trackable complex. An occlusive dressing is an air- and water-tight dressing that prevents the wound from desiccation and protects from trauma. In this work, a fluorescent silver complex was prepared through combination of $AgClO_4$ and dansyl imidazole (ImD) to yield $[Ag(ImD)_2]ClO_4$. The complex was then incorporated within a carboxymethyl cellulose/polyethylene glycol hydrogel and a dressing was obtained by sealing the material between a sterile gauze and an adhesive layer of surgical tape. The aim of the study was to achieve readily trackable release of silver via visualisation of the blue-green fluorescence generated by the compound. Thanks to the straight-forward spectroscopic assessment of the release of silver, in fact, the platform could offer the possibility to easily evaluate the exhaustion time of a dressing. The biological characterisation displayed improved antibacterial efficiency *E. coli* and *S. aureus* as compared to colloidal silver and AgNPs. The release of the complex was then evaluated, showing higher rates for the composition with lower concentration, probably because it reaches a more dynamic state faster, thus facilitating the movement of the ions out of the polymeric network (DeBoer, Chakraborty and Mascharak, 2015).

Along with silver, other metals have been introduced as additives to obtain antibacterial features. Among these, copper has been largely used for this purpose thanks to its bactericidal effect as well as biological properties such as angiogenesis. For instance, copper oxide (CuO) containing biocomposites have been developed in the form of aerogels for chronic wound healing applications. This type of wounds is in fact characterised by impaired angiogenesis that limits the blood supply to the wound. Furthermore, an optimal level of moisture is required in order to promote epithelialisation and collagen deposition. In this context, the combination of copper-containing mesoporous bioglasses (Cu-MBGs) and nanofibrillated cellulose was investigated. MBGs are sol-gel produced glasses with ordered mesoporosity that present higher bioactivity as compared to melt-derived glasses thanks to the increased surface area. These materials demonstrated to trigger vascularisation in wounds thanks to the release of calcium ions from their network. Cu-MBGs was combined with NFC to obtain an aerogel through lyophilisation technique. The composite was then tested *in vitro* with respect to its antibacterial, angiogenic and cytotoxic effect. The assessment towards fibroblasts showed an inversely proportional correlation between the cell viability and the copper content, whereas the opposite was true with the inhibition of *E. coli*. Finally, the aerogel promoted the expression of angiogenic growth factors of fibroblasts, namely vascular endothelial growth factor (VEGF) and fibroblast growth factor (FGF). In light of the results obtained, the authors suggested that an optimal threshold should be determined when using copper for biomedical applications to avoid toxicity due to local accumulation (Wang *et al.*, 2016).

Another class of active agents broadly used to dope polymers is flavonoids, a class of natural substances mostly known for their antibacterial properties. Flavonoids are low molecular weight compounds characterised by a polyphenolic structure consisting of three aromatic rings, more specifically, C_6, C_3 and C_6, where the C_3 presents an oxygen. Several types of flavonoids have been isolated, including flavones, flavonols and chalcones, showing different mechanisms of action depending on their structure (Farhadi *et al.*, 2019). In a

study by Jeong *et al.*, a flavonoid, galangin, was introduced into a modified cellulose matrix through complexation. Galangin is in fact able to inhibit β-lactamase, the enzyme responsible for the antibiotic resistance in MRSA strains. First, cellulose was functionalised with cyclosophoraose (Cys) using epychlorohydrine. After this, galangin was added and stabilised through hydrophobic interaction. Good biocompatibility towards dermal fibroblasts was observed for the hydrogel developed, with results comparable to the positive control. In addition to this, the antibacterial activity assessment showed high levels of inhibition up to 72 hours after incubation, with bacterial reduction of almost 100% against *S. aureus* (Jeong *et al.*, 2016).

An alternative strategy that has been extensively researched to confer antibacterial features to cellulose is its chemical functionalisation. Several groups can be attached to the backbone, including amino groups and sulphur-containing compounds. A study conducted by Dahoua *et al.* reported the grafting copolymerisation of cellulose fluff pulp in order to achieve antibacterial activity and improved swelling capacity. Cellulose fibres present in fact lower absorption ability due to the presence of crystalline regions that restrict the mobility of the polymer chains. In light of this, acrylic acid (AA), a hydrophilic monomer, and acrylonitrile (AN), a hydrophobic monomer, were graft polymerised using ceric ammonium nitrate as the initiator. The copolymer was then cross-linked by replacing various amounts of acrylic acid with ethylene glycol dimethacrylate (EDMA), a bifunctional monomer used as a cross-linking agent for hydrogel formation. In the second part of the research, cellulose was reacted with thiourea to confer antibacterial properties and then grafted with acrylonitrile, obtaining cellulose-thiocarbamate-graft-polyacrylonitrile copolymer. The product was then characterised and tested to assess its activity against *E. coli*, *P. aeruginosa* and *Bacillus subtilis*. Promising results were obtained, especially in the case of *B. subtilis* and *P. aeruginosa* even after washing with hot water, proving that a permanent chemical modification was achieved (Dahou *et al.*, 2010).

Recently, increasing attention has been focused on the functionalisation of microcrystalline cellulose (MCC) to develop antibacterial materials. MCC is

obtained from cellulose by acid hydrolysis in order to partially remove the amorphous regions from the fibres. This treatment results in the production of cellulose with high specific area, thus facilitating its chemical modification with other monomers. In a study of 2015, *N*-halamine compounds were used to confer antibacterial activity to MCC. After grafting of methacrylamide (MAM) onto MCC, the copolymer (MAM-g-MCC) underwent chlorination by treatment with sodium hypochlorite, and the chlorine content over time was checked throughout the storage period. Antibacterial tests were carried out against *S. aureus* and *E. coli*, showing 100% inactivation of both strains within 10 minutes of contact time (Y. Liu *et al.*, 2016). Microcrystalline cellulose was also used as a substrate for amination in order to achieve amino-cellulose based nanofibres with antimicrobial features. The modified cellulose was produced via nucleophilic displacement reaction starting from cellulose-*p*-toluenesulphonic acid ester (tosylate) to obtain 6-deoxy-6-trisaminoethyl-amino (TEAE) cellulose. The product was then subjected to electrospinning to form nanofibres in order to yield a material with high surface area. Finally, polyvinyl alcohol (PVA) was added as a stable fibre-forming additive to assist the process. The antibacterial assays performed against *S. aureus* and *K. pneumoniae* showed a significant inhibition of the growth for both bacteria (Roemhild *et al.*, 2013).

Bacterial cellulose has also been extensively used as an alternative to plant-derived cellulose for the development of antibacterial dressings. Once again, the use of active metals has been widely explored thanks to their high efficiency. In the research of Gupta *et al*. silver zeolites (AgZ) were used as silver(I) sources. Silver ions can in fact be leached out of the anionic cavities of AgZ upon cationic exchange. AgZ impregnated cellulose (BC-AgZ) was prepared by incorporation of zeolites into the pellicles together with BC-$AgNO_3$, which was obtained using silver nitrate as the ion source. It was observed that a higher amount of silver was transferred to the surrounding environment in the case of BC-AgZ. Furthermore, as expected, the sample yielded constant silver release up to 96 hours, whereas a plateau was reached for $AgNO_3$ after 3 days. The results obtained were reflected by the antibacterial assay carried out on Gram negative and Gram positive

strains, where improved long-term efficiency was detected for the zeolite-containing specimen even after 96 hours of incubation (Gupta *et al.*, 2016).

Other therapeutic metal ions have been used along with silver to develop antibacterial cellulose-based substrates for wound healing. Among these, a very common one is zinc and its oxidised form, zinc oxide. In this respect, one example is the work of Khalif *et al*. on the production of a dressing based on BC and ZnO nanoparticles (ZnO-NPs) for burn wounds treatment. The material was prepared through impregnation of the polymer matrix with ZnO-NPs previously obtained by treatment of zinc nitrate with NaOH. The composite was then tested with respect to its antibacterial properties against the most common bacterial strains found in burn wounds (e.g. *S. aureus* and *P. aeruginosa*). Furthermore, an *in vivo* study was carried out on BALB^{c} type mice to evaluate the performance on burn wounds and compare it to a positive control consisting of BC and silver sulphadiazine ointment. The histological analysis evidenced good tissue regeneration comparable to the positive control and good healing rate, whereas formation of necrotic tissue and ulceration were detected in the untreated group (Khalid *et al.*, 2017). A different approach was also reported involving the use of solution plasma process (SPP) to achieve *in situ* formation of ZnO from zinc ions. Zinc sources (namely, nitrate and acetate) were incorporated into the BC network and reduced using SPP via formation of reducing radical oxygen species such as hydroxyl radical and hydroperoxyl radical, but also anionic ones like oxygen anion, super oxide anion and electrons. As expected, the antibacterial activity estimation against *S. aureus* and *E. coli* demonstrated increasing effect for higher concentration of zinc in a proportional manner (Janpetch, Saito and Rujiravanit, 2016). Along with simple immersion of the membranes in a zinc solution, other methods have been reported for the incorporation of the ions. One example is ultrasound irradiation, which has proved to result in good incorporation efficiency, as confirmed by the antibacterial assays carried out on the composite using *S. aureus* and *E. coli* (Shahmohammadi Jebel and Almasi, 2016).

Another important group of active agents is represented by natural antibacterial compounds. In the study by Siddhan *et al*., two different herbal extracts, namely

bitter gourd and tridax daisy, were utilised for impregnation of both BC and plant-derived cellulose. Interestingly, the antibacterial study evidenced that both materials were active, however, BC exerted greater biocidal activity against *S. aureus* and *E. coli* as compared to vegetal cellulose. This result was explained by the authors as related to its porous nanostructure, which can ensure higher liquid absorption and, therefore, higher incorporation efficiency (Siddhan, Sakthivel and Basavaraj, 2016).

Although less explored, chemical modification of bacterial cellulose to achieve antibacterial properties was also investigated as an alternative strategy for the development of inherently active wound dressings. In the study conducted by Fernandes *et al.*, grafting of aminoalkyl groups onto the surface of the nanofibrillar network was performed to obtain grafted BC membranes. To achieve this, the nanofibrils were treated with a solution of 3-aminopropyltrimethoxysilane (APS) to form Si-O-C bonds with the hydroxyl groups of cellulose. The mechanism of such modification involved the hydrolysis of the silane derivative to give the corresponding silanol and the adsorption onto BC through hydrogen bonding. This was then followed by generation of Si-O-Si bridges (from self-condensation of silanols) and Si-O-cellulose bridges (through reaction with the hydroxyl groups of cellulose). The effect of the introduction of the amino groups was evaluated by testing the dehydrated modified membranes against *S. aureus* and *E. coli*, showing efficient growth inhibition after 24 hours. The antibacterial effect was ascribed to a combination of the amino groups as well as to the presence of hydrophobic chains, which might play a role in the interaction with the membrane of the bacteria. Furthermore, the *in vitro* assays performed using human adipose-derived mesenchymal stem cells proved that modified cellulose membranes possessed no cytotoxicity, confirming their potential use for biomedical applications (Fernandes *et al.*, 2013).

In this study, various strategies for the chemical/physical modification of bacterial cellulose to develop inherently active wound dressings have been explored. As previously explained in section 1.1.9, this approach can in fact allow to overcome the limitations related to the incorporation of leachable antibacterial

agents, i.e. volatility and stability of the compound (especially in the case of low molecular weight molecules) and exhaustion upon complete release from the matrix. In addition to this, in this work BC was kept hydrated both during the functionalization and after, and all the biological studies were carried out on wet pellicles as the material was intended to be used as a hydrogel to be applied on dry wounds. Finally, novel reactions were investigated for the covalent attachment of antibacterial functional groups, both in aqueous and organic solvents, and the results in terms of biological performance were compared and discussed.

1.2.4 Chitosan-based hydrogels

Chitosan is a semi-crystalline polysaccharide produced through deacetylation treatment of chitin in the presence of sodium hydroxide. Chitin is the second most abundant polymer after cellulose, and can be found in nature as a structural component of the exoskeleton of crustaceans and of the cell wall of fungi. Thanks to the great degree of biocompatibility and biodegradability of chitosan as well as its innate bactericidal nature, this polymer is one of the most commonly used in the biomedical field, for instance to develop artificial skin, wound dressings, ophthalmologic devices (i.e. contact lenses) and drug delivery systems. As a general assumption, the distinction between chitin and chitosan is based on the degree of deacetylation of *N*-acetyl-glucosamine to yield *N*-glucosamine units. The chitosan structure consists of β(1→4) linked *N*-acetyl-glucosamine and glucosamine units, with a minimum degree of deacetylation (DD) of circa 50-60% (Domard and Domard, 2002). This semi-crystalline polymer is insoluble in common organic solvents and aqueous solutions above pH = 7. The presence of free amino groups results in increased solubility in aqueous solutions with respect to chitin, as these moieties undergo protonation at pH < 6.5 (Yang *et al.*, 2015). Despite this, the poor solubility of chitosan still poses a challenge to its processing. Various studies have been carried out to improve its solubility in aqueous solutions, for instance by grafting of polyethylene glycol chains onto chitosan. The results indicated improved solubility and lower susceptibility to

pH variation for higher amount of PEG (Bhattarai, Matsen and Zhang, 2005; Jeong *et al.*, 2008). The amino groups are also responsible for the intrinsic antimicrobial properties of chitosan against a wide range of bacterial strains and fungi. In addition to this, the polysaccharide can be easily functionalised thanks to these reactive groups, turning chitosan into an attractive candidate for the development of antibacterial biomaterials with tailorable properties (Ravi Kumar, 2000; Khor and Lim, 2003; Di Martino, Sittinger and Risbud, 2005).

The mode of action of the bactericidal effect of chitosan has been deeply investigated. It is widely acknowledged that the inhibitory action relies on various processes such as chelation of the metal ions in the bacterial cell wall and interaction with intracellular DNA. The principal mechanism explaining the disruption of the bacterial cell wall followed by release of the intracellular components is thought to be related to the electrostatic interactions between the positive C_2-linked amino groups and the negatively charged constituents of the external bacterial membrane (**Figure 1.12**) (Rabea *et al.*, 2003; Raafat *et al.*, 2008; Kong *et al.*, 2010). This hypothesis has been confirmed by several studies focused on investigating the effect of various parameters on the antibacterial activity. First, the DD of chitosan was evaluated with respect to its biological effect. Higher degree of deacetylation (and, therefore, higher number of free amino groups) caused, as expected, an increase in the antimicrobial efficiency against the strains tested, i.e. *Staphylococcus aureus* and *Escherichia coli* (Li, Wu and Zhao, 2016). Together with the degree of deacetylation, the influence of the molecular weight on the antibacterial activity has also been studied. Several works showed a higher effect of low-molecular weight chitosan against Gram negative strains, probably thanks to the facilitated penetration of the polymer through the membrane. On the other hand, Gram positive strains were found to be more susceptible to high-molecular weight chitosan, probably as a result of the formation of a film that prevents the cellular nutrient intake (No *et al.*, 2002; Zheng and Zhu, 2013). Finally, the correlation between the total exposed surface area and the antibacterial properties of the polymer have been researched. It has been observed that chitosan nanoparticles cause superior inhibition compared to

bulk chitosan and chitosan microparticles, probably because of the increased surface area (Qi *et al.*, 2004; Mohammadi, Hashemi and Masoud Hosseini, 2016). In this sense, one example is the work proposed by Bedel *at al*. on the development of a chitosan/poly(ethylene glycol) diacrylate (CS/PEGM) hydrogel in the presence of porogens such as $NaHCO_3$ or PEG. It was observed that hydrogels with higher degree of interconnection between the pores were more efficient in inhibiting bacterial growth as compared to hydrogels with smaller surface area (Bedel *et al.*, 2015). This finding was in line with previous results, as it indicated the main mechanism of antibacterial activity of chitosan to be a surface-related phenomenon.

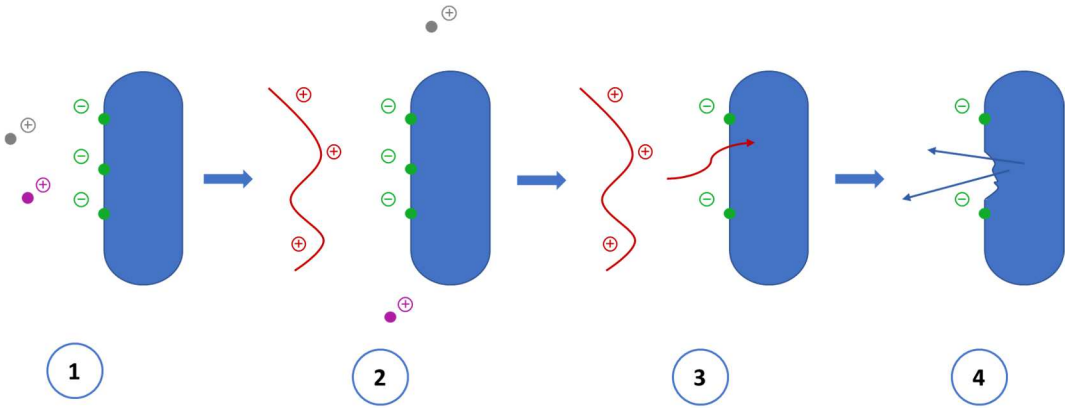

Figure 1.12 Mechanism of action of antibacterial activity of chitosan:

1. Normal bacterial cell with negatively charged compounds in the bacterial membrane (i.e. teichoic acids and phosphate groups) stabilised by calcium and magnesium ions;

2. Displacement of the cationic species upon competition with positively charged chitosan for the anionic sites of the cell wall;

3. Disruption of the membrane/penetration of the chitosan chains through the cell;

4. Release of intracellular components and cell death.

In the context of wound healing, chitosan represents one of the most widely used polymers for the development of dressings of different types thanks to its biological properties such as biocompatibility, biodegradability, hydrophilicity and innate bactericidal nature (Jayakumar *et al.*, 2011). However, the main limitation to the use of plain chitosan as an antibacterial material is related to the low activity at basic pH, when the amino groups are not protonated and, therefore, not active.

In light of this, various studies have been directed towards the enhancement of the antibacterial properties of chitosan at basic pH. In most cases, the incorporation of active agents has been proposed as a valid strategy to ensure activity despite the pH variation. In this context, several reports can be found in literature involving the use of metal ions such as silver, copper and zinc as leachable compounds. Among these, silver is the most common therapeutic ion in the biomedical field. For instance, chitosan-based hydrogels have been fabricated incorporating silver nanoparticles. The hydrogel was obtained through combination of chitosan and acetic acid using silver nitrate as the ion source. Micro- and nano-hydrogels were then produced by using a concentration of chitosan lower than the critical value (Kozicki *et al.*, 2016). In a different work, the formation of polyelectrolyte complexes was achieved through combination of positively charged chitosan with anionic xanthan gum (containing COO^- groups). Ag^+ ions were first stabilised by the hydroxyl and carboxyl groups of xanthan and consequently added to the system. AgNPs were then formed by nucleation of the silver ions, as observed through SEM imaging. Finally, the dressing was biologically tested with respect to its antibacterial and cytotoxic properties. The results showed strong inhibitory capacity against Gram negative and Gram positive strains without causing any adverse effect on the viability of fibroblasts, making the material suitable for application on wounds and burnt skin (Rao *et al.*, 2016).

Apart from silver, numerous works proposed the use of zinc (and zinc oxide) as a valid alternative. In the article by Wahid *et al.*, nanocomposite hydrogels were developed using carboxymethyl chitosan (CMCh). CMCh was cross-linked in the presence of epichlorohydrin, whereas ZnO was subsequently obtained through incorporation of zinc nitrate followed by alkaline treatment of zinc ions with NaOH. The material demonstrated increasing bactericidal effect against *E. coli* and *S. aureus* in a directly proportional trend to zinc concentration, with poor results observed for the hydrogel without Zn, probably due to the cross-linking process that decreases the amount of free amino groups (Wahid *et al.*, 2016). In a similar study, chitosan cross-linking was achieved using methyl trimethoxy

silane as the cross-linker and zinc hydroxide as the ion source. The antiproliferative assessment revealed good efficiency against Gram positive and Gram negative bacteria as well as antifungal activity for up to two weeks after incubation (Shafiq *et al.*, 2014).

A different strategy was proposed by Wang *et al.*, which involved the use of honey as a natural additive to improve the antibacterial effect of chitosan. In addition to this, gelatine was incorporated in the structure to absorb the excess of exudates. The hydrogel sheets developed were then tested *in vivo* on Kunming mice and New Zealand rabbits using a burn wound model and their performance was compared to the behaviour of a commercial ointment. After 8 days, higher degree of wound contraction (i.e. approximation of the wound edges) was observed for the test group as compared to the untreated and the control, with faster healing rate. Furthermore, no signs of infection were detected, whereas bacterial contamination occurred in the untreated group (Wang *et al.*, 2012).

Along with loading of leachable agents, chemical modification of chitosan structure has been extensively explored to enhance its antibacterial properties. In the work reported by Dragostin *et al.*, the functionalisation of chitosan with different derivatives of sulphonamides was investigated. These compounds are widely used in the biomedical field thanks to their biological properties such as antifungal, antimalarial and, mainly, antibacterial activity. Sulphonamides, in fact, are able to exert a bacteriostatic effect by inhibiting the growth of bacteria. The most common sulphonamides are *p*-aminobenzenesulphonamides. This class of compounds has proved to inhibit bacterial growth through competition with *p*-aminobenzoic acid, which is required for the biosynthesis of folic acid in bacteria (Gomes and Gomes, 2005). In this study, several sulphonamides were reacted with chloroacetyl chloride to yield the corresponding *N*-chloroacetyl sulphonamides. After this, chitosan derivatives were obtained through substitution of the amino groups, as confirmed by the presence of amide peaks in the NMR. The positive free amino groups of the polymer were then cross-linked with negatively charged sodium tripolyphosphate (TPP) to improve chemical stability of the final product, especially in an acidic environment. The

materials were tested with respect to their biological properties, showing that the presence of sulphonamide moieties improved the antibacterial properties of chitosan against both Gram positive and Gram negative strains. Moreover, *in vivo* assessment on male Wistar rats of one of the derivatives (i.e. chitosan-sulphadiazine) demonstrated improved healing as compared to the control group treated with plain chitosan (Dragostin *et al.*, 2016).

Quaternisation of chitosan via formation of quaternary ammonium groups has also been performed to improve the antibacterial properties of chitosan in non-acidic pH. One example of such an approach was described by Zhou *et al.*, where the functionalisation of the polymer was achieved through ring-opening reaction with 2,3-epoxypropyl trimethyl ammonium chloride. The biological performance of the quaternised chitosan fibres (QCF) produced was then evaluated and compared to pristine chitosan. It was observed that quaternised derivatives presented higher antibacterial activity against *S. aureus*, broader spectrum of activity and higher killing rate. Moreover, functionalised fibres presented high liquid absorbance capacity, hence allowing the formation of cohesive gels after absorption of exudates that could trap bacteria (Zhou *et al.*, 2012). Quaternary ammonium groups containing chitosan was also produced in order to develop an antibacterial hydrogel by γ-irradiation. Various radiation conditions were tested, and their effect on parameters such as gel content, swelling ability and water evaporation rate was investigated. Since this approach could result in the degradation of the chitosan chains, two biocompatible polymers, namely polyvinyl alcohol (PVA) and polyethylene oxide (PEO), were incorporated in the matrix to improve the stability and mechanical strength of the material. The antibacterial activity of the hydrogel was then assessed, showing excellent inhibitory effect against *S. aureus* and *E. coli* (Fan *et al.*, 2015).

Aims and objectives

This research project was aimed at developing inherently active antibacterial hydrogels, i.e. hydrogels presenting antibacterial activity upon structural modification, as opposed to the incorporation of leachable agents. The materials are intended to be used as primary dressings on various types of chronic wounds, from dry to moderately exuding, depending on the hydrating/absorbing ability of the substrates as well as the pre-treatment they are subjected to.

The incorporation of antibacterial features was accomplished via chemical functionalisation of bacterial cellulose as well as through a composite fabrication approach. In particular, the following objectives were set and achieved:

1. *Production and purification of bacterial cellulose*

First, the fermentation of *Gluconacetobacter xylinus* in static conditions to produce bacterial cellulose (BC) was studied over time. The purification process was then carried out by optimisation of previously published protocols for the medical use of BC to ensure complete removal of the residual biomass through high-temperature alkaline treatment. The chemical structure of the polymer was confirmed using solid-state techniques such as Fourier-Transform Infrared (FT-IR) and Energy Dispersive X-ray (EDX) spectroscopy. The viscoelastic properties of the hydrogel were studied through rheological measurements to evaluate the stiffness under typical skin tissue engineering stress conditions. In addition to this, the hydrating ability of the material was assessed by calculation of the water content, and the weight variation in liquid media was determined to investigate its stability during the utilisation timeframe (i.e. between two dressing changes);

2. *Surface modification of bacterial cellulose in aqueous system*

The pellicles were chemically modified to introduce antibacterial functionalities (namely, quaternary ammonium groups and hydrophobic moieties) in the structure. According to the literature review carried out, this is the first time that the reaction proposed, i.e. ring-opening of two epoxides in basic conditions, was performed on never-dried bacterial cellulose pellicles with the aim to maintain

the hydrogel structure of the substrate. The material was chemically characterised through EDX and X-ray Photoelectron Spectroscopy (XPS), whereas its mechanical properties were assessed through rheological studies. A biological evaluation was then carried out using both prokaryotic and eukaryotic cells in order to investigate the antibacterial activity upon direct contact and the cytotoxicity/wound healing ability towards keratinocytes;

3. *Surface modification of bacterial cellulose in anhydrous system*

Bacterial cellulose was then modified following a novel method consisting in the derivatisation of the hydroxyl groups in anhydrous conditions upon solvent exchange to yield, once again, a material that maintained the initial hydrogel structure. The functionalisation involved two reaction steps, i.e. Schotten-Baumann substitution to introduce double bonds, followed by introduction of a cationic ammonium group and a thioether in the backbone through thiol-ene addition. The structure of the resulting hydrogel was determined through EDX and XPS analysis and rheological assays were performed to study the viscoelastic behaviour. The biological assessment of the hydrogel was carried out through evaluation of the antibacterial activity upon direct contact and direct/indirect cytotoxicity estimation;

4. *Bacterial cellulose/copper-chitosan composite development*

Two natural-polymers based systems, namely functionalised bacterial cellulose and copper(II)-loaded chitosan, were combined for the first time via solvent casting technique to produce two hydrogels with increasing copper content. To achieve this, bacterial cellulose pellicles were subjected to wet mechanical grinding and the fibres obtained were functionalised to introduce antibacterial features and dispersed within a chitosan matrix. Morphological evaluation of the structure was performed through Scanning Electron Microscopy (SEM). The swelling behaviour of the composites was determined as well as their mechanical properties. The antibacterial and cytotoxic effect upon direct and indirect contact were then studied without and with cellulose addition.

Chapter II

Materials and methods

2.1 Materials

2.1.1 Chemicals

All the chemicals used in this study were purchased from Sigma-Aldrich (now Merck kGaA, Darmstadt, Germany), Thermo Fischer Scientific Inc. (Waltham, MA, USA) and VWR International (Radnor, PA, USA). Copper-loaded chitosan was obtained through collaboration with Dr Lukas Gritsch within the framework of HyMedPoly, a Marie Skłodowska-Curie Actions (MSCA) project funded by the Horizon 2020 Research and Innovation Programme.

2.1.2 Bacterial strains

Gram negative *Gluconacetobacter xylinus* JCM10150 was used to produce bacterial cellulose. The strain was obtained from the culture collection of the University of Westminster, London, UK. Antibacterial assays were performed using the strains indicated in the international standard ISO 22916:2007 in order to ensure the reproducibility and comparability of the results obtained. In particular, *Staphylococcus aureus* subsp. aureus Rosenbach 6538™ and *Escherichia coli* (Migula) Castellani and Chalmers ATCC® 8739™ were used, which were purchased from ATCC® (American Type Culture Collection), Manassas, VA, USA.

2.1.3 Cell line

The cytotoxicity studies were performed using *in vitro* spontaneously transformed keratinocytes (HaCaT) from histologically normal skin (Catalog #: T0020001) as a preliminary assessment of the biocompatibility of the materials developed towards the most external layer of the epidermis. The cells were bought from AddexBio, San Diego, CA, USA.

2.2 Experimental methods

2.2.1 Gluconacetobacter xylinus fermentation

Bacterial cellulose (BC) was produced by *Gluconacetobacter xylinus* using a modified Hestrin and Schramm medium with glucose as the main carbon source. The production medium composition consisted of glucose (50 g/L), yeast extract (5 g/L) and $CaCO_3$ (12 g/L). The final pH was adjusted to 5.5 using HCl 1 M and NaOH 1 M. The glucose was sterilised in autoclave at 110 °C for 10 minutes in order to avoid thermal degradation of the sugar, while all the other components and the glassware were sterilised in autoclave at 121 °C for 20 minutes. Pre-inoculation was carried out by inoculation of 10 mL of production medium into 20 mL glass vials using frozen bacterial glycerol stocks. The stocks were prepared by freezing 500 µL of 40% v/v glycerol solution in water and 500 µL of bacterial culture. As *Gluconacetobacter xylinus* is an aerobic bacterium, the vials were kept slightly open in order to ensure sufficient flow of oxygen throughout the fermentation period. The vials were incubated at 30 °C in static conditions. When the cellulose pellicles had formed at the interface between the liquid culture and the air, 3 mL of inoculum were transferred into 500 mL Erlenmeyer flasks containing 300 mL of production medium. Static fermentation was then carried out at 30 °C for 5-7 days, until a thickness of 1-1.5 cm was achieved. The cellulose pellicles were then harvested and washed several times under distilled water.

2.2.2 Temporal profiling of the biosynthesis

A temporal profiling of the *Gluconacetobacter xylinus* fermentation was carried out in order to monitor the growth of bacteria and the polymer production. The optical density at 600 nm 1 mL of culture collected at regular intervals for 72 hours was measured using a Single Beam Spectrophotometer, SB038, Cadex Inc. For the pH measurement, 1 mL of culture was collected and centrifuged at 13,870 x g for 10 minutes (Heraeus Pico 17 Centrifuge, Thermo Fisher Scientific, MA, US). The supernatant was then transferred to a test tube and the pH was measured using a Seven Compact pH meter (Mettler Toledo Ltd., Leicester). Finally, the growth of the pellicles was visually evaluated. Two different methods

were used in order to compare the impact of external interference on the growth of cellulose. For method A, the samples were directly taken from the growth medium using a 1 mL pipette. For method B, the medium was collected using a 5 mL syringe and a syringe filter (diameter: 17 mm, pore size: 0.2 µm) to suction the liquid through a flexible pipe previously fixed in the flask. In both cases the profiling was performed in triplicate. Three flasks were also incubated and used as a control (no sample was taken) to compare the cellulose growth trend.

2.2.3 Bacterial cellulose purification

The pellicles produced were subjected to purification treatment to remove the residual biomass. In order to achieve medical grade purity, different methods were investigated. Method A involved washing of cellulose with NaOH 0.1 M at 80 °C for 80 minutes under continuous agitation. This procedure was repeated three times, followed by wash with distilled water until neutral pH was obtained on a pH indicator strip CF 0-14. For method B, the cellulose pellicles were subjected to treatment with 3% NaOH (= 0.75 M) for 12 hours under stirred conditions at room temperature, followed by wash with distilled water until neutral pH was reached. The process was repeated four times. The samples were then incubated with 3% HCl (= 0.82 M) for four hours and washed with distilled water until no acidic traces were detected by pH measurement. After this, a sterilisation in autoclave at 110 °C for 10 minutes was carried out. Finally, method C consisted in treating the pellicles first with NaOH 1 M for two hours at 80 °C and then washing with distilled water until reaching a neutral pH of the medium. The treatment was reiterated before subjecting the membranes to sterilisation in autoclave at 110 °C for 10 minutes. A colony forming assay was carried out in order to evaluate the presence of any residual *Gluconacetobacter xylinus* cell. Three 1 cm^2 samples were cut from non-treated cellulose as well as from each of the treated pellicles. The samples were incubated with 10 mL of production medium (prepared as described in section 2.2.1) for 1.5 hours under continuous agitation at 30 °C. After this time, the liquid was collected and diluted with fresh medium to obtain a final dilution of 1:100, 1:10,000 and 1:1,000,000. 100 µL from each

dilution (in triplicate) were then spread over a nutrient agar plate using an L-shaped spreader and incubated at 30 °C for 48 hours in static conditions. The presence of the colonies was visually evaluated.

2.2.4 Chemical functionalisation in wet conditions

The surface of the purified bacterial cellulose membranes was functionalised in order to introduce antibacterial groups. To achieve this, two different types of epoxides containing quaternary ammonium groups and hydrophobic tails were used. The modification was performed through a one-step reaction in water. The pellicles were placed in a round-bottom flask filled with distilled water and NaOH as the catalyst at a concentration of 5% w/w with respect to the weight of cellulose (dry). After 15 minutes of pre-treatment of the samples with the base at room temperature under stirred conditions, glycidyl trimethylammonium chloride (GTMAC; MW = 151.63 g/mol; ρ = 1.13 g/mL) and glycidyl hexadecyl ether (GHDE; MW = 298.50 g/mol) were added. The stoichiometric ratio of both reagents was calculated considering the number of hydroxyl groups per monomer unit of glucose (MW of glucose = 180.56 g/mol; number of hydroxyl groups per unit = 3). The epoxides were then introduced with a ratio of 3:1 of GTMAC with respect to GHDE. The reaction was carried out at 65 °C in a water bath for 4 hours under continuous stirring conditions. After this time, the samples were washed with distilled water until neutral pH was obtained with a pH indicator.

2.2.5 Chemical functionalisation in dry conditions

Cellulose modification was also conducted in anhydrous conditions in order to minimise secondary reactions due to the effect of the water on the reagents, i.e. base-catalysed hydrolysis of the epoxides. Cellulose pellicles were dehydrated by progressive solvent exchange using anhydrous tetrahydrofuran (THF). The wash with THF was repeated six times for one day under continuous stirring conditions. The modification was then performed in two steps. First, the surface hydroxyl groups were functionalised using acryloyl chloride (MW = 90.506

g/mol; ρ = 1.136 g/mL) in the presence of triethylamine (TEA; MW = 101.19 g/mol; ρ = 0.726 g/mL). Both reagents were added in excess to the stoichiometric ratio with respect to the hydroxyl groups. The reaction was carried out in THF at 0 °C in ice-water bath under inert atmosphere using a flow of Argon for 3 hours in continuous stirring conditions. The hydrochloride salt of triethylamine (triethylammonium chloride) produced was removed at the end of the reaction by washing the pellicles several times with distilled water. The second step consisted of a thiol-ene Michael-type addition between the acrylate groups introduced in the first step and the thiol groups of cysteamine hydrochloride (2-mercaptoethylamine hydrochloride; MW = 113.61 g/mol) using 4-(dimethylamino) pyridine (DMAP; MW = 122.17 g/mol; ρ = 1.01 g/mL) as the catalyst. Both reagents were added in stoichiometric ratio with respect to the hydroxyl groups of the glucose unit. The reaction was carried out in water at room temperature in continuous stirring conditions for 4 hours. Finally, the pellicles were collected and washed for several hours with distilled water until neutral pH was reached with a pH indicator.

2.2.6 Grinding of bacterial cellulose

A composite based on modified bacterial cellulose and copper-loaded chitosan was also developed. In order to obtain a dispersion to be used for physical blending with chitosan, bacterial cellulose pellicles were mechanically ground. First, the samples were roughly chopped using a stationary electric blender. After this, the cellulose bits were collected and transferred to a plastic beaker, immersed in water and finely ground using an immersion blender. The homogeneous suspension was then centrifuged at 4,335 x g (Heraeus Multifuge X1 Centrifuge, Thermo Fisher Scientific, MA, US) for 20 minutes to collect the fibres.

2.2.7 Chemical functionalisation of ground bacterial cellulose

The ground cellulose was chemically modified to introduce antibacterial functionalities. The fibres were first transferred to a round-bottom flask and

dispersed in water by magnetic agitation. The reaction was carried out following the procedure described in 2.2.5. After this, the fibres were collected by centrifugation at 4,335 x g for 20 minutes and washed several times until neutral pH was measured with a pH indicator.

2.2.8 Copper-loaded chitosan preparation

Copper-loaded chitosan was obtained through collaboration with Dr Lukas Gritsch within the framework of the HyMedPoly project. The material was prepared following a previously published protocol using medium molecular weight chitosan with a degree of deacetylation (DD) between 75-85% and molecular weight of ~190-310 kDa (product number: 448877, Sigma-Aldrich) (Gritsch *et al.*, 2018). Anhydrous $CuCl_2$ (MW = 134.45 g/mol; purity 99%) was used for the modification of the polymer. The preparation of the copper(II)-chitosan complex (CuChi) was carried out through *in situ* precipitation method. Chitosan was first dissolved in 3% v/v acetic acid at 40 °C to obtain a final concentration of 2% w/v. After this, $CuCl_2$ was added to the solution and kept under stirred conditions for one hour. Various amounts of $CuCl_2$ were introduced to obtain complexes with increasing copper content. Two copper(II)-chitosan formulations were used in this study: copper(II)-chitosan 3 (CuChi3) and copper(II)-chitosan 12 (CuChi12), where 3 and 12 are the percent ratios between the Cu(II) ions and the free amino groups of chitosan (i.e. non acetylated). In particular, for CuChi3 the weight of copper is 1% with respect to chitosan, while in CuChi12 there is a 4% w/w concentration of copper. The calculation of the $CuCl_2$ required was made considering only the primary amines as the coordination sites. The complexes were precipitated by alkaline treatment using a 0.5 M NaOH solution and the hydrated spheres were washed with distilled water until neutral pH was reached. The pellets were then dried in oven at 37 °C for 24 hours and subjected to dry milling treatment to obtain a fine powder. The process was carried out using a planetary micro mill Pulverisette 7 premium line equipped with ZrO_2 beads (Fritsch GmbH, Germany) by

performing 5 cycles of 5 minutes each at 700 rpm. Finally, the powder was manually sieved using a mesh size of 150 μm.

2.2.9 Bacterial cellulose/copper-chitosan composites production

The bacterial cellulose/copper-chitosan composites were produced by solvent casting technique. 4 g of each CuChi formulation were dissolved in 2% v/v acetic acid solution to obtain a final concentration of 4% w/v of chitosan. The complexes were kept at 50 °C in a water bath under vigorous stirred conditions overnight to completely dissolve the polymer. The films containing ground bacterial cellulose were prepared using the same method. 10% w/w of bacterial cellulose (= 0.4 g, corresponding to 1.2 g of hydrated cellulose) previously functionalised in water was added to the solution of CuChi3 and CuChi12 to obtain, respectively, CuChi3/BC and CuChi12/BC. The mixture was further stirred and vortexed for several minutes. Chitosan without copper was also produced using the same method and used as a control. Before being poured into a 60 mm petri dish, the solutions were subjected to ultrasonic degassing treatment for 10 minutes using Ultrawave U50 bath (Cardiff, UK) to eliminate all the bubbles. The films were dried in incubator at 30 °C for two days and then treated with NaOH 0.1 M twice to remove the residual acetates. Finally, a wash with distilled water was carried out followed by drying at 37 °C for two days. To avoid wrinkling during the dehydration, a weight of about 500 g was placed uniformly on top of each film. The samples were cut using a 6 mm stainless steel hole puncher.

2.3 Morphological analysis

The morphology of the pellicles before and after chemical modification was evaluated using a JOEL 5610LV scanning electron microscope (SEM). The same equipment was used for the analysis of the chitosan-based composites (with and without cellulose). The samples were placed on 8 mm diameter aluminium stubs and gold-coated for 2 min using a gold sputtering device (EMITECH-K550). Operating pressure of $7x10^{-2}$ bar and deposition current of 20 mA for 2 min were

used. The analysis was carried out at the Eastman Dental Institute, Department of Biomaterials and Tissue Engineering, University College London, UK.

The structure of ground bacterial cellulose was also studied by SEM analysis to evaluate the structure of the fibrils after physical grinding. The analysis was performed at the University of Erlangen-Nürnberg Friedrich-Alexander, Department of Materials Science and Engineering, Erlangen, Germany. The samples were first gold-coated using a Q150T S coating system (Quorum Technologies, United Kingdom). A LEO 435 VP scanning electron microscope was then used for the imaging (LEO Electron Microscopy Ltd., Cambridge, UK and Ultra Plus, Zeiss, Jena, Germany).

2.4 Chemical characterisation

2.4.1 Fourier Transform Infrared Spectroscopy

The chemical structure of the bacterial cellulose pellicles and the chitosan-based films was studied by attenuated total reflectance Fourier transform infrared (ATR-FTIR) spectroscopy using a Spectrum Two Spectrometer (PerkinElmer, Massachusetts, USA). The analysis was performed in the spectral range of 4000 to 400 cm^{-1}; window material: CsI, 10 scans and resolution of 4 cm^{-1}. Prior to the analysis, the samples were dehydrated for 24-48 hours (depending on the thickness) under a fume hood.

2.4.2 Energy-Dispersive X-ray Spectroscopy

Energy dispersive X-ray (EDX) spectroscopy was used to perform a qualitative elemental analysis of the materials developed. The analysis was carried out both on the cellulose pellicles before and after each type of modification as well as on the copper(II)-chitosan based composites. The cellulose samples were first subjected to water evaporation for 24-48 hours under a fume-hood (depending on the thickness). The preparation of the samples was then carried out following the procedure described in section 2.3. The study was performed in parallel to the SEM analysis using the same equipment described in section 2.3 for the study of the cellulose pellicles and the chitosan composites.

2.4.3 X-ray Photoelectron Spectroscopy

X-ray photoelectron spectroscopy (XPS) was also conducted in order to quantify the degree of functionalisation. Samples of non-modified cellulose as well as samples of cellulose modified in wet conditions were analysed at the School of Chemistry, Cardiff University, UK using a Thermo Escalab 220iXL system. The analysis was performed using an Al K-alpha monochromated X-ray source and data was elaborated using CASAXPS (Casa Software Ltd, Teignmouth, UK). For all the samples, both survey and high-resolution spectra were recorded. For the cellulose functionalised in dry conditions, the measurements were carried out at the Nano Imaging and Material Analysis Centre at the University College Dublin using an Axis Ultra^{DLD} (Kratos Ltd., UK), equipped with Al Kα (1486.7 eV) X-ray source. All sample films were outgassed before analysis for 12 h under ultra-high vacuum. In both cases, since the XPS facilities were not always readily available as they belonged to different departments or universities with respect to the ones where this work was carried out, it is important to consider the timeframe between the reactions and the analyses, as it could have had an effect on the data obtained due to eventual alteration of the chemical structure upon a storage period.

2.5 Physical characterisation

2.5.1 Evaluation of the water content of bacterial cellulose

The water content of the pellicles produced was determined by evaluation of the weight before and after drying under a fume-hood for 24 hours. 9 samples of 1 cm^2 from three different pellicles were used in order to have a statistically valid sample. The percentage of water was calculated using the formula:

$$Water\ \% = \frac{A - B}{A} x\ 100$$

A = Weight of the sample wet

B = Weight of the sample dry

2.5.2 Rheological measurements

The rheological properties of the cellulose pellicles were evaluated using a Discovery HR-2 Rheometer (TA Instruments). The analysis was performed on non-modified cellulose, cellulose after sterilisation treatment and cellulose after modification in aqueous and anhydrous conditions. Three 1 cm^2 samples were cut from each type of cellulose and tested in wet form. A parallel plate geometry (diameter: 8 mm) was used for all the measurements and the gap was set at 3.85 mm for all the samples. First, the linear viscoelastic region (LVR) was determined by an oscillation sweep test using a stress of increasing amplitude (0.01-100 Pa) and a constant frequency of 1.0 Hz. All the other tests were performed using a stress within the LVR. Variations of storage modulus and loss modulus of each sample were evaluated through frequency sweep analysis. The test was carried out using a stress of 6 Pa, a temperature of 32 °C and a frequency ranging between 0.1 and 50 Hz. The variations of storage modulus and loss modulus with the temperature were also estimated by temperature ramp assay. This was performed using a stress of 6 Pa and a frequency of 1 Hz. The temperature range considered was 10-60 °C, with a rate of 5 °C/min.

2.5.3 Static contact angle measurements

A static contact angle study was carried out to evaluate the wettability of the copper(II)-chitosan based composites with and without the incorporation of bacterial cellulose. The analysis was conducted by sessile drop method at room temperature using an Attension® Theta contact angle meter by Biolin Scientific AB (Gothenburg, Sweden). A droplet (< 50 µL) of distilled water was deposited using a manual micro-syringe on the surface of a flat sample previously cut from each film. The contact angle (both left and right side) was optically measured from the shape of the meniscus using a digital camera. The images were acquired from the moment of contact of the drop with the sample for 10 seconds with a frame interval of 0.07 frames/s (142 frames per sample). The images were analysed using OneAttension software to calculate the average contact angle.

2.5.4 Tensile Testing

Tensile testing of the copper(II)-chitosan films with and without bacterial cellulose was performed in order to evaluate the mechanical properties of the composites developed. The test was carried out using a 5942 Single Column Testing System (Instron®, Norwood, MA, US) equipped with a 500 N load cell. The specimens were subjected to increasing load until failure by applying a deformation rate of 2 mm/min. The assay was carried out at room temperature using a gauge length of 25.5 mm. The films were cut into strips of 4.5-6 mm (width) × 35 mm (length) and thickness of about 0.15-0.30 mm. Prior to the test, the thickness and the width of each specimen in different areas was measured using a stainless steel digital caliper and taken into account for the determination of the cross-sectional area. The data were acquired and analysed using a BlueHill 3 software. Young's modulus (E), Ultimate tensile strength (σ_u) and Elongation at break (ε_u) were calculated for each sample in quadruplicate.

2.6 Stability studies

2.6.1 Stability of bacterial cellulose in aqueous media

The stability of the cellulose pellicles in liquid media before and after the modification was studied over a period of 7 days (i.e. maximum average period between two consecutive dressing changes). Three samples of 1 cm^2 from each type of cellulose were used for the test (i.e. non-functionalised, functionalised in dry conditions and functionalised in wet conditions). The stability in phosphate buffer solution and keratinocytes growth medium was assessed by comparing the initial hydrated weight to the hydrated weight of each sample after 1 day, 3 days, 5 days and 7 days. The samples were placed in 24-well plates with 2 mL of medium and incubated in static conditions at 32 °C. The percentage weight variation (ΔW) at each time point was calculated using the following formula:

$$\Delta W\% = \frac{W_x}{W_0} x\ 100$$

W_x = Weight of the sample at time x

W_0 = Weight of the sample at time 0

2.6.2 Swelling profile of copper-chitosan based films

The swelling profile in aqueous medium of the copper-chitosan based composites with and without bacterial cellulose was studied. The specimens were cut in triplicate from each type of film, i.e. CuChi3, CuChi12, CuChi3/BC and CuChi12/BC, using a stainless-steel hole puncher with a diameter of 6 mm. The initial dry weight of each sample was measured and used as the reference. The samples were placed in a 24-well plate and immersed in 2 mL of PBS at room temperature under static conditions. After 30 minutes and 1 hour the specimens were collected and the excess of water was removed with tissue paper. The weight was then measured and the percent water uptake (WU%) for each type of film was calculated using the formula below:

$$WU\% = \frac{W_x - W_d}{W_d} x\ 100$$

W_x = Weight of the sample at time x

W_d = Weight of the dry sample

2.6.3 Stability of copper-chitosan based films in aqueous medium

The stability of each composition in aqueous medium was also evaluated over a period of 30 days. The specimens were cut in triplicate from each type of film using a stainless-steel hole puncher with a diameter of 6 mm. The samples were incubated in 2 mL of PBS at 32 °C under static conditions. The initial weight of the samples (hydrated) was measured after removing the water excess with a tissue paper. The same procedure was followed at each time point, i.e. 1 day, 3 days, 6 days, 10 days, 20 days and 30 days. The weight variation at each time compared to the initial weight was calculated as described below:

$$\Delta W\% = \frac{W_x}{W_0} x\ 100$$

W_x = Weight of the sample at time x

W_0 = Weight of the sample at time 0

2.7 Biological characterisation

2.7.1 Antibacterial activity evaluation

2.7.1.1 Bacterial culture methods

The antibacterial activity of all the materials developed was evaluated against *Staphylococcus aureus* subsp. aureus Rosenbach 6538™ and *Escherichia coli* (Migula) Castellani and Chalmers ATCC® 8739™ (from here onwards referred to as, respectively, *S. aureus* and *E. coli*). Selective mannitol agar was used as the solid culture medium for *S. aureus*, while MacConkey agar was used for *E. coli*. The plates were prepared by streaking a loop of inoculum from glycerol stocks. The plates were then incubated overnight at 37 °C in static conditions. A single colony was used to inoculate 150 mL of nutrient broth No. 2 in a 500 mL Erlenmeyer flask. The inoculum was kept in the incubator at 37 °C in shaking conditions (120 rpm) until log phase was reached (approximately 16 hours). The optical density (OD) was then measured at 600 nm. The inoculum for each test was prepared by dilution of the culture from a concentration of 0.5 MacFarland, which corresponds to an OD_{600} = 0.132 and an approximate bacterial cell density of $1.5x10^8$ CFU/mL (= colony forming units/mL). The culture was diluted using nutrient broth diluted 1:500 according to the final concentration required for each assay.

2.7.1.2 SEM analysis

The proliferation of bacteria on the surface of pristine cellulose and cellulose modified in water was also visually evaluated by scanning electron microscopy for qualitative assessment. Three 1 cm^2 samples of each type of cellulose were sterilised by autoclave treatment and placed onto agar plates. 25 µL of *S. aureus* inoculum at 0.5 MacFarland concentration were pipetted directly on the surface of each sample. The pellicles were incubated in static conditions at 37 °C. After 48 hours, the samples were transferred into 6-well plates and covered with a solution of 2% formaldehyde in order to fix the bacterial cells on the substrate and kept at 0-5 °C overnight. On the next day, the samples were dehydrated by solvent exchange technique using ethanol at increasing concentration (50%, 70%,

90% and absolute). The samples were then dried for 24 hours under a fume cupboard. SEM analysis was conducted on each sample in order to evaluate the amount and the morphology of the cells on each sample.

2.7.1.3 Live/dead viability assay

A bacterial live/dead viability assay was performed on unmodified cellulose samples and samples modified in aqueous conditions after incubation for 24 hours with *S. aureus*. Three 2.5 cm^2 samples were sterilised in autoclave and placed onto agar plates. 50 µL of *S. aureus* inoculum at a cell concentration of 2.5-10x10^5 CFU/mL were pipetted directly on the surface of each sample. The plates were then incubated for 24 hours at 37 °C in static conditions. After this time, the bacterial inoculum was recovered from each sample and transferred onto glass slides. The cells were then stained using a LIVE/DEAD™ *Bac*Light™ Bacterial Viability Kit (Catalogue number: L7012). A 1:1 mixture of two different stains was prepared, namely SYTO® 9, a green-fluorescent nucleic acid stain that penetrates all bacteria in a population, both with intact and damaged membranes, and propidium iodide, a red-fluorescent nucleic acid stain that diffuses only through damaged membranes. 3 µL of this mixture were added onto each glass slide, and the viability of the cells was evaluated using a confocal microscope (Leica TCS SP2). The cells were viewed using filter sets with an excitation wavelength in the range of 480-500 nm for SYTO 9 stain and 490-635 nm for propidium iodide.

2.7.1.4 Direct contact test

A quantitative evaluation of the antibacterial activity upon direct contact with all the materials developed was performed following a modified ISO22916 procedure. The test was conducted on cellulose modified both in aqueous and anhydrous environment as well as on the chitosan-based composites using two different strains, i.e. Gram positive *S. aureus* and Gram negative *E. coli*. For the cellulose samples, non-modified BC was used as the control, while for the chitosan/BC ones, polyethylene terephthalate (PET) and pristine chitosan were

utilised. A known number of bacterial cells of *S. aureus* or *E. coli* was then seeded on the surface of each specimen. The assay was carried out as described below:

- *Cellulose modified in aqueous conditions:*

Three 2.5 cm^2 samples of functionalised cellulose as well as six 2.5 cm^2 samples of non-functionalised cellulose were used. Prior to the assay, all the specimens were subjected to sterilisation treatment by autoclave. 100 µL of *S. aureus* or *E. coli* inoculum at a cell concentration of 1.2 x 10^6 CFU/mL were pipetted directly on the surface of each sample.

- *Cellulose modified in anhydrous conditions:*

Three 1 cm^2 samples of functionalised cellulose as well as six 1 cm^2 samples of non-functionalised cellulose were used. Prior to the assay, all the specimens were subjected to sterilisation treatment in autoclave. 25 µL of *S. aureus* or *E. coli* inoculum at a cell concentration of 3 x 10^5 CFU/mL were pipetted directly on the surface of each sample.

- *Copper(II)-chitosan composites:*

Three 0.28 cm^2 disks were used from each type of film, i.e. CuChi3, CuChi12, CuChi3/BC and CuChi12/BC, as well as from a plain chitosan film. Six 0.28 cm^2 PET discs were also cut with a puncher and utilised as the control. All the samples were pre-treated by conditioning in phosphate buffer saline (PBS) solution for 30 minutes and sterilised by UV treatment for 15 minutes on each side. 10 µL of *S. aureus* or *E. coli* inoculum at a cell concentration of 3 x 10^5 CFU/mL were pipetted directly on the surface of each sample.

Three of the control samples as well as three of each type from the modified pellicles and copper(II)/chitosan composites were incubated in static conditions at 37 °C for 24 hours, while the remaining three control samples were washed to evaluate the number of bacterial cells recovered at time 0. Each sample was transferred to a 15 mL Falcon tube or to a 1 mL Eppendorf vial (respectively, the bacterial cellulose samples and the chitosan-based specimens) and washed using sterile PBS. The bacterial cells were detached from the sample surface by vortexing for 3 minutes. Several 10-fold dilutions were then prepared using PBS. 10 µL of each dilution (in triplicate) were plated onto nutrient agar plates using

the drop plate technique. When the drops were completely dry, the plates were placed upside down in the incubator at 37 °C in static conditions for 20 hours. The same method was used for the recovery of bacteria both at time 0 and after 24 hours for both bacterial strains. The number of viable cells was evaluated by colony counting considering the dilution factor and normalised with respect to the sample size. The antibacterial activity (*R*) was calculated using the following formula, according to the ISO22196 standard:

$$R = log(a)\,[unmodified] - log(a)\,[modified]$$

where *a* is the average of the viable bacterial cells recovered after 24 hours expressed as CFU/(mL*cm^2). The result was also calculated as the percentage of the reduction in the number of viable bacterial cells recovered:

$$R\% = \frac{(a)\,[unmodified] - (a)\,[modified]}{(a)\,[unmodified]} * 100$$

2.7.1.5 Indirect antibacterial activity

The indirect antibacterial efficiency of the BC/CuChi composites was studied by evaluation of the activity of the copper released from the samples over time. Three discs with a diameter of 6 mm were cut in triplicate from each type of composite, i.e. CuChi3, CuChi12, CuChi3/BC and CuChi12/BC using a hole puncher and incubated in nutrient broth No. 2 at 37 °C for 9 hours. Prior to the test, the samples were pre-conditioned in PBS for 30 minutes and sterilised by UV treatment for 15 minutes on each side. The specimens were placed in a 24-well plate with 1 mL of nutrient broth. The medium was collected after 30 minutes, 2 hours, 3 hours, 6 hours and 9 hours and replaced with fresh nutrient broth. The assay was then performed by transferring 180 µL of the eluate from each sample and each time point in triplicate to 96-well plates. Nutrient broth No. 2 was used as the control. 20 µL of bacterial inoculum at 10 x 0.5 MacFarland concentration were added to each well. The multi-wells were incubated at 30 °C in mild shaking conditions (100 rpm) overnight. On the following day, the trays were collected and the OD at 600 nm was measured using a FluoStar Optima plate reader (SMG Labtech). The antibacterial activity (*R*) of the eluates was

calculated as the % reduction of the OD at 600 nm compared to the control, which was calculated as described below:

$$R\% = \frac{A_{control} - Ax}{A_{control}} * 100$$

where $A_{control}$ is the absorbance value of the control (i.e. bacteria with nutrient broth) and A_x is the absorbance value of the sample considered.

2.7.2 Biocompatibility studies

2.7.2.1 Cell culture conditions

Keratinocyte HaCaT cells were cultured in polystyrene tissue culture flasks using Dulbecco's modified Eagle medium (DMEM) supplemented with 10% v/v fetal bovine serum (FBS), 1% v/v sodium pyruvate and 1% v/v penicillin/streptomycin. All reagents were purchased from Gibco™. The cells were incubated at 37 °C in 5% CO_2 atmosphere. When 90% of confluency was reached, the cells were passaged with a 1:3 or 1:5 ratio using 3 mL of 0.25% trypsin/ethylenediaminetetraacetic acid (EDTA) to detach them upon incubation of the reagent for a few minutes with the cells. The activity of trypsin was inhibited by 1:4 dilution using FBS supplemented growth medium. Cells were then centrifuged at 120 x g for 5 min, and the pellet obtained was resuspended in 3 mL of media. The count of the cells was carried out using a Neubauer counting chamber by trypan blue exclusion method. The cell viability after direct/indirect contact of the cells with the cellulose samples was quantified by Alamar Blue assay. Alamar Blue is a colorimetric redox indicator of living cells metabolic activity based on resazurin, a blue-coloured, non-fluorescent and non-toxic reagent. Resazurin can penetrate through the cell membrane of healthy cells, where it is reduced to resofurin, a highly fluorescent pink-coloured compound. The conversion of resazurin to resofurin is due to the metabolic mitochondrial activity, which is a function of the aerobic respiration. The absorbance of resofurin was measured using a spectrophotometer.

2.7.2.2 Indirect cytotoxicity of bacterial cellulose

The indirect cytotoxicity of unmodified and modified cellulose was studied to evaluate the presence of toxic leachable compounds. 1 cm^2 samples from non-functionalised and functionalised cellulose in wet and dry environment were sterilised by autoclaving and incubated in a 24-well plate with 1 mL of growth medium for 24 hours at 37 °C in 5% CO_2 atmosphere. On the same day, the cells were seeded in a 24-well plate at a concentration of 50,000 cells per well and incubated with 1 mL of growth medium in the same conditions. After 24 hours, the medium was removed from the cells and the conditioned medium was added. Unconditioned medium was used as the positive control, while pure dimethyl sulfoxide (DMSO) was used as the negative control. All the samples as well as the positive and negative control were prepared in triplicate. The cells were incubated with the eluates for 24 hours at 37 °C in 5% CO_2 atmosphere. On the next day, the samples were removed from the wells and the medium was replaced with 1 mL of fresh medium supplemented with 10% Alamar Blue. The plate was then incubated in the same conditions as the cells for further 4 hours. After this time, 200 µL of the solution from each well were transferred into a 96-well plate. The absorbance (A) was measured at 570 nm and normalised to the absorbance at 600 nm using a FluoStar Optima plate reader (SMG Labtech). The absorbance of the tissue culture plate (TCP) without cells with 10% Alamar Blue solution was subtracted from the normalised absorbance values of each sample, including the positive control. The cell viability was then calculated by comparing each value to the positive control using the formula below:

$$Cell\ viability = \frac{A_x}{A_p} x\ 100$$

A_x = absorbance of the solution – absorbance of TCP/10% Alamar Blue

A_p = absorbance of the positive control – absorbance of TCP/10% Alamar Blue

2.7.2.3 Direct cytotoxicity of bacterial cellulose

A quantitative evaluation of the cell viability after direct contact with the functionalised cellulose (for both reactions) was performed following a modified

ISO 10993-5 procedure for the biological evaluation of medical devices. 1 cm^2 samples of non-functionalised and both types of functionalised cellulose were sterilised by autoclave and pre-conditioned by incubation with 1 mL of growth medium for 24 hours in 24-well plates at 37 °C in 5% CO_2 atmosphere. On the same day, the cells were seeded in a 24-well plate at a concentration of 50,000 cells per well and incubated with 1 mL of growth medium in the same conditions. All the samples were prepared in triplicate as well as positive and negative control. After 24 hours, the medium was removed from the cells and the samples were placed directly onto the cell layer. 1 mL of fresh medium was added into each well. Growth medium was used as the positive control, while pure DMSO was used as the negative control. The cells were incubated with the samples for several days at 37 °C in 5% CO_2 atmosphere. Cell viability was evaluated after 1, 3 and 6 days by Alamar Blue assay. At each time point, the medium was replaced with 1 mL of 10% solution of Alamar Blue in growth medium. The plate was then incubated in the same conditions for 4 hours. After this time, 200 µL of the solution from each well were transferred into a 96-well plate. The absorbance was measured at 570 nm and 600 nm and the cell viability was calculated as described in section 2.7.2.2. After 6 days of incubation with the samples, cells were stained in order to evaluate their morphology. Two different stains were used for this purpose, i.e. rhodamine phalloidin and DAPI (4',6-diamino-2-phenylindole, dilactate). First, the cells were fixed with a 4% formaldehyde-based fixation buffer and incubated for 30 minutes at room temperature. After this, the excess was removed through washing with PBS solution for three times. 0.1% Triton X-100 in PBS was then added in order to increase the permeability and incubated for 3-5 minutes, followed by washing with PBS three times. Finally, a solution containing 8 µL/mL rhodamine phalloidin and 1 µL/mL DAPI was added for staining. The images were acquired with a confocal microscope Leica TCS SP2.

2.7.2.4 In vitro scratch assay

The ability of keratinocytes to migrate and proliferate to achieve wound closure in the presence of the cellulose samples was also evaluated through *in vitro*

scratch assay. 1 cm^2 samples in triplicate of non-functionalised cellulose and cellulose functionalised in wet conditions were sterilised by autoclave and pre-conditioned with 1 mL of growth medium for 24 hours at 37 °C in 5% CO_2 atmosphere. On the same day, the cells were seeded in a 24-well plate at a concentration of 100,000 cells per well and incubated with 1 mL of growth medium in the same conditions. After 24 hours, the medium was removed from the cells and a scratch was made in the cell monolayer using a 200 µL pipette tip. The cells were then washed with 1 mL of Hank's balanced salt solution to remove the cell debris. A reference point next to the scratch was made with an ultrafine tip marker. The cellulose samples were then placed directly onto the cell layer and 1 mL of fresh medium was added into each well. Growth medium was used as the positive control, while pure DMSO was used as the negative control. The progressive coverage of the scratched area by the cells was observed using an Olympus CKX41 microscope, bright field, magnification 40x and 100x. The images were acquired using a QIClick™ CCD Camera from QImaging. The modification of the pictures was performed using GIMP, an open source software. The contrast was minimised while the brightness was increased in order to achieve a clear distinction between the cells (white pixels) and the scratch (black pixels). The analysis of the image was then carried out using ImageJ (National Institutes of Health, USA). The width of the scratch at time 0 was set as 100%, corresponding to 0% of coverage. The percentage of coverage of the scratch by the cells was considered as the ratio between white pixels and black pixels and was quantified over time by measuring the number of black pixels in the image.

2.7.2.5 Cytotoxicity of chitosan-based composites

The cytotoxicity of the copper-chitosan based films without and with bacterial cellulose was quantified. The toxicity of copper was evaluated by adapting the ISO 10993-5 procedure previously described for biological evaluation of medical devices. Samples of diameter of 6 mm were cut from each formulation (i.e. CuChi3, CuChi12, CuChi3/BC and CuChi12/BC) and sterilised by UV treatment for 15 minutes per side. After this, a pre-conditioning was carried out by

incubation in PBS for 30 minutes at room temperature. On the first day, the cells were seeded in a 24-well plate at a concentration of 50,000 cells per well and incubated with 1 mL of growth medium at 37 °C in 5% CO_2 atmosphere. After 24 hours, the specimens were placed on permeable supports for cell culture and put into the wells seeded with the cells with 1 mL of fresh medium. Transwell® polycarbonate membranes with a pore size of 8.0 μm were used for this purpose (Corning® Inc, New York, US). The viability of the cells with growth medium only was set as the positive control, while pure dimethyl sulfoxide (DMSO) was used as the negative control. All the samples were prepared in triplicate as well as the positive and negative control. The cells were incubated with the samples for several days in the same conditions. Cell viability was evaluated after 1, 3 and 6 days by Alamar Blue assay. At each time point, the supports were removed and the samples were washed with 1 mL of Hank's balanced salt solution. The medium was then replaced in each well with 1 mL of 10% solution of Alamar Blue in growth medium. The plate was incubated in the same conditions for further 4 hours. After this time, 200 μL of the solution from each well were transferred into a 96-well plate. The absorbance was measured at 570 nm and 600 nm and the cell viability was calculated as described in section 2.7.2.2.

2.7.2.6 Cytotoxicity of copper released from the chitosan-based composites

The toxicity of the copper released from the composites prepared over time was also evaluated by indirect assay. Circular samples of 6 mm of diameter were cut from each formulation (i.e. CuChi3, CuChi12, CuChi3/BC and CuChi12/BC) and sterilised by UV treatment for 15 minutes per side. After this, a pre-conditioning was carried out by incubation in PBS for 30 minutes at room temperature. The samples were then incubated in 1 mL of keratinocytes growth medium at 37 °C in 5% CO_2 atmosphere for several days. After 1, 3 and 6 days, the eluate from each well containing the samples (in triplicate) was collected and replaced with fresh medium. After this, the keratinocytes were seeded in a 24-well plate at a concentration of 50,000 cells per well and incubated overnight with 1 mL of growth medium at 37 °C in 5% CO_2 atmosphere. Upon cell attachment, the

eluates collected were transferred to the 24-well plate and incubated in the same conditions for 24 hours. Positive and negative control were also prepared in triplicate using, respectively, normal growth medium and pure DMSO. On the next day, the medium was replaced with 1 mL of fresh medium supplemented with 10% Alamar Blue. The plate was then incubated in the same conditions as the cells for 4 hours. After this time, 200 µL of the solution from each well were transferred into a 96-well plate. The absorbance was measured at 570 nm and 600 nm and the cell viability was calculated as described in section 2.7.2.2.

2.8 Statistical analysis

The data are shown as the arithmetic mean ± standard deviation (STD). Statistical analysis was carried out by performing one-way analysis of variance (ANOVA) with Tukey post-hoc test between two or more groups to determine if there were statistically significant differences between populations. A significance below 0.05 was used ($\alpha < 0.05$). The test was performed using GraphPad Prism 8.1.0 software (GraphPad Software Incorporated).

Chapter III

Production and characterisation of bacterial cellulose

3.1 Introduction

The inherent biocompatibility of the majority of the natural polymers available today has turned these materials into some of the most studied for applications in the biomedical field. This feature relies, mainly, in their similarities with the extracellular matrix (ECM) components as well as with polymers already present in the human body, including collagen, hyaluronic acid and nucleic acids. Thanks to their great degree of biocompatibility as well as tailorable mechanical and physical properties, polymers of natural origin have been extensively used for several applications, ranging from tissue engineering and skin repair to bone or dental repair/replacement and drug delivery (Aravamudhan *et al.*, 2014; Olatunji, 2016). The main categories of natural polymers are polysaccharides, polypeptides and polyesters, which can be derived either from plants or animals. Among these, an important class is represented by bacteria derived polymers. Bacteria are in fact able to synthesise polysaccharides, polyesters, polyamides and polyanhydrides, which are employed in a wide range of biological functions such as structural, nutritional (nutrients storage) and protective, among others. The bioproduction of these polymers occurs through conversion of various carbon sources, resulting in their accumulation both in the intracellular or, more commonly, extracellular environment (Rehm, 2010). Although the first bacterial polymer discovery took place in the mid-nineteenth century, only in the recent decades they have been attracting attention on an industrial scale. Several polymers are currently produced and have relevance in the biomedical field, including various polysaccharides (mostly extracellular) such as alginate (Rehm and Valla, 1997), cellulose (Lin *et al.*, 2013), xanthan (Petri, 2015), dextran (Naessens *et al.*, 2005), hyaluronic acid (Kogan *et al.*, 2006), intracellular polyesters like polyhydroxyalkanoates (Philip, Keshavarz and Roy, 2007) and polyamides, mainly poly-ε-lysine and poly-γ-glutamic acid (Shih, Shen and Van, 2006; Ogunleye *et al.*, 2015).

Thanks to its unusual features, microbial cellulose is one of the most studied bacterial polymers, especially in the biomedical context. This polysaccharide is in fact produced with a great degree of purity, as it does not contain other

components such as lignin and hemicellulose that are present in plant-derived cellulose. Moreover, it possesses excellent mechanical properties, therefore it is widely used as a reinforcement for the development of high-performance composites. From the structural point of view, bacterial cellulose presents a highly porous and crystalline nanofibrillar structure that, thanks also to the high water holding ability and hydrophilicity, turns this material into a naturally-formed hydrogel, particularly suitable for applications in skin tissue engineering and wound healing (Picheth *et al.*, 2017).

Bacterial cellulose is externally secreted by several strains such as *Gluconacetobacter* (formerly *Acetobacter*), *Agrobacterium*, *Aerobacter*, *Achromobacter*, *Azotobacter*, *Rhizobium*, *Sarcina*, *Salmonella* and *Escherichia*. On an industrial scale, this polymer is currently produced using two different methods, i.e. static (or surface) culture and agitated (or submerged) culture. Fermentation in static conditions is probably the most common and easiest method to carry out, and it allows the production of homogeneous and flat pellicles that form at the surface of the culture. Due to their accumulation at the air-liquid interface, however, this process requires wide surface area to increase the production yield as well as long culture period, therefore it is not convenient from an industrial point of view. The fermentation in agitated culture, on the contrary, allows to overcome this drawback, although, due to the rapid proliferation, it results in the accumulation of non-producing mutants. Moreover, due to the insolubility of cellulose, in shaking conditions the biopolymer is produced as a dispersed slurry of highly inhomogeneous pellets. Another disadvantage of this approach is the limited oxygen supply as compared to the surface culture. To address this limitation, an airlift reactor could be used, which involves supplying air or oxygen-enriched air from the bottom of the tank, resulting in improved oxygen circulation in the culture. Although there is no significant variation in the microstructure of the cellulose produced in the two processes, it is important to consider the final application when choosing the appropriate fermentation technique (Watanabe *et al.*, 1998; Shoda and Sugano, 2005; Lin *et al.*, 2013).

In this chapter, the production of bacterial cellulose through static fermentation of *Gluconacetobacter xylinus* is reported. The material was thoroughly purified in order to obtain a biomass-free pellicle suitable for biomedical applications. In particular, the outstanding water holding ability of the material turns it into an optimal candidate for wound healing, particularly in the case of dry wounds that require additional moisture. The mats were chemically characterised to confirm their structure, and their morphology was studied through SEM analysis. Moreover, the rheological properties of the hydrogel were investigated as well as their stability in liquid media at a typical wound-bed temperature.

3.2 Results

3.2.1 Fermentation of Gluconacetobacter xylinus

In this study, bacterial cellulose was produced through fermentation of *Gluconacetobacter xylinus* in the presence of glucose as the main carbon source. In order to obtain a flat and homogeneous pellicle to be used for wound dressing, strictly static fermentation conditions were applied. The formation of the pellicles usually required 5-7 days to obtain a thickness of about 1 cm. The polymer biosynthesis occurred at the interface between the culture medium and the air in order to maximise the oxygen supply (**Figure 3.1**).

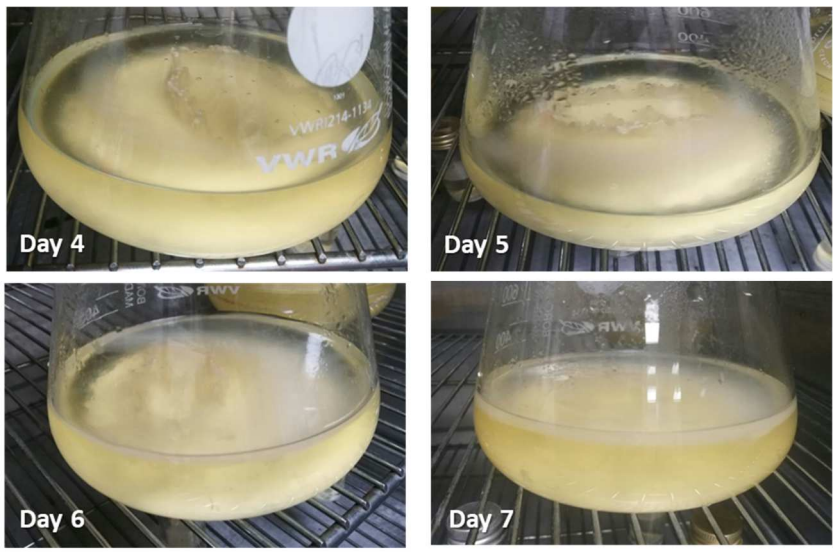

Figure 3.1 Bacterial cellulose production by fermentation of *Gluconacetobacter xylinus*

After four days of incubation, it was possible to observe the bacteria floating to the gas-liquid interface and the formation of the pellicle by secretion of the cellulose fibres in the medium (**Figure 3.2**).

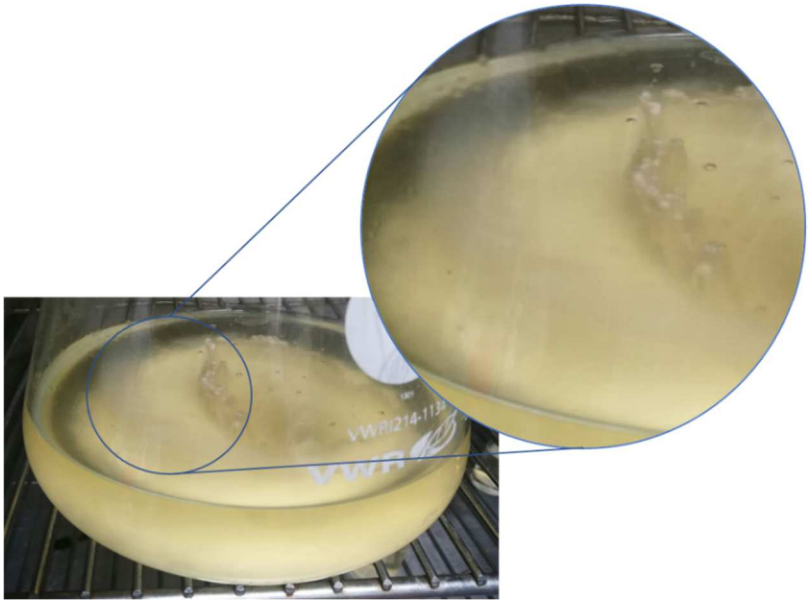

Figure 3.2 Bacterial cellulose pellicle formation after four days of incubation

The polymer yield for the biosynthesis as well as the productivity rate were evaluated by considering the weight of the pellicle both in wet conditions and after drying for 24 hours. The monomer conversion was also calculated by considering the amount of glucose used as the carbon source (**Table 3.1**).

Table 3.1 Polymer yield, glucose conversion and productivity rate for bacterial cellulose biosynthesis. Glucose conversion was calculated by comparing the amount of glucose added in the production medium with the final polymer yield.

	Polymer concentration (mg/mL)	Glucose conversion (%)	Productivity rate (mg/mL*day)
Wet cellulose	97	2	16.2
Dry cellulose	1	2	0.2

The fermentation process was monitored in order to evaluate the growth of bacteria and the polymer production. Two different methods were investigated to understand the effect of external interference on the bacterial fermentation, i.e.

the disturbance applied by the collection of the culture samples from the medium. For method A, the collection of the culture was carried out using a pipette, while for method B a tube was secured to the internal wall of the flask and culture medium was suctioned using a syringe (**Figure 3.3**).

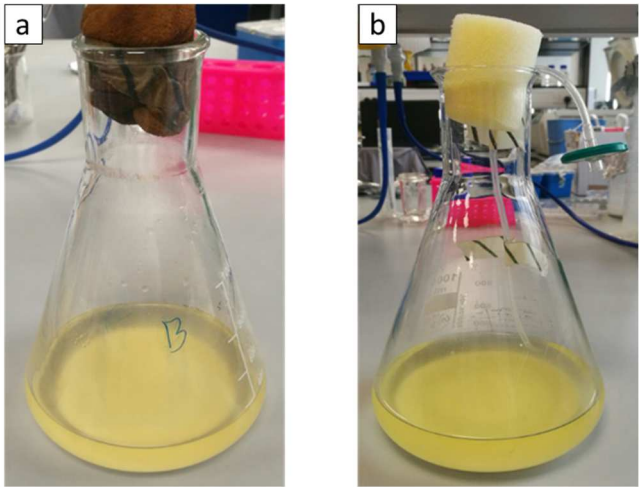

Figure 3.3 Flask preparation for method A and method B of bacterial fermentation profiling

The pH and the optical density were measured over time for both the profiling methods (**Figure 3.4**). In both cases, however, the disturbance of the bacterial growth led to the lack of pellicle formation, therefore it was not possible to evaluate the polymer yield over time.

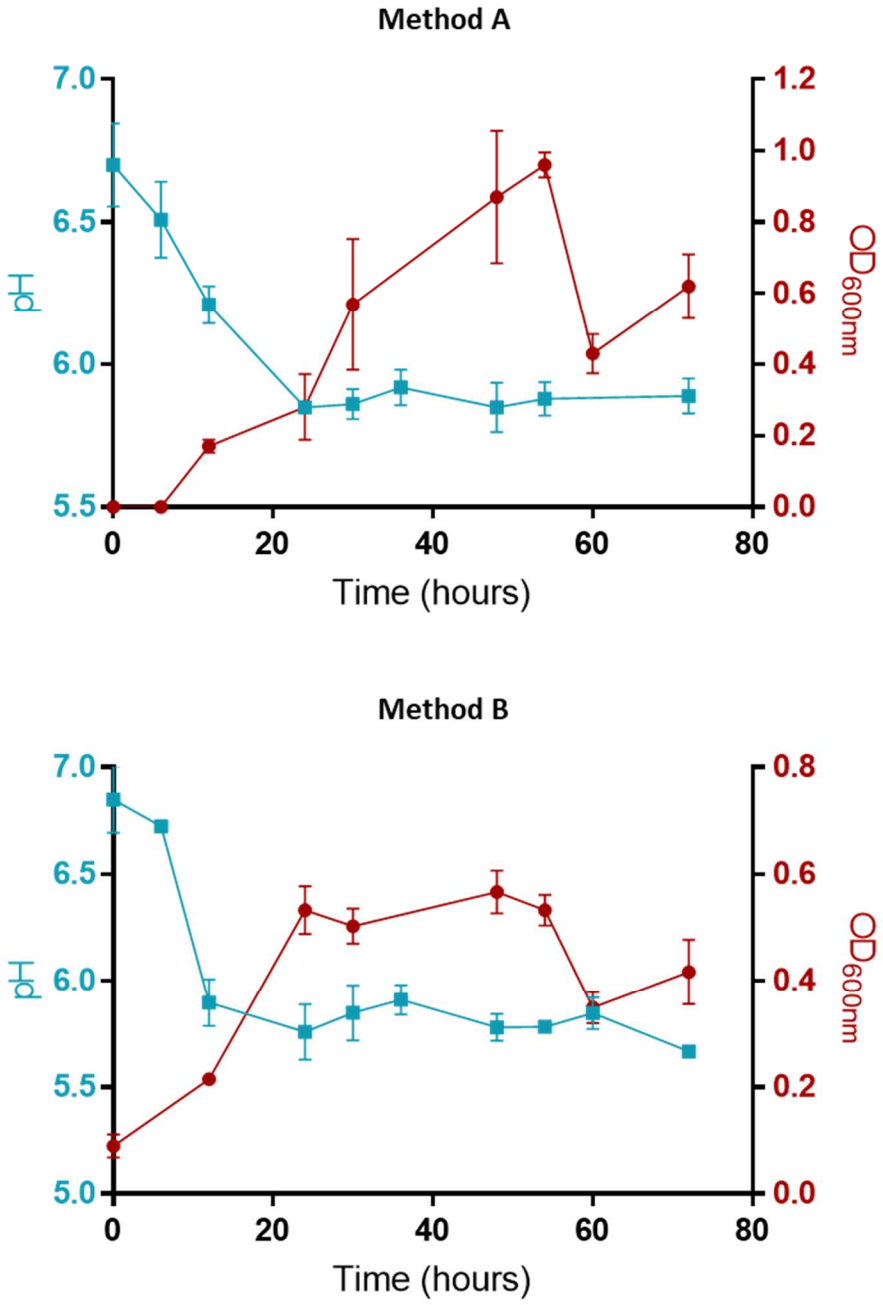

Figure 3.4 Temporal profiling of bacterial cellulose production (method A and method B)

For both methods, an increase in the optical density was observed until 48 hours as a result of the bacterial proliferation, followed by a decrease on the third day of fermentation. This effect could be ascribed to the agglomeration of bacteria and formation of the pellicle. Higher OD values were observed for method A, with a maximum absorbance of about 1 after 54 hours, while for the second method a maximum of ≈ 0.6 was reached after 48 hours. It is possible that the presence of the tube within the flask was interfering with the cells, thus resulting

in lower bacterial proliferation. The pH of the medium showed the same trend for method A and method B, with a quick decrease from 6.8 to 5.8-5.9 after 20 hours due to the production of acidic by-products such as gluconic acids. In both cases, no pellicle formation was detected, but only production of disaggregated fibres dispersed throughout the culture medium.

3.2.2 Purification of bacterial cellulose

The purification of the pellicles produced was optimised in order to ensure the complete removal of all the biomass from the fibrous network. Various treatments were investigated involving acid or basic wash at different temperatures, which are summarised in **Table 3.2**.

Table 3.2 Summary of different purification treatments

	Reagent	T (°C)	Time	Reiteration	Sterilisation
Method A	NaOH 0.1M	80	80 mins	3x	-
Method B	1) 3% NaOH (0.75M) 2) 3% HCl (0.82 M)	RT RT	12 hours 4 hours	4x 1x	Autoclave
Method C	NaOH 1 M	80	2 hours	2x	Autoclave

The outcome of the different treatments was studied through colony forming assay. Samples from each pellicle were incubated with the *Gluconacetobacter xylinus* growth medium in shaking conditions, and the culture was spread over agar plates to evaluate the presence of residual bacterial cells (**Figure 3.5**).

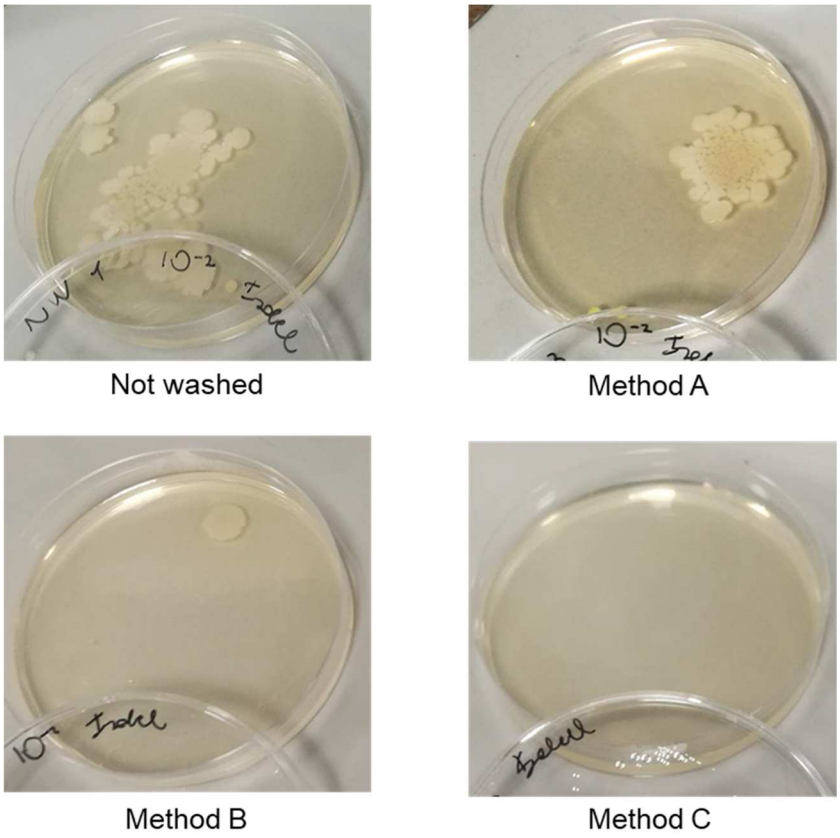

Figure 3.5 Colony forming assay for different bacterial cellulose purification treatments and control (unwashed pellicle)

The assay showed a massive presence of bacteria for the unwashed pellicle as well as for the method A as compared to methods B and C. This was most probably due to the sterilisation by autoclaving, which allowed to kill the residual biomass thanks to the high pressure/temperature process. In particular, method C did not show the presence of any residual colony. The effectiveness of this procedure could be ascribed to the high concentration of sodium hydroxide (1 M) as well as the high temperature (80 °C). Although method B involved longer washing time (12 hours repeated for 4 times, while method C lasted only 80 minutes), lower base concentration and, especially, significantly lower temperature were used, thus resulting in lower killing and washing efficiency.

The difference in the aspect of the cellulose pellicles before and after purification process (method C) was also visually observed. The pellicle appeared yellowish and opaque before the washing, whereas the high-temperature treatment resulted in a white and more transparent material (**Figure 3.6**).

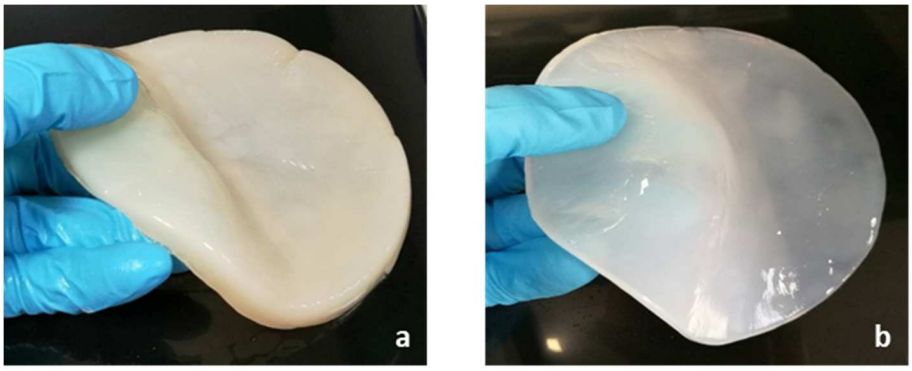

Figure 3.6 Bacterial cellulose pellicle before (a) and after (b) purification treatment

Finally, the presence of residual bacterial cells in the cellulose network was investigated through SEM analysis (**Figure 3.7**).

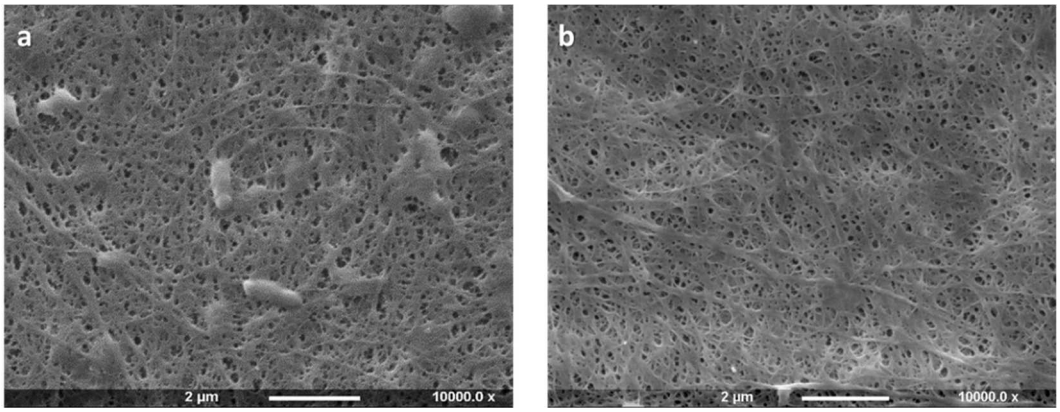

Figure 3.7 SEM images of bacterial cellulose pellicles before (a) and after (b) purification treatment

The images clearly showed the presence of *Gluconacetobacter xylinus* cells in the untreated sample. The morphology and size of the cells was within the range expected for this strain (Sievers and Swings, 2015). The cells appeared to be rod-shaped, with a rod size of about 0.4 µm (width) x 1.4 µm (length). In particular, the cells were trapped within the fibrous network of cellulose, as the polymer chains are secreted extracellularly as self-assembled microfibrils. This unique feature provides the structure with a high degree of porosity, resulting in the ability to immobilise water molecules within its interstitial spaces. Furthermore, it was observed that no degradation of the fibres occurred upon purification, even after the high-temperature sterilisation. In light of the results obtained,

method C was used for the purification and sterilisation of all the cellulose samples used in this study.

3.2.3 Chemical characterisation

The chemical structure of the bacterial cellulose pellicles was studied through attenuated total reflection Fourier-transform infrared spectroscopy (ATR FT-IR) (**Figure 3.8**).

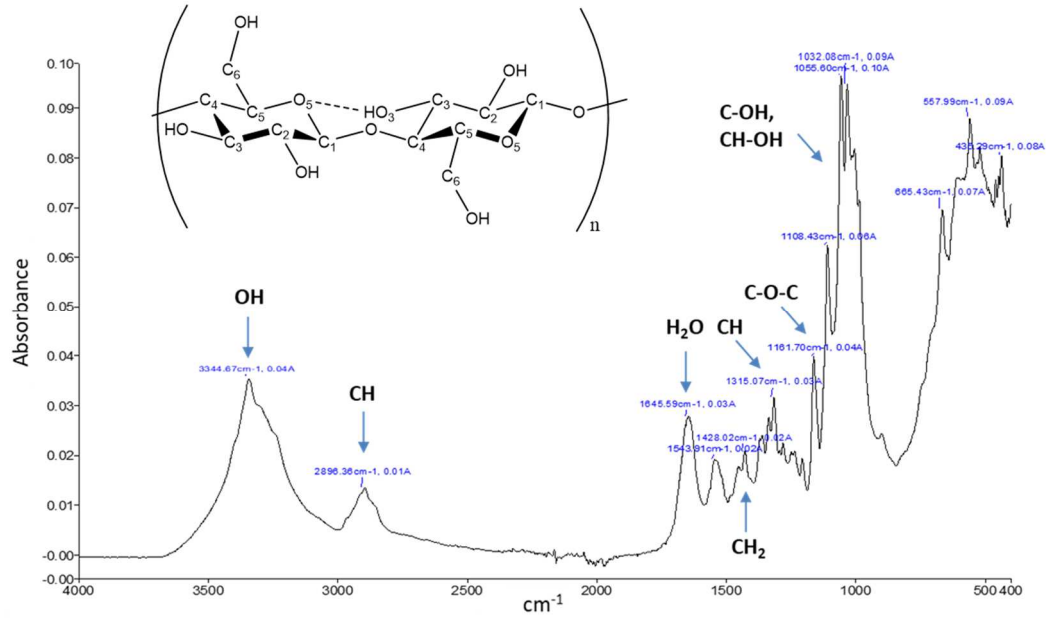

Figure 3.8 ATR FT-IR spectrum and chemical structure of bacterial cellulose

The analysis showed the presence of an intense signal at ≈ 3345 cm^{-1} corresponding to the intramolecular O_3H-O_5 hydrogen bond. The symmetric bending of the CH_2 group was detected in the spectrum, with an absorbance of 1428 cm^{-1}. It was also possible to observe the peak related to the β (1→4) glucosidic linkage (C_1-O-C_4) at 1161 cm^{-1}. Finally, the absorption bands at 1108, 1055 and 1032 cm^{-1} were compared to literature data, and it was found that they were previously attributed to the C_2-O_2H, C_3-O_3H and C_6H_2-O_6H vibrations, respectively (Feng *et al.*, 2012; Grube *et al.*, 2016).

Overall, the assignment of the peaks and the comparison of the spectrum obtained with already published studies on the same substrate confirmed that the pellicles produced presented the structure expected for a cellulosic polymer.

The elemental composition of the material obtained was confirmed through EDX analysis (**Figure 3.9**).

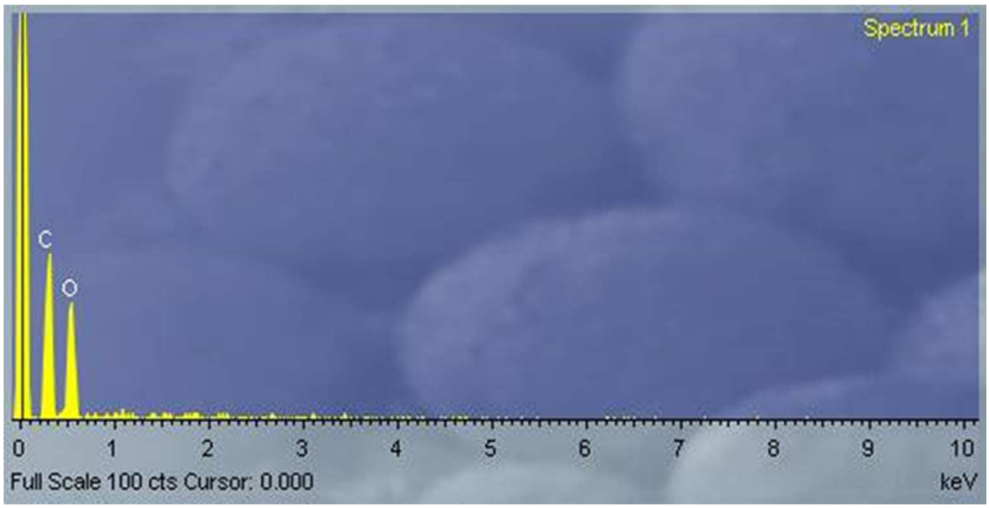

Figure 3.9 EDX spectrum of plain bacterial cellulose. Au and Pd peaks (resulting from the coating pre-treatment) were removed for clarity purposes.

The analysis revealed the presence of carbon and oxygen, as expected for cellulose. Moreover, no other elements were detected in the spectrum, indicating that the purification treatment successfully removed the impurities. However, it is important to mention that EDX analysis presents a detection limit of about 0.1% w/w (circa 1000 ppm), which means that it cannot detect trace elements (Nasrazadani and Hassani, 2016). This effect is reflected in the accuracy, where a relative error of ±5% has been observed for bulk constituents, i.e. elements with a weight percent higher than 10%, and ±10% of relative error for minor constituents, with 1-10% w/w, whereas in the case of trace constituents (<1% w/w) the relative error has been found to be ±25% (Newbury and Ritchie, 2015).

3.2.4 Water content evaluation

The water content of the cellulose mats produced was evaluated in order to investigate the degree of hydration of the material. To estimate this, the difference of the weight of cellulose samples before and after a drying period of 27 hours under a hood was measured. The percent of water was calculated as follows:

$$Water\ \% = \frac{(A - B)}{A}\ x\ 100 = 97.53\%$$

where A is the weight of the wet specimen and B is the weight of the specimen after drying.

As expected, the pellicles presented extremely high water concentration, which allows the material to behave as a self-standing hydrogel. The moisture incorporated during the biosynthesis is in fact retained within the highly porous structure, turning the material into an optimal substrate for wound healing applications, in particular, as a dressing for dry wounds requiring additional hydration. It was also noted that the drying process required a much longer period when the samples were exposed to air as compared to the fume hood, with a total time of 4-5 days necessary for complete desiccation. This is an important feature as usually a dressing is changed after a minimum of 3-5 days from the application. It was not possible, on the other hand, to rehydrate the samples after this, probably because of the collapse of the structure upon slow solvent evaporation.

3.2.5 Rheological properties

The bacterial cellulose pellicles were characterised with respect to their rheological properties before and after sterilisation in autoclave in order to assess the influence of the process on the viscoelastic behaviour of the material. In particular, frequency sweep and temperature ramp tests were carried out, and the storage and loss modulus (respectively, G' and G'') were evaluated. Both tests were performed in the linear viscoelastic region (LVR), which was identified through oscillatory strain sweep test.

The frequency sweep analysis (also called small amplitude oscillatory shear, SOAS) showed that both materials behaved as self-standing gels, with the storage modulus (G') higher than the loss modulus (G'') for all the frequencies considered (**Figure 3.10**).

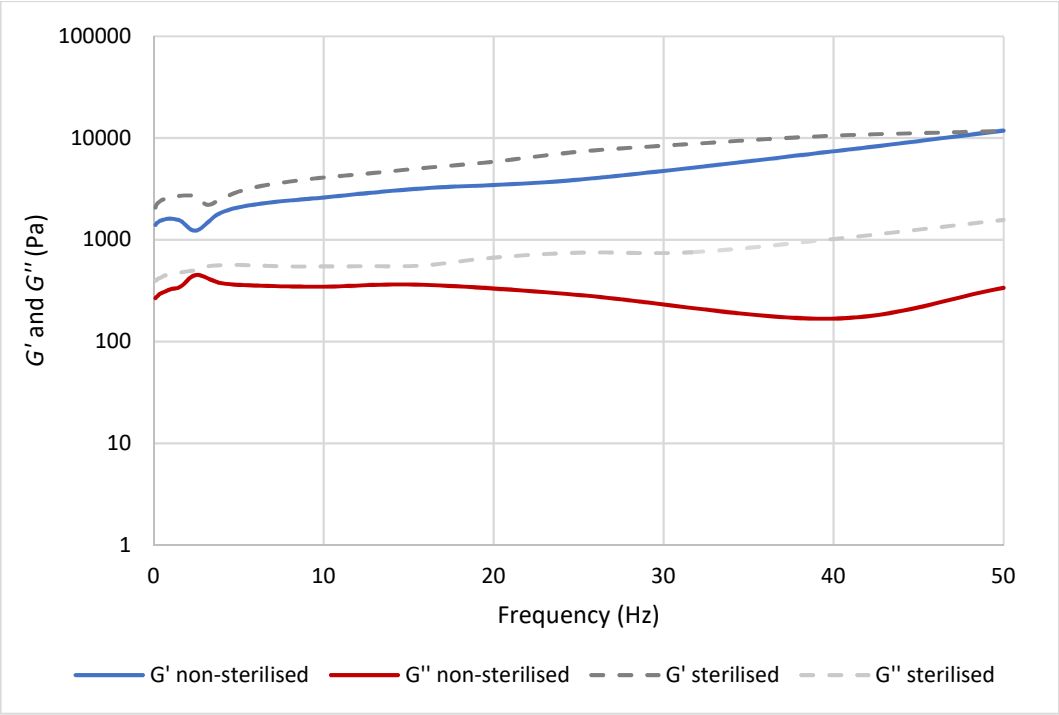

Figure 3.10 Frequency sweep test; T = 32 °C, preload = 6 Pa.

For the non-sterilised cellulose, it was observed that the loss modulus presented an almost zero-order linear trend with minimal variation upon increase of the frequency (average *G''* = 300 Pa). This result showed that the viscous behaviour of the pellicle was not affected by the change in the oscillatory shear rate applied. More specifically, no increase in the deformation energy dissipated during the oscillation (which expresses the liquid-like response of the material) was detected. The storage modulus (*G'*), on the other hand, increased proportionally with respect to the frequency, from 1400 Pa to about 11800 Pa at 50 Hz. This trend proved that at higher frequencies the material behaved more like an elastic solid with higher resistance to deformation, rather than like a viscous liquid. The storage modulus represents in fact the deformation energy stored during the shear process, therefore it is an indication of the stiffness.

The same behaviour was noted for the cellulose pellicles after sterilisation, with the storage modulus higher than the loss modulus for all the frequencies, proving that its gel-like viscoelastic properties were retained. The loss modulus evaluation exhibited higher values as compared to the untreated samples, with a final *G''* value of about 1500 Pa at 50 Hz. This effect indicated that the viscous

component of the mechanical behaviour was affected by the increase in the oscillation frequency, resulting in higher liquid-like response. As regards the storage modulus, the values obtained were very similar to the non-sterilised cellulose, with a maximum of about 11700 Pa at 50 Hz. Once again, the analysis showed an increase in the storage modulus proportional to the frequency change.

The effect of the temperature variation on the viscoelastic properties of the pellicles was also studied by temperature ramp test (**Figure 3.11**).

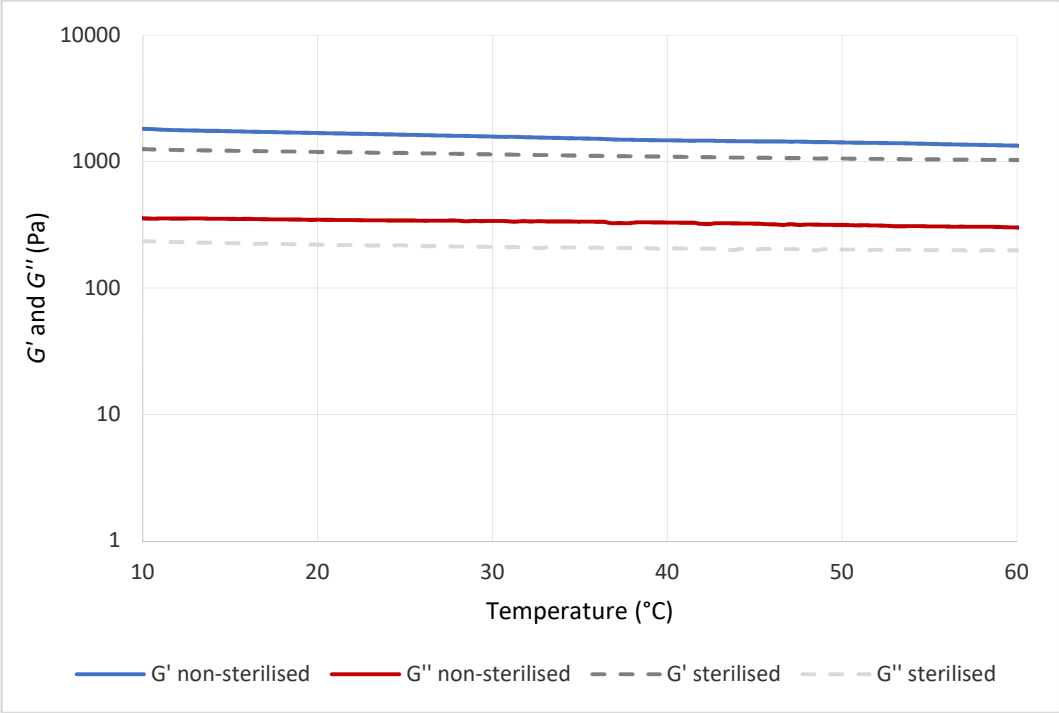

Figure 3.11 Temperature ramp test; f = 1 Hz, preload = 6 Pa, rate = 5°C/min.

The analysis was first conducted on the pellicles before sterilisation. As for the frequency sweep, the hydrogel showed a solid-like behaviour (i.e. $G' > G''$) in the entire range of temperatures considered, confirming that the material is easy to handle and self-standing. Again, the loss modulus did not show significant variations, with a minimal decrease from 350 Pa to 300 Pa. On the contrary, the storage modulus decreased from 1800 Pa at 10 °C to about 1300 Pa at 60 °C. This result indicated that at higher temperature the material showed a more liquid-like behaviour, as expected for an elastic solid.

The test was then performed on the sterilised pellicles to evaluate the effect of the treatment on the viscoelastic properties of the material. Overall, both the storage modulus and the loss modulus exhibited lower values as compared to the untreated samples. This effect could be ascribed to the degradation happening as a consequence of the high-temperature process to which the pellicles were subjected. However, the pellicles retained a solid-like behaviour at all the temperatures considered, proving that there was no major variation in the structure. The storage modulus decreased from almost 1260 Pa at 10 °C to about 1000 Pa at 60 °C. Although both values were lower than in the case of the untreated sample, it was observed that the variation of *G'* with temperature was lower. In particular, a decrease of about 28% was detected without sterilisation, whereas after the treatment the storage modulus showed a decrease of 18%. The same trend was noted for the loss modulus, with a decrease from about 235 Pa to almost 200 Pa at 60 °C (circa 30% lower than the non-sterilised).

3.2.6 Stability studies

The stability of the pellicles in liquid media was studied over a period of 7 days, which is beyond the maximum average time between two consecutive wound dressing changes. The test was conducted at 32 °C to evaluate the weight variation at a typical wound-bed temperature. The samples were incubated both in PBS solution and keratinocytes growth medium and their weight was measured over time (**Figure 3.12**). The study showed no statistically significant difference between the weight variation of the samples in the two types of medium.

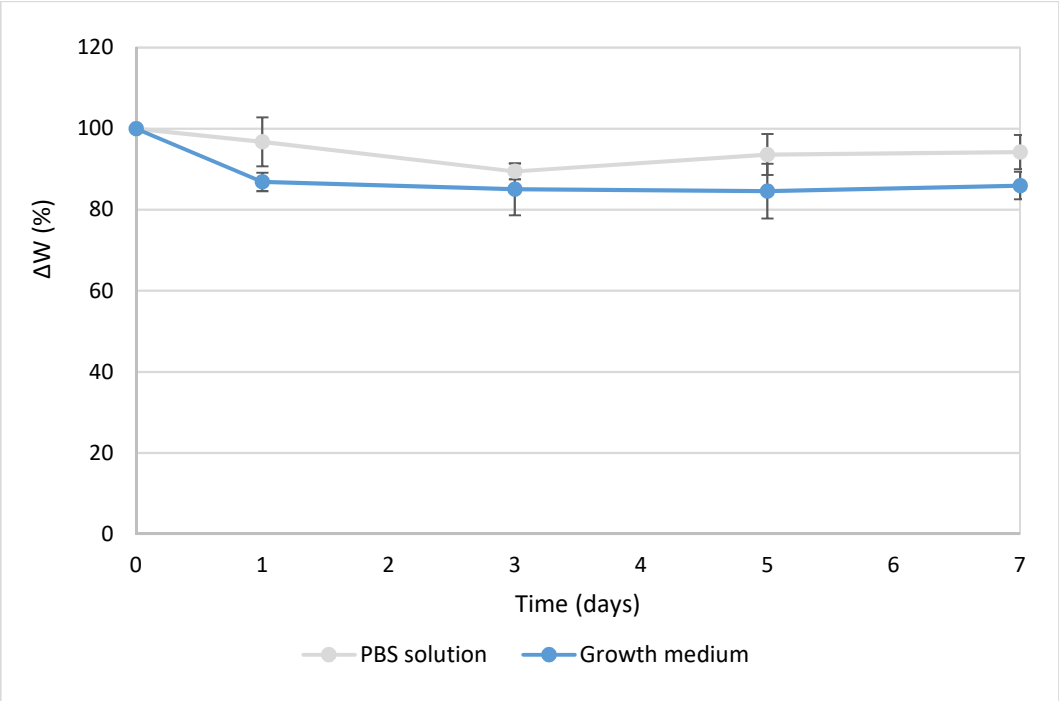

Figure 3.12 Stability of bacterial cellulose samples in PBS solution and keratinocytes growth medium at 32 °C under static conditions.

This result proved that the presence of the nutrients in the keratinocytes growth medium did not have a higher impact on the degradation of the material. As regards the weight variation in the PBS solution, the samples retained about 90-95% of their initial weight, with no statistical decrease over time at any time point ($p>0.05$). In the case of the cell culture medium, a significant weight loss was observed after 24 hours, with a decrease of about 15%. After this time, the weight reached a plateau and no statistical variation was detected for up to 7 days of incubation. This effect was probably due to the solvent exchange taking place in the samples, from the initial distilled water to the medium in which the samples were soaked.

3.3 Discussion

In this chapter, the biosynthesis of bacterial cellulose pellicles through fermentation of *Gluconacetobacter xylinus* was reported as well as its optimised purification and chemical/mechanical characterisation. The production of the polymer was carried out in static conditions using glucose as the principal carbon

source. The most common medium used for the growth of *Gluconacetobacter xylinus* (formerly known as *Acetobacter xylinum*) is the Hestrin and Schramm (HS) medium. The composition of such medium was published in 1954 by Hestrin and Schramm. The mixture included glucose (2% w/v), yeast (0.5% w/v) and peptone (0.5% w/v) (Schramm and Hestrin, 1954). In this study, a variation of the HS medium was used, consisting of glucose, yeast extract and $CaCO_3$. More recent studies proved in fact that the presence of metal ions such as calcium or magnesium leads to an increase in the production yield (Son *et al.*, 2003; Hungund and Gupta, 2010; Hong *et al.*, 2011). Over the past decades, a wide range of growth medium compositions has been investigated, with different carbon sources. Glucose, mannitol, sucrose and fructose are some of the most common sugars used for this purpose. Among these, glucose has been found to give the highest cellulose yield in several studies focused on the fermentation of *Gluconacetobacter* species with a single carbon source in static conditions. As regards the nitrogen supply, corn steep liquor, beef extract and various peptones have been employed, but lower yield was obtained as compared to yeast extract (Son *et al.*, 2001; Jia *et al.*, 2004; Castro *et al.*, 2012).

During the fermentation, the pH dropped from 6.8 (immediately after inoculation) to about 5.8-5.9 in less than 24 hours. This effect could be ascribed to the production of acidic by-products by the bacteria. More specifically, previous studies showed that glucose is converted into (keto)gluconic acids by membrane-bound enzyme glucose dehydrogenase (GDH) (Shigematsu *et al.*, 2005; Kuo, Teng and Lee, 2015). As a consequence, the conversion of glucose for cellulose production results in lowered efficiency, with lower BC yield. Moreover, the acidic pH negatively affects the cell viability, as the optimal pH for the bacterial growth is in the range of 5-7. Although in this work the pH decrease was quite low (circa one unit), it is important to consider this issue on an industrial scale. One alternative is the administration of a limited initial glucose supply to avoid the conversion of the excess glucose into gluconic acids or the control of the pH during the fermentation. However, such approaches are difficult to be put in

place for static surface cultures (Vandamme *et al.*, 1998; Esa, Tasirin and Rahman, 2014; Kuo, Teng and Lee, 2015).

The purification of the pellicles was optimised in order to achieve a suitable cellulosic material for applications in wound healing. As mentioned in the introduction of this chapter, cellulose of bacterial origin presents, among other advantages, higher purity as compared to plant-derived cellulose, which requires harsh and costly chemical or mechanical treatments to remove lignin and hemicellulose (Moon *et al.*, 2011). On the other hand, bacterial cellulose pellicles contain residual biomass and medium components that must be removed to minimise the risk of adverse effects on the skin. Most of the studies previously published on the production and purification of BC for various applications involved alkaline treatments at different temperatures, eventually followed by a wash in acid conditions (Svensson *et al.*, 2005; Maneerung, Tokura and Rujiravanit, 2008; Yang *et al.*, 2012; Costa *et al.*, 2017). However, it has been proven that a concentration of NaOH higher than 6% can lead to structural modification of the pellicle, with consequences on its mechanical properties and its 3D-network (Reiniati, Hrymak and Margaritis, 2016). In this work, three different methods were investigated, with increasing alkali concentration up to 4% (i.e. 1 M). It was also observed that high temperature was required together with basic conditions to obtain good killing and washing efficiency, as demonstrated by the colony forming assay performed on the samples.

The presence of bacterial cells as well as the morphology of the pellicles before and after purification was evaluated through SEM analysis. The images showed that the process successfully removed the cells without affecting the porous nanofibrillar network of the mat. The fibrils did not exhibit any significant degradation or variation in the orientation, maintaining the random organisation present in the untreated sample. In particular, cellulose chains can be arranged in various patterns resulting in different allomorphs, namely cellulose I, II, III and IV. Native cellulose presents a cellulose I structure, which indicates a parallel arrangement of the chains. More specifically, this phase consists of two crystalline forms, i.e. I_α and I_β. Cellulose I_α consists of a triclinic unit cell with one

chain, while cellulose I_β has a monoclinic unit cell containing two chains. Diffractometric studies on the structure of BC produced by *Gluconacetobacter xylinus* showed that it usually includes both forms, with a higher content of cellulose I_α (Nishiyama, Langan and Chanzy, 2002; Holtzapple, 2003; Czaja, Romanovicz and Brown, 2004).

The chemical structure of the pellicles was confirmed by FT-IR analysis. The spectrum showed the presence of the typical cellulose peaks, including the β (1→4) glucosidic linkage (C_1-O-C_4), which indicated the polymerisation of the glucose units, and the signals relative to the vibrations of the hydroxyl groups of the ring (Feng *et al.*, 2012; Grube *et al.*, 2016). This result, together with the outcome of the EDX study, confirmed the chemical structure of the biomaterial.

The mechanical properties of the pellicles, on the other hand, were assessed through rheological measurements. Samples before and after purification/sterilisation treatment were analysed in order to evaluate the effect of the process and detect any structural degradation. For both tests performed, i.e. frequency sweep (or small amplitude oscillatory shear, SOAS) and temperature ramp, the dynamic moduli (namely, storage modulus and loss modulus, respectively G' and G'') were measured. As a general assumption, the mechanical behaviour of a viscoelastic material can be approximated to the one of an elastic solid in case of $G' > G''$ or a viscous liquid for $G' < G''$ (Yan and Pochan, 2010). In this study, the cellulose pellicles were found to behave as self-standing hydrogels with $G' > G''$ both before and after sterilisation treatment at all the frequencies considered and in the entire temperature range analysed. The storage modulus values obtained from the frequency sweep test gave similar results for the two specimens, especially at higher frequencies (≈ 11830 Pa for the untreated *vs* ≈ 11730 Pa for the sterilised at 50 Hz). Furthermore, an increase of one order of magnitude in the storage modulus from 0.1 to 50 Hz was observed for both samples. This is a typical feature of hydrogels, which usually present a more solid-like response at increased frequencies, i.e. higher stiffness upon fast motions on a short time-scale. Both dynamic moduli of the materials tested were compared to previously published results, and it was observed that the pellicles

produced in this study indicated similar or higher mechanical performance as compared to other BC samples as well as different synthetic or natural polymers-based hydrogels. The temperature ramp analysis showed the same trend as compared to literature. In particular, it was found that most hydrogels exhibited a liquid-like behaviour at temperatures higher than 35-40 °C, probably because of degradation of the crystalline regions, which resulted in the breakdown of the 3D-network (Van Den Bulcke *et al.*, 2000; Huang *et al.*, 2010; Roy *et al.*, 2010; Smith, Kennedy and Higginbotham, 2010; Zuidema *et al.*, 2014). This effect was not noted in the case of BC, as the membranes retained a solid structure and good mechanical properties even at 60 °C. This is a critical aspect for a wound dressing, as a hydrogel needs to be easy to handle and to remove (for dressing change), stiff enough to sustain the cell growth and the tissue surrounding the wound but also adaptable to its shape (Boateng *et al.*, 2008; Kocen *et al.*, 2017).

Finally, the stability of the hydrogel in liquid medium was studied over 7 days of incubation both in PBS solution and keratinocytes growth medium. The study confirmed that the purification and sterilisation treatments did not affect the degradability of the pellicles over the timeframe considered, yielding a stable material.

3.4 Conclusions

In this chapter, the production of bacterial cellulose by fermentation of *Gluconacetobacter xylinus* in static conditions was described. The pellicles were subjected to purification treatment in order to remove the residual bacterial cells embedded in the polymeric network as well as the nutrients from the culture medium. After this, the biomaterial was characterised with respect to its morphological, chemical and mechanical properties. The presence of a nanofibrillar porous network was confirmed through SEM analysis. Its unique 3D-structure offers an advantage over plant-derived cellulose, especially for applications in wound healing and skin tissue engineering. This feature results in fact in great water holding ability, which is of crucial importance in the case of dry wounds as additional moisture is required to promote skin regeneration and

avoid the formation of necrotic tissue that can delay the healing process. Moreover, the polymer showed good mechanical properties even after alkaline treatment and sterilisation at high pressure/temperature, as confirmed by rheological measurements, with no significant degradation or loss of the 3D-structure. This is particularly important for a biomaterial, as the sterilisation in autoclave allows to avoid the use of toxic reagents such as ethylene oxide, which can be difficult to remove prior to the commercialisation/application, or expensive irradiation processes that can degrade the chemical structure of the substrate. Overall, the pellicles obtained showed excellent applicability as biomedical materials. Furthermore, their production and purification were achieved through a cost-effective and easy process, which is fundamental from an industrial point of view. The rough price per gram of bacterial cellulose was in fact calculated taking into accounts the variable costs (excluding utilities), resulting in a competitive 1.266 £/g to obtain a pure biomaterial with high properties such as biocompatibility and mechanical strength.

Chapter IV

Bacterial cellulose modification under aqueous conditions

4.1 Introduction

The use of bacterial cellulose for wound healing purposes has been widely investigated due to its unique biological and mechanical properties as well as green and low-cost method of production. However, it does not present inherent antibacterial properties. As antibiotic resistance continues to rise and infection-related mortality rate keeps increasing, it is crucial to develop dressings that are able to fight bacteria without triggering resistance mechanisms.

Chemical modification of polysaccharides has been the subject of extensive research, mostly thanks to the renewable nature of these polymers and their great degree of biocompatibility. Different types of reactions have been studied, depending on the substrate and the kind of modification required. The most widespread strategies involve nucleophilic attack of oxygen (or, less commonly, nitrogen), electrophilic attack of carbon, oxidation and reaction of the carboxylic acids. The use of the saccharide oxygen as a nucleophile results in the formation of an ester or an ether, depending on the alkylating agent (Cumpstey, 2013; Liu, Willför and Xu, 2015). In this study, two epoxides were employed as the oxygen-alkylating agents, namely glycidyl trimethylammonium chloride (GTMAC) and glycidyl hexadecyl ether (GHDE), containing, respectively, a quaternary ammonium group and a hydrophobic alkyl chain as antibacterial functionalities.

As discussed in the introduction chapter, quaternary ammonium groups are widely used substrates for the development of biocides with application in textile (Kim, Kim and Rhee, 2010; Simoncic and Tomsic, 2010; Liu *et al.*, 2014), water disinfection (Chaidez, Lopez and Castro-del Campo, 2007; Abid *et al.*, 2010) and, especially, biomedical and healthcare fields (Vasilev, Cook and Griesser, 2009; Zubris, Minbiole and Wuest, 2016; Jiao *et al.*, 2017; Makvandi *et al.*, 2018). These compounds are generally obtained through alkylation of a neutral amine following a procedure known as Menschutkin reaction (or, more recently, quaternisation) consisting of a bimolecular nucleophilic substitution (S_N2). The attack occurs on a tertiary amine at the aliphatic carbon attached to a leaving group (i.e. the halide), yielding the formation of two ions of opposite sign. The most common alkylating agents are bromides and chlorides, although the more

active are alkyl fluorosulfonates, tosylates and iodides. The reaction is usually conducted in polar solvents such as acetonitrile in order to stabilise the transition state and, thus, increase the rate of the reaction (Sasson, 1997; Okeke, Snyder and Frukhtbeyn, 2019). This approach has been extensively used to improve or introduce antibacterial properties in a wide range of natural and synthetic polymers such as chitosan (Tan *et al.*, 2013; Martins *et al.*, 2014), cellulose (Song *et al.*, 2010), polycarbonates (Ng *et al.*, 2014), polyethyleneimine (Gao, Zhang and Zhu, 2007) and polymethacrylates (Álvarez-Paino *et al.*, 2015; Tejero *et al.*, 2015). The bactericidal properties of such compounds rely on the electrostatic interaction between the cationic ammonium and the negatively charged bacterial cell membrane. After this, the hydrophobic alkyl side chains of the quaternary ammonium groups are able to permeate into the intramembrane region through the lipid regions of the cell wall, ultimately leading to leakage of cytoplasmic material and cell lysis. The anionic nature of the bacterial cell membrane turns this class of reagents into non-selective biocides with a broad spectrum of activity. However, it is important to mention that, due to the structural conformation of Gram negative strains, which present an additional external layer known as outer membrane, quaternary ammonium based compounds show higher activity towards Gram positive bacteria (Jennings, Minbiole and Wuest, 2015; Xue, Xiao and Zhang, 2015). In this context, several studies have been directed towards the assessment of the effect of these agents on the development of antibacterial resistance. Previous works indicated that some bacterial species are able to express genes that code for the production of transmembrane efflux pumps. These proteins are responsible for the specific extrusion of quaternary ammonium groups, thus lowering the susceptibility of bacteria towards their action (Jennings, Minbiole and Wuest, 2015). On the other hand, it has been observed that highly charged quaternary ammonium compounds with flexible alkyl chains did not induce resistance, as opposed to rigid and monocationic structures (Minbiole *et al.*, 2016). Although there still is ongoing debate whether the prolonged use of quaternary ammonium containing biocides might trigger bacteria to increase their tolerance and to what degree, it

is generally acknowledged that the non-specific action of quaternary ammonium compounds makes this effect less likely (Buffet-Bataillon *et al.*, 2012; Gerba, 2015).

The second reagent used for the modification of the cellulose pellicles presents a long alkyl chain (C14) as a substituent of the epoxide ring. Such a structure has been proven to perform a disruptive action towards the bacterial cell wall. This effect is based on the hydrophobic interaction between the alkyl chain and the external bacterial cell wall. In particular, in the case of Gram positive strains this is composed of cross-linked peptidoglycan complexed with teichoic and lipoteichoic acids, whereas the outer membrane of Gram negative bacteria consists of lipopolysaccharides, proteins and phospholipids. The hydrophobic interaction results in the insertion of the alkyl chain into the lipid region of the cell wall, causing the rupture of the membrane followed by bacterial death (Denis, Rodriguez-Villalobos and Struelens, 2010; Wiener and Horanyi, 2011; Zheng *et al.*, 2016). In particular, it is fundamental to consider the length of the chain when assessing the antimicrobial efficiency of the moiety. It has been shown that for Gram positive strains the optimal antibacterial effect is achieved with a chain length of C12-C14, while for Gram negative it was found to be in the C14-C15 range. For a chain length below C4 no antimicrobial properties were detected, probably due to the impossibility to cross the hydrophobic region of the membrane (Devínsky *et al.*, 1990; Zhao and Sun, 2008).

In this chapter, an environmental-friendly method for the surface modification of bacterial cellulose pellicles to introduce functional groups with biocidal activity is reported. The process involved the derivatisation of the hydroxyl groups of glucose through a base-catalysed ring-opening reaction using two epoxides in an aqueous system. The chemical structure of the modified material was studied through solid-state techniques (i.e. EDX and XPS analyses). Furthermore, the mechanical properties were investigated through rheological measurements and compared to the ones of the unmodified pellicles. The biological activity was then evaluated towards bacteria and keratinocyte cells. In particular, the antibacterial activity upon direct contact was assessed both qualitatively and quantitatively, whereas the cytotoxicity was studied over 6

days of direct incubation with the cells and through indirect assay. Finally, the stability of the hydrogels was studied over 7 days in liquid medium.

4.2 Results

4.2.1 Functionalisation in aqueous conditions

The cellulose membranes produced through bacterial fermentation did not possess any inherent antibacterial activity. To achieve such feature, specific functional groups were chemically introduced by surface modification. In particular, quaternary ammonium groups as well as hydrophobic chains were attached to the hydroxyl groups of glucose through base-catalysed ring-opening reaction (**Figure 4.1**).

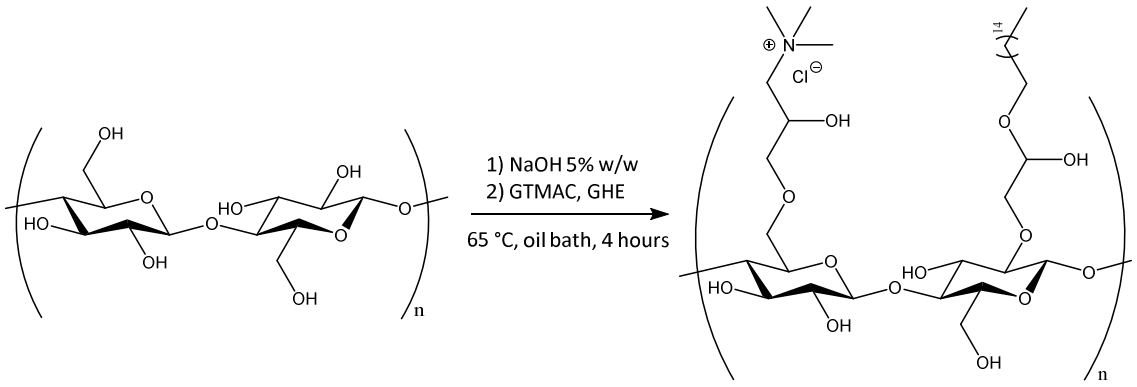

Figure 4.1 Chemical functionalisation of bacterial cellulose hydroxyl groups by reaction with GTMAC and GHDE

The reaction involved the use of two different epoxides, namely glycidyl trimethylammonium chloride (GTMAC) and glycidyl hexadecyl ether (GHDE) (**Figure 4.2**).

Figure 4.2 Chemical structure of a) GTMAC and b) GHDE

The functionalisation of the hydrogels was achieved through basic pre-treatment using 5% w/w NaOH with respect to cellulose (dry weight) for the deprotonation of the surface hydroxyl groups of cellulose. After this, the two epoxides were added to the reaction mix simultaneously. The reaction was performed in an aqueous environment due to the high percentage of water contained in the membranes as well as the solubility of the reagents and the catalyst. The procedure did not affect the integrity of the material, as no evident degradation occurred after the modification. The pellicles retained in fact their initial weight as well as the appearance, with no macroscopic change in colour or macrostructure.

4.2.2 Chemical characterisation

The functionalised cellulose was characterised in order to investigate the degree of substitution. In particular, due to the insolubility of cellulose in the majority of the solvents, the characterisation was carried out through the use of solid-state techniques. Firstly, energy dispersive X-ray spectroscopy was utilised to check the effective presence of the elements belonging to the functional groups introduced (**Figure 4.3**). The study did not allow to detect the incorporation of GHDE as carbon and oxygen were already present in the cellulose structure. However, the spectrum clearly showed the appearance of the peaks related to chlorine and nitrogen from the GTMAC reagent. Furthermore, although the EDX analysis is not quantitatively reliable, it was possible to observe that the intensity of the signals related to the chlorine and nitrogen atoms was much lower as compared to carbon and oxygen. This was probably ascribable to the functionalisation process that occurred at the surface of the hydrogel only, while the bulk material was composed of glucose chains containing carbon and oxygen atoms in large quantities.

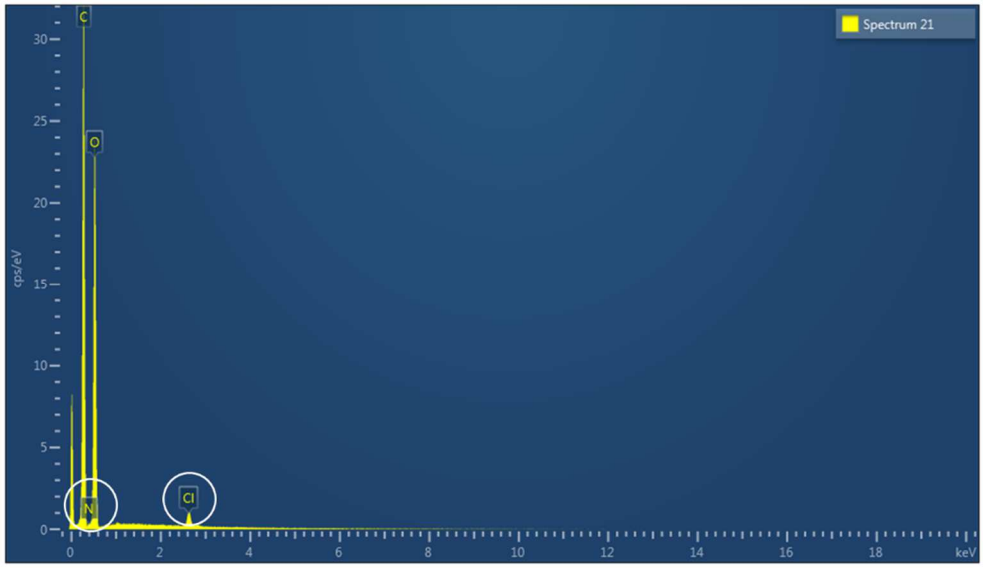

Figure 4.3 Energy-dispersive X-ray (EDX) spectrum of functionalised cellulose samples

In order to have a better understanding of the yield of the reaction, X-ray photoelectron spectroscopy was used to analyse the composition of plain cellulose and modified samples (**Figure 4.4**).

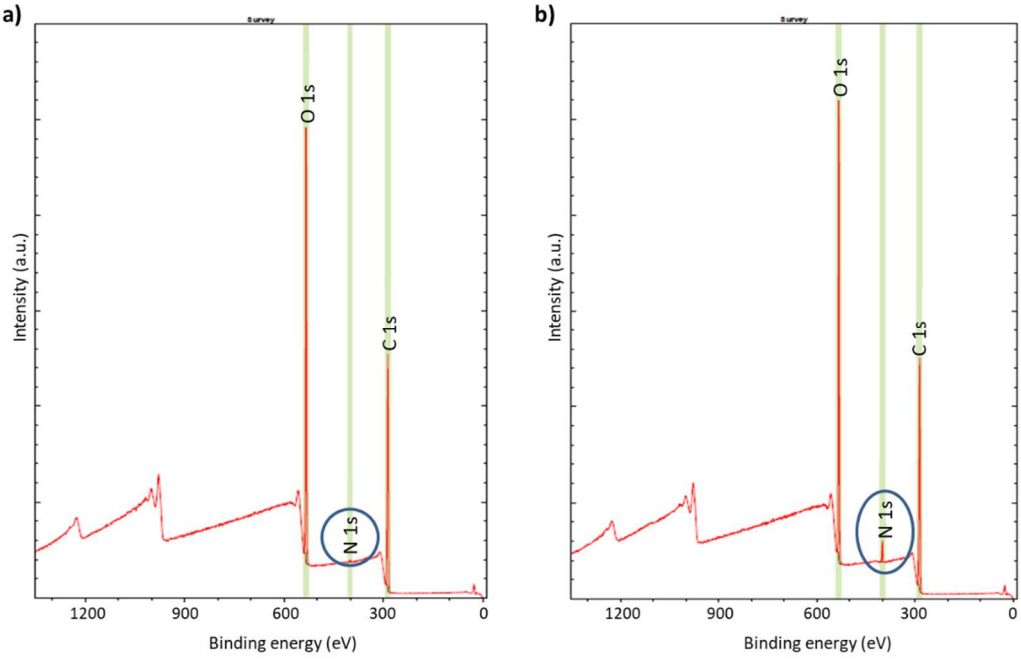

Figure 4.4 XPS spectra of a) unmodified and b) modified cellulose

The analysis allows to quantitatively assess the surface composition of the samples through determination of the energy of the photoelectrons emitted from

the surface upon irradiation with soft X-rays (generally 1-3 keV) in vacuum. In particular, the elemental distribution shown in the spectra refers to the chemical composition of the samples in the external 10-50 Å of the surface (Burrell, 2001). For this reason, the XPS was particularly suitable for the characterisation of the modified cellulose as the functionalisation occurred on the surface of the hydrogel at the interface with the liquid, where the reagents and the catalyst were dissolved. The quantification of the elemental composition for each sample was calculated through determination of the area of the spectral peaks (**Table 4.1**).

Table 4.1 Elemental analysis of non-functionalised and functionalised cellulose. The area of the peak related to each element is reported as well as its relative amount.

	Element	Area	Atomic %
Non-functionalised cellulose	O 1s	2386607.93	38.35
	C 1s	1303162.96	61.36
	N 1s	11008.54	0.29
Functionalised cellulose	O 1s	2072893.74	35.83
	C 1s	1215029.43	61.54
	N 1s	93556.40	2.63

An increase in the nitrogen content was detected upon functionalisation (from 0.29 to 2.63 of atomic percent) as a result of the introduction of the quaternary amino groups of GTMAC. Again, the amount of carbon and oxygen remained almost constant due to their predominance in the material. However, a decrease in the relative oxygen content was observed in the modified cellulose (from 38.35% to 35.83%), while the amount of carbon did not show any significant reduction. This result indicated the successful incorporation of GHDE. The reagent contains in fact long alkyl chains with a carbon to oxygen ratio of 9:1, whereas the ratio in glucose is 1.2:1, which is more similar to the ratio obtained for the unmodified sample (i.e. 1.6:1) as compared to the modified one (i.e. 1.7:1). The presence of nitrogen in the non-functionalised cellulose could be attributed to residual traces of the growth medium components or environmental-derived impurities.

4.2.3 Rheological properties

The mechanical properties of the bacterial cellulose pellicles upon functionalisation were assessed through evaluation of their viscoelastic behaviour. In particular, the rheological studies were carried out following the same protocols used for the analysis of the unmodified samples in order to obtain comparable results on the mechanical performance of the hydrogels. The storage and loss modulus (respectively, *G'* and *G''*) for frequency sweep and temperature ramp tests were determined and compared with the values previously obtained. As regards the frequency sweep assay, it was noted that even after the functionalisation the hydrogel retained a self-standing structure, with storage modulus higher than loss modulus at all the frequencies considered (**Figure 4.5**).

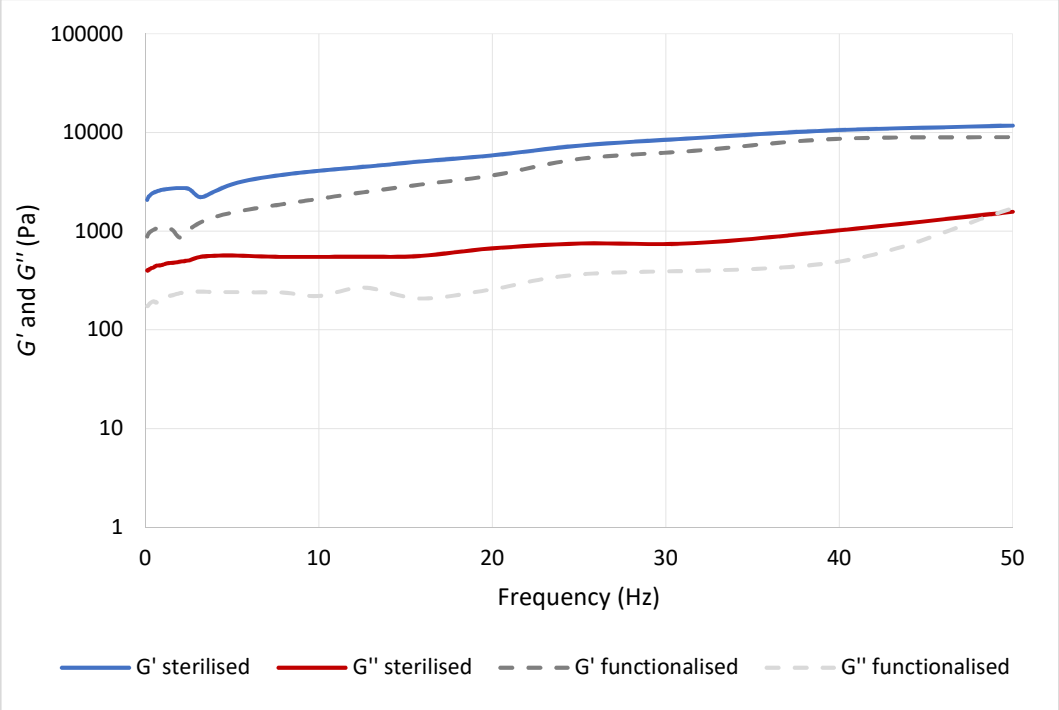

Figure 4.5 Frequency sweep test; T = 32 °C, preload = 6 Pa.

This is a crucial feature and the most important information obtainable from rheological measurements of biomedical materials, as a dressing needs to be easy to handle during the application. The two graphs exhibited a similar trend for both viscous and elastic moduli. In particular, *G'* increased proportionally with the frequency, while *G''* presented lower variation throughout the test. This

result means that the elastic component of the mechanical behaviour of the material was more affected by the increase in the shear rate, which is a typical feature of hydrogels. Although both samples exhibited a more elastic-like response to the stimuli, it was possible to observe that the functionalisation induced a slight decrease of the storage modulus from 2000 Pa in the case of pristine cellulose to almost 900 Pa for the modified sample at 0.1 Hz. The same tendency was noted at higher frequencies, where the maximum for the unmodified specimen was about 11700 Pa *vs* ≈ 9000 Pa for the modified one. As regards the viscous component of the behaviour, which is expressed by the loss modulus, for both hydrogels a linear increase of about 1000 Pa was detected from 0.1 Hz up to about 35-40 Hz. At higher rate, i.e. in the 40-50 Hz region, it was possible to observe a higher increase, especially in the case of the modified cellulose, with a final *G''* value of about 1570 Pa and 1700 Pa, respectively for the plain and the functionalised sample. These values indicated a more liquid-like response of the pellicles at higher oscillation frequencies.

The effect of the temperature variation on the viscoelastic properties of the hydrogels was then studied through temperature ramp assay, and both dynamic moduli were evaluated from 10 to 60 °C (**Figure 4.6**).

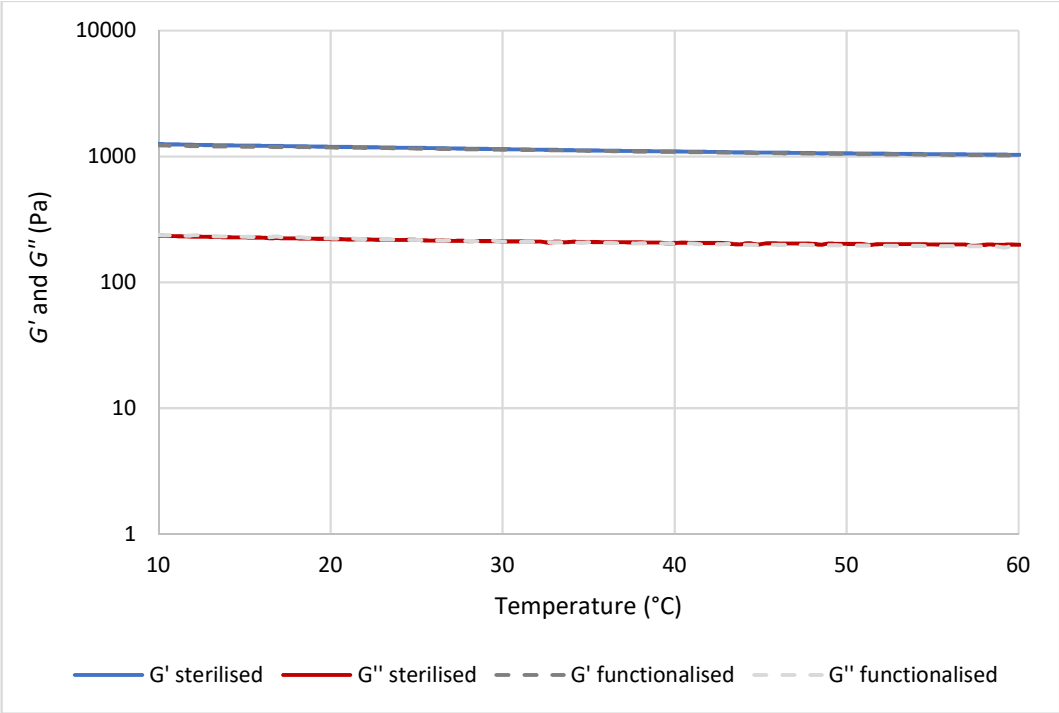

Figure 4.6 Temperature ramp test; f = 1 Hz, preload = 6 Pa, rate = 5°C/min.

In this case, there was no evident variation in both storage and loss moduli for the unmodified and modified samples. As for the frequency sweep, the hydrogels showed a solid-like behaviour ($G' > G''$) at all the temperatures considered, i.e. high resistance to deformation. Minimal decrease was observed in the storage modulus at low temperature after the reaction, with a value of 1230 Pa at 10 °C for the functionalised cellulose, whereas for the plain cellulose it was found to be almost 1260 Pa at the same temperature. The same trend was detected at higher temperatures, with values of about 1030 Pa and 1020 Pa, respectively, for the unmodified and modified pellicles. In both cases, a decrease of ≈17-18% in the storage modulus was registered with the increase in the temperature. This result indicated that the materials behaved more like a viscous liquid at higher temperatures, as expected for a solid. However, the presence of a high amount of water (i.e. 97%) did not have a massive effect on the mechanical properties, with the samples retaining a solid structure with good degree of stiffness up to 60 °C. As regards the loss modulus, the two hydrogels showed once again very similar behaviour, with only a slight decrease in the values at increasing temperatures (about 236 Pa to 200 Pa for the unmodified and about 237 Pa to 190 Pa for the

modified cellulose). This result indicated that there was no significant effect of the temperature on the viscous component of the mechanical behaviour, with minimal liquid-like response as compared to the solid-like (expressed by *G'*, which was much higher than *G''*). The assay confirmed that the functionalisation process did not adversely affect the 3D structure and the viscoelastic properties of the material, which maintained a solid network in the range of temperatures tested.

4.2.4 Stability studies

The effect of the functionalisation on the degradation of the pellicles was investigated through determination of the weight variation (ΔW) over time. In particular, the test was conducted both in PBS solution and keratinocytes growth medium at 32 °C, which is the average temperature of an acute wound-bed. The results were then compared with the values obtained for the unmodified hydrogel to detect any eventual variation in the stability (**Figure 4.7** and **Figure 4.8**).

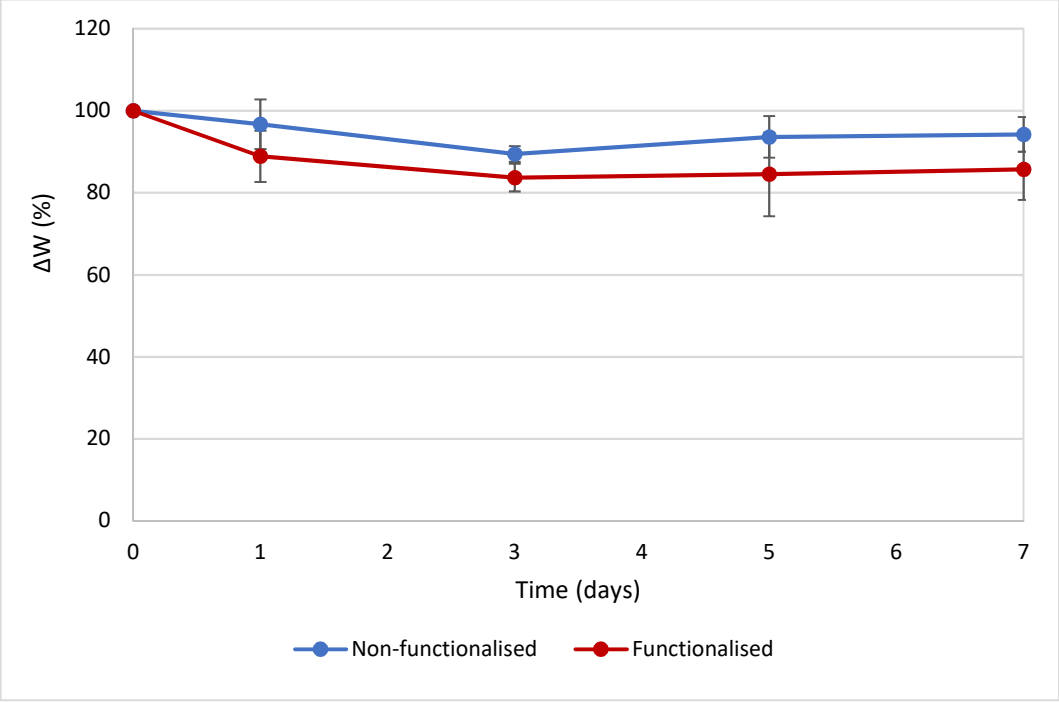

Figure 4.7 Stability of unmodified and modified bacterial cellulose samples in PBS solution at 32 °C under static conditions.

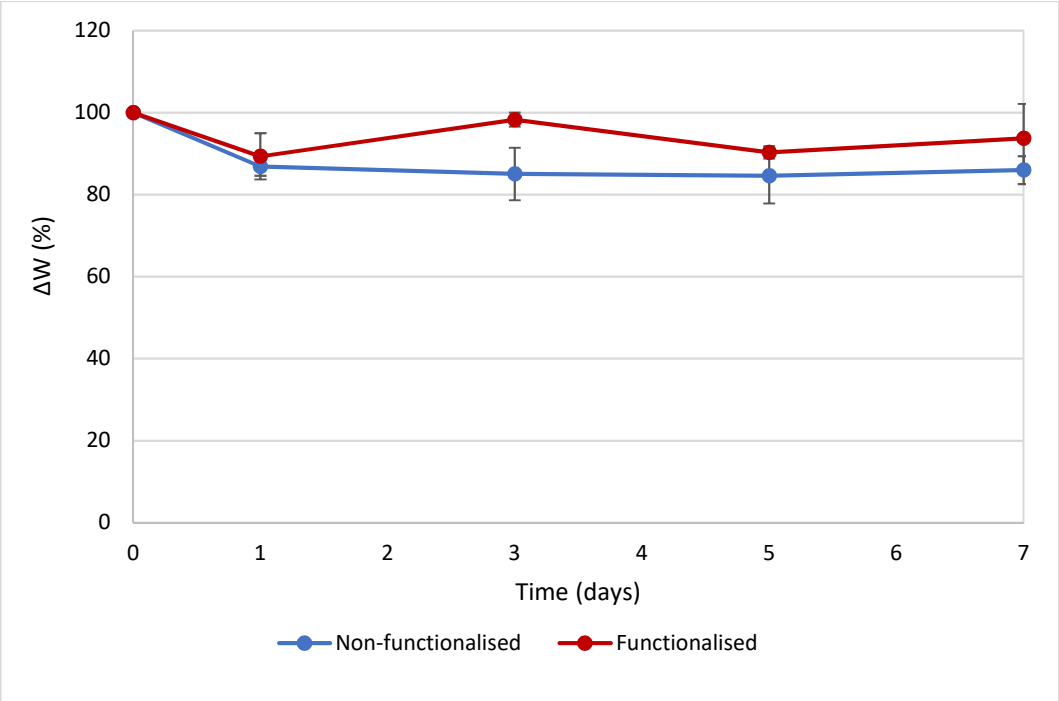

Figure 4.8 Stability of unmodified and modified bacterial cellulose samples in keratinocytes growth medium at 32 °C under static conditions.

The results suggested that the modification carried out on the pellicles did not massively affect the stability of the material over the time considered. As regards the behaviour in PBS solution, the functionalised sample showed a plateau in the weight after about 3 days, when it reached 85% of the initial wet weight. This value remained constant for up to 7 days after incubation in the medium. The weight of the unmodified hydrogel, on the other hand, showed a higher degree of variation over time. However, it was possible to note that after 3 days the sample lost about 10% of the initial weight, and the values remained very similar until day 7, with total weight loss of about 5-10%. Overall, the two materials did not show any statistically significant difference at any time point ($p>0.05$), proving that the weight variation followed the same trend. In the case of incubation in keratinocyte growth medium, the tendency appeared to be reverse, with the non-functionalised reaching a plateau in the weight after 3 days (final value: 85% of the initial weight). The weight of the functionalised cellulose decreased by 10% after 2 days of incubation, with a final weight of 90-93% as compared to day 0. Once again, the two sets of data did not differ significantly for the time points considered, with the only exception being day 3 ($p=0.01$).

4.2.5 Biological characterisation

4.2.5.1 Antibacterial activity evaluation

The modification carried out on BC was focused on the development of an inherently active hydrogel for wound healing applications. To achieve this, the surface modification of the pellicles was carried out through functionalisation of the hydroxyl groups. As confirmed by the characterisations performed, the antibacterial moieties introduced were found to be permanently attached to the glucose chains rather than physically incorporated in the matrix. In light of this, the killing capacity of the functionalised material upon direct contact was studied. Different methods, both qualitative and quantitative, were followed. Furthermore, two bacterial strains were used, i.e. Gram positive *Staphylococcus aureus* subsp. aureus Rosenbach 6538™ and Gram negative *Escherichia coli* (Migula) Castellani and Chalmers ATCC® 8739™.

First, the presence of bacterial cells after direct incubation with the unmodified and modified samples for 24 hours was qualitatively evaluated by SEM analysis. The images were acquired in different areas of the samples in order to have a complete overview of the survival rate of the bacteria on the specimens (**Figure 4.9**). It was possible to observe that the major part of the surface area of the modified cellulose appeared to be clear with almost no cells, apart from some colonised regions. This result could probably be ascribed to the inhomogeneity of the reaction due to the biphasic conditions required by the insolubility of the membranes. Despite this drawback, a much lower number of cells was detected on the functionalised sample, confirming the successful inclusion of the antibacterial groups.

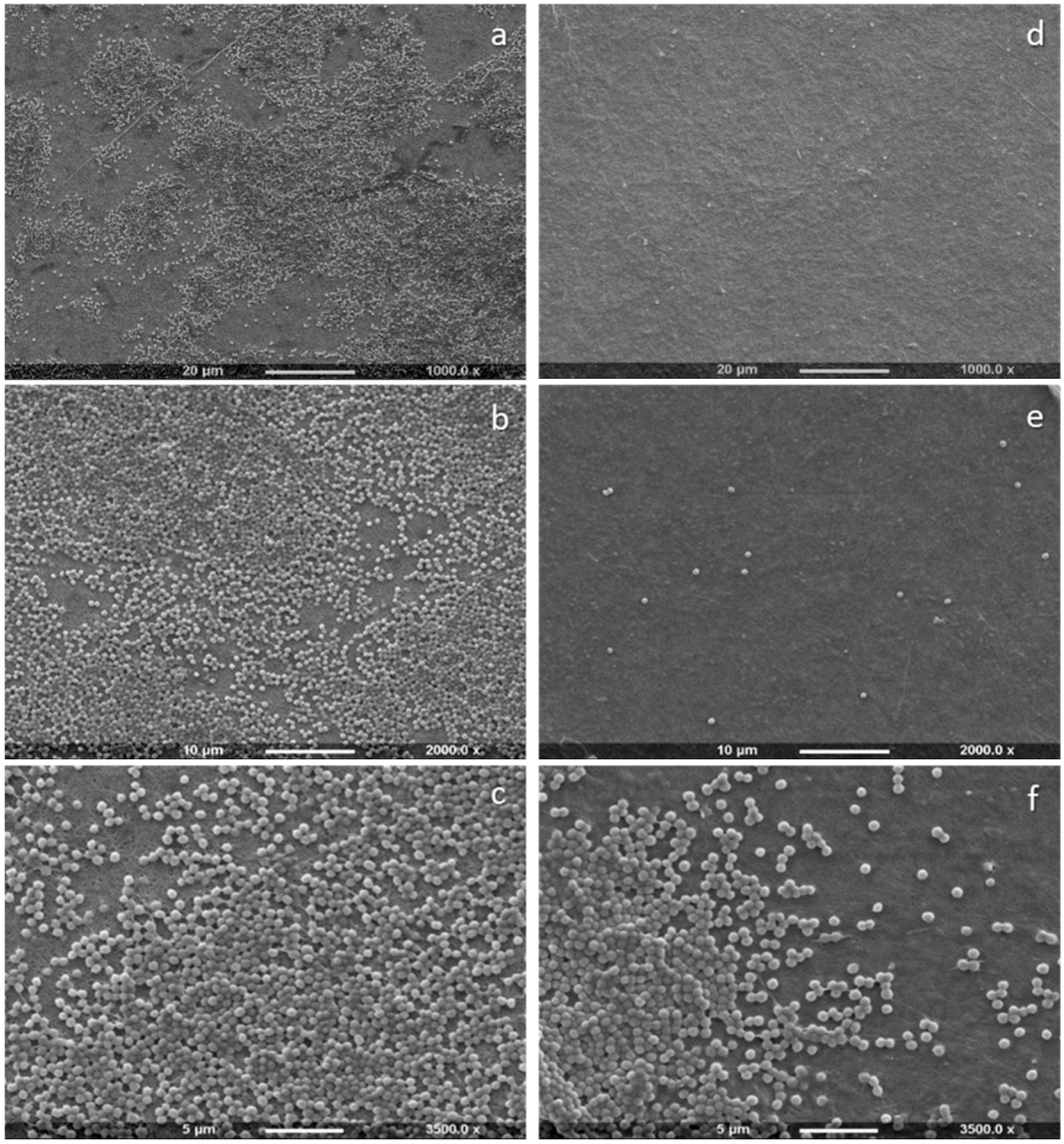

Figure 4.9 SEM images of non-functionalised BC (a, b and c) and functionalised BC (d, e and f)

The bacterial cell viability after incubation with the cellulose samples was then studied using a LIVE/DEAD™ *Bac*Light™ Bacterial Viability Kit. Propidium iodide (PI), a red-fluorescent nucleic acid stain that diffuses through damaged membranes was used to detect dead cells together with SYTO® 9, a green-fluorescent nucleic acid stain able to penetrate bacteria with both intact and damaged membranes. Since its fluorescence is reduced in the presence of PI (i.e. in case of dead cells), SYTO® 9 is only visible in case of live cells, which are therefore stained green. The cells were recovered from the samples after incubation for 24 hours and visualised using a confocal microscope (**Figure 4.10**).

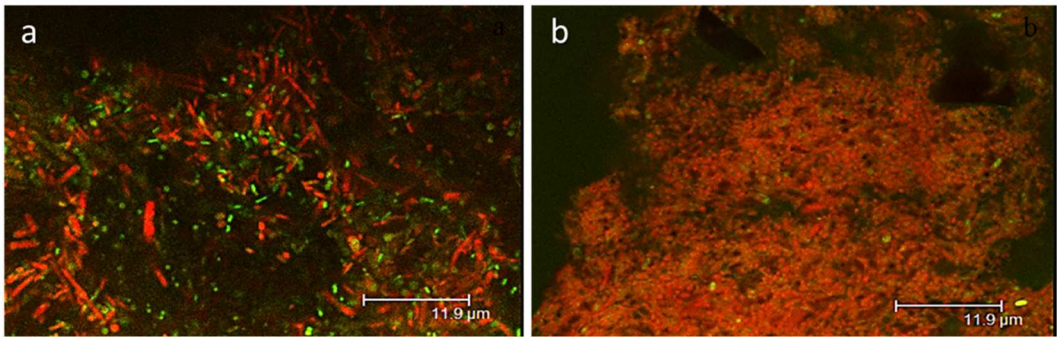

Figure 4.10 Live/dead viability assay performed on the bacterial cells recovered from a) non-functionalised and b) functionalised cellulose samples after 24 hours of incubation. The cells were transferred on a glass slide and imaged using a set of FITC and Texas Red filters.

The images showed a massive predominance of dead bacteria among the cells recovered from the modified cellulose sample, whereas a higher number of cells was found to be alive after contact with the unmodified pellicle. Such difference indicated that the functionalisation had an adverse effect on the viability of bacteria upon direct contact. Moreover, the cells seeded on the surface of the plain cellulose specimen displayed two different morphologies, i.e. round-shaped and rod-shaped. The round-shaped morphology is typical of *cocci*, a class of bacteria that includes the *Staphylococcus aureus* strain. From the analysis, these cells appeared to be stained green, which means that they survived after the incubation period. The rod-shaped cells, on the other hand, characterise the *bacilli*, and, in this case, were identified as *Gluconacetobacter xylinus* JCM10150 (the BC-producing strain). It is possible that some residual *Gluconacetobacter xylinus* cells were still present in the pellicle, as they excrete the fibres in the environment surrounding the membrane, thus embedding themselves in the matrix. However, it should be noted that the purification/sterilisation treatment successfully killed such bacteria, as confirmed by the red-coloured staining. The images related to the modified sample, on the other hand, did not show any green-stained cell, indicating that they were no longer alive after contact with the antibacterial surface of the hydrogel.

A quantitative evaluation of the antibacterial properties of the membrane was performed using a slightly modified ISO22196 protocol. This standard procedure allows in fact the determination of the activity upon direct contact against specific

Staphylococcus aureus and *Escherichia coli* strains. The assay involved the seeding of the bacterial inoculum at known cell concentration directly on the surface of the samples. After 24 hours, the cells were retrieved by washing the specimens with PBS solution and quantified through drop plate technique (Naghili *et al.*, 2013). The average number of viable cells recovered after incubation was determined considering the dilution factor and the surface area of the material. The test was first conducted against *S. aureus*. The antibacterial activity (R) was then calculated using the formula below, as indicated in the protocol:

$$R = log(a)[non - functionalised] - log(a)[functionalised] = 0.32 \pm 0.04$$

The percent antibacterial activity ($R\%$) was also determined as follows:

$$R(\%) = \frac{a(T24)Non-functionalised - a(T24)Functionalised}{a(T24)Non-functionalised} * 100 = (53 \pm 11)\%$$

where a is the number of bacterial cells recovered from each specimen after 24 hours of incubation (CFU/mL*cm^2).

The results showed that the number of cells growing on the surface of the modified pellicle was reduced by more than half as compared to the unmodified one, with a statistically significant reduction of about one order of magnitude in the bacterial population after 24 hours.

The test was also performed against an *Escherichia coli* strain to evaluate the antibacterial properties of modified cellulose against Gram negative bacteria. The same ISO22196 procedure was used to quantify the antibacterial efficiency, and similar results were obtained. The R and $R\%$ were determined using the same formulae as for the *S. aureus*:

$$R = log(a)\,[non - functionalised] - log(a)\,[functionalised] = 0.25 \pm 0.08$$

$$R(\%) = \frac{a(T24)Non-functionalised - a(T24)Functionalised}{a(T24)Non-functionalised} * 100 = (43 \pm 11)\%$$

where a is the number of bacterial cells recovered from each specimen after 24 hours of incubation (CFU/mL*cm^2).

Although the decrease in the bacterial cell count was lower as compared to the Gram positive bacteria, it was observed that, once again, a reduction by almost half in the number of cells seeded on the surface of the hydrogel was achieved

after 24 hours. The difference between the unmodified and the modified samples was found to be statistically significant ($p<0.05$), indicating that the functionalisation successfully inhibited the bacterial growth. This result was particularly important, as Gram negative bacteria are usually characterised by a higher degree of resistance to traditional antibiotics, typically because of the presence of the external additional layer (outer membrane) that makes it much more difficult for the bactericidal agent to access the cell.

Overall, the assay showed that the material induced a significant decrease in the proliferation of both Gram positive and Gram negative bacteria as a result of the functionalisation performed, making the hydrogel a suitable substrate for the development of an inherently active antibacterial wound dressing.

4.2.5.2 Cytotoxicity studies

The biocompatibility of the cellulose pellicles (both plain and after functionalisation) was assessed through determination of the indirect and direct cytotoxicity. Normal human keratinocyte type cells were used in this study, as the hydrogel was intended for applications in wound healing. First, the indirect cytotoxicity was determined by quantitative evaluation of the cell viability in the medium incubated for 24 hours with the samples (**Figure 4.11**). This test was performed in order to investigate if any leachable product released from the membranes would result in an adverse effect on the cellular growth.

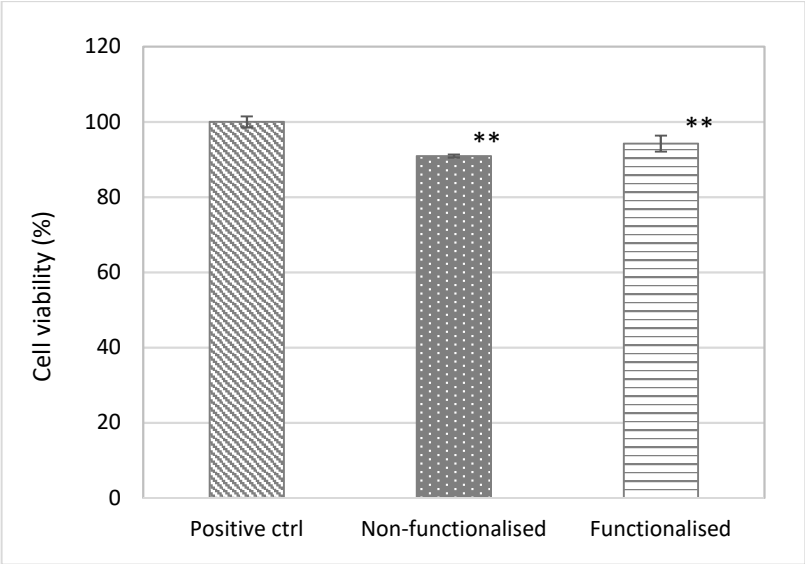

Figure 4.11 Viability of HaCat cells upon contact with undiluted eluates from the BC samples. Positive control: keratinocytes growth medium. The non-functionalised and the functionalised samples were found to be significantly different as compared to the positive control (**=$p<0.01$), whereas no statistically relevant difference was observed between the non-functionalised and the functionalised cellulose.

The results of the Alamar Blue assay showed a great degree of biocompatibility for both samples, with cell viability values higher than 90%. Furthermore, no statistically significant difference was observed between the unmodified and the modified pellicle, indicating that the functionalisation performed did not introduce any leachable compound that caused a cytotoxic effect on keratinocytes.

The direct cytotoxicity of the hydrogels was then evaluated following a standard method (ISO 10993-5) for the biological evaluation of medical devices. The cells were put in direct contact with the samples and the viability was evaluated after 1, 3 and 6 days by Alamar Blue assay (**Figure 4.12**).

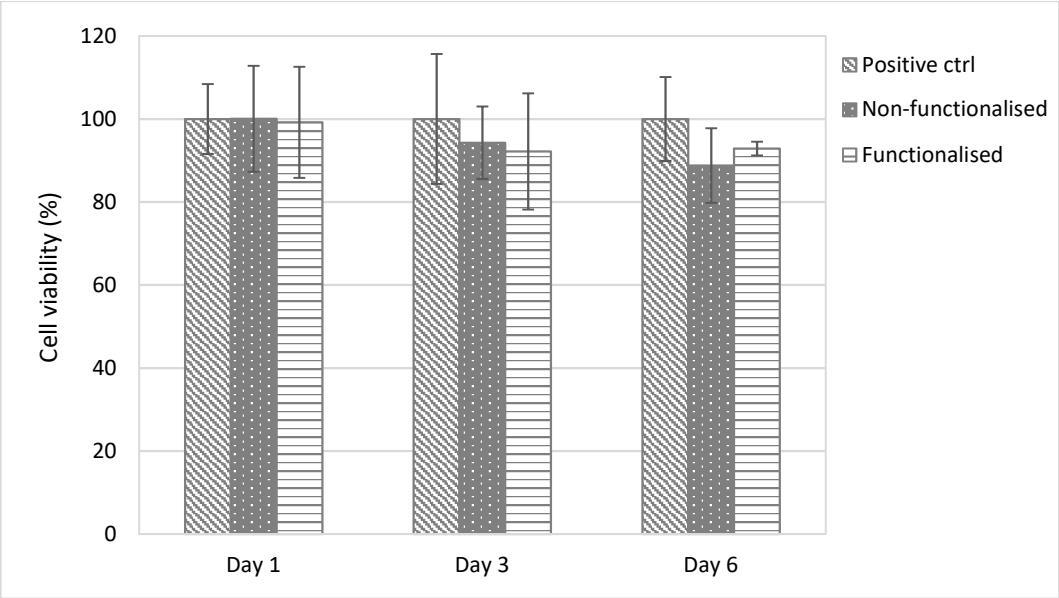

Figure 4.12 Viability of HaCat cells upon direct contact with the BC samples. Positive control: keratinocytes growth medium. No statistically significant difference was observed between the cellulose samples and the positive control at any time point ($p>0.05$).

The assay confirmed the results previously obtained for the cytotoxicity upon indirect contact. On day 1, both samples showed ≈ 100% cell viability, with no statistically significant difference as compared to the positive control ($p>0.05$). On the third day, the viability was found to be higher than 90% (respectively, 94% and 92% for the unmodified and modified pellicles). After 6 days of incubation with the samples, the cell viability was almost 90% for the neat cellulose and about 93% for the functionalised one. In particular, no statistically significant difference was observed between the two materials and the positive control at any of the time points considered. The cellulose pellicles showed a great degree of biocompatibility, comparable with the positive control even after direct contact for long periods, indicating that the modification performed did not alter the biological properties of the substrate towards eukaryotic cells.

The morphology of the cells after 6 days of direct contact with the hydrogels was then evaluated through fluorescent staining of nuclei and actin filaments with, respectively, DAPI and phalloidin and compared to the control group. The images were acquired using a confocal microscope after fixation of the samples (**Figure 4.13**).

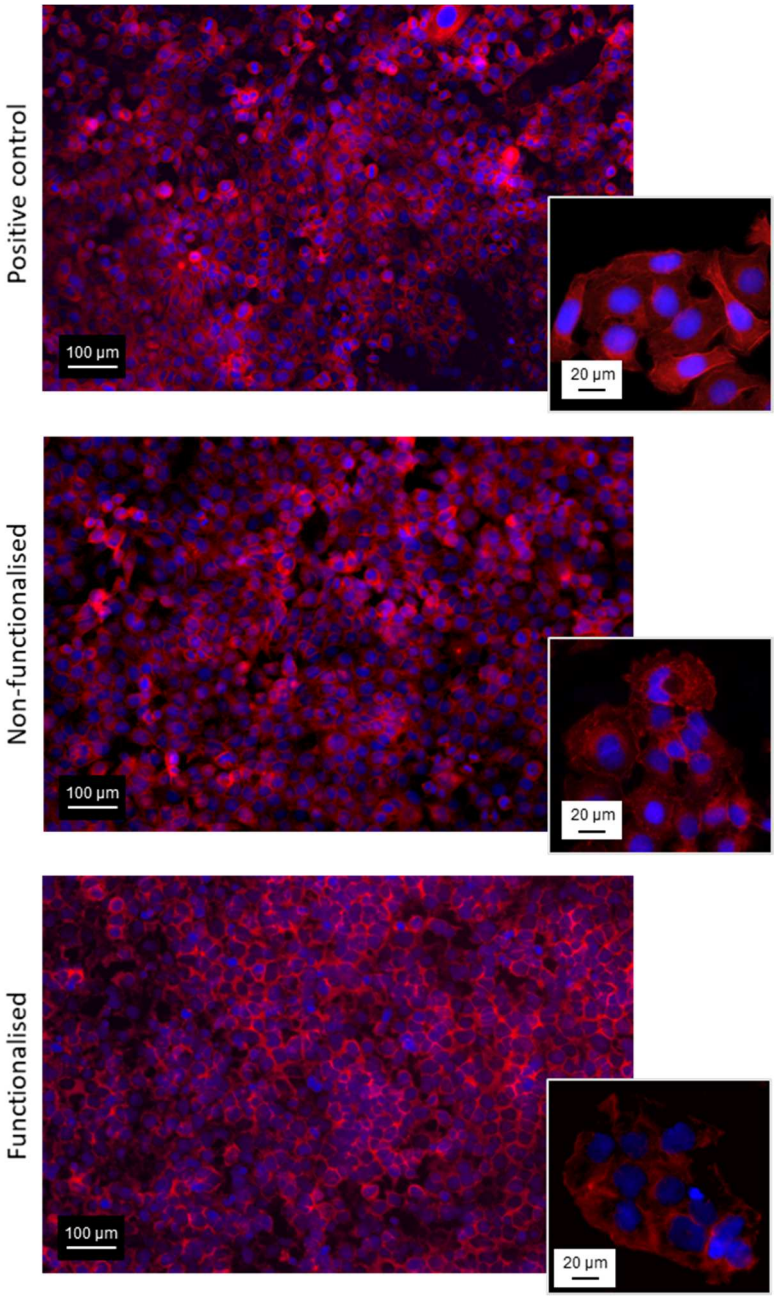

Figure 4.13 Confocal microscopies of keratinocytes after 6 days of incubation with cellulose stained using phalloidin/DAPI

All the images showed the presence of a homogeneous monolayer of adherent keratinocytes. No qualitative difference in the morphology was observed for the three groups, confirming that the presence of cellulose (both before and after functionalisation) did not negatively affect the growth and proliferation of the cells. In particular, a polygonal morphology typical of keratinocytes was detected, and the cells appeared to be arranged in a 'cobblestone' pattern. The nuclei appeared to be spherical, surrounded by a homogeneous cytoplasmic

region. The size and structure of the cells was found to be the same for the ones in contact with the samples and for the positive control, with an average diameter of about 15-20 μm.

The wound healing capacity of the hydrogels was then investigated by performing an *in vitro* scratch assay using keratinocyte cells. This test allows to evaluate the migratory and proliferative potential of cells without and in the presence of cellulose samples by creating a scratch in the cell monolayer and observing the cells behaviour over time until wound closure. The wound margins were monitored over 7 days until complete closure of the scratch. The images showed that for both samples as well as the positive control almost complete closure was observed after 5 days. The presence of the two hydrogels did not inhibit cell migration to the site of the wound, and the recovery rate was found to be very similar for the three conditions. After two days, the scratch area appeared to be covered with keratinocytes, proving that the cells were alive and active from both proliferative and migratory point of view (**Figure 4.14** and **Figure 4.15**).

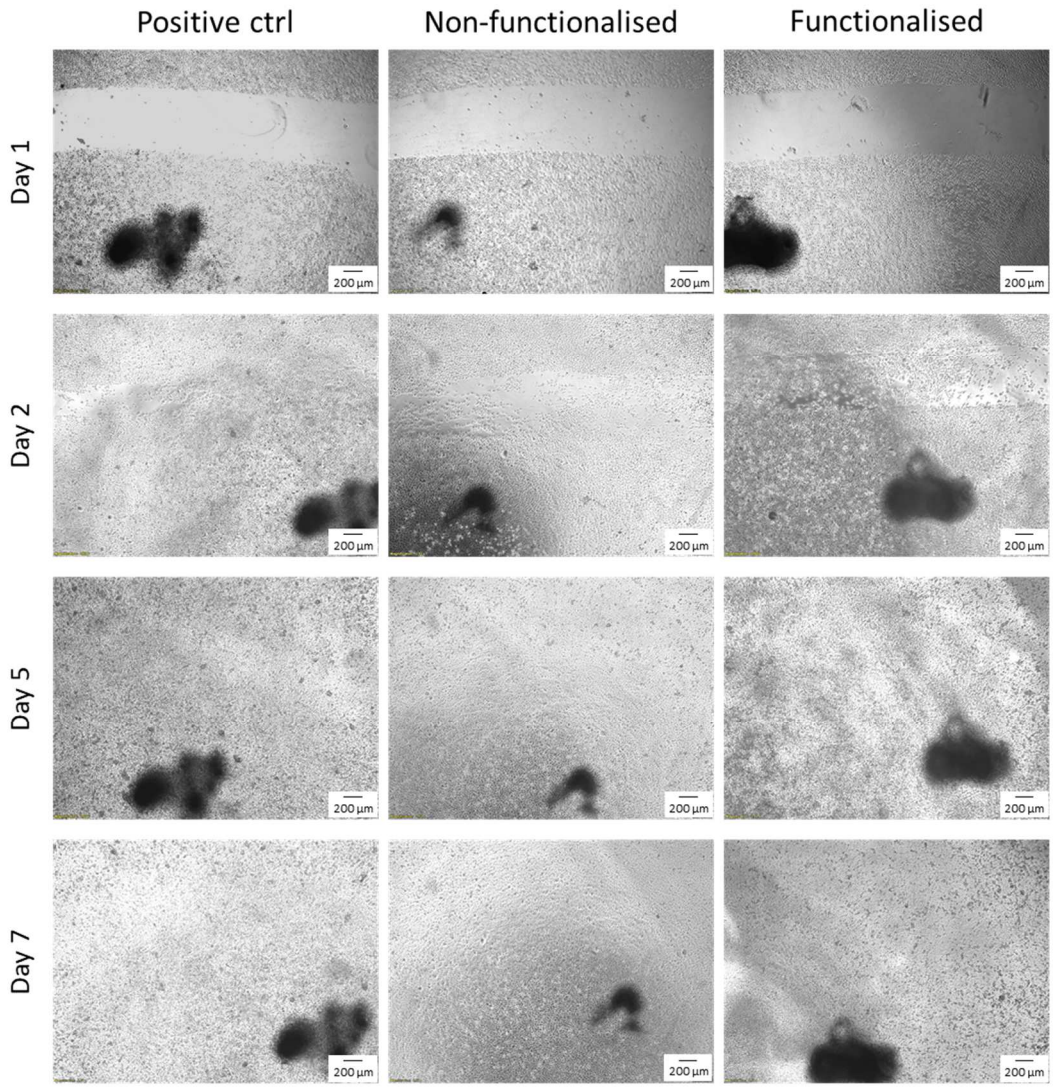

Figure 4.14 *In vitro* scratch test at different time points (40x). The black mark in the images is the reference for the scratch. Positive control: keratinocytes growth medium

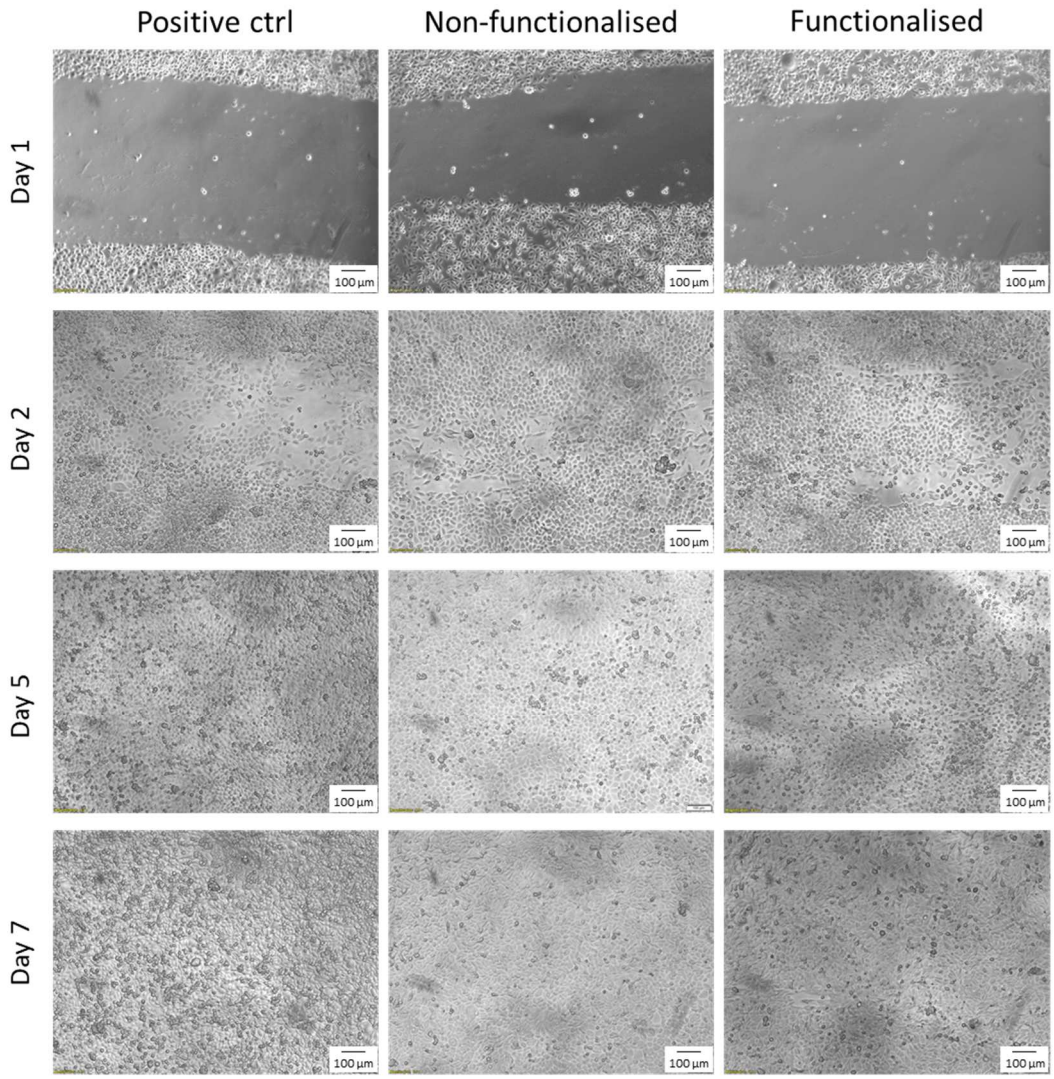

Figure 4.15 *In vitro* scratch test at different time points (100x).
Positive control: keratinocytes growth medium

After a first qualitative assessment, the images were analysed in order to evaluate the rate of the wound closure in the presence of unmodified and modified cellulose as compared to the positive control. The percent of the scratch covered by the cells was quantified using an image processing programme that allowed to distinguish between the area covered by cells (simplified as white pixels) and the area not covered by cells (black pixels) (**Figure 4.16**).

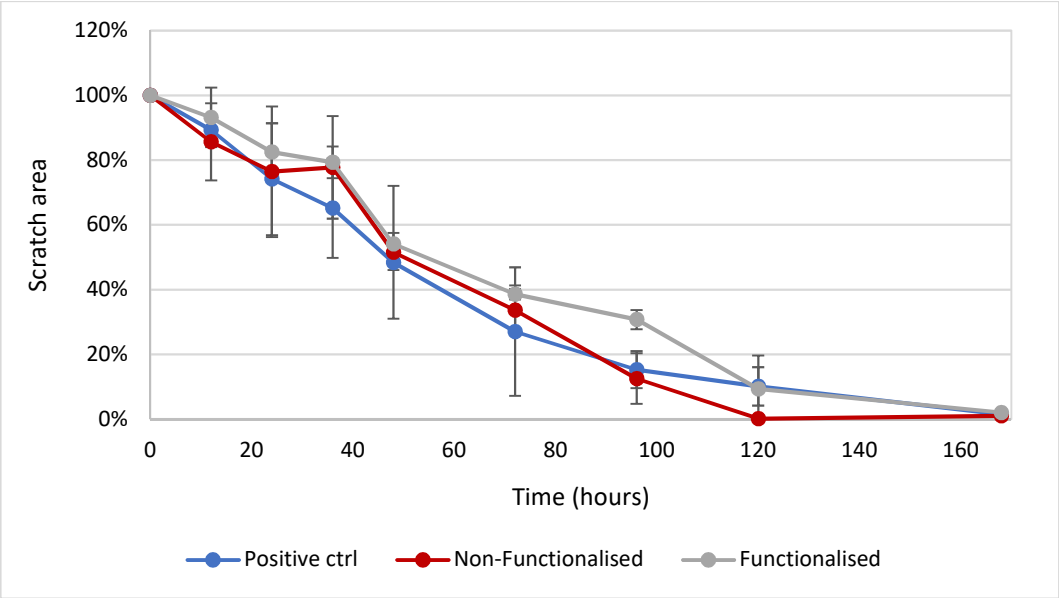

Figure 4.16 Evaluation of the scratch area over time as the ratio between black pixels at time x and black pixels at time 0 (set as 100%, i.e. no coverage by cells).

The graph highlighted that the wound progression in the presence of the cellulose samples and the positive control followed similar trend, with almost total coverage of the damaged area by the cells after 5 days of incubation. In particular, for the unmodified cellulose group 100% of wound closure was reached, whereas both the modified and the positive control presented a value of 90%. The statistical analysis carried out for each time point showed no significant difference between the two hydrogels and the control, with $p<0.05$ only in the case of the functionalised material at 96 hours ($p=0.045$ for functionalised *vs* control and $p=0.031$ for functionalised *vs* non-functionalised). This was calculated both for singular time points and for the whole set of data. Overall, for the three groups a linear decrease of the scratch area was observed up to 5 days, showing that the proliferation and migration rate of keratinocytes was not affected by the presence of the pellicles.

4.3 Discussion

This chapter focused on the production of an inherently antibacterial hydrogel based on bacterial cellulose through surface modification. In particular, a chemical derivatisation of the hydroxyl groups of cellulose was carried out in

order to obtain a wound dressing with bactericidal activity upon direct contact. The material was also characterised with respect to its chemical, mechanical and biological properties.

Two different reagents were used to attach antibacterial functionalities to the polymer backbone, i.e. glycidyl trimethylammonium chloride (GTMAC) and glycidyl hexadecyl ether (GHDE). The two compounds were selected because of the presence of an epoxide ring in their structure as well as that of an antibacterial moiety. GTMAC is in fact an epoxide containing a cationic quaternary ammonium group. As discussed in the introduction to this chapter, quaternary ammonium groups are efficient antibacterial compounds that have been widely studied for application in various fields including water disinfection, textiles and biomedical, especially in the context of polymers modification. In particular, the reagent presents a tetraalkylammonium salt moiety, with a chloride as the negative counterion. The second reagent, GHDE, was introduced in the reaction mix with a ratio of 1:3 as compared to the GTMAC. This was chosen as a hydrophobic platform for the delivery of the biocidal residues through the lipid membrane of bacteria (Zhao and Sun, 2008).

The surface modification of cellulose to introduce quaternary ammonium groups was investigated by Salajkovà *et al.* in 2012. The study, however, focused on the treatment of nanocrystalline cellulose as a colloidal dispersion obtained through acidic hydrolysis of softwood pulp (Salajková, Berglund and Zhou, 2012). In this research, a similar approach was used for the introduction of antibacterial groups through heterogeneous reaction in order to maintain the hydrogel-like structure of bacterial cellulose membranes. The functionalisation of the pellicles was carried out via base-catalysed ring-opening reaction in the presence of sodium hydroxide. The reaction consisted in the alkylation of the oxygen, resulting in etherification of the hydroxyl groups. The process involved a pre-treatment of the hydrogel with a base to achieve the deprotonation of the surface hydroxyl groups of glucose followed by simultaneous addition of the two epoxides. The reaction is believed to proceed as a regioselective nucleophilic attack (probably

via S_N2 mechanism) of the oxygen to the less hindered electrophilic carbon of the epoxide ring (Padwa and Murphree, 2000; Smith, 2010).

The main drawback of the aqueous-based functionalisation performed in this research is the low degree of substitution due to the competition with water, in particular, the hydrolysis of the alkylating agent in basic conditions (Salajková, Berglund and Zhou, 2012). This was confirmed by the low amount of nitrogen detected in the structure through EDX and XPS analyses of the material. On the other hand, as also indicated by the carbon to oxygen ratio of the samples before and after modification, it was possible to observe that the two epoxides were successfully introduced in the matrix. Moreover, prior to the characterisation, the pellicles were thoroughly washed for several hours under shaken conditions until neutral pH was reached in order to ensure the complete removal of any unreacted reagent not covalently bound to the substrate.

As regards the mechanical properties of the material, rheological assays were carried out to assess the effect of the functionalisation on the viscoelastic behaviour of the hydrogel. As previously described in chapter III, the storage and loss moduli of the specimens was measured as a function of the frequency and temperature variations through frequency sweep and temperature ramp assay, respectively. Both analyses highlighted the solid-like behaviour of the materials, which behaved as self-standing hydrogels ($G' > G''$) under all the conditions considered. The frequency sweep test resulted in very similar behaviour for the two samples, with a significant increase of the storage modulus as a response to higher oscillation rate, whereas the loss modulus (which refers to the viscous component) did not exhibit the same degree of variation in the range of frequencies applied. As already discussed, this is a typical feature of hydrogels, which present increasing solid-like response in a directly proportional manner to the frequency. In particular, the storage modulus values showed a decrease in the case of the modified sample especially at low frequencies, probably ascribable to the high temperature and basic treatment required for the reaction that resulted in a slight degradation of the structure. The same tendency was noted for the loss modulus, although the maximum G'' observed for the unmodified

was 1570 Pa *vs* 1700 Pa for the modified one at 50 Hz. Nevertheless, even after the functionalisation, the hydrogel retained an elastic-like behaviour with good degree of stiffness. The properties of the materials upon temperature variation were also evaluated. In this case, no significant variation was observed between the two specimens, with very similar values for both dynamic moduli in the entire range considered. The storage modulus showed in fact 1-2% variation between the samples, confirming that the treatment did not have any adverse effect on the elastic component of the mechanical behaviour of the pellicle upon temperature increase. The same result was obtained for the measurement of the loss modulus, with only slightly higher values for the unmodified cellulose. Overall, the membranes retained good mechanical properties with highly solid-like response up to 60 °C, which is a crucial feature in order to have easy to handle and self-sustaining dressings suitable for commercialisation and clinical application.

The weight variation of the hydrogels in liquid media was also studied over 7 days. For both samples, an average 85-90% of the initial weight was retained in PBS solution and keratinocytes growth medium with no statistically relevant difference between them at any time point. This result confirmed that the modified pellicles constitute a suitable material to be used for wound healing applications thanks to their mechanical properties as well as stability over time.

Finally, a biological characterisation was carried out in order to investigate the effect of the functionalisation towards both prokaryotic and eukaryotic cells. First, the antibacterial efficiency was evaluated against Gram positive and Gram negative strains. All the assays were performed by determination of the activity upon direct contact of the bacteria with the samples. This approach was adopted because no leachable compounds were introduced in the matrix, as the antibacterial groups were incorporated via covalent bonding with the polymer backbone. A preliminary assessment was conducted by qualitative evaluation of the cell proliferation and viability after direct contact of a *Staphylococcus aureus* strain with the samples. The cells were seeded on the surface of the hydrogels (both unmodified and modified) and incubated for 24 hours; after this time, the

presence of the bacteria was visually studied through SEM analysis. The images clearly showed that the treated membrane presented a lower number of cells, probably as a result of the antibacterial effect of the groups attached to the glucose chains. However, it was possible to observe the presence of some colonised regions even on the surface of the functionalised sample. This was probably due to the inhomogeneous derivatisation of the hydroxyl groups, which resulted in anisotropy in the bactericidal efficacy. Heterogeneous reactions present in fact some limitations as compared to the homogeneous ones. Specific parameters must be taken into account for solid-liquid phase interactions, such as the surface area of the solid as well as its morphology (including shrinking, porosity, defects and phase change). This is extremely important, as the surface area might not be entirely reactive and accessible to the reactant dissolved in the liquid phase. Furthermore, mass and heat transfer kinetics need to be considered. In particular, the diffusion of the particles is regulated by several factors, such as mass, concentration and temperature, which affect the rate of the reaction (Ramsden, 2011; Salmi *et al.*, 2013).

The viability of the bacterial cells after direct contact with the hydrogels was then studied using a live/dead bacterial staining based on propidium iodide (red) and SYTO® 9 (green). The assay highlighted that the bacteria incubated with the functionalised sample appeared to be mostly dead after 24 hours, whereas in the case of the non-functionalised, green (viable) cells were observed by confocal microscopy. This result confirmed that the surface modification carried out on the cellulose hydrogel negatively impacted not only the proliferation but also the viability of the bacteria seeded on the sample. In addition to this, on the surface of the unmodified membrane it was possible to detect the presence of two cell morphologies, i.e. round and rod shaped, clearly belonging to two different strains. In particular, the round-shaped cells were stained green, meaning that the *S. aureus* (which is a *coccus* round-shaped strain) survived upon direct contact with plain cellulose. The rod-shaped cells, on the other hand, were attributed to *G. xylinus*, the strain used for the production of the pellicles. The cellulose production is in fact achieved through secretion of the fibrils from pores located

on the membrane, resulting in the cells being completely embedded in the matrix and, therefore, difficult to remove (Benziman *et al.*, 1980; Kondo *et al.*, 2012). On the other hand, these bacteria appeared to be dead, probably as a result of the high-temperature alkaline purification treatment to which the pellicles were subjected before the functionalisation.

A quantitative study of the antibacterial efficiency was also carried out by adapting a standard ISO test (ISO22196) for the evaluation of the activity upon direct contact. The assay was performed against *S. aureus* and *E. coli* in order to investigate the effect of the antibacterial groups on both Gram positive and Gram negative strains. The results were quite similar, with a promising 53% decrease in the bacterial cells count for the *S. aureus* and 43% in the case of *E. coli* for the modified as compared to the unmodified sample. The lower activity towards Gram negative strains could be ascribed to the difference in the cell membrane as compared to the Gram positive ones. The external structure of Gram negative bacterial cells presents in fact an additional external layer known as outer membrane, which is mainly composed of glycolipid lipopolysaccharides and glycerol phospholipids. This functions as a barrier against toxic compounds such as antibiotics and, more generally, any biocide (Miller, 2016). Because of this structural feature, Gram negative bacteria are considered as a threat in the medical world as they develop much higher resistance towards traditional treatments. In this context, there are a few antibacterial substances that proved to be effective even against Gram negative strains. Among these, quaternary ammonium containing compounds have been found to be active towards a broad spectrum of microorganisms. As mentioned in the introduction to this chapter, their mechanism of action is believed to rely on the electrostatic interaction between the cationic ammonium group and the negatively charged bacterial cell wall. After this first attraction, the lipophilic alkyl chains of such groups are able to penetrate through the hydrophobic bacterial membrane, causing its disruption. In particular, it has been observed that high concentrations of quaternary ammonium groups can solubilise cell membrane components through formation of micellar aggregates or act through denaturation of

structural proteins and enzymes. In addition to this, the non-selectivity of the attack makes it more difficult for bacteria to develop resistance towards cationic ammonium groups, as this would require a structural modification of their cell wall (Buffet-Bataillon *et al.*, 2012; Jennings, Minbiole and Wuest, 2015).

The biocompatibility of the materials was investigated both via direct and indirect cytotoxicity assay towards keratinocytes. As regards the indirect assay, the two hydrogels were first incubated with the culture medium for 24 hours. After this time, the eluates were transferred to a multi-well with previously seeded cells and their viability was measured after further 24 hours. For both materials, more than 90% of the cells was found to be viable as compared to the positive control, proving that no toxic substances were released from the matrix in the interval considered. A direct cytotoxicity study was then conducted using the same cell line over a period of 6 days, as the average frequency of the dressing change in case of hydrogels has been indicated as 1-3 days (Purser, 2010; Sood, Granick and Tomaselli, 2014). Once again, the cell viability was found to be ≥90% even after 6 days of incubation, proving that the contact with the samples did not affect the viability of the keratinocytes. Furthermore, no statistically significant difference was observed between the two groups and the positive control at any time point ($p>0.05$). The results are in line with previously published studies, confirming that quaternary ammonium compounds do not adversely affect the cell viability upon contact. In particular, it has been observed that quaternisation of various polymers including chitosan (Peng *et al.*, 2010), polyethyleneimine (Milović *et al.*, 2005) and poly(ethylene glycol) methacrylate (Stratton, Rickus and Youngblood, 2009) resulted in highly antibacterial effect without inducing significant cytotoxic effects. After 6 days of incubation with the samples, the cells were fixed and stained using DAPI (for the nuclei) and phalloidin (for the cytoplasm) in order to evaluate their morphology. All the groups (i.e. positive control, non-functionalised and functionalised cellulose) presented an adherent monolayer of keratinocytes showing the polygonal morphology typical of keratinocytes and a 'cobblestone' pattern of growth (Koehler *et al.*, 2011). The diameter of the cells was in the range of 15-20 μm, which is in line with previously

published data (Sun *et al.*, 2007). More specifically, it was observed that young keratinocytes cultures were characterised by regular shape and smaller size, whereas at late passages they assumed an irregular morphology and larger size (up to 50 μm) (Soroka *et al.*, 2008).

The wound healing ability of keratinocytes in the presence of the cellulose-based hydrogels was evaluated through an *in vitro* scratch assay. The results showed that the progression of the wound followed the same trend for the control and the two samples, with no statistically significant difference between the three groups at any time point. After 5 days, the scratch appeared to be almost completely closed for all the samples, with 90-100% coverage of the damaged area by the cells. Furthermore, after only 12 hours 10-15% of the wound area was already repopulated, confirming that the cells were viable and migrating. The rate of wound closure observed in this study was found to be in the same range as previous studies, therefore the presence of the pellicles did not affect the normal healing process. Keratinocytes are in fact believed to start migrating after 6 to 24 hours upon wounding and begin to express keratin after 8-24 hours. This is of crucial importance, as the migration of cells to the site is a rate limiting event in wound healing. In particular, it has been proven that keratinocytes have lower migration rate as compared to dermal fibroblasts. Previous studies suggested in fact that fibroblasts are the first cell type to migrate together with endothelial cells. After this, keratinocytes move to the area to initiate the re-epithelialisation, which is then followed by a last migratory phase of fibroblasts for tissue remodelling, the last stage of wound healing (Usui *et al.*, 2008; Walter *et al.*, 2010).

4.4 Conclusions

In this chapter, the development of an inherently active antibacterial wound dressing based on bacterial cellulose was reported. As cellulose lacks intrinsic bactericidal properties, a derivatisation of its surface hydroxyl groups was carried out in a water-based system through base-catalysed heterogeneous reaction with two different epoxides. The material produced was then characterised both chemically and mechanically. The rheological measurements

did not highlight any major degradation of the structure after the reaction, confirming the solid-like nature of the hydrogel. The antibacterial assays showed that the functionalisation caused an inhibitory effect against Gram positive and Gram negative strains upon direct contact, as confirmed by both qualitative and quantitative tests. Furthermore, the modified membrane did not show any cytotoxic effect upon incubation with keratinocytes for up to 6 days. The scratch assay highlighted that the keratinocytes retained good migratory and proliferative ability even in the presence of the hydrogels, with no statistically significant difference between the wound closure rates for the samples and control. Overall, the results obtained from this study indicated that the pellicles constitute a promising substrate for application as a dressing in the case of infected dry wounds. The process here described represents in fact a valuable strategy to turn bacterial cellulose into a versatile platform with tailorable properties thanks to the possibility to introduce various functional groups as required by the final application.

Chapter V

Bacterial cellulose modification under anhydrous conditions

5.1 Introduction

In chapter IV, the development of an antibacterial dressing based on bacterial cellulose was discussed. In particular, an environmental-friendly method was proposed for the surface modification of the pellicles in order to introduce active functional groups. However, the biological characterisation carried out on the material highlighted some limitations, probably due to the low derivatisation yield as a consequence of the presence of water during the reaction. In this section, an alternative method is reported aimed at improving the yield and, therefore, the antibacterial efficiency of the hydrogel. In particular, the derivatisation of the hydroxyl groups of glucose was achieved through a two step-functionalisation involving a Schotten-Baumann coupling followed by a thiol-ene Michael type addition.

The Schotten-Baumann reaction was first reported by Schotten and Baumann in 1884-1886 (Schotten, 1884; Baumann, 1886) and it is an example of a nucleophilic acyl substitution. The classical procedure involves the acylation of an amine or an alcohol through coupling with an acyl halide (usually acyl chloride) to yield, respectively, an amide or an ester. In particular, the nucleophilic amino or hydroxyl group can displace the acyl halide (or other leaving group, for Schotten-Baumann variations) via nucleophilic addition to the electron deficient carbonyl, followed by expulsion of the halide. This step results in the generation of a proton and a chloride ion in the form of one equivalent of acid. The presence of a base is therefore required to neutralise the acid, as its addition to the unreacted amine (or alcohol) would make the electron pair no longer available, resulting in a decrease of the final yield. An aqueous base solution (generally sodium hydroxide) is often used, with consequent formation of a biphasic aqueous/organic system, which is referred to as "*Schotten-Baumann conditions*". This can allow the simultaneous neutralisation of the acid as well as its extraction, whereas the reagents and the product remain in the organic phase (usually, dichloromethane, tetrahydrofuran or diethyl ether). An excess of water, however, can result in the hydrolysis of the acyl halide, especially if this is soluble in the aqueous phase. To overcome this issue, the aqueous base should be added

slowly to the reaction mixture or, as in in this study, an organic base can be used to minimise the hydrolysis (Asano and Matsubara, 2009). Tertiary amines such as triethylamine and pyridine are commonly used in this type of reactions as they can subtract the acid by formation of insoluble salts, i.e. triethylamine hydrochloride and pyridinium chloride, respectively (Jursic and Neumann, 2001; Fang, 2004; Shukla, 2014).

Thiol-alkene additions, on the other hand, belong to a class of so-called *click* reactions, i.e. highly selective, regiospecific and efficient reactions that yield easily removable or no side products. Furthermore, click reactions take place in mild and solvent-less or aqueous conditions. Among these, cycloadditions, azide/alkyne additions and thiol-ene reactions are some of the most widely studied in the context of click chemistry. Thiol-ene reactions, in particular, can occur in two different ways, i.e. through free-radical addition to the double carbon bond or via catalysed Michael addition. Most commonly, radical thiol-ene reactions are light-mediated and can proceed without or in the presence of a photo-initiator. Thanks to their versatility and simplicity, they are widely used for the polymerisation of a variety of monomeric substrates, modification of polymers and basic synthesis. If the alkene involved in the reaction is electron-deficient (for example, acrylates, acrylonitriles and unsaturated ketones), a Michael type addition can take place as an alternative to the traditional radical thiol-ene reaction. In this case, the use of catalysts such as strong bases, Lewis acids and metal-based systems is necessary to overcome the activation energy (Hoyle and Bowman, 2010). In particular, the reaction can be initiated through base-catalysed or nucleophile-mediated addition. Triethylamine is among the most used bases for such reactions, although it has been proven that primary and secondary amines are more efficient, resulting in an almost quantitative yield. In addition to this, nitrogen-centred compounds like imidazole and dimethyl amino pyridine (DMAP) demonstrated higher effectiveness in several cases (Lowe, 2014).

In this chapter, an alternative method for the surface functionalisation of bacterial cellulose is described. The treatment involved a solvent exchange step to be

carried out prior to the modification in order to remove the water from the structure. After this, the modification of the hydroxyl groups was first conducted in anhydrous conditions, followed by a thiol-ene Michael type reaction upon rehydration of the hydrogel. The material was characterised with respect to its chemical and morphological structure in order to evaluate the results of the reaction as well as any eventual degradation. Furthermore, the mechanical properties were studied through rheological measurements. Finally, a biological characterisation was carried out to investigate the effect on both bacteria and eukaryotic cells. The antibacterial effect was determined against Gram positive and Gram negative bacteria, whereas the cytotoxicity was tested using keratinocytes. Finally, the stability of the samples in liquid media was assessed and compared with unmodified cellulose.

5.2 Results

5.2.1 Functionalisation in anhydrous conditions

The modification of bacterial cellulose was carried out in anhydrous conditions in order to improve the functionalisation yield and, therefore, the antibacterial properties of the material. Initially, the water was removed from the hydrogel and replaced with an organic solvent (i.e. tetrahydrofuran, THF) through solvent exchange process. The reaction was then carried out in two steps under different conditions (**Figure 5.1**).

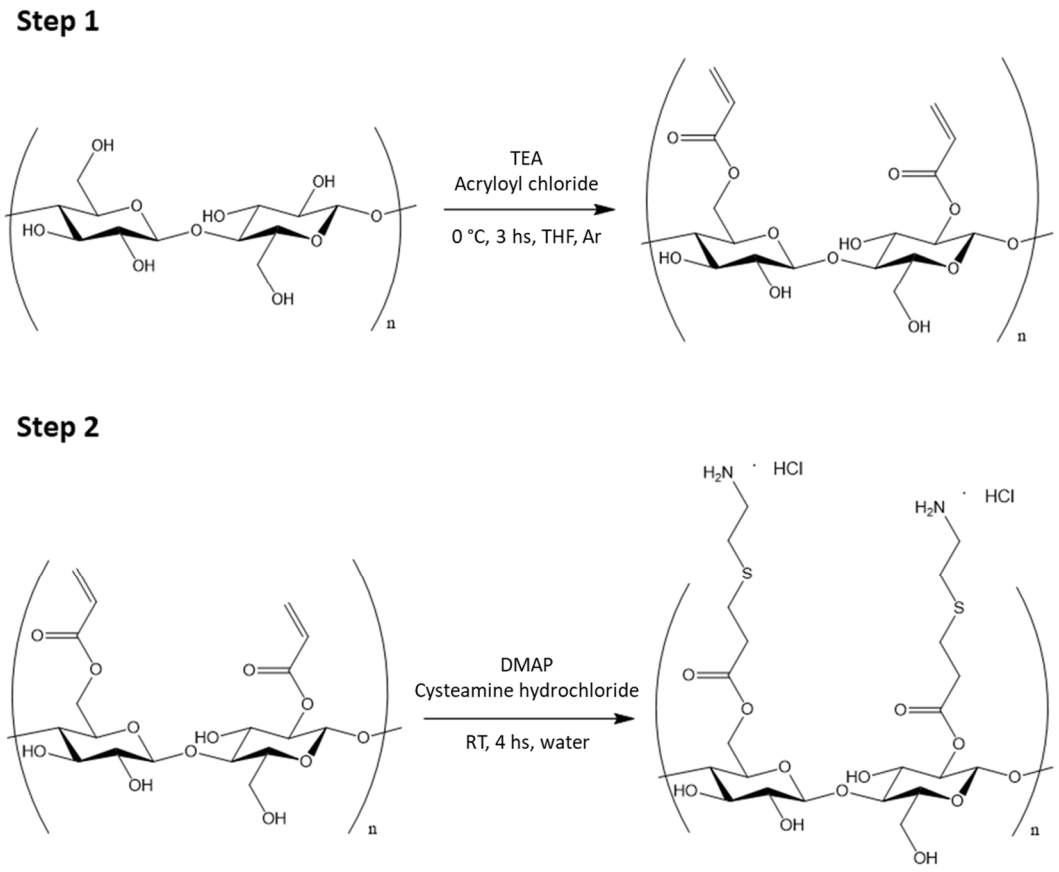

Figure 5.1 Derivatisation of BC hydroxyl groups through reaction with acryloyl chloride (step 1) and cysteamine (step 2)

The surface hydroxyl groups were acrylated using acryloyl chloride in anhydrous setting under inert atmosphere in order to introduce double bonds in the structure as binding moieties. After this, the water was incorporated again in the structure by washing of the pellicle to remove the solvent. Cysteamine hydrochloride was then used as the functionalisation reagent to achieve antibacterial properties due to its amino group. A thiol-ene Michael type addition was performed in water between the double bonds of cellulose and the thiol groups of cysteamine (**Figure 5.2**).

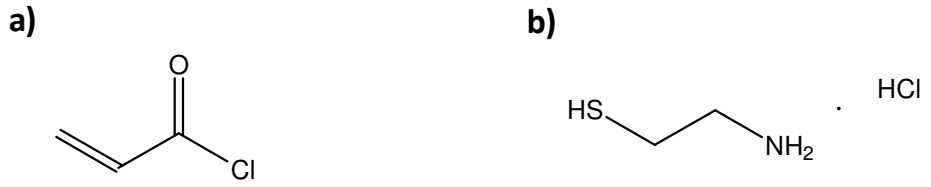

Figure 5.2 Chemical structure of a) acryloyl chloride and b) cysteamine hydrochloride

The derivatisation of the hydroxyl groups of glucose was achieved by treatment with an acyl chloride in the presence of a base (namely triethylamine, TEA) in order to isolate the hydrochloric acid that was produced during the reaction. The second step, on the other hand, was conducted in water in the presence of 4-dimethylaminopyridine (DMAP) as the base catalyst.

In order to assess the degree of degradation of the material under the conditions applied, the morphology of the fibrillar structure of cellulose after functionalisation was studied through SEM analysis (**Figure 5.3**).

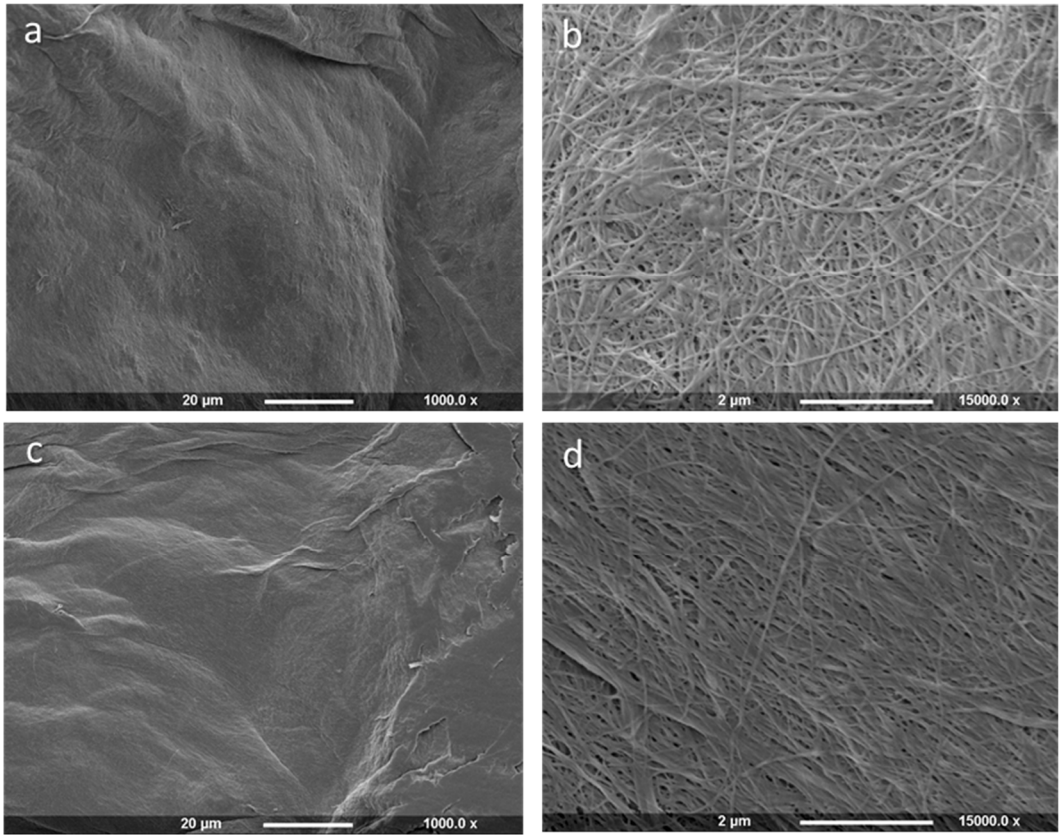

Figure 5.3 SEM analysis of non-modified (a and b) and modified cellulose (c and d)

It was possible to note that even after treatment with an organic solvent and basic catalysis the nanofibrillar structure typical of bacterial cellulose was retained, with no major degradation happening at the microscopic level.

5.2.2 Chemical characterisation

As for the cellulose functionalised in aqueous conditions, the modified material was characterised using solid-state techniques because of the insolubility of cellulose. First, a qualitative evaluation of the elemental composition of the hydrogel was carried out through energy-dispersive X-ray spectroscopy (EDX) (**Figure 5.4**).

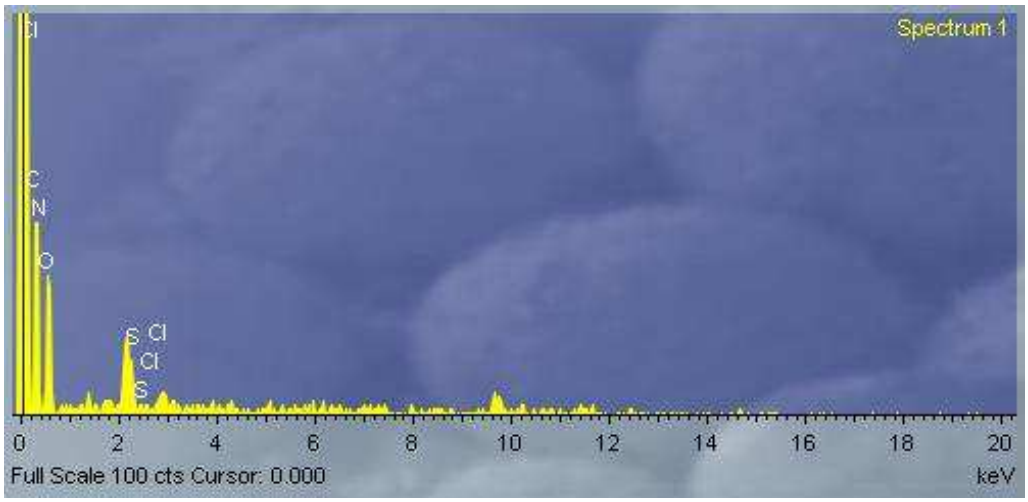

Figure 5.4 Energy-dispersive X-ray (EDX) spectrum of functionalised cellulose samples

In addition to carbon and oxygen (the elements constituting the glucose backbone), the spectrum showed the presence of nitrogen, sulphur and chlorine. Although the EDX is not a quantitatively reliable analysis, the successful incorporation of the thiol and amino groups of cysteamine was confirmed.

X-ray photoelectron spectroscopy was also conducted on the modified hydrogel in order to further investigate the degree of derivatisation. Once again, nitrogen and sulphur were detected on the surface of the functionalised cellulose sample, confirming the thiol-ene reaction between the acrylate group and cysteamine (**Figure 5.5**).

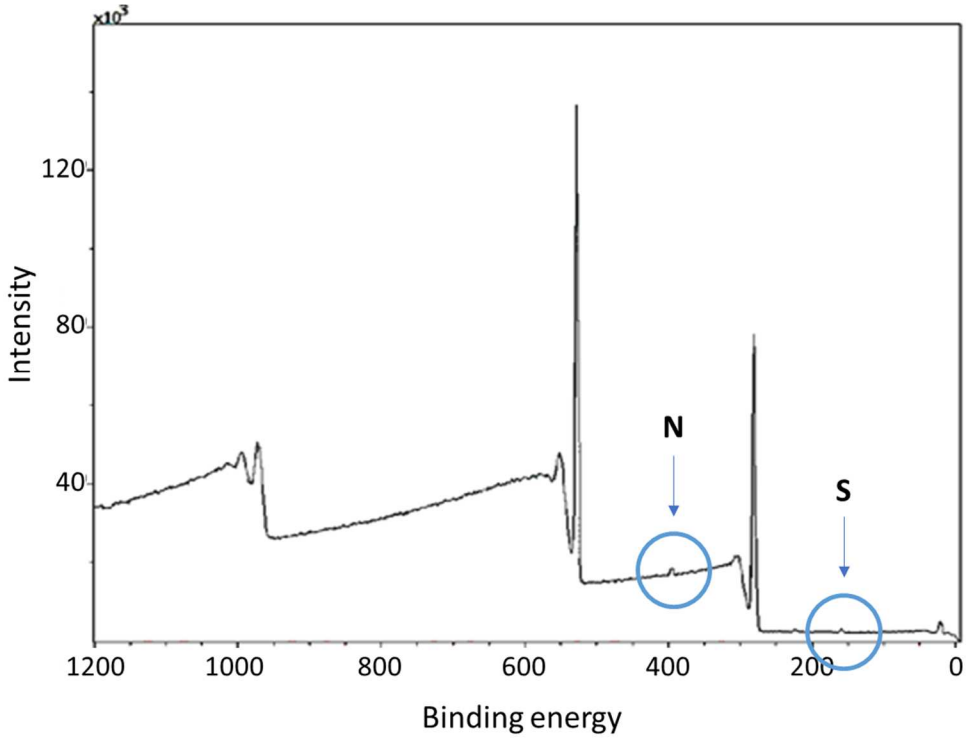

Figure 5.5 XPS spectrum of modified cellulose

The relative amount of each element was also calculated through determination of the area of the corresponding peak. The values were compared with the ones obtained for the non-modified sample in order to evaluate the effect of the reaction performed (**Table 5.1**).

Table 5.1 Elemental analysis of non-functionalised and functionalised cellulose. The area of the peak related to each element is reported as well as its relative amount.

	Element	Area	Atomic %
Non-functionalised cellulose	O 1s	2386607.93	38.35
	C 1s	1303162.96	61.36
	N 1s	11008.54	0.29
Functionalised cellulose	O 1s	529520.0	34.32
	C 1s	375464.0	64.34
	N 1s	10472.0	1.06
	S 2p	4044.0	0.28

The table shows the presence of both nitrogen and sulphur on the surface of the sample, which confirmed the functionalisation performed. In particular, the

nitrogen content in the functionalised pellicle was found to be more than threefold as compared to neat cellulose, with an increase of about 265%. Furthermore, the sulphur was only detected in the modified cellulose, as a confirmation of the thiol-ene reaction. As observed in chapter IV, the presence of nitrogen in the non-modified hydrogel was probably due to traces of the growth medium components or environmental impurities.

5.2.3 Rheological properties

As for the pellicles modified in aqueous conditions, the mechanical properties of the hydrogel after functionalisation were studied through rheological measurements. In particular, frequency sweep and temperature ramp tests were carried out in order to determine the variation of the storage modulus (*G'*) and loss modulus (*G''*). The assays were conducted at 32 °C, which has been reported in literature as the average wound-bed temperature.

The frequency sweep analysis showed that even after the treatment the material presented storage modulus higher than loss modulus at all frequencies, confirming that it maintained a self-standing solid-like structure (**Figure 5.6**).

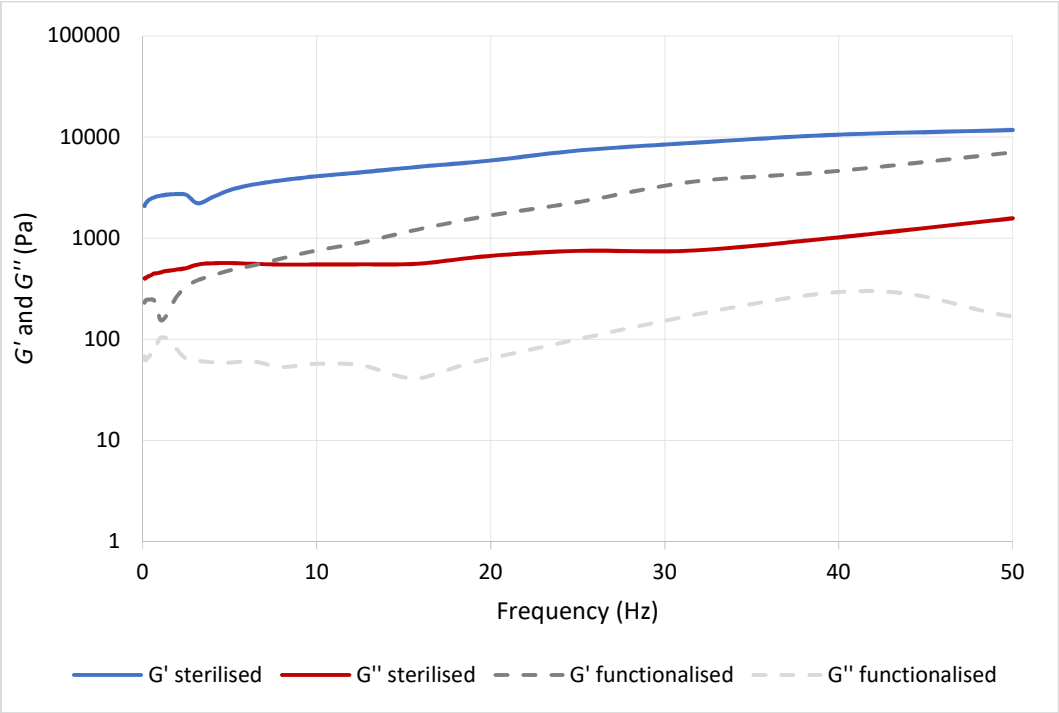

Figure 5.6 Frequency sweep test; T = 32 °C, preload = 6 Pa.

The graphs highlighted that for both materials the storage modulus increased massively in the range considered, whereas for the loss modulus lower average variation was observed. As already discussed in previous chapters, this is a typical feature for hydrogels, which are usually characterised by an increase in the storage modulus values as a response to the increase in the shear rate. The main difference in the viscoelastic behaviour of the two samples was detected at low frequencies, with the storage modulus decreasing from about 2000 Pa for the unmodified cellulose to circa 230 Pa for the modified one at 0.1 Hz and a final *G'* value of more than 7000 Pa for the treated sample *vs* circa 11700 Pa for the untreated one. A similar result was noted for the loss modulus, which expresses the viscous component of the mechanical performance, i.e. the liquid-like response of the specimen. In the region analysed, *G''* showed an almost linear trend, with values in the range of 70-370 Pa in the case of the functionalised hydrogel, whereas for the non-functionalised an increase from 400 to 1570 Pa was observed. Overall, the test evidenced a certain degree of degradation of the pellicles as a consequence of the reaction performed. However, it was possible to

notice that the hydrogel presented a solid and handleable structure with elastic response for the oscillatory shear rate considered.

The dependence of the viscoelastic behaviour to the temperature variation was assessed through temperature ramp assay. The dynamic moduli of the functionalised sample were measured in the 10-60 °C range and compared with the values obtained for the unmodified cellulose (**Figure 5.7**).

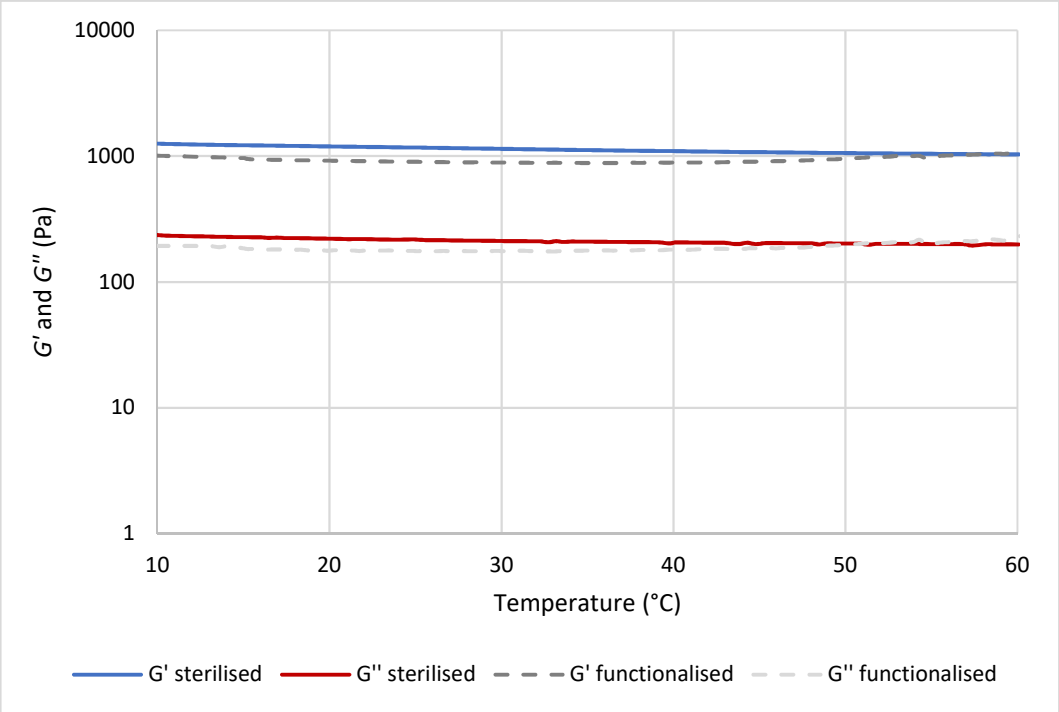

Figure 5.7 Temperature ramp test; f = 1 Hz, preload = 6 Pa, rate = 5 °C/min.

As for the frequency sweep assay, the results indicated that the material behaved as a solid hydrogel with self-standing structure even at high temperature (up to 60 °C). The test indicated that the functionalisation did not have a drastic effect on the elastic component of the mechanical behaviour, with similar values of *G'* in the interval considered. In particular, the storage modulus at 10 °C was about 1260 Pa for the unmodified sample and 1000 Pa for the modified one. A slight decrease of circa 100-120 Pa was then observed in the case of the functionalised cellulose up to physiological temperature followed by an increase in the final section of the interval, with an overall variation of about 10% that was considered as not significant. As regards the loss modulus, the same results were obtained

for the two hydrogels, with a *G''* that showed almost no variation in the range considered. The untreated specimen had in fact loss modulus of about 220 Pa (at 10 °C) to 200 Pa (at 60 °C), whereas for the treated one it was found to be ≈180-230 Pa. The test highlighted that no major degradation occurred as a result of the functionalisation, with very similar response to the temperature variation for the two samples both for the elastic and the viscous component. The hydrogels presented similar mechanical properties, with good resistance to deformation and minimal liquid-like response up to 60 °C.

5.2.4 Stability studies

The weight variation (ΔW) over time in liquid media was studied for the modified pellicles and compared to the non-functionalised ones to determine the stability of the material after chemical treatment. In particular, the test was carried out both in PBS solution and in keratinocytes growth medium at 32 °C, which is the average wound-bed temperature, in order to investigate the behaviour of the hydrogel under physiological conditions of pH **(Figure 5.8** and **Figure 5.9**).

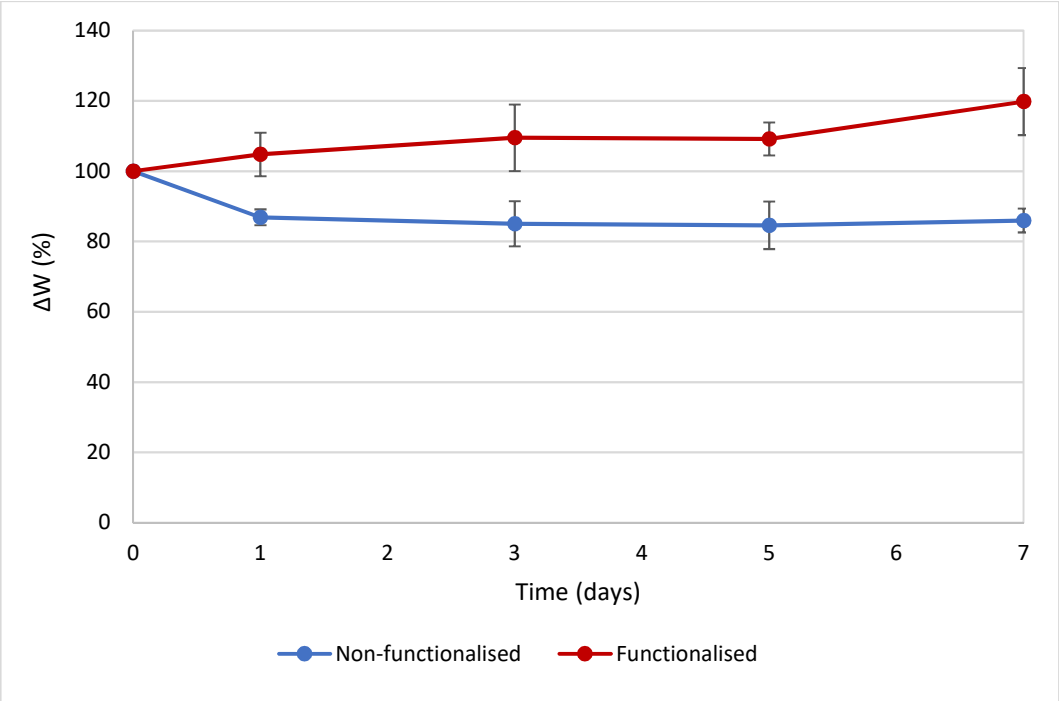

Figure 5.8 Stability of unmodified and modified bacterial cellulose samples in PBS solution at 32 °C under static conditions.

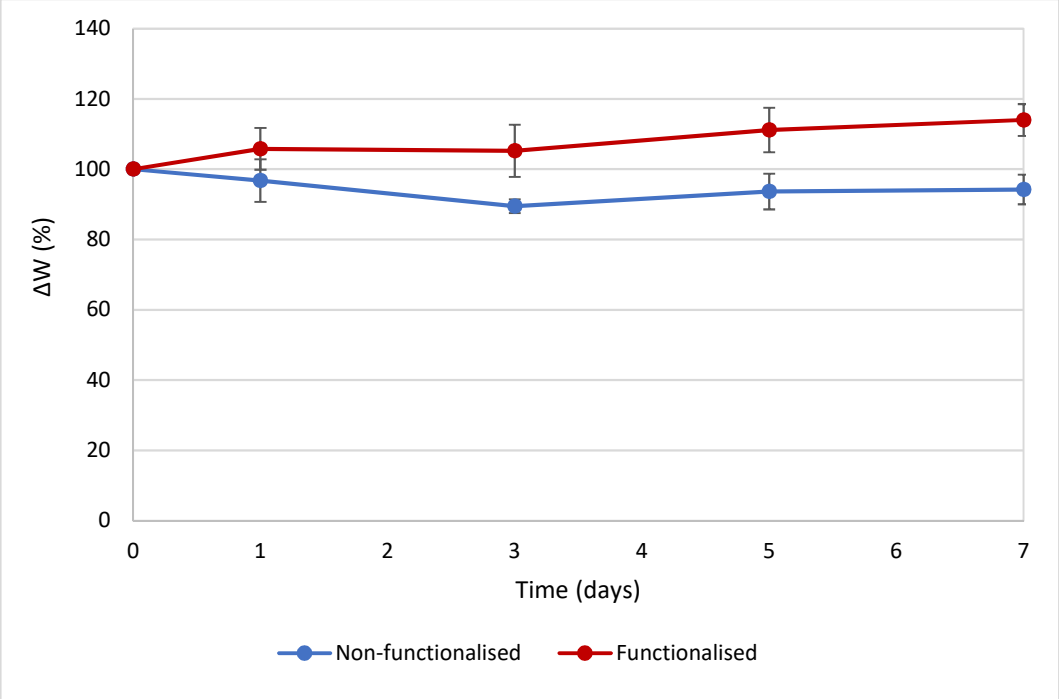

Figure 5.9 Stability of unmodified and modified bacterial cellulose samples in keratinocytes growth medium at 32 °C under static conditions.

The assay showed that for the modified cellulose samples an increase in the weight was observed over 7 days in the liquid media. As regards the incubation

in PBS solution, after 24 hours a non-significant increase of 5% in the weight of the functionalised sample was observed, with no further variation for up to 3 days. After 5 days, the weight of the sample seemed to reach a plateau, with a final value of about 115% with respect to the initial weight. As compared to the unmodified hydrogel, from day 3 the weight of the treated sample was found to be significantly higher. This might be explained with a higher grade of hydrophilicity as a result of the introduction of amino groups. On the other hand, this could also be ascribed to a certain degree of degradation, mostly related to the solvent exchange carried out prior to the reaction, which could have altered the cellulose network. Overall, however, the samples maintained a solid structure even after 7 days, with no evident disruption of the fibrillar system. The values obtained for the test performed in keratinocytes growth medium were found to be very similar. The weight of the treated membrane showed an increase of 5% after 24 hours, with a final variation of 20% after 7 days in the medium. As a general trend, no statistically significant difference was detected in the behaviour of the material in PBS solution and keratinocytes growth medium ($p=0.21$).

5.2.5 Biological characterisation

5.2.5.1 Antibacterial activity evaluation

The antibacterial properties of the cellulose pellicles upon chemical modification were assessed through evaluation of the activity against a Gram positive (i.e. *Staphylococcus aureus* subsp. aureus Rosenbach 6538™) and a Gram negative (i.e. *Escherichia coli* (Migula) Castellani and Chalmers ATCC® 8739™) strains. First, the presence of residual leachable reagents was studied through agar diffusion assay. This was carried out in order to confirm that the washing process had successfully removed all the toxic compounds not covalently attached to the polymer backbone (**Figure 5.10**).

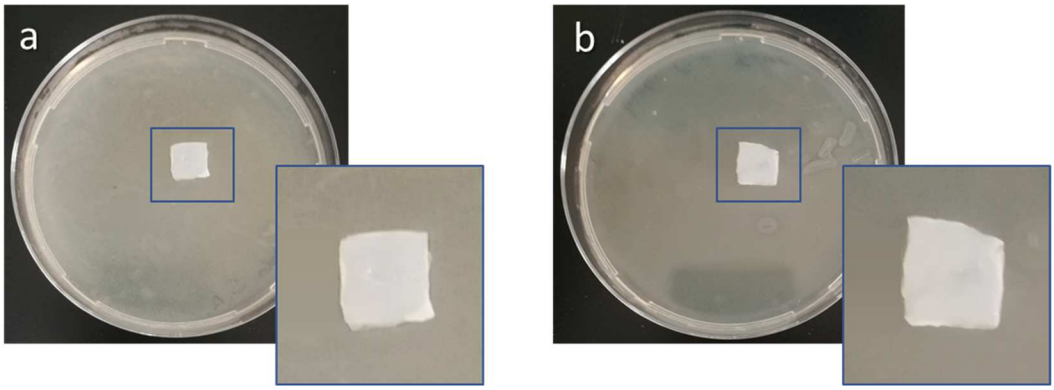

Figure 5.10 Agar diffusion assay of functionalised cellulose against a) *S. aureus* and b) *E. coli*

The images clearly showed that no inhibition zone was detected for both strains after incubation with the samples. This result confirmed that no leachable substance was released over time that could cause an adverse effect on the growth and proliferation of bacteria. This was particularly important as quite toxic reagents were used during the functionalisation of the pellicles, such as 4-(dimethylamino)pyridine (DMAP) as the base catalyst.

After this assay, the antibacterial activity of the hydrogel was studied upon direct contact with bacteria. The same ISO22196 protocol used for the cellulose functionalised in aqueous conditions was applied, and the efficacy of the material was tested against *S. aureus* and *E. coli*. The assay involved a period of incubation of a known number of bacteria on the surface of the samples, followed by recovery of the cells and quantification through drop plate technique.

The test was first conducted against *S. aureus* using the unmodified cellulose sample as the reference. The antibacterial activity (R) was calculated using the formula below, as indicated in the protocol:

$$R = log(a)\,[non-functionalised] - log(a)\,[functionalised] = 2.07 \pm 0.07$$

The percent antibacterial activity ($R\%$) was also determined as follows:

$$R(\%) = \frac{a(T24)Non-functionalised - a(T24)Functionalised}{a(T24)Non-functionalised} * 100 = (99.2 \pm 0.1)\%$$

where a is the number of bacterial cells recovered from each specimen after 24 hours of incubation (CFU/mL*cm^2).

The results obtained highlighted the high inhibitory efficiency of the material against the growth of bacteria. More than 99% of reduction was observed in fact in the bacterial cell count as compared to plain cellulose after only 24 hours of incubation with the sample.

The test was then performed against a Gram negative strain, namely *E. coli*, following the same standard protocol (ISO22196) as for *S. aureus*. Once again, plain cellulose was used as the reference in order to obtain comparable results. The antibacterial activity (R) and the percent antibacterial activity ($R\%$) were calculated using the same formulae previously described for Gram positive bacteria:

$$R = log(a)\,[non-functionalised] - log(a)\,[functionalised] = 2.7 \pm 0$$

$$R(\%) = \frac{a(T24)Non-functionalised - a(T24)Functionalised}{a(T24)Non-functionalised} * 100 = (99.85 \pm 0)\%$$

where a is the number of bacterial cells recovered from each specimen after 24 hours of incubation ($CFU/mL*cm^2$).

Once again, the assay resulted in excellent inhibition of the bacterial growth in the case of the functionalised cellulose sample as compared to the untreated one. Almost 100% reduction was achieved after 24 hours of incubation, proving that the material had a drastic effect even against Gram negative strains. This is a crucial aspect in the development of antibacterial wound dressings and biomaterials in general, as Gram negative bacteria are generally much more resistant to the effect of antibiotics and other biocides thanks to the presence of an external additional membrane.

Overall, the material showed high inhibitory efficiency against both Gram positive and Gram negative bacteria. Over 99% of bacterial cell count reduction was achieved upon direct contact with the functionalised cellulose membrane, with no statistically significant difference between the two strains. The result indicated that the functional groups introduced are highly active against bacteria. Furthermore, they were found to be successfully attached to the glucose chains, as no inhibition of the growth was detected in the area around the sample during the agar diffusion assay.

5.2.5.2 Cytotoxicity studies

The biocompatibility of the bacterial cellulose pellicles after surface functionalisation was evaluated using keratinocyte cells (HaCat). The cytotoxicity was assessed through both direct and indirect assay in order to study the release of any leachable toxic compound as well as to determine the proliferation and viability of the cells after direct incubation with the samples. First, the cell viability upon contact with the eluates after 24 hours of incubation with the hydrogels (non-functionalised and functionalised) was estimated through Alamar Blue assay (**Figure 5.11**).

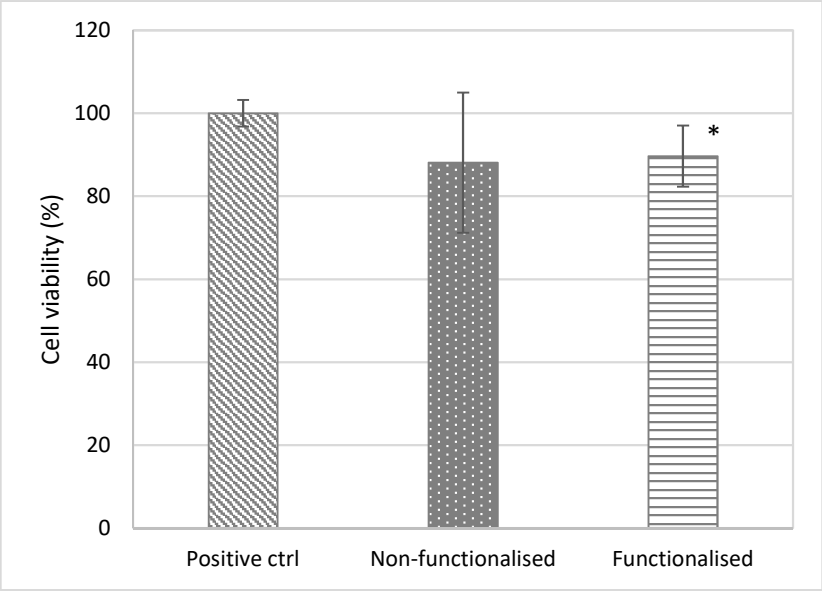

Figure 5.11 Viability of HaCat cells upon contact with undiluted eluates from the BC samples. Positive control: keratinocytes growth medium. No statistically significant difference was observed between the non-functionalised sample and the positive control, whereas the functionalised cellulose was significantly different as compared to the positive control (*=$p<0.05$).

The results of the test did not reveal any significant toxicity for both non-functionalised and functionalised cellulose. Both samples showed in fact a cell viability of almost 90%, with no statistically relevant difference between the untreated and the treated hydrogel ($p=0.5$). The study confirmed that no cytotoxic compound was released from the material over 24 hours of incubation, proving that the washing procedure for the unreacted reagents was successful.

After this, the cytotoxicity of unmodified and modified cellulose upon direct contact with keratinocytes was evaluated over a period of 6 days. As previously described in chapter IV, the test was conducted following a standard protocol (ISO 10993-5) for the biological characterisation of medical devices. The cell viability was measured after 1, 3 and 6 days using Alamar Blue (**Figure 5.12**).

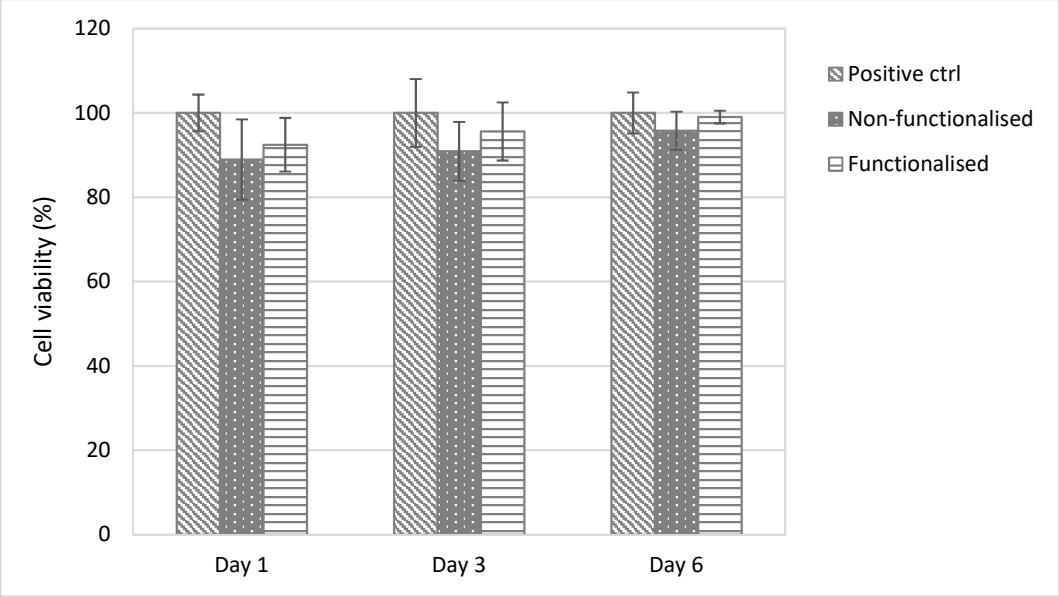

Figure 5.12 Viability of HaCat cells upon direct contact with the BC samples. Positive control: keratinocytes growth medium. No statistically significant difference was observed between the cellulose samples and the positive control at any time point ($p>0.05$).

Both samples resulted in high biocompatibility at all time points considered, with values of cell viability in the range of 90-100%. In particular, no statistically significant difference was detected between the non-functionalised, the functionalised and the positive control groups, with p values always higher than 0.05. Although not significant ($p>0.05$), the viability showed an increase in the interval studied, probably because of the initial environmental stress caused by the presence of the specimen. This trend suggested that the cells were able to adjust to the material after only 24 hours of incubation. After 6 days, 95% and 99% of cell viability were observed for the non-functionalised and the functionalised sample, respectively. This result indicated that the reaction performed did not have an adverse effect on the growth and proliferation of the

keratinocytes even upon direct long-term contact, with optimal degree of biocompatibility comparable to the positive control.

5.3 Discussion

In this chapter, an alternative method for the surface modification of bacterial cellulose to introduce antibacterial groups was proposed to overcome the limitations described in chapter IV. In particular, a strategy for the functionalisation of the hydroxyl groups of glucose in an organic solvent was investigated in order to improve the degree of substitution and, consequently, the antibacterial efficiency. The material was then characterised with respect to its chemical and physical properties as well as its biological functionalities.

Prior to the reaction, the pellicles were subjected to a solvent exchange procedure to replace the water with an organic solvent, namely tetrahydrofuran (THF). This step was particularly important in the interests of the modification, as BC presents a high content of water molecules trapped within the interstices of the fibrillar network (i.e. 97% w/w, as described in chapter III). The presence of water could have in fact interfered with the first reaction carried out, which was aimed at the derivatisation of the hydroxyl groups through substitution with acryloyl chloride. More specifically, a Schotten-Baumann reaction was performed in THF using triethylamine as the catalyst. In this type of reactions, an excessive amount of water can result in the hydrolysis of the acyl halide (in this case, acryloyl chloride) with formation of the corresponding acid, which is not reactive towards amino or hydroxyl groups. For this reason, it was necessary to perform this step under anhydrous conditions (i.e. under argon atmosphere) to minimise the generation of side products. Furthermore, as mentioned in the introduction to this chapter, triethylamine was added as the base catalyst in order to neutralise the acid produced during the substitution, preventing it from reacting with the hydroxyl groups and, therefore, inactivating them. Due to its exothermicity, the Schotten-Baumann is usually conducted at room temperature or below. In this study, the modification was carried out in ice-bath to reduce the accumulation of heat and prevent an eventual thermal runaway, although, due

to the scale of the reaction, such a possibility was rather unlikely. Most importantly, the acyl halide hydrolysis proceeds significantly faster at higher temperatures, thus resulting in lower concentration of the chloride and therefore slower reaction kinetics (Queen, 1967). Previous studies indicated the interval between -3 °C and 5 °C as the optimal range, although examples of temperature up to 30-40 °C with good esterification rate are reported (Tsuda, 1964; Dean, Matzner and Tibbitt, 1989; Nithyanandan *et al.*, 2011; Braun *et al.*, 2013).

The second step of the reaction was carried out in water after rehydration of the pellicles. A thiol-alkene addition was performed between acrylated BC and cysteamine hydrochloride in order to covalently attach active amino groups to the glucose backbone. Thiol-ene additions belong to the class of *click* reactions, i.e. simple, fast and selective reactions. Furthermore, they have the advantage to yield easily removable or no side products at all. In this study, a thiol-ene Michael type addition was carried out in the presence of DMAP as the base catalyst. Nitrogen-centred compounds such as DMAP and imidazole have been found to be highly efficient for this type of reactions. In particular, superior catalytic activity was observed as compared to primary and tertiary amines, including the commonly used TEA. This was explained by the nucleophile-catalysed mechanism adopted by the catalyst to generate the thiolate anion, rather than the base-catalysed pathway. The hypothesis would explain why the use of TEA, a weaker nucleophile, results in a slower reaction kinetics (Xi *et al.*, 2012).

After the reaction, the hydrogel was thoroughly washed to ensure the removal of any residual reagent or catalyst. The morphology of the pellicles was then evaluated and compared to untreated samples. The SEM analysis carried out highlighted that the nanofibrillar network typical of bacterial cellulose was retained, showing that no microscopic variation was generated after the functionalisation. A chemical characterisation of the pellicles was then performed using solid-state techniques due to the insolubility of cellulose. Both EDX and XPS analyses confirmed the incorporation of nitrogen and sulphur, as an indication of the successful two-step modification performed.

The mechanical properties of the functionalised hydrogel were assessed through rheological measurements to evaluate the effect of the reaction on the viscoelastic behaviour. As for previous tests, the storage modulus and loss modulus variations were studied as a function of frequency and temperature (respectively, frequency sweep and temperature ramp assay). For both analyses, it was possible to observe that the sample retained a solid-like response, with *G'* always higher than *G''*. This result indicated that the material showed good degree of stiffness and resistance to deformation in the range of frequencies and temperature considered. More specifically, the frequency sweep study evidenced a significant increase in the storage modulus at higher oscillation rates for both samples, although lower values were obtained in the case of the modified one. At 0.1 Hz, the modified specimen presented in fact a decrease of one order of magnitude in the storage modulus as compared to plain cellulose. This difference was drastically reduced in the high frequency range, with a reduction of 40% in the *G'* values for the treated specimen. As regards the loss modulus, an average 70-80% decrease was detected, with a zero-order linear trend for both materials. Similar results were obtained for the temperature ramp assay in the 10-60 °C range. Once again, the test highlighted that the material maintained a self-standing structure after the functionalisation even at high temperature. Furthermore, lower difference between the *G'* and *G''* values of the unmodified and the modified sample was observed, with only a 20% decrease in the storage modulus of the treated one at low temperature. Overall, the test highlighted that the derivatisation performed did not have a drastic effect on the viscoelastic behaviour of the hydrogel. It was noted, however, that a certain degree of degradation occurred, especially as evidenced by the frequency sweep analysis. This result could probably be ascribed to the functionalisation procedure to which the pellicles were subjected. Along with alkaline treatments, cellulose can in fact be dissolved upon contact with specific solvents. Depending on the action of the solvents on the chemical structure, they can be classified as non-derivatising and derivatising, i.e. solvents that are able to dissolve cellulose by interfering with the intramolecular bonds only and solvents that yield a

derivative of the polymer (Heinze and Koschella, 2005). Although THF is not considered to be a strong solvent for cellulose, it has been reported that a THF/water system could improve the dissolution of plant-derived cellulose through disruption of the intramolecular hydrogen bonding by THF. This effect is probably greatly reduced in the case of bacterial cellulose, which presents a high degree of crystallinity, since the amorphous regions are the most subject to the dissolution (Jiang *et al.*, 2018). Nevertheless, it is possible that the solvent exchange procedure involving progressive substitution of the water with THF might have an effect on the structure of the hydrogel.

The stability of the modified hydrogel in liquid media was then evaluated over 7 days and compared to untreated cellulose. Both in PBS solution and keratinocytes growth medium an increase in the weight of the functionalised sample was detected, with final ΔW of about 15-20%. As previously mentioned, it is possible that the solvent exchange and basic treatment to which the pellicles were subjected might have caused a certain degree of degradation. The incorporation of water can in fact indicate disaggregation of the polymer chains, resulting in higher interstitial space. Nevertheless, the hydrogel maintained a solid structure throughout the assay, with minimal variation as compared to the untreated specimen. Overall, the study highlighted that even after the harsh treatment performed to induce antibacterial activity, the material retained good structural properties with no significant weight loss in the period considered.

Finally, a biological characterisation of the hydrogel was carried out to evaluate the effect of the surface modification on both bacterial and human cells. The antibacterial efficiency of the material was investigated against Gram positive (*S. aureus*) and Gram negative (*E. coli*) strains. First, an agar diffusion assay was conducted to detect the presence of any leachable substance, i.e. residual unreacted reagents or catalysts, as the treatment proposed focused on the development of an inherently antibacterial wound dressing through covalent functionalisation of the substrate, rather than on the physical incorporation of active compounds. For both types of bacteria, no inhibition zone was detected in the area around the sample, showing that no toxic compounds were released over

time. This result confirmed that the washing procedure successfully removed all the reagents not permanently attached to the polymer backbone. After this, a quantitative evaluation of the antibacterial activity upon direct contact of bacteria with the sample was conducted following a standard procedure (ISO22196). The same method described in the previous chapters was adopted in order to obtain comparable results. In both cases, the treated sample caused a reduction of >99% in the bacterial cell count with respect to plain cellulose after 24 hours of incubation. In this context, there is no universally accepted regulation regarding the definition of antibacterial dressings and minimum activity required. FDA reports indicated a 3 to 4 log reduction in the bacterial cell count as the acceptable value for antibacterial dressings, although this depends on the kind of wound and material as well as the degree of bacterial contamination (FDA, 2016). Nevertheless, the results obtained are in line with previously published works and commercially available materials, and further studies should be aimed at determining the antibacterial activity with higher accuracy (Simões *et al.*, 2018). The assay proved that the modification introduced effective antibacterial features even against Gram negative strains. The results obtained suggested that the reaction yielded a higher degree of substitution as compared to the one described in chapter IV. The cysteamine hydrochloride was probably more homogeneously attached to the glucose chains, due to the efficiency of both the Schotten-Baumann reaction and the thiol-ene addition. As regards the chemical structure of the modified cellulose, both the terminal amino group as well as the thioether in γ-position were probably involved in the antibacterial action of the substrate. The use of cysteamine hydrochloride as an antimicrobial compound has in fact been investigated for a wide range of applications, including as mucolytic and antibiofilm agent for the treatment of cystic fibrosis (Charrier *et al.*, 2014). Cysteamine presents a primary amine hydrochloride residue, which exerts a biocidal effect due to the cationic nature of nitrogen (Xie, Liu and Chen, 2007; Oliva *et al.*, 2017). In addition to this, the thioether generated after the thiol-ene addition with acryloyl chloride probably contributed to the overall activity of the hydrogel. Organo-sulphur groups such as thiols, thioethers, thioesters,

sulfoxides and disulphides are extensively used as bacterial inhibitors (Gülerman *et al.*, 2001; Kim, Kubec and Musah, 2006; Ling *et al.*, 2014). Although the mechanism of action has not been fully defined yet, it is acknowledged that sulphur-based compounds can interfere with different biological targets depending on the reactivity and the substituents (Heldreth and Turos, 2005). In particular, it has been found that thioethers are more efficient biocides as compared to oxidised species like sulfoxides and sulfones. Furthermore, increased activity was detected for the derivatives with longer alkyl chains, most probably thanks to the higher lipophilicity that allowed the penetration of the cell membrane through hydrophobic interactions (Zhao and Sun, 2008).

As regards the effect of the membranes on human cells, the cell viability after indirect and direct contact with the samples was determined through Alamar Blue assay. A keratinocyte cell line was used for this purpose, as the material was intended for wound healing applications. For both tests, no cytotoxic effect was induced by the material. The indirect assay showed cell viability of almost 90% for both hydrogels after incubation with the eluates. As already suggested by the agar diffusion assay, this result indicated that any potentially toxic reagent used during the modification process had been successfully removed from the network. After this, the cytotoxicity upon direct contact with the dressings was evaluated over a period of 6 days following a standard procedure for the characterisation of medical devices. In both cases (i.e. untreated and treated cellulose) the viability was found to be above 90%, with increasing values in the interval of time considered. This effect might be due to the initial cellular stress generated by the presence of an interfering event. The alteration of the physicochemical conditions of the extracellular environment (most commonly, change of temperature) can in fact affect the growth and proliferation of the cells, which have to adapt to the new environment. The mechanisms of the adaptation usually depend on the type and intensity of the stress, and can range from re-arrangement of molecular pathways to chemotactic movements, i.e. movement of a living system as a result of a chemical stimulus (Al-Fageeh and Smales, 2006; Rabouille and Alberti, 2017; Tu and Rappel, 2018). In this study, a non-significant

increase in the cell viability was observed as compared to the positive control, which could probably be ascribed to the presence of the hydrogels. After 6 days of incubation, the cell viability of the group incubated with the functionalised cellulose sample was found to increase from 90% (after 24 hours) to 99%, indicating that the modification process did not affect the long-term biocompatibility of the material.

5.4 Conclusions

This chapter focused on an alternative method for the modification of bacterial cellulose in order to develop an antibacterial material for wound healing applications. More specifically, a different treatment was investigated to improve the reaction yield and, therefore, the antibacterial efficiency of the hydrogel. As opposed to the method proposed in chapter IV, in this case the derivatisation of the hydroxyl groups was conducted in an organic solvent to minimise the effect of water on the reaction. Double bonds were in fact introduced in the structure through acrylation by Schotten-Baumann reaction. After this, the pellicles were rehydrated and a thiol-ene Michael type addition was carried out to incorporate active amino groups. The chemical structure of the material was confirmed by solid-state techniques, whereas the mechanical properties were studied by rheological measurements. The modified pellicles were then biologically characterised with respect to their behaviour towards both bacteria and eukaryotic cells. In particular, the activity upon direct contact with Gram positive and Gram negative strains was investigated, resulting in a high inhibition efficiency with >99% of reduction in the bacterial cell count as compared to unmodified cellulose. On the other hand, the cytotoxicity evaluation highlighted good biocompatibility towards keratinocytes both after indirect and direct contact, with cell viability higher than 90% for up to 6 days of incubation. Overall, the results obtained proved that the modification proposed yielded an inherently active wound dressing with good mechanical and biological properties. Furthermore, despite the harsh conditions used, no structural degradation was observed, with the hydrogel retaining a solid network in the conditions tested.

Chapter VI

Production of bacterial cellulose/ copper-chitosan composites

6.1 Introduction

In chapter IV, the development of a chemically modified hydrogel through surface modification of bacterial cellulose was described. The pellicles were functionalised in an aqueous system to minimise the steps of the reaction and the environmental impact. However, the hydrogel demonstrated an antibacterial activity of about 50% against Gram positive and Gram negative bacterial strains. To improve these results, the material was combined with another antibacterial agent to obtain higher inhibition for the development of an effective wound healing patch with improved biological properties. To achieve this, the pellicles were mechanically ground to produce cellulose fibres, which were then chemically modified to introduce antibacterial groups. A chitosan/cellulose composite was then produced by physical incorporation of such fibres within a chitosan-based network containing copper(II) ions with antibacterial properties.

Chitosan is a polysaccharide easily obtained through deacetylation of chitin, the second most abundant polymer in nature after cellulose, hence this polymer is widely available at low price. Thanks to its great degree of biocompatibility, it has been largely used in the biomedical field for numerous applications. Moreover, the presence of primary and secondary amino groups confers to chitosan a pH-dependent antibacterial and antifungal activity. There are, however, a few drawbacks related to the use of chitosan on its own. First of all, since the antibacterial properties originate from its polycationic nature, they are strictly dependent on the pH at which chitosan is used. The polymer also shows quite low mechanical properties, in particular, high brittleness with low deformation at break, which limit its utilisation in load-bearing applications. To overcome these issues, different approaches have been investigated. As regards the antibacterial efficiency of chitosan, several types of modifications have been performed to ensure activity at higher pH. Thanks to the presence of reactive groups, chemical modification of chitosan has been widely investigated, for instance through the introduction of sulphur-based moieties or quaternisation of the amino groups (Jia, Shen and Xu, 2001; Vallapa *et al.*, 2011; Mohamed and Al-mehbad, 2013; Ahmad *et al.*, 2015). Incorporation of external agents was also

explored to ensure activity under all conditions. A variety of compounds was used to this purpose, such as metal ions, natural substances (Thakhiew, Devahastin and Soponronnarit, 2013) and active polymers (Tan *et al.*, 2009; Anisha *et al.*, 2013).

In this context, the use of copper as an antibacterial agent for the enhancement of chitosan activity has recently been attracting attention in the biomedical field (Qi *et al.*, 2004; Mekahlia and Bouzid, 2009; Tripathi *et al.*, 2012; Covarrubias, Trepiana and Corral, 2018). Copper is an essential element for humans, as it is a central component of several metalloenzymes with various functions including haemoglobin formation and aerobic respiration. Thanks to its ability to easily undergo transition between two different oxidation states, i.e. Cu(I) and Cu(II), the biological role of copper is mainly related to redox enzymatic reactions. However, this particular feature is also responsible for its toxicity at high concentrations. During this transition, copper can in fact generate toxic reactive oxygen species (ROS) through Fenton-type reactions, with consequent oxidative damage if these species are not deactivated. Furthermore, it can exert its toxicity through competing with other metal ions such as zinc and iron for the binding sites of proteins or, thanks to its high affinity to sulphur-containing residues, it can inactivate them through depletion of the thiol groups (Camakaris, Voskoboinik and Mercer, 1999; Osredkar, 2011). For this reason, several copper proteins are committed to maintaining copper homeostasis in order to minimise the risks related to its toxicity. On the other hand, the antibacterial properties of copper rely on the same processes happening in eukaryotic cells, i.e. oxidative stress, competition with metal ions for binding sites of proteins and thiol depletion. However, in prokaryotic organisms copper has a limited biological role, therefore their homeostatic system is mainly based on the protection from copper rather than on its utilisation (Festa and Thiele, 2011; Rensing and McDevitt, 2013).

As regards the improvement of the mechanical performance of chitosan, different methods have been investigated. Chemical cross-linking of the chitosan chains, for instance, has been carried out as it results in higher stiffness (Rivero, García

and Pinotti, 2010), with the degree of cross-linking directly related to the mechanical properties of the material (Silva *et al.*, 2004; Chiono *et al.*, 2008; Chen *et al.*, 2009). Loading of a reinforcing agent to develop chitosan-based composites with higher mechanical properties is also reported in literature. Inorganic materials have been widely used as reinforcing agents; some examples are oxidised carbon nanotubes (Spinks *et al.*, 2006; Fan *et al.*, 2012), graphene (Fan *et al.*, 2010) and graphene oxide (Han *et al.*, 2011; Zuo *et al.*, 2013), calcium phosphate (Zhang and Zhang, 2001), calcium carbonate or silica to produce bone substitutes and cements for bone repair (Muzzarelli and Muzzarelli, 2002), halloysite nanotubes (Liu *et al.*, 2012). In addition to this, a highly efficient technique for the enhancement of the mechanical properties of chitosan consists in the incorporation of natural or synthetic fibres as reinforcing agents. A variety of natural materials has been used to produce fibres thanks to their renewable and biodegradable nature (Cheung *et al.*, 2009), including chitosan itself (Albanna *et al.*, 2012), lignin (thanks to its polyanionic nature) (Wang, Loo and Goh, 2016), silk fibroin (Mirahmadi *et al.*, 2013) and chicken feather derived keratin (Flores-Hernández *et al.*, 2014).

In this context, great attention has been focused on the use of cellulose in combination with chitosan thanks to its excellent mechanical properties and structural similarity between the two polymers. Several studies have been directed towards the development of such composites (Khan *et al.*, 2012; H.P.S *et al.*, 2016); in particular, nano-sized structures such as nanocrystalline cellulose and bacterial cellulose showed considerable advantages over plant-derived cellulose thanks to their unique features. Their morphology gives in fact these materials high stiffness and strength as well as transparency when combined with other polymers (Fernandes *et al.*, 2011).

In this chapter, the preparation of composites based on copper(II)-chitosan and modified bacterial cellulose is reported. Two different copper(II)-chitosan compositions were evaluated in order to determine the influence of copper on the mechanical and especially the biological properties of the scaffolds. The morphology of the composites developed was analysed by scanning electron

microscopy (SEM) to ensure that no phase separation occurred from the coupling of the two polymers. Moreover, the incorporation and dispersion of the cellulose fibres within the chitosan network was visually investigated. The films were then characterised from the chemical point of view to confirm the presence of both copper(II) and modified cellulose by elemental analysis through energy dispersive X-ray spectroscopy (EDX). The wettability of the systems before and after loading of bacterial cellulose was evaluated as well as their degradation in liquid medium. Finally, the biological properties of the scaffolds were assessed to have a clear understanding of the influence of cellulose on the system. The cytotoxicity of the materials was studied using a keratinocyte cell line (HaCat), while the antibacterial activity was estimated against both Gram positive and Gram negative strains, i.e. *Staphylococcus aureus* and *Escherichia coli*, respectively.

6.2 Results

6.2.1 Production of bacterial cellulose fibres

The cellulose mats produced through bacterial fermentation were mechanically ground in order to obtain homogeneous fibres for incorporation in a chitosan-based matrix (**Figure 6.1**). The process was carried out in wet conditions to avoid the collapse of the 3D-network of cellulose. The morphology of ground bacterial cellulose was studied by SEM in order to evaluate if the fibrillar structure was retained after mechanical grinding of the pellicle (**Figure 6.2**).

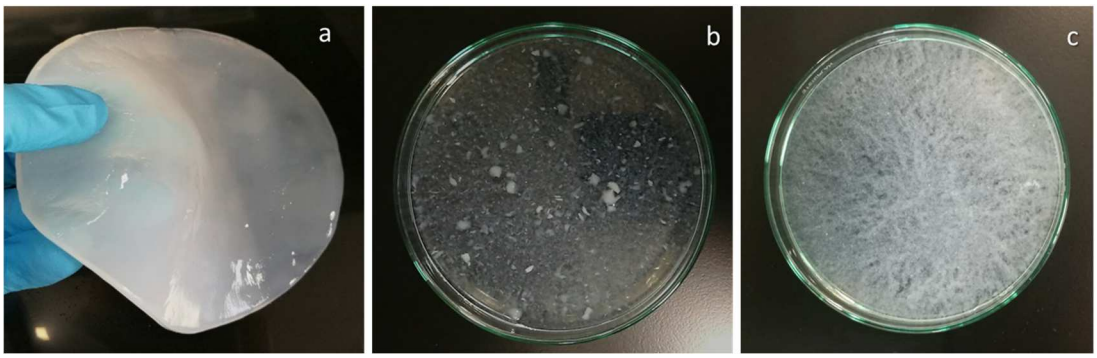

Figure 6.1 Production of cellulose fibres through mechanical grinding: a) bacterial cellulose pellicle, b) cellulose after grinding with normal blender, c) cellulose after homogenisation with immersion hand blender.

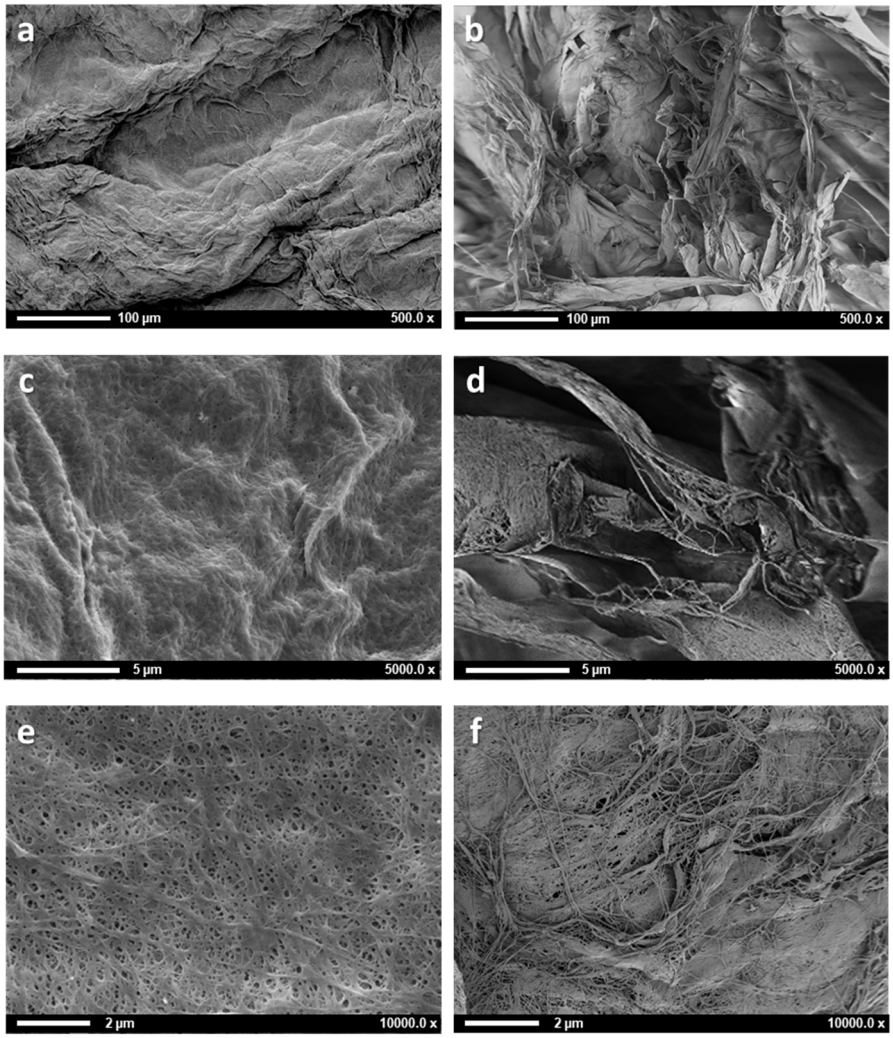

Figure 6.2 SEM images of bacterial cellulose before and after grinding treatment: a), c) and e) normal cellulose; b), d) and f) ground cellulose.

Ground cellulose showed an irregular structure and sharp edges, which were formed as a result of the grinding of the pellicle. However, the images also confirmed that the typical fibrillar structure of bacterial cellulose was maintained after the grinding process. This was clearly visible at higher magnifications, when it was possible to see the presence of the fibrils, although in a much more disorganised pattern as compared to normal cellulose.

After this, the fibres obtained were chemically functionalised to introduce antibacterial groups in the structure. The modification was carried out in water following the procedure described in chapter IV (**Figure 6.3**).

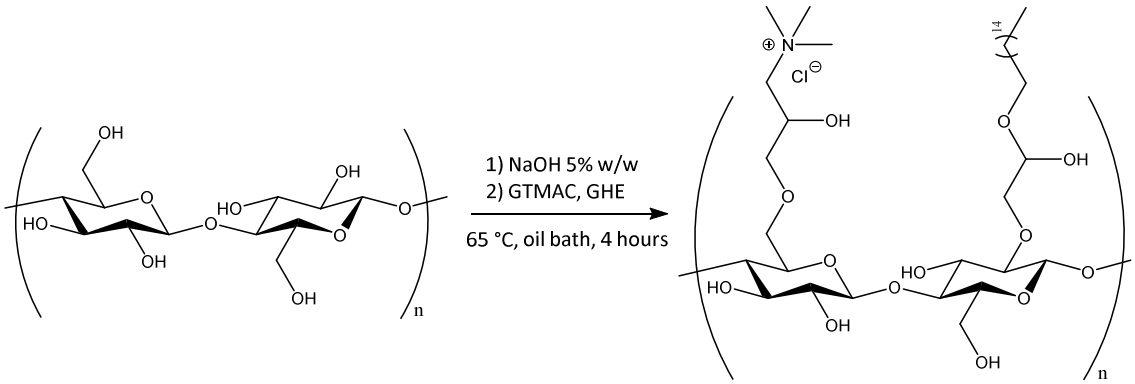

Figure 6.3 Bacterial cellulose modification in aqueous system (reaction described in chapter IV)

6.2.2 Cellulose/chitosan composites development

The modified cellulose/copper-chitosan composites were produced through solvent casting technique. Two different copper(II)-chitosan formulations were used for this purpose, namely CuChi3 and CuChi12, both without and with the addition of bacterial cellulose.

The miscibility of the two polysaccharides in the films developed was also investigated by morphological study through SEM (**Figure 6.4**).

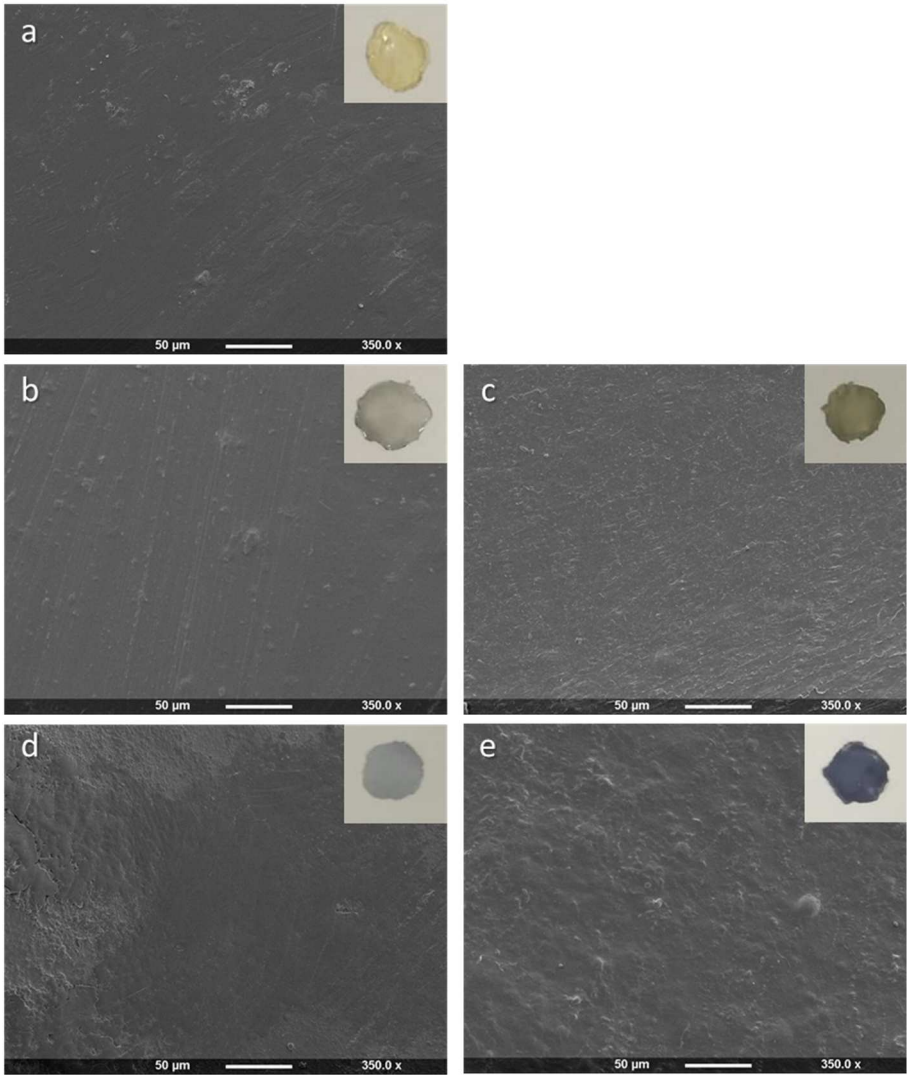

Figure 6.4 SEM images and pictures of the bacterial cellulose/copper-chitosan films: a) neat chitosan, b) CuChi3, c) CuChi3/BC, d) CuChi12 and e) CuChi12/BC.

All the samples exhibited no visible phase separation between cellulose and chitosan. The cellulose fibres appeared homogeneously dispersed in the matrix, without the formation of aggregates or voids. The surface of the cellulose-containing composites was characterised by a higher degree of roughness as compared to the chitosan control or the copper-chitosan films, which can be attributed to the presence of a second phase. Moreover, the incorporation of the modified cellulose was confirmed by the presence of the typical cellulose fibres that could be observed at higher magnification, as shown in **Figure 6.5**.

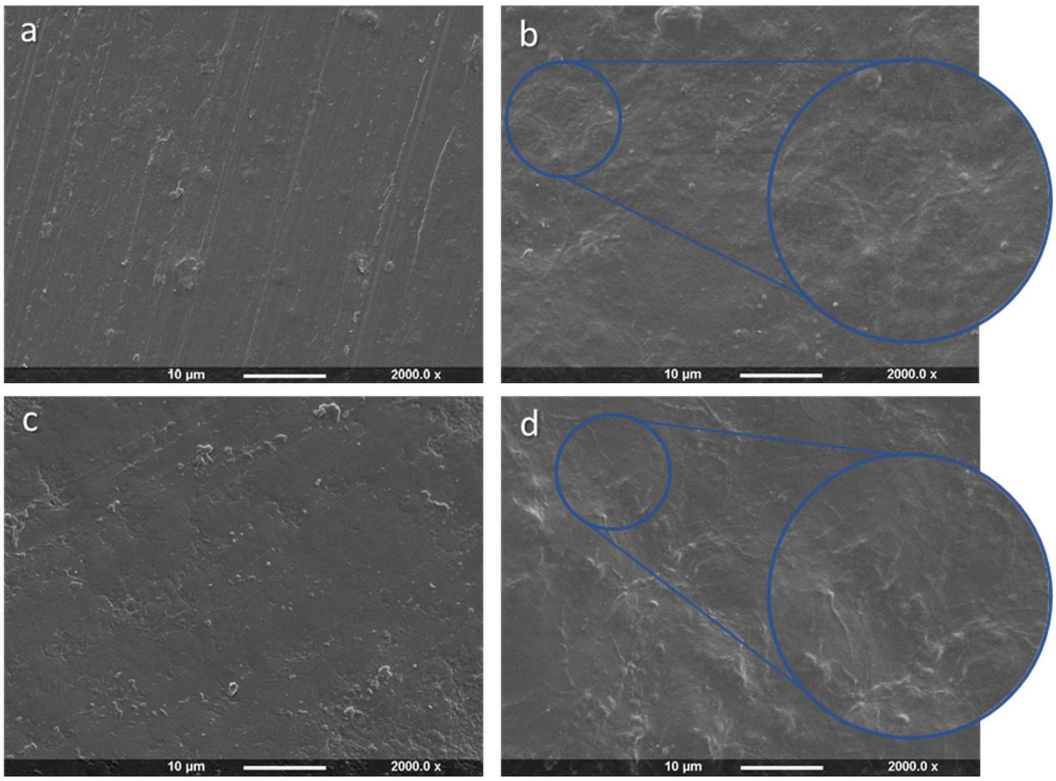

Figure 6.5 SEM images of CuChi3 and CuChi12 films without and with cellulose: a) CuChi3, b) CuChi3/BC, c) CuChi12 and d) CuChi12/BC.

To further investigate the structural organisation of the fibres in the chitosan matrix, a CuChi12/BC composite scaffold prepared by freeze-drying technique was studied by SEM (**Figure 6.6**). The analysis was carried out on a 3D freeze-dried scaffold in order to have a clear understanding of the disposition of the fibres within the chitosan network by evaluation of its cross-section.

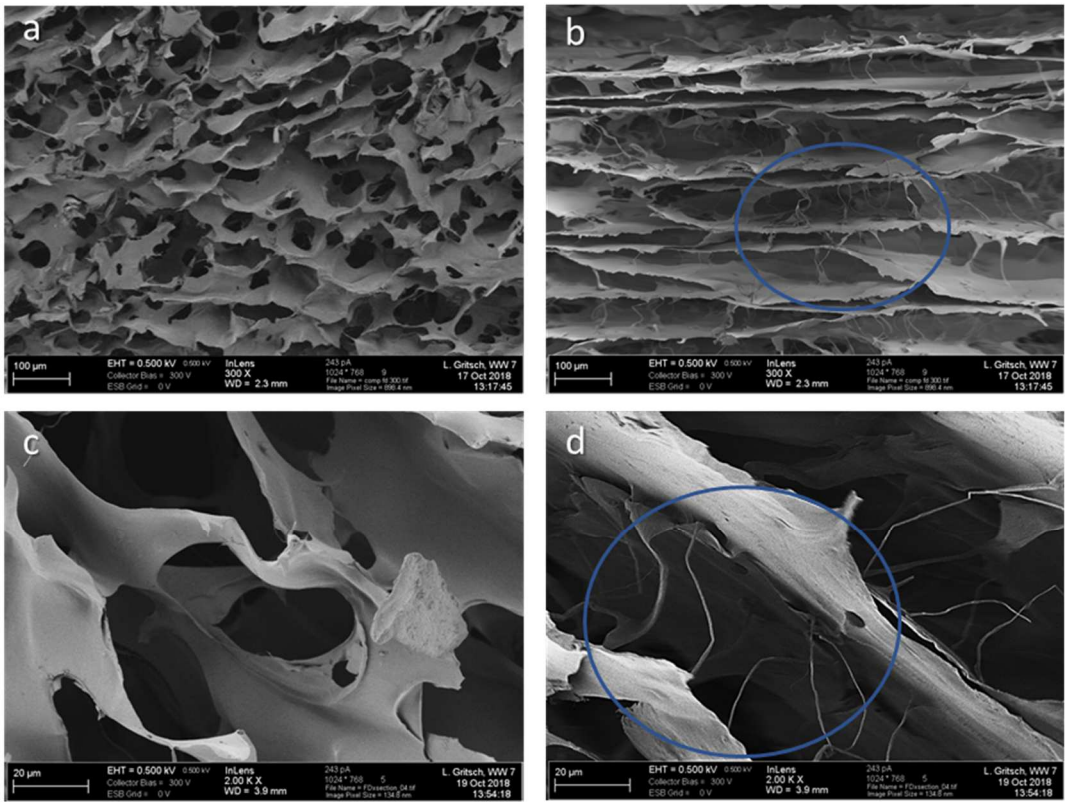

Figure 6.6 SEM images of freeze-dried copper(II)-chitosan scaffolds without and with cellulose: a) and c) CiChi12; b) and d) CuChi12/BC.

The SEM imaging of the cross-section of the chitosan/cellulose composite showed a highly organised structure with the chitosan layers interconnected by the cellulosic fibres. In addition to this, the analysis revealed that the fibres were arranged transversal to the parallel chitosan layers. The freeze-dried scaffold without cellulose, on the other hand, presented a porous network with interconnected cavities. This difference in the structure could also be due to the difference in the rate of the freeze-drying step in the scaffold fabrication, as different vessels were used for the two samples. In particular, the difference in the shape of the vessels and the position of the liquid nitrogen resulted in different temperature gradient that could have affected the formation of the crystals.

6.2.3 Chemical characterisation

The elemental composition of each film was also investigated by EDX analysis in order to confirm the presence of copper as well as the incorporation and dispersion of the modified cellulose fibres within the matrix (**Figure 6.7**).

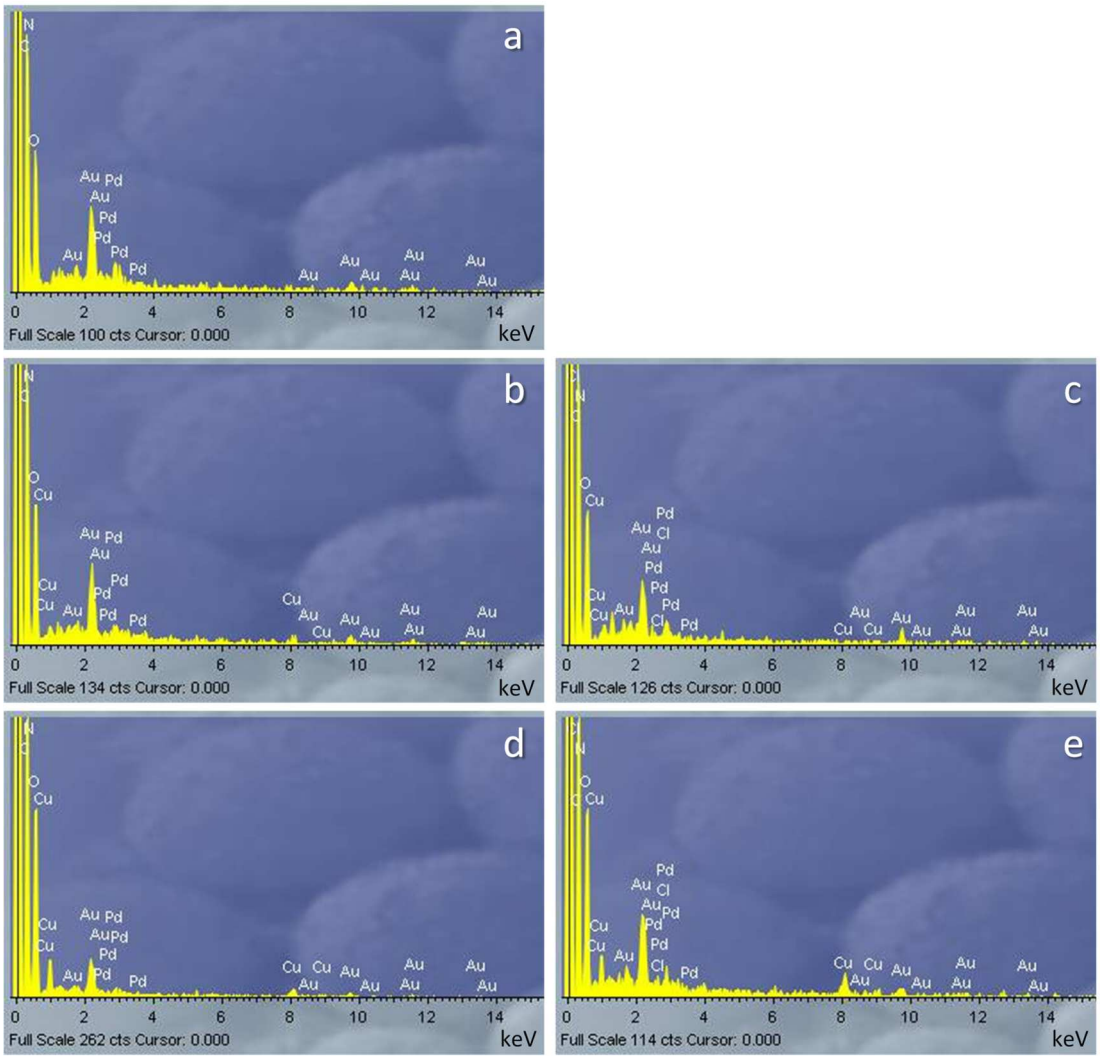

Figure 6.7 EDX spectra of CuChi3 and CuChi12 films without and with cellulose: a) Chitosan, b) CuChi3, c) CuChi3/BC, d) CuChi12 and e) CuChi12/BC.

The elemental analysis performed on the samples confirmed the expected compositions. The spectra were acquired in different areas of the specimen to evaluate the dispersion of the copper and the cellulose fibres within the matrix. The peaks relative to gold and palladium were found in each spectrum as a result of the sputter-deposition pre-treatment performed on all samples in order to enhance their conductivity. All the samples showed the presence of copper

homogeneously distributed throughout the polymer network. Moreover, the spectra of the films developed from the cellulose-containing formulations (i.e. CuChi3/BC and CuChi12/BC) showed the presence of chlorine as a result of the successful functionalisation of the cellulose fibres previously performed. The relative amounts of each element were also evaluated (**Table 6.1**).

Table 6.1 Elemental composition of each film by EDX analysis. The amount of each element is reported as the relative weight %.

Sample	C	N	O	Cl	Cu	Pd	Au	Total
Chitosan	17.56	17.75	45.09	-	-	3.64	15.97	100.00
CuChi3	19.77	17.67	44.24	-	1.76	3.49	13.07	100.00
CuChi3/BC	25.24	15.21	42.26	0.60	1.15	3.22	12.31	100.00
CuChi12	20.60	15.84	52.43	-	3.45	1.47	6.21	100.00
CuChi12/BC	25.24	12.30	43.80	0.27	4.80	2.65	10.93	100.00

The EDX technique is based on the interaction between the primary beam of protons or X-rays generated from a source and the sample. When the beam hits the sample, the electrons of the inner low-energy shells are excited to a higher energy level or expelled from the atom, leaving a vacancy in the inner shell. The second step consists in the transition of an electron from one of the outer shells to the inner shell, where it fills the vacancy. During the transition, an X-ray emission is generated, which corresponds to the difference between the high-energy level and the low-energy level. This difference is typical for each atom, as it depends on the atomic structure of the element. The reliability of the EDX analysis for quantitative evaluation of light elements is low, especially in case of $Z<11$. In particular, H and He, respectively with $Z=1$ and $Z=2$, do not have characteristic X-rays, therefore they are not detectable by EDX, as well as Li ($Z=3$), which has too low-energy characteristic X-rays. Elements with low Z have low-energy characteristic X-rays that are also subjected to strong absorption by the specimen itself, therefore the emission of these atoms is highly dependent on the

specimen shape and geometry (Shindo and Oikawa, 2002; Egerton, 2011). Nevertheless, it was possible to observe the increase in copper concentration from the CuChi3 composition to the CuChi12 one.

The chemical structure of the composites developed was further investigated through ATR FT-IR analysis (**Figure 6.8**).

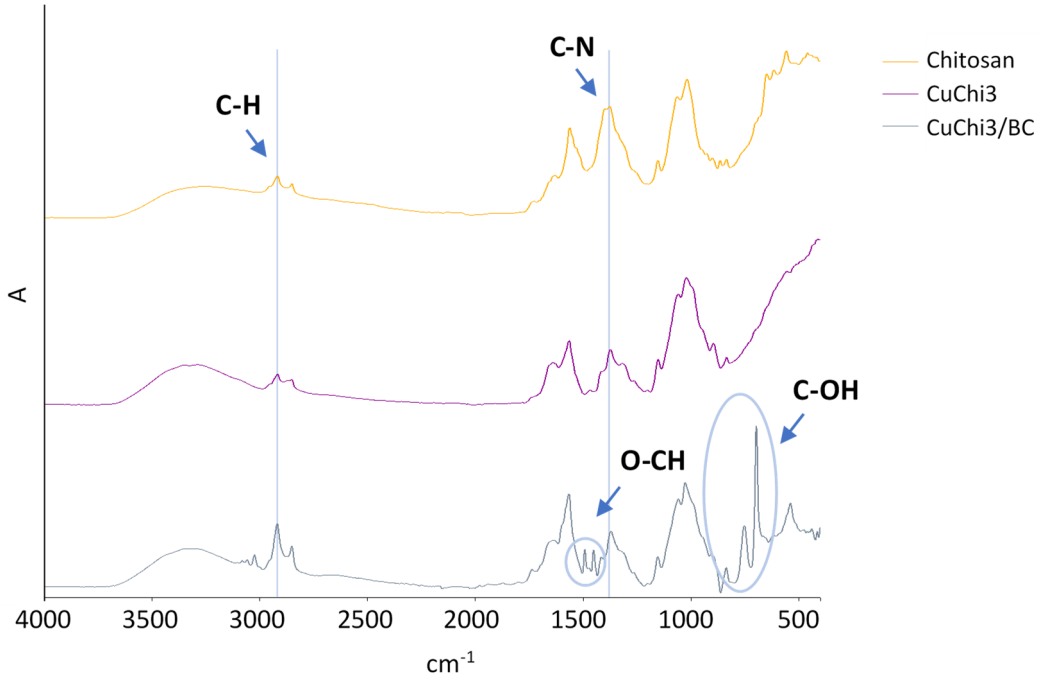

Figure 6.8 ATR FT-IR spectra of chitosan, CuChi3 and CuChi3/BC as representative samples

The spectra acquired showed the decrease in the intensity of the C-N peak from pure chitosan to the copper-loaded samples. It was also noted that the width of the absorption band was larger as compared to neat chitosan and slightly shifted towards lower wavenumbers, meaning that some interaction had occurred involving the functional groups of the bond. This result indicated the successful complexation of the copper ions by the amino groups of chitosan with consequent cross-linking of the polymer chains and, therefore, limitation of their molecular vibrations (Qu *et al.*, 2011; Gritsch *et al.*, 2018). In addition to this, it was possible to observe the characteristic peaks of cellulose in the CuChi3/BC sample. In particular, the increase of the intensity of the C-H stretching at ≈ 2890-2900 cm^{-1} as well as the presence of the H-C-H and O-C-H bending in the 1450-

1500 cm^{-1} region and C-O-C and C-C-O stretching at 650-900 cm^{-1} confirmed the successful incorporation of cellulose (Kačuráková *et al.*, 2002; Zhou *et al.*, 2007).

6.2.4 Physical characterisation

6.2.4.1 Wettability study

The hydrophilicity of the composites developed was studied to understand the influence of the cellulose fibres on the chitosan matrix. The assay was conducted on flat samples using the sessile drop technique to measure the static contact angle (**Figure 6.9**).

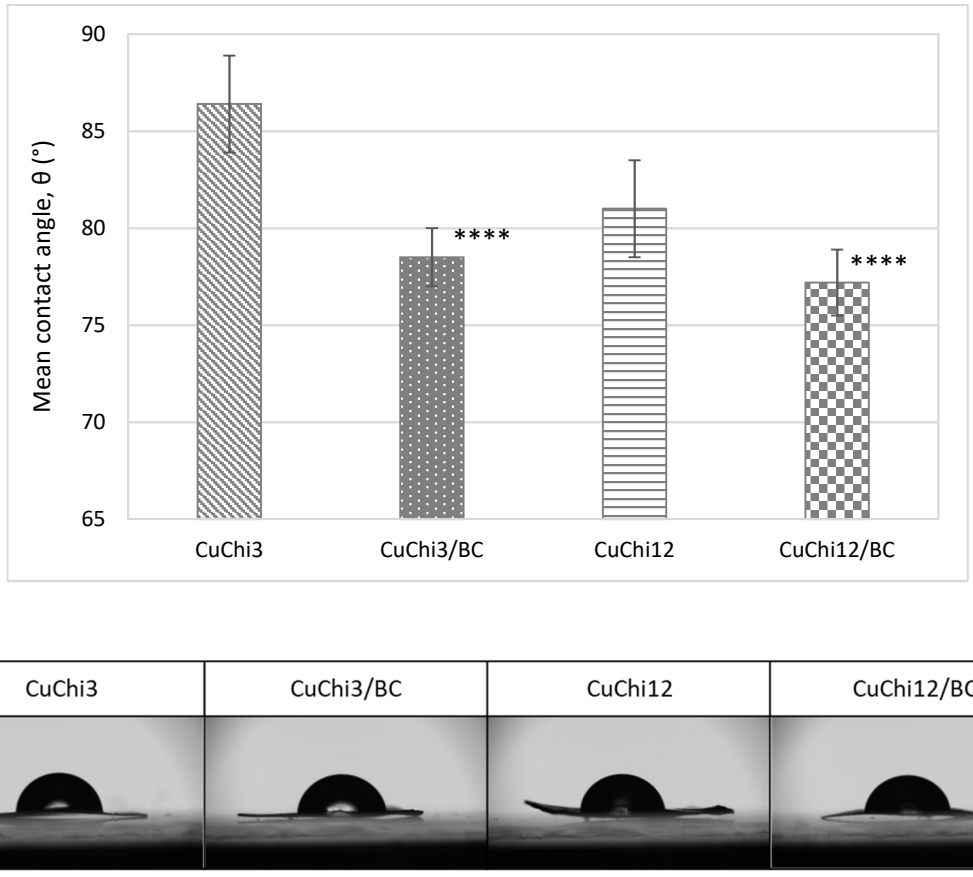

Figure 6.9 Static water contact angle of the CuChi films without and with BC (n=3) and images. No statistically significant difference was observed between the two cellulose-containing formulations ($p>0.05$), whereas both of them were significantly lower than the corresponding non-loaded samples (****=$p<0.0001$).

For both chitosan/cellulose composites (i.e. CuChi3/BC and CuChi12/BC), lower water contact angle values were observed with respect to the corresponding compositions without cellulose. As a general assumption, in case

of contact angles (ϑ) higher than 90°, the sample is indicated as hydrophobic, while if ϑ is lower than this value, it is considered hydrophilic (Yuan and Lee, 2013). All the films demonstrated a hydrophilic nature with ϑ below this threshold; however, CuChi3/BC and CuChi12/BC showed higher wettability. In particular, no statistically significant difference was observed between the two cellulose-containing formulations ($p>0.05$), whereas both of them were significantly lower than each of the non-loaded samples ($p<0.0001$).

6.2.4.2 Mechanical properties

The mechanical properties of the composites developed were evaluated to assess the influence of the presence of the cellulose fibres. The tensile test was performed after hydration of each specimen for 30 minutes (**Figure 6.10**). The Young's modulus (E), ultimate tensile strength (UTS or σ_U) and elongation at break are reported in **Table 6.2**.

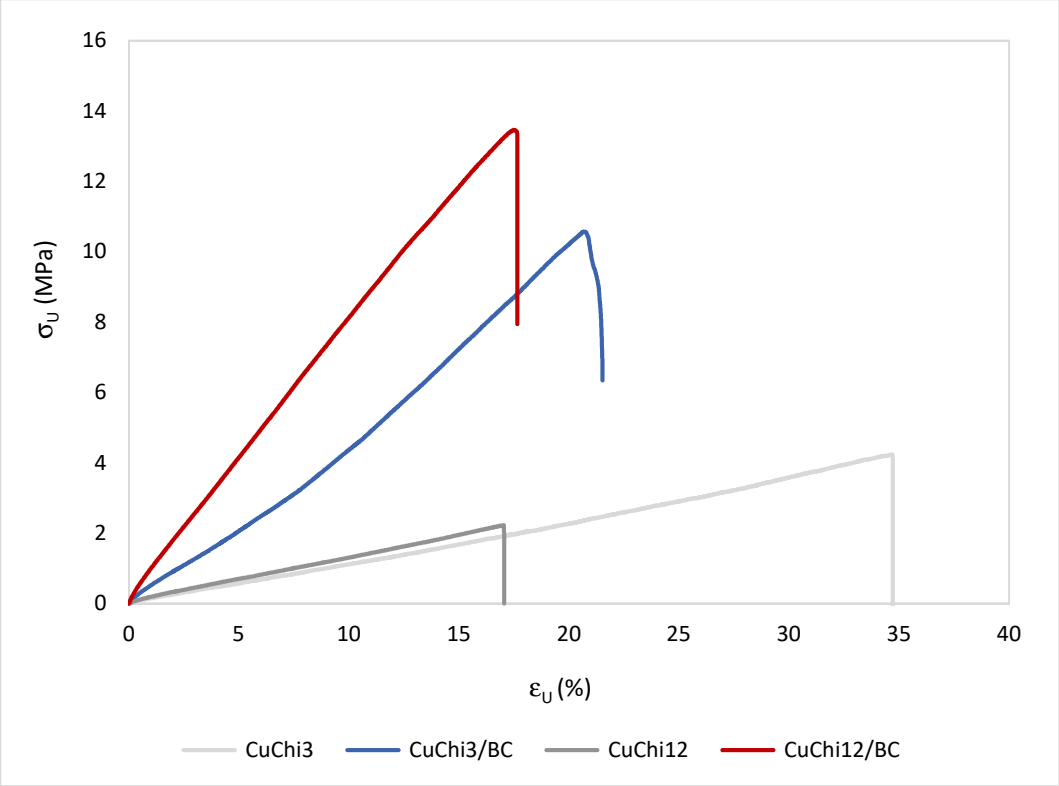

Figure 6.10 Representative stress-strain curves for each sample, i.e. CuChi3, CuChi3/BC, CuChi12 and CuChi12/BC.

Table 6.2 Mechanical properties of the copper(II)-chitosan composites after hydration pre-treatment

Sample	E [MPa]	σ_U [MPa]	ε_U [%]
CuChi3	14 ± 4	3.6 ± 0.4	32 ± 9
CuChi3/BC	43 ± 4	10 ± 1	20 ± 1
CuChi12	9 ± 3	1.5 ± 0.5	17.5 ± 0.3
CuChi12/BC	91 ± 11	12 ± 1	15 ± 2

It was possible to observe a sharp increase of both Young's modulus and ultimate tensile strength for the samples containing the cellulose fibres, while the elongation at break remained almost constant, with significantly higher values only for the CuChi3 composition as compared to the CuChi12 and CuChi12/BC specimens. In particular, a statistically significant variation was observed in the Young's modulus of the samples upon incorporation of cellulose ($p<0.05$), with a two-fold and nine-fold increase for CuChi3 and CuChi12, respectively. The moduli of the neat CuChi films, on the other end, were found to be not significantly different between each other, probably because the complexation of copper did not affect the stiffness of the material. The values of the ultimate tensile strength showed the same trend, with an increase of about 200% and 700% for the CuChi3/BC and CuChi12/BC scaffolds as compared to the non-loaded ones.

Overall, all the samples showed a brittle behaviour, with linear elastic deformation from 0 to 15-20% of elongation at break. The addition of the cellulose fibres in the copper-chitosan matrix did not cause any variation in the trend, i.e. no plastic deformation was observed. However, it resulted in significantly higher stiffness and higher resistance to fracture without increasing the brittleness of the material (as it would be expected), with no statistically relevant variation in the elongation at break.

6.2.5 Stability studies

6.2.5.1 Swelling profile

The water uptake of both copper(II)-chitosan compositions was evaluated and compared to the respective sample after incorporation of the cellulose fibres to study the influence of cellulose. The ability to swell upon absorption of water and maintain the moisture over time is in fact particularly important in wound healing, where an optimal level of hydration is crucial for the health of the wound (Ousey *et al.*, 2016). The samples were incubated in PBS solution and the weight variation over time was calculated (**Figure 6.11**).

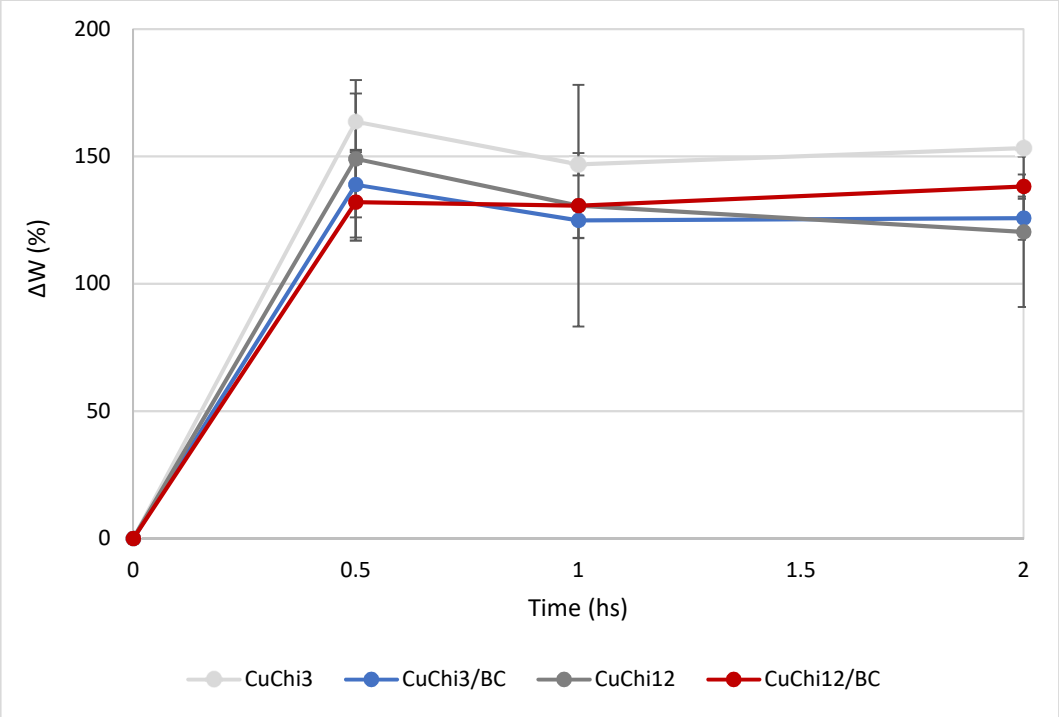

Figure 6.11 Swelling profile of the copper(II)-chitosan composites in PBS solution at room temperature.

All the samples showed a similar trend in their swelling behaviour, with no statistically relevant difference and a rapid water uptake upon incubation in the medium. Both compositions (i.e. CuChi3 and CuChi12), regardless of the incorporation of the cellulose fibres, increased their weight of about 130-160% within the first 30 minutes, with no statistically significant variation between the samples. After one hour of incubation a plateau was reached, with a slight

decrease in the weight for all the films (125-150%). Overall, all the specimens exhibited good swelling ability, with an increase of about 2.5 times of their initial dry weight and a final concentration of water of 55-60% w/w for all the compositions. The presence of the cellulose fibres did not seem to influence the water uptake.

6.2.5.2 Stability studies

The stability of the materials developed over time was studied by determination of their weight variation (ΔW) in liquid medium (**Figure 6.12**). The samples were incubated in PBS solution for 30 days at 32 °C, which is the average temperature of an acute wound bed (Fierheller and Sibbald, 2010; Power, Moore and O'Connor, 2017).

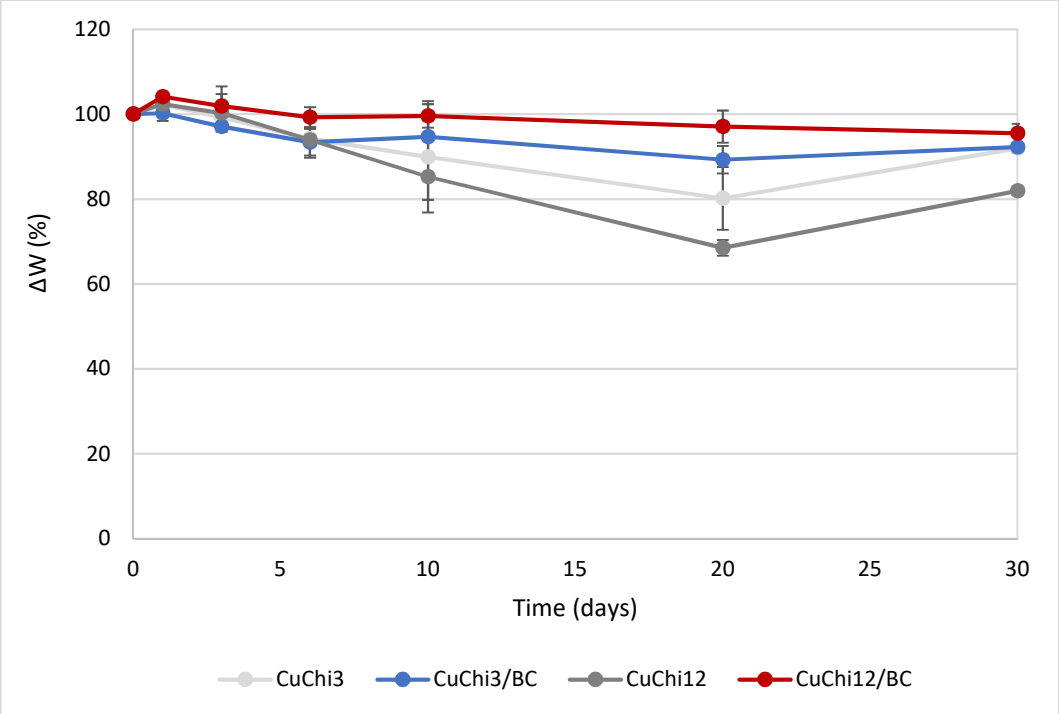

Figure 6.12 Stability of the copper(II)-chitosan composites in PBS solution at 32 °C.

In the first 6 days, all the samples retained their initial weight with no substantial weight loss (< 7%) and no statistically significant variation between each other. From day 10, two different patterns were observed: the cellulose-loaded composites showed a linear trend, while for the other two compositions a higher

weight variation took place. In particular, the weight of CuChi12/BC remained almost constant, with a final ΔW of 5% after 30 days, while for CuChi3/BC the final weight was about 90% of the initial weight. For the copper-chitosan films, on the other hand, a much higher loss was detected, with a maximum reduction after 20 days, when the weight of CuChi3 and CuChi12 was, respectively, the 80% and the 70% of the initial weight ($p<0.05$ for CuChi12 as compared to the other samples). After 30 days of incubation, an increase in the weight was observed for both compositions. The reason for the decrease of the weight after 20 days followed by an increase could be the degradation of the polymeric network and the subsequent absorption of water.

The assay highlighted the higher stability of the cellulose-loaded samples as compared to their non-loaded counterparts. This might be due to the presence of the fibres within the chitosan matrix, as they acted as a reinforcing agent by stabilising the structure and preventing the degradation of the polymeric chains in liquid medium.

6.2.6 Biological characterisation

6.2.6.1 Antibacterial activity evaluation

The antibacterial activity of the composites upon incorporation of the modified cellulose fibres was evaluated by direct and indirect contact assay. The tests were carried out using a Gram positive and a Gram negative strain in order to have a clear understanding of the inhibitory capacity of the agents. First, the antibacterial activity on contact was studied using a modified ISO procedure (ISO 22196). As previously described, the protocol involved the cultivation of the bacteria directly on the surface of the samples followed by recovery of the cells after 24 hours. The number of viable cells was determined through drop plate technique and compared to the control specimens, i.e. plain chitosan and polyethylene terephthalate (PET). The percent antibacterial activity ($R\%$) was then calculated using the formula below:

$$R\% = \frac{(a)\,[unmodified] - (a)\,[modified]}{(a)\,[unmodified]} * 100$$

where a is the number of cells recovered per specimen (CFU/mL*cm^2).

The antibacterial activity against *S. aureus* cells was calculated with respect to plain chitosan (**Figure 6.13**).

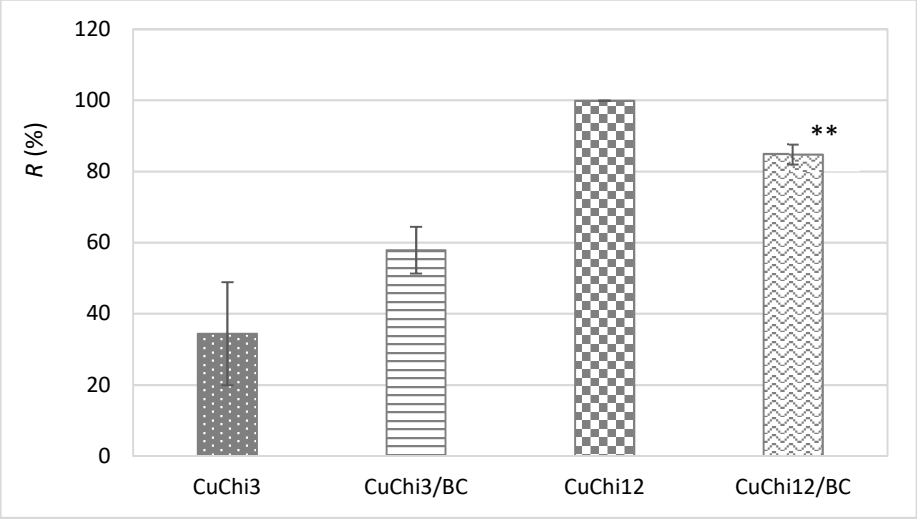

Figure 6.13 Antibacterial activity of the copper-chitosan films against *S. aureus*; control: chitosan. No statistically significant difference was observed between CuChi3 and CuChi3/BC, whereas CuChi12/BC was significantly different as compared to CuChi12 (**=p<0.01).

The assay evidenced that all the samples possess higher properties as compared to plain chitosan. In particular, the CuChi3/BC composite was found to exhibit increased activity (almost 58% *vs* 34%) with respect to the non-loaded counterpart (i.e. CuChi3), although not statistically relevant. On the other hand, the BC-loaded CuChi12 exerted slightly lower effect than CuChi12, with a 15% decrease in the $R\%$ value. This effect could be ascribed to the presence of the cellulose fibres within the network, where the hydroxyl groups could have stabilised the copper(II) ions (present in higher concentration) through hydrogen bonding.

In order to gain a more comprehensive understanding of the antibacterial effect of the materials, the same test was also carried out using PET as the control (**Figure 6.14**), as it is an inert substrate that has been proven not to positively or negatively affect the growth of bacteria. Chitosan, on the other hand, has been

reported to possess antibacterial properties thanks to the presence of amino groups in the backbone, especially in the case of Gram positive strains that lack the external membrane and are, therefore, more accessible to the action of the bactericidal agents (Raafat and Sahl, 2009; Goy, Morais and Assis, 2016).

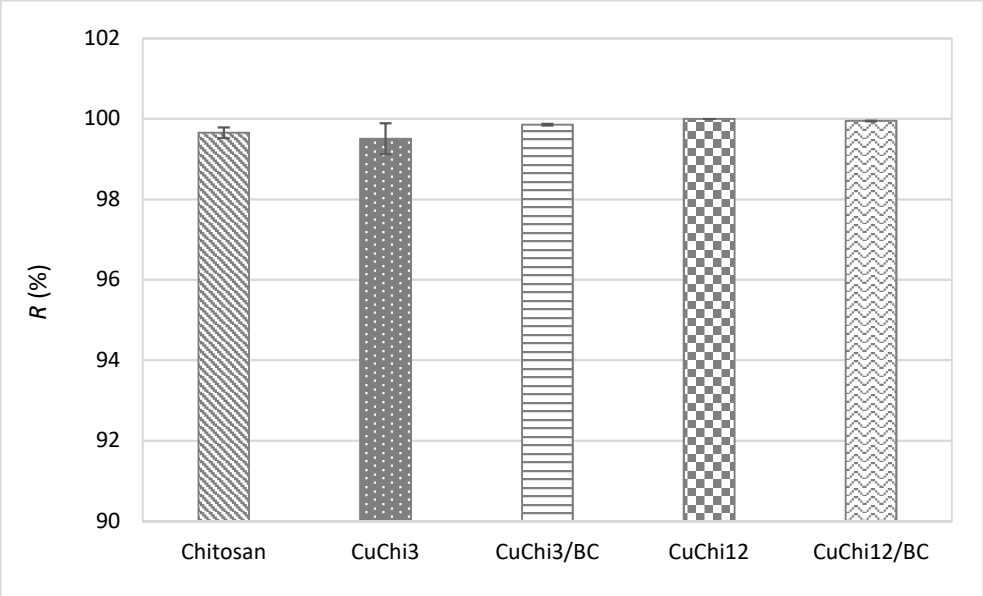

Figure 6.14 Antibacterial activity of the copper-chitosan films against *S. aureus*; control: PET. No statistically significant variation was observed between the samples ($p>0.05$).

As expected, all the samples showed excellent antibacterial activity (≥ 99%), including plain chitosan. The results highlighted that the materials developed were highly active against the growth of *S. aureus* as compared to an inert substrate, and presented improved efficiency with respect to plain chitosan (i.e. chitosan without copper or modified cellulose fibres).

The antibacterial activity upon direct contact of the samples against *E. coli* was also determined using plain chitosan as the reference (**Figure 6.15**). In this case, an antibacterial effect was observed for all the compositions, probably because untreated chitosan is less efficient in the inhibition of the proliferation of Gram negative bacteria, thus making it a suitable reference material for the quantification of the antibacterial activity.

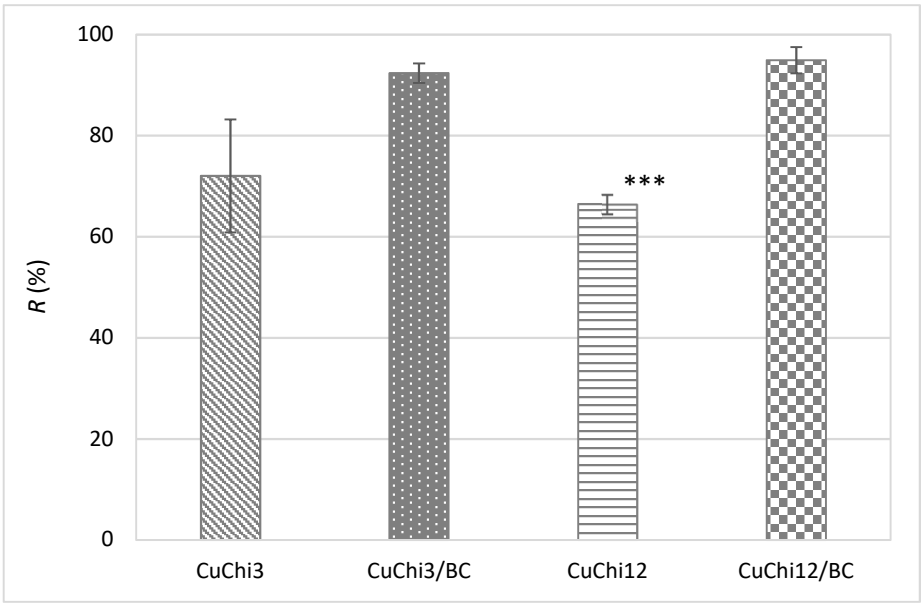

Figure 6.15 Antibacterial activity of the copper-chitosan films against *E. coli*; control: chitosan. No statistically significant difference was observed between CuChi3 and CuChi3/BC, whereas CuChi12/BC was significantly different as compared to CuChi12 (***=$p<0.001$).

As a general trend, the samples containing the functionalised cellulose fibres exhibited equal or superior antibacterial activity against *E. coli*. In particular, CuChi3/BC presented an increase of about 20% in the *R*% with respect to its non-loaded counterpart, although not statistically significant. In the case of the CuChi12 composition, on the other hand, the presence of the fibres resulted in a statistically relevant increase of the activity, with almost 95% decrease in the bacterial cell count for the CuChi12/BC sample *vs* 66% for the CuChi12.

The activity of the copper released from the chitosan-cellulose systems was also evaluated by indirect contact assay. The samples were incubated in nutrient broth and the eluates were collected at different time points and left in contact with the bacteria overnight. The test was first performed against *S. aureus* (**Figure 6.16**), showing similar results as compared to the direct contact activity evaluation.

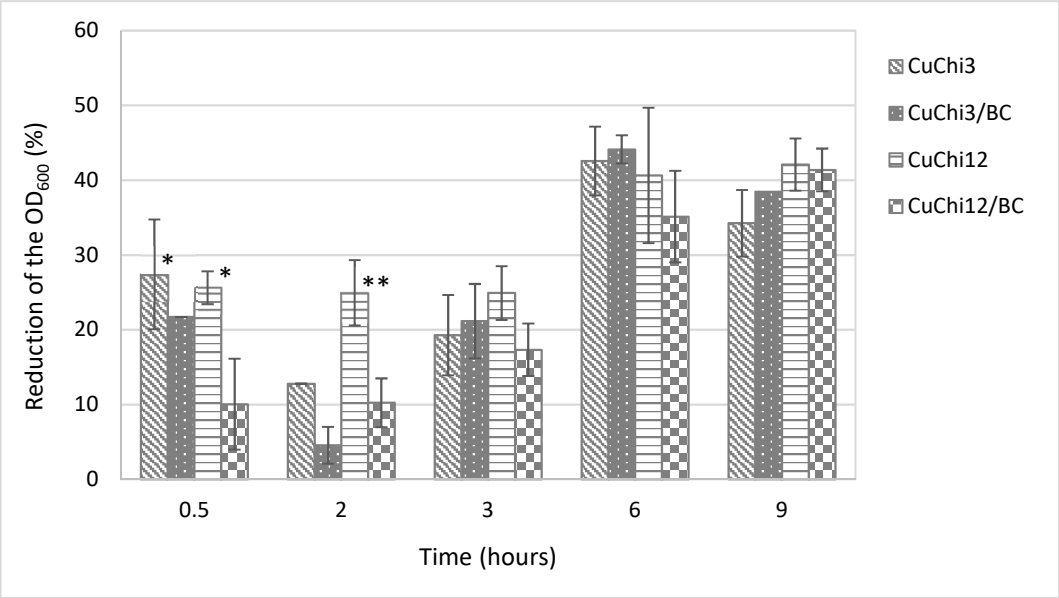

Figure 6.16 Indirect antibacterial activity evaluation against *S. aureus*. After 30 minutes, the reduction caused by CuChi3 and CuChi3/BC was found to be significantly different than the corresponding BC-loaded samples (*=$p<0.05$), while after 2 hours CuChi12 was significantly different than CuChi12/BC (**=$p<0.01$). No statistically significant difference was observed between any of the compositions after 3, 6 and 9 hours.

All the samples caused a reduction in the OD measured at 600 nm upon contact with *S. aureus* as compared to the positive control. No statistically significant variation was observed between the two copper-chitosan compositions for most of the time points, despite the difference in copper concentration. This might be due to the interaction between the metal ions and the amino groups of chitosan, which act as ligands for copper and prevent it from being completely released into the medium. After 2 hours, significantly higher antibacterial effect was obtained for the CuChi12 sample as compared to the other three compositions ($p<0.05$), probably because of the higher concentration of copper. On the other hand, the CuChi12/BC did not show the same trend: it is possible that the cellulose fibres provided binding sites for the copper ions due to the presence of the hydroxyl groups, thus causing a lower rate of copper release. After 3 hours, all the specimens showed similar antibacterial effect, with no statistically significant difference ($p>0.05$ for all the samples at 3 hours, 6 hours and 9 hours). Moreover, after 6 hours, no further reduction was detected in the bacterial cells count, probably as a result of the stabilisation in the copper release from the samples.

The assay was also carried out against *E. coli* to evaluate the effect of the copper ions on bacterial growth (**Figure 6.17**).

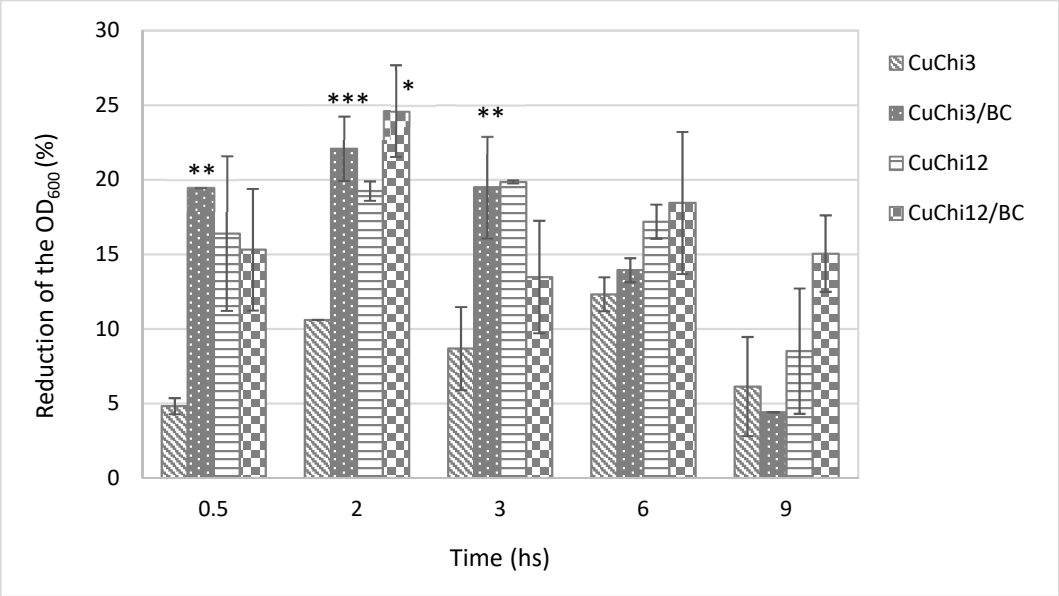

Figure 6.17 Indirect antibacterial activity evaluation against *E. coli*. After 30 minutes and 3 hours, the reduction caused by CuChi3 was found to be significantly different than the corresponding BC-loaded sample (**=$p<0.01$), while after 2 hours both CuChi3 and CuChi12 were significantly different than, respectively, CuChi3/BC and CuChi12/BC (***=$p<0.001$ and *=$p<0.05$). No statistically significant difference was observed between any of the compositions after 6 and 9 hours.

The assay showed lower inhibition efficiency against *E. coli* as compared to *S. aureus*, with a maximum of bacterial proliferation reduction of about 20-25%, whereas values of about 45% were reached after 6 hours of incubation with *S. aureus*. This confirmed the results obtained for the evaluation of the antibacterial activity upon direct contact, showing that copper has a stronger effect on Gram positive strains. Moreover, for both compositions, a higher reduction of the growth of *E. coli* was observed for the cellulose-loaded films at almost all the time points, with the maximum statistically significant difference registered between the CuChi3-based compositions in the first 3 hours ($p<0.05$ between CuChi3 and CuChi3/BC). A possible explanation for this could be the release of some of the cellulose fibres from the matrix, which could have contributed to the antibacterial activity of the samples. This phenomenon was not visible in the case of *S. aureus*. Once again, the reason for this might be that *E. coli* was less susceptible to the

antibacterial action of copper, which resulted in a higher effect of the samples loaded with the cellulose fibres. On the contrary, copper-chitosan samples showed great bacterial inhibition against *S. aureus* even without cellulose, therefore the contribution of the fibres could have been undetectable.

6.2.6.2 Cytotoxicity studies

The cellulose-chitosan composites were characterised with respect to their cytotoxicity towards keratinocytes to evaluate their suitability for wound healing applications. In particular, HaCat cells were used to measure the biological properties of the samples as well as the effect of the copper released over time through indirect contact test.

First, the cells were cultured for 6 days with the samples placed on semi-permeable supports. For all the time points considered, the CuChi3 and CuChi3/BC compositions resulted in good cell viability, with values of about 80% as compared to the positive control even after 6 days of incubation. No statistically significant difference was observed between CuChi3, CuChi3/BC and CuChi12/BC as compared to the positive control ($p>0.05$) after 24 hours of incubation. After 3 days and 6 days of incubation, however, both samples with higher copper concentration (without and with cellulose) caused statistically significant decrease in the viability, with minimum values of about 20% and 45% respectively for the specimen without and with cellulose. As regards the CuChi3 and CuChi3/BC compositions, on the other hand, no significant difference was observed with respect to the positive control after 3 days of incubation, and a final cell viability of about 80% was reached after 6 days of contact (**Figure 6.18**).

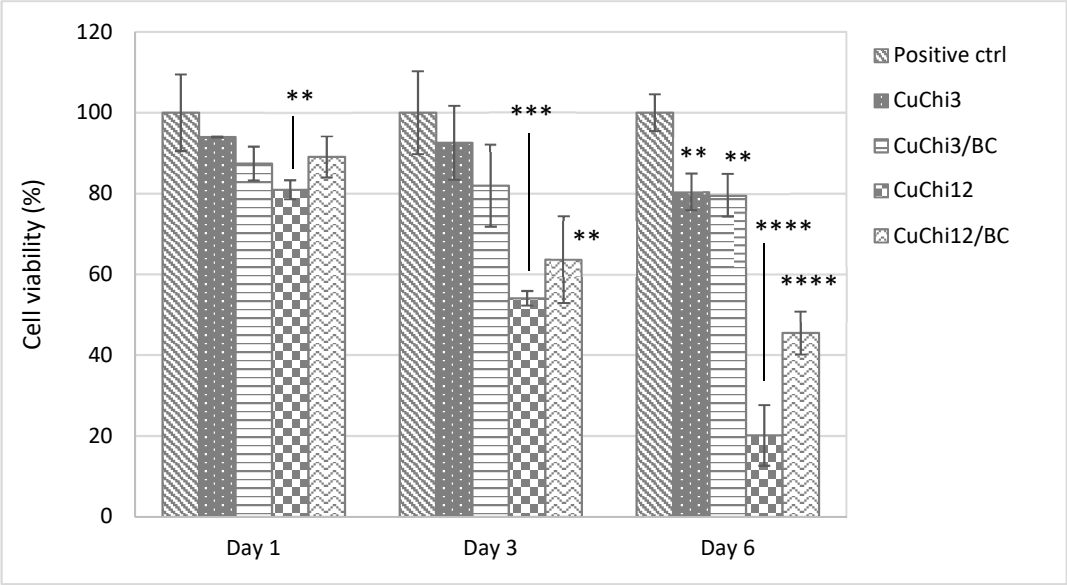

Figure 6.18 Viability of HaCat cells upon contact with the copper-chitosan films without and with cellulose placed on semi-permeable supports. Positive control: keratinocytes growth medium After 1 day, only CuChi12 was found to be significantly different than the positive control (**=p<0.01), while after 3 days both CuChi12 and CuChi12/BC were significantly different (***=p<0.001 and **=p<0.01). After 6 days, all the samples were found to be significantly different than the positive control (**=p<0.01 and ****=p<0.0001).

The results obtained clearly highlighted that high concentrations of copper caused an adverse effect towards the cells. This was further confirmed by evaluation of the cytotoxic effect of the copper released over 6 days from each composition (**Figure 6.19**).

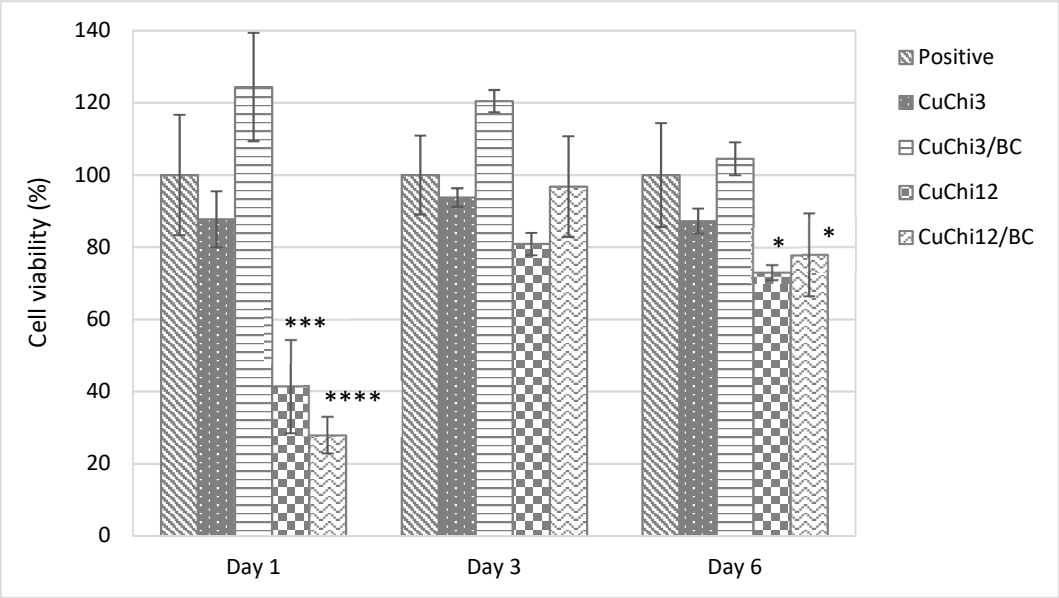

Figure 6.19 Viability of HaCat cells upon contact with undiluted eluates from the copper-chitosan films without and with cellulose. Positive control: keratinocytes growth medium. After 1 day and 6 days, the cell viability for CuChi12 and CuChi12/BC was found to be significantly different than the positive control (*=$p<0.05$, ***=$p<0.001$ and ****=$p<0.0001$). No statistically significant difference was observed between the compositions after 3 days of incubation ($p>0.05$).

For the CuChi3 composition, statistically significant increase in the cell viability was detected after 1 and 3 days for the composite loaded with the cellulose fibres ($p<0.05$). This might be due to the release of some of the fibres from the scaffold, which could have improved the viability of the cells. The CuChi12 and CuChi12/BC samples, on the contrary, caused a massive decrease on the cell viability after the first 24 hours of incubation ($p<0.05$ as compared to the positive control). It is possible that a burst release of copper resulted in a cytotoxic effect on the cells. On the other hand, no statistically relevant variation in the viability was observed for the CuChi3 and CuChi3/BC compositions after 6 days, proving that the amount of copper released was below the cytotoxicity threshold.

Overall, the biological characterisation of the materials allowed the determination of an optimal threshold that could ensure good antibacterial efficiency as well as low cytotoxicity towards keratinocytes. Based on the results obtained, the CuChi3 and CuChi3/BC compositions resulted in good cell viability even after 6 days of incubation with the cells, confirming them to be the most suitable substrates for the development of antibacterial wound healing patches.

6.3 Discussion

In this chapter, the development of novel chitosan/cellulose based systems through physical incorporation of chemically modified bacterial cellulose fibres was reported. To achieve this, copper(II)-loaded chitosan (CuChi) was used as the bulk material for the fabrication of composites with applicability in wound healing. The copper-chitosan was obtained through collaboration within the framework of the HyMedPoly project. The material was produced following the procedure described in literature by Gritsch *et al.* (Gritsch *et al.*, 2018). For this purpose, two copper(II)-chitosan compositions were used with increasing copper concentration, namely CuChi3 and CuChi12. The influence of copper on the properties of the final materials, especially on its biological behaviour, was therefore investigated.

The chitosan/cellulose composites were obtained upon grinding and loading of bacterial cellulose within the copper-chitosan matrix. Because of its insolubility in most of aqueous and organic solvents, numerous studies focused on the production of cellulose nanofibrils without dissolution of the polymer. Several methods have been reported in literature, which can be classified in two main strategies, i.e. the conventional mechanical disintegration and the more recent biological/chemical processes (Lavoine *et al.*, 2012; Abdul Khalil *et al.*, 2014; Nechyporchuk, Belgacem and Bras, 2016). In this study, a mechanical wet grinding treatment was performed to obtain the fibrils. The drawbacks of the conventional mechanical treatments are mainly related to the lower degree of fibrillation achieved as compared to the chemical ones. To enhance the fibrillation efficiency, high energy consumption or specific pre-treatments are required, with an increase in the final costs. For this reason, recent studies have been focused on the development of new chemical strategies, especially on an industrial scale. On the other hand, the mechanical approach does not result in any modification of the cellulose structure, whereas the biological/chemical ones involve the use of other agents and cannot be performed in water. To avoid derivatisation of the polymer structure, a mechanical process was adopted in this study. As confirmed by the elemental composition obtained from EDX analysis, this allowed to

produce chemically pure never-dried cellulose fibres. Furthermore, the morphological evaluation highlighted the presence of the fibrillar network of cellulose, which was retained upon grinding. After this, the fibres were chemically functionalised with the aim to introduce antibacterial groups following the procedure described in chapter IV. The reaction was carried out in aqueous system directly on the fibres in order to achieve higher degree of derivatisation thanks to the increased surface area available as compared to the cellulose pellicles.

The composites were then produced through solvent-casting technique. The miscibility between the two polymers was studied by SEM analysis for all the compositions. As expected from previous studies, no visible phase separation was observed for any of the compositions. The presence of the fibres was clearly visible in cellulose-loaded samples, with homogeneous dispersion in the chitosan matrix. The interaction between the two polysaccharides was investigated in depth by Holmberg *et al.*, who justified the attraction between the polymers as a result of the bridging between some extended chains of cellulose and the chitosan surface. The polyelectrolyte nature of chitosan might also have contributed to this long-range attraction, with van der Waals forces taking place between the amino groups of chitosan and the hydroxyl groups of cellulose that resulted in weak intermolecular bonding (Holmberg *et al.*, 1997). The SEM images of the freeze-dried chitosan/cellulose scaffold seemed to validate such hypothesis, as the cellulose fibres were arranged transversally between the chitosan layers.

The materials developed were then characterised with respect to their chemical and physical properties. The chemical analysis confirmed the successful incorporation and dispersion of the cellulose fibres within the chitosan matrix, as observed by EDX analysis. The elemental composition of each sample showed the presence of copper, with increasing concentration from the CuChi3 to the CuChi12 compositions, as well as chlorine (in the case of the samples loaded with modified cellulose fibres), which was introduced upon functionalisation of the cellulose fibres. The chemical composition was further investigated by ATR FT-IR analysis. The spectra of the copper-loaded samples (i.e. CuChi3 and

CuChi3/BC) showed a decrease in the intensities of the peak related to the C-N bond as a result of the complexation of copper by the amino groups of chitosan. Furthermore, the characteristic peaks of cellulose were detected in the CuChi3/BC sample, confirming the incorporation of the fibres in the chitosan network.

The tensile test carried out on the composites highlighted the reinforcing effect of cellulose. As previously mentioned, the use of fibres as reinforcing agents to improve the mechanical properties of a substrate has been widely explored to enhance the applicability of chitosan. This study confirmed that the presence of the cellulose fibres resulted in significantly higher mechanical performance and stability as compared to non-loaded samples. The Young's modulus and the ultimate tensile strength of the samples containing the fibres showed, in fact, a significant increase as compared to the neat copper-chitosan films. According to previous studies, non-porous films of neat chitosan usually show an elastic modulus of about 5-7 MPa, while for the cellulose/chitosan composites here described values of circa 40 MPa and 90 MPa were obtained respectively for the CuChi3/BC and CuChi12/BC samples (Francis Suh and Matthew, 2000; Le *et al.*, 2012; Ahmed *et al.*, 2017). Surprisingly, the addition of the cellulose fibres did not result in the embrittlement of the material, as a decrease in the elongation at break would be expected upon addition of reinforcing agents.

The swelling capacity of the copper(II)-chitosan composites as well as their stability in liquid medium was studied. Upon incubation in liquid medium, all the materials showed a weight increase of about 130-160% within the first 30 minutes. After this period, the weight reached a plateau and no massive variation was observed over time, showing that the water uptake of each sample led to the development of a stable hydrogel. This was ascribed to the coordination of the copper(II) ions by the amino groups of chitosan, which resulted in the formation of a cross-linked network that behaved as a hydrogel in liquid medium. The most common coordination numbers for copper(II) ions are four, five and six, with different geometries expected, such as tetrahedral or square planar geometry (n=4), square pyramid or trigonal bipyramid (n=5) or octahedral (n=6). In

addition to these, copper-based complexes with different coordination numbers have been observed (Gaazo, 1976; Chaurin, Constable and Housecroft, 2006). Although it is not clear which geometry is adopted in the coordination of copper by the amino and hydroxyl groups of chitosan, previous studies suggested that inter-molecular cross-linking occurred as a result of the bonding between copper and ligands from different chitosan chains ('*bridge* model'). In particular, the formation of complexes with four ligands was observed (Schlick, 1986; Rhazi *et al.*, 2002). In addition to this, the wettability of the films was studied through determination of the static water contact angle. It is generally acknowledged that in the case of contact angle higher than 90° the material is considered to be hydrophobic, whereas if it is lower, the sample is referred to as hydrophilic. The test showed that the cellulose-loaded compositions presented significantly higher contact angle values as compared to the neat copper-chitosan. This effect could probably be ascribed to the incorporation of cellulose within the chitosan matrix. Cellulose presents, in fact, a high degree of hydrophilicity thanks to the presence and structural position of three hydroxyl groups in the glucose ring (Lindman *et al.*, 2017).

The hydrophilic nature of the composites turns these materials into optimal substrates for the development of dressings that can be applied to different types of wounds. The copper-chitosan/cellulose patches can be applied in a dry form to exuding wounds. The fluids can in fact be absorbed and firmly trapped within the matrix thanks to the swelling ability of the material, thus preventing the maceration of the peri-wound skin as a consequence of prolonged contact with moisture (Ousey *et al.*, 2016). On the other hand, the films can also be used for dry wounds upon hydrating pre-treatment to obtain a stable hydrogel that can ensure a good level of moisture during the wound healing process.

The stability of the samples in liquid medium was also studied over a period of 30 days. All the compositions showed good retention of their wet weight in the first 10 days of incubation. After this time, a weight loss of about 20-30% was detected for the neat copper-chitosan films, while the cellulose-loaded composites maintained their initial weight, with an overall variation of about 5%

and 10%, respectively, for CuChi12/BC and CuChi3/BC over 30 days. This effect could be ascribed to the stabilising effect of the cellulose fibres to the chitosan network, which resulted in the reinforcement of the structure by preventing the degradation of the material in moist environment.

As mentioned in the introductory section of this chapter, it is crucial to control the concentration of copper in order to minimise its toxicity in the case of copper-based materials for biomedical applications. Copper acts as an antibacterial agent by causing cellular damage through oxidative stress, competition with other metal ions for the binding sites of proteins and depletion of thiol groups. On the other hand, it is also an essential trace element for humans, as it is a constituent of several metalloenzymes with different functions. However, it can have a toxic effect even towards eukaryotic cells if homeostasis is not controlled. In this study, an optimal copper concentration threshold was identified to ensure both good bacterial inhibition and low cytotoxicity towards keratinocytes.

As regards the antibacterial effect of the materials, their activity upon direct contact with bacteria was determined with respect to plain chitosan. In the case of *S. aureus*, no significant difference was observed between the CuChi3 composition and its BC-loaded counterpart, although the *R*% showed an increase from about 34% to almost 58%, respectively. The CuChi12, on the other hand, caused slightly higher reduction as compared to the CuChi12/BC samples, probably as a result of the binding of the copper(II) ions by the hydroxyl groups of cellulose. As chitosan has been reported in literature as an effective antibacterial agent, particularly in the case of Gram positive strains, an inert control, namely polyethylene terephthalate (PET), was used to quantify the antibacterial activity of the composites (Raafat and Sahl, 2009; Goy, Morais and Assis, 2016). As expected, when compared to PET all the samples resulted in almost total inhibition of the proliferation, with over 99% reduction in the bacterial cell count within 24 hours. The same test was then carried out against *E. coli* using chitosan as the reference. It was found that the presence of copper caused circa 80% and 65% decrease of the bacterial cells number (respectively, for CuChi3 and CuChi12). Furthermore, enhanced antibacterial effect was

observed for the samples loaded with the modified cellulose fibres, with *R%* values of over 90% for both formulations. A similar trend was noted upon evaluation of the antibacterial effect after indirect contact, with a maximum bacterial growth reduction of 20% for *E. coli* and 45% for *S. aureus*. Moreover, in the case of *E. coli*, significantly higher inhibition was observed for the samples containing cellulose at all time points. Although both copper and quaternary ammonium groups (from the cellulose fibres) are known to be effective against both Gram positive and Gram negative bacteria, the cell wall structure of Gram negative strains usually results in higher tolerance towards bactericidal agents thanks to the presence of an additional external layer (Exner, 2017). Previous studies confirmed that copper is more efficient in inhibiting Gram positive strains as compared to Gram negative strains exposed to the same copper concentrations, probably as a result of the lower permeability of the cell (Raffi *et al.*, 2010; Azam *et al.*, 2012). Hence, the contribution of the modified fibres might have been decisive in the evaluation of the antibacterial activity of the system against *E. coli*, whereas no statistically relevant difference was detected between the activity of non-loaded and loaded samples against *S. aureus*.

As regards the biological assessment using keratinocytes, it was noted that the CuChi3 composition did not show any massive cytotoxic effect even after 6 days of incubation with the cells. The viability was, in fact, higher than 80% with respect to the positive control for both cellulose-containing and neat samples. On the other hand, the films produced using the CuChi12 formulation caused a decrease in the viability, with values of about 60% after 3 days of incubation. The assay allowed to estimate a threshold value for the copper concentration that can ensure good antibacterial effect without resulting in high cytotoxicity towards keratinocytes, namely 2% w/w copper concentration with respect to chitosan.

6.4 Conclusions

In this chapter, the development of copper(II)-chitosan based composites by incorporation of modified bacterial cellulose fibres was reported. The materials showed excellent applicability in wound healing thanks to the antibacterial

properties of the system, which relies on the combined effect of copper-chitosan and the quaternary ammonium groups of modified cellulose. The results showed high inhibition of both Gram positive and Gram negative strains upon direct contact with the samples. An optimal copper concentration threshold was also identified to ensure low cytotoxicity towards keratinocytes for up to 6 days of contact. An enhancement in the mechanical properties of neat copper-chitosan films was observed after incorporation of the fibres, with increase in the tensile strength and elastic modulus of both compositions without embrittlement of the structure. The use of natural cellulose fibres as reinforcing agents, on the other hand, does not affect the biodegradability of the material, turning these composites into suitable substrates for the fabrication of environmental-friendly antibacterial wound dressings.

Chapter VII

Conclusions and future work

7.1 Conclusions

The work presented in this thesis was focused on the development of an antibacterial wound dressing through chemical/physical modification of bacterial cellulose. In particular, two different strategies were investigated for the surface functionalisation of the hydrogel and the results were compared from both the mechanical and biological point of view. In addition to this, copper-loaded chitosan was used as a substrate to incorporate ground cellulose in order to achieve a composite with enhanced properties.

First, the production of bacterial cellulose through fermentation of *Gluconacetobacter xylinus* was reported. The biosynthesis was carried out under static conditions using a variation of the Hestrin and Schramm medium containing glucose as the main carbon source. A temporal profiling of the fermentation was also attempted, although it was not possible to achieve the formation of the polymer as any interference caused by sample collection resulted in the inhibition of the biosynthesis. However, it was possible to observe a drop in the pH after less than 24 hours, probably as a result of the conversion of glucose into acidic by-products. After this, the pellicles were subjected to purification in order to kill and remove any residual biomass. Different methods were studied to optimise the washing process, and a combination of high temperature and basic conditions followed by sterilisation in autoclave was found to be the most successful one, as confirmed by colony forming assay and scanning electron microscopy (SEM). The morphological analysis of the material evidenced the typical nanofibrillar network of bacterial cellulose, with no evident degradation upon washing procedure. Due to the insolubility of cellulose in most aqueous and organic solvents, the chemical structure and composition of the pellicles was confirmed using solid-state techniques such as Fourier-transform infra-red (FT-IR) and energy dispersive X-ray (EDX) spectroscopies. Finally, the mechanical properties of the sample before and after purification/sterilisation were assessed through rheological assays. Frequency sweep and temperature ramp tests were conducted and the storage modulus (G') and loss modulus (G'') values were measured. For both specimens, an elastic-like response was detected

with *G'* higher than *G''* at all conditions, highlighting the solid nature of the hydrogels. The stability in liquid media was also studied in phosphate buffer saline (PBS) solution and keratinocytes growth medium, and no significant degradation in the interval considered was detected.

The cellulose membranes exhibited good applicability as wound dressing substrates, with high mechanical properties even after sterilisation and high water content (more than 97%), which ensures optimal hydration level during all wound healing stages. However, the lack of inherent antibacterial properties prevents the use of plain cellulose in the case of infected wounds. For this reason, various strategies for its surface modification were investigated to introduce antibacterial functionalities. An environmental-friendly aqueous-based reaction was first performed under basic conditions using sodium hydroxide as the catalyst. The hydroxyl groups of cellulose were deprotonated and derivatised through ring-opening reaction with two epoxides, i.e. glycidyl trimethylammonium chloride (GTMAC) and glycidyl hexadecyl ether (GHDE), bearing, respectively, a quaternary ammonium residue and a long alkyl chain. The two groups are in fact known to possess biocidal activity thanks to the cationic nature of nitrogen as well as the disruptive hydrophobic interaction of the carbon chain with the cell membrane. The reaction occurred in heterogeneous conditions probably following an S_N2 mechanism, involving nucleophilic attack of the alcoholate to the less hindered electrophilic carbon of the epoxide. The modified pellicles were then chemically characterised through EDX and X-ray photoelectron spectroscopy (XPS) to investigate the degree of derivatisation obtained. As for plain cellulose, the viscoelastic behaviour of the hydrogel was evaluated by rheological tests. The same assays previously described were performed, i.e. frequency sweep and temperature ramp. Once again, the sample showed good structural properties with a self-standing structure, and no significant difference was observed as compared to the untreated specimen even at high temperature. The material was also subjected to thorough biological characterisation in order to study the effect of the modification on both bacterial and human cells. The antibacterial efficiency upon direct contact was tested using

different methods against Gram positive and Gram negative strains and compared to pristine cellulose. Among these, a quantitative assay was performed following a standard procedure (ISO 22196). The results evidenced higher inhibitory efficiency in the case of *Staphylococcus aureus*, although significant reduction in the bacterial cell count was also observed for *Escherichia coli*. This could probably be ascribed to the presence of an external layer in the membrane of Gram negative bacteria, which results in higher resistance against the attack of antibiotics and other biocides. Furthermore, the SEM analysis showed a much lower number of cells on the surface of the modified sample, although some regions appeared to be colonised by bacteria, probably because of the inhomogeneity of the reaction occurring at the interphase between solid and liquid. The cytotoxicity of the hydrogel was studied via direct and indirect assay using keratinocytes, as the hydrogel was intended for wound healing applications. No statistically relevant difference was detected between the control group, the untreated sample and the treated one, with cell viability higher than 90% for up to 6 days of incubation. In addition to this, the morphology of the cells after 6 days of contact with the samples was evaluated via DAPI/phalloidin staining, showing in all cases the typical cobblestone pattern of growth and regular cell shape and size as compared to literature. The wound healing ability of the material was also investigated by performing an *in vitro* scratch test. The progression of the wound (i.e. the scratch) was monitored until complete closure, which took place after 5 days for both samples and the positive control. The migration rate was found to be in agreement with published reports, with 10-15% coverage of the area by the cells after 24 hours. The assay showed that the presence of the hydrogel did not impact the migratory and proliferative capacity of the cells even after the modification, which is particularly important as cell migration is the rate limiting event in wound healing processes. Furthermore, stability studies showed that no significant degradation occurred over 7 days of incubation in liquid media, turning the material into a suitable candidate for the development of an active dressing for dry wounds.

In light of the results obtained for the water-based reaction, an alternative approach was explored to improve the functionalisation yield and, therefore, the antibacterial efficiency of the hydrogel. In particular, a different chemical treatment was carried out involving surface modification in organic environment upon solvent exchange procedure. The water of the fibrillar structure was in fact replaced with tetrahydrofuran (THF) via several consecutive washings of the pellicles. This step allowed to perform a Schotten-Baumann derivatisation of the hydroxyl groups of cellulose using acryloyl chloride without formation of the corresponding carboxylic acid as a result of the hydrolysis of the acyl halide. The reaction was performed under anhydrous conditions at low temperature due to its exothermicity, and triethylamine (TEA) was added to the mixture to neutralise the hydrochloric acid generated. After this, the water was reintroduced in the structure and the pellicles were subjected to thiol-ene Michael type addition, which is one example of the so-called *click* reactions, i.e. simple, fast and selective reactions that yield quantitative and stereospecific products. The functionalisation of the double bonds of acrylated cellulose was performed using cysteamine hydrochloride in the presence of 4-dimethylaminopyridine (DMAP) as the catalyst. The material was then washed and characterised both morphologically and chemically to investigate the effect of the treatment on the structure as well as the modification yield. The SEM images clearly demonstrated that the fibrillar network was retained, whereas the EDX and XPS analyses revealed the successful incorporation of the groups. In addition to this, the mechanical properties of the pellicles were evaluated by performing rheological studies and compared to neat cellulose. The frequency sweep assay evidenced a certain degree of degradation for the modified sample, with lower values for both loss and storage moduli especially at low oscillation rates. This result could be explained by considering the treatment performed, which involved the use of basic conditions and, most importantly, the substitution of water with an organic solvent. It has been suggested, in fact, that THF is able to partially solubilise cellulose through disruption of the intermolecular hydrogen bonds. Nevertheless, the hydrogel presented a solid-like behaviour at all frequencies

and temperatures tested, indicating good resistance to deformation and stiffness. The antibacterial efficiency upon functionalisation was then investigated following the same standard procedure previously reported. In this case, the contact of bacteria with the samples resulted in almost total inhibition, with over 99% of cell count reduction as compared to the control for both *S. aureus* and *E. coli*. The result was most probably due to the more homogeneous surface modification and improved derivatisation yield. Furthermore, the presence of both a terminal amine hydrochloride moiety and a thioether in γ-position might have equally contributed to the biocidal action of the hydrogel. Cationic nitrogen groups and sulphur-based compounds are in fact well known bacterial inhibitors, which can act through disruption of the cell membrane and interference with metabolic pathways. After this, the biocompatibility of the hydrogel towards keratinocytes was estimated through indirect and direct contact test. Cell viability above 90% were observed at all time points upon contact with the functionalised samples. In particular, no significant difference was detected as compared to the positive control and increasing viability values were registered over 6 days of incubation, indicating that the cells successfully adapted to the presence of the material. Finally, the weight variation in liquid media at 32 °C was evaluated to assess the stability of the modified hydrogel. In both cases, an increase of about 15-20% in the weight was noted, probably ascribable to partial degradation of the fibrillar structure. It is possible, in fact, that the solvent exchange procedure caused disaggregation of the chains, resulting in higher interstitial space. Despite this, the material retained a solid nature in the timeframe considered with no massive structural degradation.

Along with surface functionalisation of bacterial cellulose pellicles, a different strategy was explored for the development of a natural polymer-based wound dressing with antibacterial features. In particular, copper(II)-loaded chitosan (CuChi) was used as the bulk material for the fabrication of a composite incorporating ground bacterial cellulose. The material was provided by an external collaborator in the context of the HyMedPoly project. Two different formulations were utilised with increasing copper content, i.e. CuChi3 and

CuChi12, having, respectively, 1% and 4% w/w copper concentration with respect to chitosan. The cellulose fibrils were obtained by mechanical wet grinding procedure to enhance the fibrillation efficiency without altering the chemical structure. The composites were then produced via solvent casting technique to yield the formation of four different compositions without and with addition of cellulose, i.e. CuChi3, CuChi12, CuChi3/BC and CuChi12/BC. The miscibility of the two polymers was investigated through SEM analysis, and no evident phase separation was observed. Furthermore, higher magnifications highlighted the successful incorporation and dispersion of the fibres in the chitosan matrix. The materials were then chemically characterised through EDX and FT-IR. The elemental analysis showed the presence of copper together with carbon and oxygen; furthermore, for the cellulose-loaded films, nitrogen and chlorine peaks were detected in the spectra. The results were confirmed by the FT-IR study, which demonstrated the complexation of copper by the amino groups of chitosan and the incorporation of cellulose. The addition of the fibres was expected to enhance the mechanical properties of the scaffold, as bacterial cellulose is widely used as a reinforcing agent thanks to its high strength. The results obtained from the tensile test carried out on the loaded samples supported this hypothesis, with significantly higher Young's modulus and ultimate tensile strength as compared to the neat ones. Interestingly, the specimens did not show significant embrittlement, with no substantial decrease in the elongation at break. The behaviour of the composites was then evaluated towards both bacteria and eukaryotic cells. Copper is known to be an essential trace element for humans, however, it can exert a toxic effect at high concentrations. In light of this, the aim of the study was to find an optimal threshold to achieve both antibacterial efficiency and biocompatibility. The CuChi3 formulation showed over 99% of bacterial cell count reduction for *S. aureus* both without and with cellulose, whereas the incorporation of cellulose resulted in an increase of the efficiency from circa 80% to more than 92% in the case of *E. coli*. The same trend was confirmed for the evaluation of the indirect antibacterial activity, highlighting the relatively higher resistance of Gram negative strains against bactericidal agents.

As regards the cytotoxicity assay, good cell viability was observed for up to 6 days after contact with the CuChi3 samples. In particular, the presence of cellulose resulted in enhanced biocompatibility at all time points. Finally, the stability of the materials was examined in liquid media. In all cases, an increase in the weight of about 130-160% was detected in the first 30 minutes of incubation, followed by a plateau. These findings evidenced the chelating nature of the amino groups of chitosan towards the copper ions, which resulted in the formation of a complex that behaved as a hydrogel upon water uptake. After this, no evident degradation occurred over 30 days, with lower weight loss for the cellulose-loaded specimens probably due to the stabilising effect of the fibres. As for the cellulose membranes, the hydrating ability of a dressing is particularly important in the case of dry wounds, where additional moisture is required to avoid the formation of necrotic tissue. In addition to this, the swelling capacity of the composites can be exploited in the case of exuding wounds, as the materials are able to absorb the fluids and prevent the maceration of the peri-wound skin.

7.2 Concluding remarks

In conclusion, the production and purification of bacterial cellulose was optimised with the aim to obtain a suitable substrate for further modification. Different strategies were then explored to achieve surface derivatisation of the pellicles. In particular, this work focused on the development of an inherently antibacterial hydrogel to be used in wound healing. The functionalisation treatments described here were found to be successful in the introduction of active groups, although the cellulose modified under anhydrous conditions proved to be more efficient in the bacterial inhibition without generating adverse effect on the growth and proliferation of keratinocytes. The main drawback of the process appeared to be the degradation of the membranes, which was probably caused by the solvent exchange performed. Nevertheless, the material maintained a solid structure in the conditions considered. Finally, an alternative approach was investigated, involving the use of chitosan as the bulk polymer and ground cellulose as an additive to obtain an antibacterial composite through

solvent casting technique. The presence of cellulose resulted in enhanced mechanical and biological performances, yielding a stable hydrogel that can be used for both dry and exuding wounds due to its swelling capacity.

7.3 Future work

This study focused on the use of bacterial cellulose as a platform for the development of an antibacterial wound dressing. Various strategies were investigated, although further studies can be carried out to gain a more comprehensive knowledge of the behaviour of the materials as well as to explore alternative approaches.

Because of the widespread use of bacterial cellulose as a biomedical polymer, it is particularly important to earn a deeper understanding of its biosynthesis mechanism. This can be obtained by performing a detailed temporal profiling of the fermentation of *Gluconacetobacter xylinus* or other cellulose-producing strains. Different parameters can be measured over time, such as glucose and nitrogen consumption, biomass content and cellulose yield. To achieve this, a method for sample collection that does not interfere with the polymer secretion has to be implemented. This might be carried out, for instance, in a suitable static bioreactor that can allow the production of homogeneous pellicles without requiring human intervention to acquire and analyse the culture. Gaining information about the polymer synthesis on a bench scale can in fact result in increased yield, with economic advantages and lower fermentation time. In addition to this, the purification of the membranes can be further optimised in order to decrease the washing time and the reagent consumption without affecting the structure and purity of the final product. Finally, it would be interesting to develop a method for the determination of the molecular weight of cellulose by solubilisation in suitable media that are able to dissolve the fibrillar network by disruption of the hydrogen bonding system without causing degradation or alteration of the chemical structure. The most common examples of non-derivatising cellulose solvents are ionic liquids and solvent/inorganic salt systems such as LiCl/DMac (Sen, Martin and Argyropoulos, 2013).

As regards the modification carried out in water, future studies should focus on the optimisation of the reaction to improve the yield and homogeneity of the derivatisation. The method proposed is a simple and environmental-friendly procedure not involving the use of toxic volatile solvents that can lead to the fabrication of an efficient antibacterial hydrogel. However, biological characterisations highlighted the need to improve the reaction conditions to achieve higher bactericidal activity, especially against Gram negative bacteria. Different parameters can be taken into account, such as reaction time, concentration of the reagents, catalyst, pH and temperature. This can be carried out, for instance, using a design of experiment (DOE) tool. Furthermore, more comprehensive biocompatibility assessment can be conducted, for example, through evaluation of the cytotoxicity towards fibroblasts or by performing an *in vivo* wound healing assay.

The hydrogel treated in anhydrous conditions, on the other hand, showed high biological performance against bacteria, probably as a result of improved functionalisation. Once again, future work should be aimed at further investigating the biological behaviour of the material towards both prokaryotic and, especially, eukaryotic cells. As for the cellulose modified in water-based system, the effect on fibroblasts should be assessed as well as the *in vitro*/*in vivo* wound healing capacity of the hydrogel.

Finally, novel chitosan/cellulose composites were developed and characterised from the mechanical and biological point of view. The presence of cellulose fibres in the matrix resulted in enhancement of the performances of the composite. In light of the encouraging results obtained, it is worth looking into the incorporation of fibres functionalised in anhydrous conditions to increase the bactericidal efficiency of the final material. Differential Scanning Calorimetry can then be carried out to evaluate the compatibility between the two polymers (cellulose and chitosan) and the effect of cellulose modification on the stability of the composite. In parallel to this, future studies can be directed towards the fabrication of skin tissue engineering scaffolds with adequate morphology and porosity. In fact, although cellulose is intrinsically endowed of ideal nanofibrillar

topography that can guide and regulate cell adhesion and spreading, the formation of wide pores in the micrometric range (circa 400 μm) is required to guarantee cell migration and, further on, tissue infiltration throughout the third dimension of the scaffold. For this purpose, different fabrication techniques can be explored using a chitosan/cellulose system. Among these, the most widely known is freeze drying, however, the use of supercritical CO_2 to induce micro- and nano- porosity in chitosan hydrogels recently emerged as a more rapid and efficient alternative approach (Ji *et al.*, 2011; Cabezas *et al.*, 2012; Moghadam *et al.*, 2017).

Overall, the strategies presented in the context of this thesis resulted in the development of promising materials with applicability in the context of wound healing. In all cases, it is crucial to gain a deeper understanding of their biological behaviour before working on the scale-up of the production as well as on their commercialisation as competitive natural polymers-based dressings. Further biological characterisation should be performed, investigating how the materials affect cell proliferation, differentiation and gene expression. 2D and 3D *in vitro* skin models infected with bacteria can be used for this purpose, followed by *in vivo* wound healing studies. Various *in vivo* wound models are available, including incision, excision and burn wound. Different biochemical parameters can be considered when assessing the technologies developed in this work. Examples of relevant tests that can be performed are estimation of collagen expression, contraction area, epithelisation period and histology. In addition to this, future studies can investigate the antiproliferative effect upon direct contact against other pathogenic bacteria (besides the ones used in this research work) that are commonly found in chronic wounds, such as *Pseudomonas* and *Streptococcus*. These tests can be performed both simultaneously, through *in vitro* models infected using multiple strains, or sequentially, i.e. by sequential exposure of the materials to different microorganisms. Finally, the robustness of the hydrogels over time can be further assessed, for instance through assessment of their mechanical properties after a storage period or after performing a comprehensive biological characterization.

References

Abdelrahman, T. and Newton, H. (2011) 'Wound dressings: principles and practice', *Surgery (Oxford)*, 29(10), pp. 491–495. doi: 10.1016/j.mpsur.2011.06.007.

Abdul Khalil, H. P. S. *et al.* (2014) 'Production and modification of nanofibrillated cellulose using various mechanical processes: A review', *Carbohydrate Polymers*, 99, pp. 649–665. doi: 10.1016/j.carbpol.2013.08.069.

Abid, C. K. V. Z. *et al.* (2010) 'Synthesis and characterization of quaternary ammonium PEGDA dendritic copolymer networks for water disinfection', *Journal of Applied Polymer Science*, p. NA-NA. doi: 10.1002/app.31510.

Ahmad, M. *et al.* (2015) 'Preparation and characterization of antibacterial thiosemicarbazide chitosan as efficient Cu(II) adsorbent', *Carbohydrate Polymers*, 132, pp. 164–172. doi: 10.1016/j.carbpol.2015.06.034.

Ahmed, J. *et al.* (2017) 'Mechanical, thermal, structural and barrier properties of crab shell chitosan/graphene oxide composite films', *Food Hydrocolloids*, 71, pp. 141–148. doi: 10.1016/j.foodhyd.2017.05.013.

Al-Fageeh, M. B. and Smales, C. M. (2006) 'Control and regulation of the cellular responses to cold shock: the responses in yeast and mammalian systems', *Biochemical Journal*, 397(2), pp. 247–259. doi: 10.1042/BJ20060166.

Albanna, M. Z. *et al.* (2012) 'Improving the mechanical properties of chitosan-based heart valve scaffolds using chitosan fibers', *Journal of the Mechanical Behavior of Biomedical Materials*, 5(1), pp. 171–180. doi: 10.1016/j.jmbbm.2011.08.021.

Altay, E. *et al.* (2015) 'Influence of alkyl chain length on the surface activity of antibacterial polymers derived from ROMP', *Colloids and Surfaces B: Biointerfaces*, 127, pp. 73–78. doi: 10.1016/j.colsurfb.2015.01.020.

Álvarez-Paino, M. *et al.* (2015) 'Effect of glycounits on the antimicrobial properties and toxicity behavior of polymers based on quaternized DMAEMA',

Biomacromolecules, 16(1), pp. 295–303. doi: 10.1021/bm5014876.

Anderl, J. N., Franklin, M. J. and Stewart, P. S. (2000) 'Role of Antibiotic Penetration Limitation in Klebsiella pneumoniae Biofilm Resistance to Ampicillin and Ciprofloxacin', *Antimicrobial Agents and Chemotherapy*, 44(7), pp. 1818–1824. doi: 10.1128/AAC.44.7.1818-1824.2000.

Anderson, D. J. *et al.* (2014) 'Strategies to Prevent Surgical Site Infections in Acute Care Hospitals: 2014 Update', *Infection Control & Hospital Epidemiology*, 35(6), pp. 605–627. doi: 10.1086/676022.

Anisha, B. S. *et al.* (2013) 'Chitosan–hyaluronic acid/nano silver composite sponges for drug resistant bacteria infected diabetic wounds', *International Journal of Biological Macromolecules*, 62, pp. 310–320. doi: 10.1016/j.ijbiomac.2013.09.011.

Aravamudhan, A. *et al.* (2014) 'Natural Polymers', *Natural and Synthetic Biomedical Polymers*. Elsevier, pp. 67–89. doi: 10.1016/B978-0-12-396983-5.00004-1.

Asano, K. and Matsubara, S. (2009) 'Amphiphilic Organocatalyst for Schotten-Baumann-Type Tosylation of Alcohols under Organic Solvent Free Condition', *Organic Letters*, 11(8), pp. 1757–1759. doi: 10.1021/ol900125y.

Augustine, R. *et al.* (2013) 'Biopolymers for Health, Food, and Cosmetic Applications', *Handbook of Biopolymer-Based Materials: From Blends and Composites to Gels and Complex Networks*, pp. 801–849. doi: 10.1002/9783527652457.ch27.

Awadhiya, A. *et al.* (2017) 'Synthesis and characterization of agarose–bacterial cellulose biodegradable composites', *Polymer Bulletin*, 74(7), pp. 2887–2903. doi: 10.1007/s00289-016-1872-3.

Azam, A. *et al.* (2012) 'Antimicrobial activity of metal oxide nanoparticles against Gram-positive and Gram-negative bacteria: a comparative study', *International Journal of Nanomedicine*, p. 6003. doi: 10.2147/IJN.S35347.

Badawy, M. E. I. and Rabea, E. i. (2011) 'A Biopolymer Chitosan and Its

Derivatives as Promising Antimicrobial Agents against Plant Pathogens and Their Applications in Crop Protection', *International Journal of Carbohydrate Chemistry*, 2011, pp. 1–29. doi: 10.1155/2011/460381.

Bang, S. *et al.* (2017) 'Preventing postoperative tissue adhesion using injectable carboxymethyl cellulose-pullulan hydrogels', *International Journal of Biological Macromolecules*, 105, pp. 886–893. doi: 10.1016/j.ijbiomac.2017.07.103.

Basu, A. *et al.* (2017) 'On the use of ion-crosslinked nanocellulose hydrogels for wound healing solutions: Physicochemical properties and application-oriented biocompatibility studies', *Carbohydrate Polymers*, 174, pp. 299–308. doi: 10.1016/j.carbpol.2017.06.073.

Basu, A., Vadanan, S. V. and Lim, S. (2018) 'A Novel Platform for Evaluating the Environmental Impacts on Bacterial Cellulose Production', *Scientific Reports*, 8(1), p. 5780. doi: 10.1038/s41598-018-23701-y.

Baumann, E. (1886) 'Ueber eine einfache Methode der Darstellung von Benzoësäureäthern', *Berichte der deutschen chemischen Gesellschaft*, 19(2), pp. 3218–3222. doi: 10.1002/cber.188601902348.

Bedel, N. S. *et al.* (2015) 'Effects of pore morphology and size on antimicrobial activity of chitosan/poly(ethylene glycol) diacrylate macromer semi-IPN hydrogels', *Journal of Applied Polymer Science*, 132(43). doi: 10.1002/app.42707.

Benziman, M. *et al.* (1980) 'Cellulose biogenesis: Polymerization and crystallization are coupled processes in Acetobacter xylinum', *Proceedings of the National Academy of Sciences*, 77(11), pp. 6678–6682. doi: 10.1073/pnas.77.11.6678.

Bhattarai, N., Matsen, F. A. and Zhang, M. (2005) 'PEG-Grafted Chitosan as an Injectable Thermoreversible Hydrogel', *Macromolecular Bioscience*, 5(2), pp. 107–111. doi: 10.1002/mabi.200400140.

Boateng, J. S. *et al.* (2008) 'Wound Healing Dressings and Drug Delivery Systems: A Review', *Journal of Pharmaceutical Sciences*, 97(8), pp. 2892–2923. doi:

10.1002/jps.21210.

Braun, D. *et al.* (2013) *Polymer Synthesis: Theory and Practice*. Berlin, Heidelberg: Springer Berlin Heidelberg. doi: 10.1007/978-3-642-28980-4.

Brown, L. *et al.* (2015) 'Through the wall: extracellular vesicles in Gram-positive bacteria, mycobacteria and fungi', *Nature Reviews Microbiology*, 13(10), pp. 620–630. doi: 10.1038/nrmicro3480.

Buffet-Bataillon, S. *et al.* (2012) 'Emergence of resistance to antibacterial agents: the role of quaternary ammonium compounds--a critical review.', *International journal of antimicrobial agents*, 39(5), pp. 381–9. doi: 10.1016/j.ijantimicag.2012.01.011.

Van Den Bulcke, A. I. *et al.* (2000) 'Structural and Rheological Properties of Methacrylamide Modified Gelatin Hydrogels', *Biomacromolecules*, 1(1), pp. 31–38. doi: 10.1021/bm990017d.

Burrell, M. C. (2001) 'Chemical Analysis, Electron Spectroscopy', in *Encyclopedia of Materials: Science and Technology*. Elsevier, pp. 1142–1149. doi: 10.1016/B0-08-043152-6/00214-X.

Cabezas, L. I. *et al.* (2012) 'Production of biodegradable porous scaffolds impregnated with indomethacin in supercritical CO2', *The Journal of Supercritical Fluids*, 63, pp. 155–160. doi: 10.1016/j.supflu.2011.12.002.

Caló, E. and Khutoryanskiy, V. V. (2015) 'Biomedical applications of hydrogels: A review of patents and commercial products', *European Polymer Journal*, 65, pp. 252–267. doi: 10.1016/j.eurpolymj.2014.11.024.

Camakaris, J., Voskoboinik, I. and Mercer, J. F. (1999) 'Molecular Mechanisms of Copper Homeostasis', *Biochemical and Biophysical Research Communications*, 261(2), pp. 225–232. doi: 10.1006/bbrc.1999.1073.

Castro, C. *et al.* (2012) 'Bacterial cellulose produced by a new acid-resistant strain of Gluconacetobacter genus', *Carbohydrate Polymers*, 89(4), pp. 1033–1037. doi:

10.1016/j.carbpol.2012.03.045.

Chaidez, C., Lopez, J. and Castro-del Campo, N. (2007) 'Quaternary ammonium compounds: an alternative disinfection method for fresh produce wash water', *Journal of Water and Health*, 5(2), pp. 329–333. doi: 10.2166/wh.2007.009b.

Chambless, J. D., Hunt, S. M. and Stewart, P. S. (2006) 'A Three-Dimensional Computer Model of Four Hypothetical Mechanisms Protecting Biofilms from Antimicrobials', *Applied and Environmental Microbiology*, 72(3), pp. 2005–2013. doi: 10.1128/AEM.72.3.2005-2013.2006.

Charrier, C. *et al.* (2014) 'Cysteamine (Lynovex®), a novel mucoactive antimicrobial & antibiofilm agent for the treatment of cystic fibrosis', *Orphanet Journal of Rare Diseases*, 9(1), p. 189. doi: 10.1186/s13023-014-0189-2.

Chauhan, A., Ghigo, J.-M. and Beloin, C. (2016) 'Study of in vivo catheter biofilm infections using pediatric central venous catheter implanted in rat', *Nature Protocols*, 11(3), pp. 525–541. doi: 10.1038/nprot.2016.033.

Chaurin, V., Constable, E. C. and Housecroft, C. E. (2006) 'What is the coordination number of copper(ii) in metallosupramolecular chemistry?', *New Journal of Chemistry*, 30(12), p. 1740. doi: 10.1039/b610306e.

Chawla, P. R. *et al.* (2009) 'Microbial cellulose: Fermentative production and applications', *Food Technology and Biotechnology*, 47(2), pp. 107–124.

Chen, M.-C. *et al.* (2009) 'Mechanical properties, drug eluting characteristics and in vivo performance of a genipin-crosslinked chitosan polymeric stent', *Biomaterials*, 30(29), pp. 5560–5571. doi: 10.1016/j.biomaterials.2009.06.039.

Cheung, H. *et al.* (2009) 'Natural fibre-reinforced composites for bioengineering and environmental engineering applications', *Composites Part B: Engineering*, 40(7), pp. 655–663. doi: 10.1016/j.compositesb.2009.04.014.

Chiono, V. *et al.* (2008) 'Genipin-crosslinked chitosan/gelatin blends for biomedical applications', *Journal of Materials Science: Materials in Medicine*, 19(2),

pp. 889–898. doi: 10.1007/s10856-007-3212-5.

Costa, A. F. S. *et al.* (2017) 'Production of Bacterial Cellulose by Gluconacetobacter hansenii Using Corn Steep Liquor As Nutrient Sources', *Frontiers in Microbiology*, 8. doi: 10.3389/fmicb.2017.02027.

Costerton, J. W. (1999) 'Bacterial Biofilms: A Common Cause of Persistent Infections', *Science*, 284(5418), pp. 1318–1322. doi: 10.1126/science.284.5418.1318.

Covarrubias, C., Trepiana, D. and Corral, C. (2018) 'Synthesis of hybrid copper-chitosan nanoparticles with antibacterial activity against cariogenic Streptococcus mutans', *Dental Materials Journal*, 37(3), pp. 379–384. doi: 10.4012/dmj.2017-195.

Cumpstey, I. (2013) 'Chemical Modification of Polysaccharides', *ISRN Organic Chemistry*, 2013, pp. 1–27. doi: 10.1155/2013/417672.

Czaja, W., Romanovicz, D. and Brown, R. malcolm (2004) 'Structural investigations of microbial cellulose produced in stationary and agitated culture', *Cellulose*, 11(3/4), pp. 403–411. doi: 10.1023/B:CELL.0000046412.11983.61.

Dahou, W. *et al.* (2010) 'Preparation and biological characterization of cellulose graft copolymers', *Biochemical Engineering Journal*, 48(2), pp. 187–194. doi: 10.1016/j.bej.2009.10.006.

Davies, D. (2003) 'Understanding biofilm resistance to antibacterial agents', *Nature Reviews Drug Discovery*, 2(2), pp. 114–122. doi: 10.1038/nrd1008.

Dean, B. D., Matzner, M. and Tibbitt, J. M. (1989) 'Polyarylates', in *Comprehensive Polymer Science and Supplements*. Elsevier, pp. 317–329. doi: 10.1016/B978-0-08-096701-1.00159-2.

DeBoer, T. R., Chakraborty, I. and Mascharak, P. K. (2015) 'Design and construction of a silver(I)-loaded cellulose-based wound dressing: trackable and sustained release of silver for controlled therapeutic delivery to wound sites', *Journal of Materials Science: Materials in Medicine*, 26(10). Available at:

www.wkap.nl/journalhome.htm/0957-4530%5Cnhttp://ovidsp.ovid.com/ovidweb.cgi?T=JS&PAGE=reference&D=emed13&NEWS=N&AN=2015416093.

Deka, S., Sharma, A. and Kumar, P. (2015) 'Cationic Polymers and their Self-Assembly for Antibacterial Applications', *Current Topics in Medicinal Chemistry*, 15(13), pp. 1179–1195. doi: 10.2174/1568026615666150330110602.

Denis, O., Rodriguez-Villalobos, H. and Struelens, M. J. (2010) 'The problem of resistance', in *Antibiotic and Chemotherapy*. Elsevier, pp. 24–48. doi: 10.1016/B978-0-7020-4064-1.00003-8.

Devínsky, F. *et al.* (1990) 'Cut-off Effect in Antimicrobial Activity and in Membrane Perturbation Efficiency of the Homologous Series of N,N-Dimethylalkylamine Oxides†', *Journal of Pharmacy and Pharmacology*, 42(11), pp. 790–794. doi: 10.1111/j.2042-7158.1990.tb07022.x.

Dhivya, S., Padma, V. V. and Santhini, E. (2015) 'Wound dressings – a review', *BioMedicine*, 5(4), p. 22. doi: 10.7603/s40681-015-0022-9.

Domard, A. and Domard, M. (2002) 'Chitosan : Structure-properties relationship and biomedical applications', *Polymeric Biomaterials*, pp. 187–212.

Donlan, R. M. (2001) 'Biofilm Formation: A Clinically Relevant Microbiological Process', *Clinical Infectious Diseases*, 33(8), pp. 1387–1392. doi: 10.1086/322972.

Dragostin, O. M. *et al.* (2016) 'New antimicrobial chitosan derivatives for wound dressing applications', *Carbohydrate Polymers*, 141, pp. 28–40. doi: 10.1016/j.carbpol.2015.12.078.

Drury, J. L. and Mooney, D. J. (2003) 'Hydrogels for tissue engineering: scaffold design variables and applications.', *Biomaterials*, 24(24), pp. 4337–51. Available at: http://www.ncbi.nlm.nih.gov/pubmed/12922147.

Du, H. *et al.* (2016) 'Injectable cationic hydrogels with high antibacterial activity and low toxicity', *Polymer Chemistry*, 7(36), pp. 5620–5624. doi:

10.1039/C6PY01346E.

Egerton, R. F. (2011) *Electron Energy-Loss Spectroscopy in the Electron Microscope*. Boston, MA: Springer US. doi: 10.1007/978-1-4419-9583-4.

Esa, F., Tasirin, S. M. and Rahman, N. A. (2014) 'Overview of Bacterial Cellulose Production and Application', *Agriculture and Agricultural Science Procedia*, 2, pp. 113–119. doi: 10.1016/j.aaspro.2014.11.017.

Exner, M. (2017) 'Antibiotic resistance: What is so special about multidrug-resistant Gram-negative bacteria?', *GMS Hygiene and Infection Control*, 12, pp. 1–24. doi: 10.3205/dgkh000290.

Fan, H. *et al.* (2010) 'Fabrication, Mechanical Properties, and Biocompatibility of Graphene-Reinforced Chitosan Composites', *Biomacromolecules*, 11(9), pp. 2345–2351. doi: 10.1021/bm100470q.

Fan, J. *et al.* (2012) 'Mechanical reinforcement of chitosan using unzipped multiwalled carbon nanotube oxides', *Polymer*, 53(2), pp. 657–664. doi: 10.1016/j.polymer.2011.11.060.

Fan, L. *et al.* (2013) 'Preparation, characterization and the effect of carboxymethylated chitosan-cellulose derivatives hydrogels on wound healing', *Journal of Applied Polymer Science*, 128(5), pp. 2789–2796. doi: 10.1002/app.38456.

Fan, L. *et al.* (2015) 'Preparation and characterization of quaternary ammonium chitosan hydrogel with significant antibacterial activity', *International Journal of Biological Macromolecules*, 79, pp. 830–836. doi: 10.1016/j.ijbiomac.2015.04.013.

Fang, J. (2004) 'The chemical modification of a range of starches under aqueous reaction conditions', *Carbohydrate Polymers*, 55(3), pp. 283–289. doi: 10.1016/j.carbpol.2003.10.003.

Farhadi, F. *et al.* (2019) 'Antibacterial activity of flavonoids and their structure-activity relationship: An update review', *Phytotherapy Research*, 33(1), pp. 13–40. doi: 10.1002/ptr.6208.

FDA (2016) 'GENERAL AND PLASTIC SURGERY DEVICES PANEL OF THE MEDICAL DEVICES ADVISORY COMMITTEE Food and Drug Administration – Hilton Washington DC North Gaithersburg, MD'.

Feng, Y. *et al.* (2012) 'A mechanically strong, flexible and conductive film based on bacterial cellulose/graphene nanocomposite', *Carbohydrate Polymers*, 87(1), pp. 644–649. doi: 10.1016/j.carbpol.2011.08.039.

Fernandes, S. C. *et al.* (2011) 'Novel materials based on chitosan and cellulose', *Polymer International*, 60(6), pp. 875–882. doi: 10.1002/pi.3024.

Fernandes, S. C. M. *et al.* (2013) 'Bioinspired antimicrobial and biocompatible bacterial cellulose membranes obtained by surface functionalization with aminoalkyl groups', *ACS Applied Materials and Interfaces*, 5(8), pp. 3290–3297. doi: 10.1021/am400338n.

Festa, R. A. and Thiele, D. J. (2011) 'Copper: An essential metal in biology', *Current Biology*, 21(21), pp. R877–R883. doi: 10.1016/j.cub.2011.09.040.

Field, C. K. and Kerstein, M. D. (1994) 'Overview of wound healing in a moist environment', *The American Journal of Surgery*, 167(1), pp. S2–S6. doi: 10.1016/0002-9610(94)90002-7.

Fierheller, M. and Sibbald, R. G. (2010) 'A Clinical Investigation into the Relationship between Increased Periwound Skin Temperature and Local Wound Infection in Patients with Chronic Leg Ulcers', *Advances in Skin & Wound Care*, 23(8), pp. 369–379. doi: 10.1097/01.ASW.0000383197.28192.98.

Flores-Hernández, C. *et al.* (2014) 'All Green Composites from Fully Renewable Biopolymers: Chitosan-Starch Reinforced with Keratin from Feathers', *Polymers*, 6(3), pp. 686–705. doi: 10.3390/polym6030686.

Francis Suh, J.-K. and Matthew, H. W. . (2000) 'Application of chitosan-based polysaccharide biomaterials in cartilage tissue engineering: a review', *Biomaterials*, 21(24), pp. 2589–2598. doi: 10.1016/S0142-9612(00)00126-5.

Fu, L., Zhang, J. and Yang, G. (2013) 'Present status and applications of bacterial cellulose-based materials for skin tissue repair', *Carbohydrate Polymers*, 92(2), pp. 1432–1442. Available at: http://ovidsp.ovid.com/ovidweb.cgi?T=JS&PAGE=reference&D=emed11&NEWS=N&AN=23399174.

Gaazo, J. (1976) 'Plasticity of the coordination sphere of copper(II) complexes, its manifestation and causes', *Coordination Chemistry Reviews*, 19(3), pp. 253–297. doi: 10.1016/S0010-8545(00)80317-3.

Gao, B., Zhang, X. and Zhu, Y. (2007) 'Studies on the preparation and antibacterial properties of quaternized polyethyleneimine', *Journal of Biomaterials Science, Polymer Edition*, 18(5), pp. 531–544. doi: 10.1163/156856207780852523.

Gerba, C. P. (2015) 'Quaternary Ammonium Biocides: Efficacy in Application', *Applied and Environmental Microbiology*. Edited by V. Müller, 81(2), pp. 464–469. doi: 10.1128/AEM.02633-14.

Gomes, J. R. B. and Gomes, P. (2005) 'Gas-phase acidity of sulfonamides: implications for reactivity and prodrug design', *Tetrahedron*, 61(10), pp. 2705–2712. doi: 10.1016/j.tet.2005.01.034.

Goy, R. C., Morais, S. T. B. and Assis, O. B. G. (2016) 'Evaluation of the antimicrobial activity of chitosan and its quaternized derivative on E. coli and S. aureus growth', *Revista Brasileira de Farmacognosia*, 26(1), pp. 122–127. doi: 10.1016/j.bjp.2015.09.010.

Grey, J. E., Enoch, S. and Harding, K. G. (2006) 'Wound assessment', *BMJ*, 332(7536), pp. 285–288. doi: 10.1136/bmj.332.7536.285.

Gritsch, L. *et al.* (2018) 'Fabrication and characterization of copper(II)-chitosan complexes as antibiotic-free antibacterial biomaterial', *Carbohydrate Polymers*, 179, pp. 370–378. doi: 10.1016/j.carbpol.2017.09.095.

Grube, M. *et al.* (2016) 'Fourier-transform infrared spectroscopic analyses of

cellulose from different bacterial cultivations using microspectroscopy and a high-throughput screening device', *Vibrational Spectroscopy*, 84, pp. 53–57. doi: 10.1016/j.vibspec.2016.03.001.

Gülerman, N. . *et al.* (2001) 'Synthesis and structure elucidation of some new thioether derivatives of 1,2,4-triazoline-3-thiones and their antimicrobial activities', *Il Farmaco*, 56(12), pp. 953–958. doi: 10.1016/S0014-827X(01)01167-3.

Guo, S. and DiPietro, L. A. (2010) 'Factors Affecting Wound Healing', *Journal of Dental Research*, 89(3), pp. 219–229. doi: 10.1177/0022034509359125.

Gupta, A. *et al.* (2016) 'Characterisation and in vitro antimicrobial activity of biosynthetic silver-loaded bacterial cellulose hydrogels', *Journal of Microencapsulation*, 33(8), pp. 725–734. doi: 10.1080/02652048.2016.1253796.

Gurtner, G. C. *et al.* (2008) 'Wound repair and regeneration', *Nature*, 453(7193), pp. 314–321. doi: 10.1038/nature07039.

H.P.S, A. K. *et al.* (2016) 'A review on chitosan-cellulose blends and nanocellulose reinforced chitosan biocomposites: Properties and their applications', *Carbohydrate Polymers*, 150, pp. 216–226. doi: 10.1016/j.carbpol.2016.05.028.

Han, D. *et al.* (2011) 'Preparation of chitosan/graphene oxide composite film with enhanced mechanical strength in the wet state', *Carbohydrate Polymers*, 83(2), pp. 653–658. doi: 10.1016/j.carbpol.2010.08.038.

Han, G. and Ceilley, R. (2017) 'Chronic Wound Healing: A Review of Current Management and Treatments', *Advances in Therapy*, 34(3), pp. 599–610. doi: 10.1007/s12325-017-0478-y.

Heinze, T. and Koschella, A. (2005) 'Solvents applied in the field of cellulose chemistry: a mini review', *Polímeros*, 15(2), pp. 84–90. doi: 10.1590/S0104-14282005000200005.

Heldreth, B. and Turos, E. (2005) 'Microbiological Properties and Modes of Action of Organosulfur-based Anti-infectives', *Current Medicinal Chemistry -Anti-*

Infective Agents, 4(4), pp. 295–315. doi: 10.2174/156801205774322250.

Helenius, G. *et al.* (2006) 'In vivo biocompatibility of bacterial cellulose', *Journal of Biomedical Materials Research - Part A*, 76(2), pp. 431–438. doi: 10.1002/jbm.a.30570.

Hirayama, K. *et al.* (2013) 'Cellular building unit integrated with microstrand-shaped bacterial cellulose', *Biomaterials*, 34(10), pp. 2421–2427. doi: 10.1016/j.biomaterials.2012.12.013.

Hoffman, A. S. (2002) 'Hydrogels for biomedical applications.', *Advanced drug delivery reviews*, 54(1), pp. 3–12. Available at: http://www.ncbi.nlm.nih.gov/pubmed/11755703.

Høiby, N. *et al.* (2010) 'Antibiotic resistance of bacterial biofilms', *International Journal of Antimicrobial Agents*, 35(4), pp. 322–332. doi: 10.1016/j.ijantimicag.2009.12.011.

Holmberg, M. *et al.* (1997) 'Surface Force Studies of Langmuir–Blodgett Cellulose Films', *Journal of Colloid and Interface Science*, 186(2), pp. 369–381. doi: 10.1006/jcis.1996.4657.

Holtzapple, M. T. (2003) 'CELLULOSE', in *Encyclopedia of Food Sciences and Nutrition*. Elsevier, pp. 998–1007. doi: 10.1016/B0-12-227055-X/00185-1.

Hong, F. *et al.* (2011) 'Wheat straw acid hydrolysate as a potential cost-effective feedstock for production of bacterial cellulose', *Journal of Chemical Technology & Biotechnology*, 86(5), pp. 675–680. doi: 10.1002/jctb.2567.

Hoyle, C. E. and Bowman, C. N. (2010) 'Thiol-Ene Click Chemistry', *Angewandte Chemie International Edition*, 49(9), pp. 1540–1573. doi: 10.1002/anie.200903924.

Hu, W. *et al.* (2019) 'Advances in crosslinking strategies of biomedical hydrogels', *Biomaterials Science*, 7(3), pp. 843–855. doi: 10.1039/C8BM01246F.

Huang, B., Liu, M. and Zhou, C. (2017) 'Cellulose–halloysite nanotube composite

hydrogels for curcumin delivery', *Cellulose*, 24(7), pp. 2861–2875. doi: 10.1007/s10570-017-1316-8.

Huang, H.-C. *et al.* (2010) 'In situ modification of bacterial cellulose network structure by adding interfering substances during fermentation', *Bioresource Technology*, 101(15), pp. 6084–6091. doi: 10.1016/j.biortech.2010.03.031.

Huang, Y. *et al.* (2014) 'Recent advances in bacterial cellulose', *Cellulose*, 21(1), pp. 1–30. doi: 10.1007/s10570-013-0088-z.

Hui, F. and Debiemme-Chouvy, C. (2013) 'Antimicrobial N-halamine polymers and coatings: A review of their synthesis, characterization, and applications', *Biomacromolecules*, 14(3), pp. 585–601. doi: 10.1021/bm301980q.

Hungund, B. S. and Gupta, S. G. (2010) 'Production of bacterial cellulose from Enterobacter amnigenus GH-1 isolated from rotten apple', *World Journal of Microbiology and Biotechnology*, 26(10), pp. 1823–1828. doi: 10.1007/s11274-010-0363-1.

Janpetch, N., Saito, N. and Rujiravanit, R. (2016) 'Fabrication of bacterial cellulose-ZnO composite via solution plasma process for antibacterial applications', *Carbohydrate Polymers*, 148, pp. 335–344. doi: 10.1016/j.carbpol.2016.04.066.

Jayakumar, R. *et al.* (2011) 'Biomaterials based on chitin and chitosan in wound dressing applications', *Biotechnology Advances*, 29(3), pp. 322–337. doi: 10.1016/j.biotechadv.2011.01.005.

Jennings, M. C., Minbiole, K. P. C. and Wuest, W. M. (2015) 'Quaternary Ammonium Compounds: An Antimicrobial Mainstay and Platform for Innovation to Address Bacterial Resistance', *ACS Infectious Diseases*, 1(7), pp. 288–303. doi: 10.1021/acsinfecdis.5b00047.

Jeong, D. *et al.* (2016) 'Cyclosophoraose/cellulose hydrogels as an efficient delivery system for galangin, a hydrophobic antibacterial drug', *Cellulose*, 23(4),

pp. 2609–2625. doi: 10.1007/s10570-016-0975-1.

Jeong, Y.-I. *et al.* (2008) 'Preparation and spectroscopic characterization of methoxy poly(ethylene glycol)-grafted water-soluble chitosan', *Carbohydrate Research*, 343(2), pp. 282–289. doi: 10.1016/j.carres.2007.10.025.

Jeschke, M. and Rogers, A. (2016) 'Managing severe burn injuries: challenges and solutions in complex and chronic wound care', *Chronic Wound Care Management and Research*, p. 59. doi: 10.2147/CWCMR.S86762.

Ji, C. *et al.* (2011) 'Fabrication of porous chitosan scaffolds for soft tissue engineering using dense gas CO2', *Acta Biomaterialia*, 7(4), pp. 1653–1664. doi: 10.1016/j.actbio.2010.11.043.

Jia, S. *et al.* (2004) 'Cellulose production fromGluconobacter oxydans TQ-B2', *Biotechnology and Bioprocess Engineering*, 9(3), pp. 166–170. doi: 10.1007/BF02942287.

Jia, Z., Shen, D. and Xu, W. (2001) 'Synthesis and antibacterial activities of quaternary ammonium salt of chitosan', *Carbohydrate Research*, 333(1), pp. 1–6. doi: 10.1016/S0008-6215(01)00112-4.

Jiang, Z. *et al.* (2018) 'Effect of Tetrahydrofuran on the Solubilization and Depolymerization of Cellulose in a Biphasic System', *ChemSusChem*, 11(2), pp. 397–405. doi: 10.1002/cssc.201701861.

Jiao, Y. *et al.* (2017) 'Quaternary ammonium-based biomedical materials: State-of-the-art, toxicological aspects and antimicrobial resistance', *Progress in Polymer Science*, 71, pp. 53–90. doi: 10.1016/j.progpolymsci.2017.03.001.

Jones, V., Grey, J. E. and Harding, K. G. (2006) 'Wound dressings', *BMJ*, 332(7544), pp. 777–780. doi: 10.1136/bmj.332.7544.777.

Jursic, B. S. and Neumann, D. (2001) 'Preparation of N-acyl derivatives of amino acids from acyl chlorides and amino acids in the presence of cationic surfactants. A variation of the Schotten-Baumann method of benzoylation of amino acids',

Synthetic Communications, 31(4), pp. 555–564. doi: 10.1081/SCC-100000582.

Kačuráková, M. *et al.* (2002) 'Molecular interactions in bacterial cellulose composites studied by 1D FT-IR and dynamic 2D FT-IR spectroscopy', *Carbohydrate Research*, 337(12), pp. 1145–1153. doi: 10.1016/S0008-6215(02)00102-7.

Kalia, S. *et al.* (2014) 'Nanofibrillated cellulose: Surface modification and potential applications', *Colloid and Polymer Science*, 292(1), pp. 5–31. doi: 10.1007/s00396-013-3112-9.

Kapoor, G., Saigal, S. and Elongavan, A. (2017) 'Action and resistance mechanisms of antibiotics: A guide for clinicians', *Journal of Anaesthesiology Clinical Pharmacology*, 33(3), p. 300. doi: 10.4103/joacp.JOACP_349_15.

Kenawy, E. R., Worley, S. D. and Broughton, R. (2007) 'The chemistry and applications of antimicrobial polymers: A state-of-the-art review', *Biomacromolecules*, 8(5), pp. 1359–1384. doi: 10.1021/bm061150q.

Khalid, A. *et al.* (2017) 'Bacterial cellulose-zinc oxide nanocomposites as a novel dressing system for burn wounds', *Carbohydrate Polymers*, 164, pp. 214–221. doi: 10.1016/j.carbpol.2017.01.061.

Khan, A. *et al.* (2012) 'Mechanical and barrier properties of nanocrystalline cellulose reinforced chitosan based nanocomposite films', *Carbohydrate Polymers*, 90(4), pp. 1601–1608. doi: 10.1016/j.carbpol.2012.07.037.

Khor, E. and Lim, L. Y. (2003) 'Implantable applications of chitin and chitosan', *Biomaterials*, 24(13), pp. 2339–2349. doi: 10.1016/S0142-9612(03)00026-7.

Kim, H. W., Kim, B. R. and Rhee, Y. H. (2010) 'Imparting durable antimicrobial properties to cotton fabrics using alginate–quaternary ammonium complex nanoparticles', *Carbohydrate Polymers*, 79(4), pp. 1057–1062. doi: 10.1016/j.carbpol.2009.10.047.

Kim, S., Kubec, R. and Musah, R. A. (2006) 'Antibacterial and antifungal activity

of sulfur-containing compounds from Petiveria alliacea L.', *Journal of Ethnopharmacology*, 104(1–2), pp. 188–192. doi: 10.1016/j.jep.2005.08.072.

Klemm, D. *et al.* (2005) 'Cellulose: Fascinating biopolymer and sustainable raw material', *Angewandte Chemie - International Edition*, 44(22), pp. 3358–3393. doi: 10.1002/anie.200460587.

Kocen, R. *et al.* (2017) 'Viscoelastic behaviour of hydrogel-based composites for tissue engineering under mechanical load', *Biomedical Materials*, 12(2), p. 025004. doi: 10.1088/1748-605X/aa5b00.

Koehler, M. J. *et al.* (2011) 'Keratinocyte morphology of human skin evaluated by in vivo multiphoton laser tomography', *Skin Research and Technology*, 17(4), pp. 479–486. doi: 10.1111/j.1600-0846.2011.00522.x.

Kogan, G. *et al.* (2006) 'Hyaluronic acid: a natural biopolymer with a broad range of biomedical and industrial applications', *Biotechnology Letters*, 29(1), pp. 17–25. doi: 10.1007/s10529-006-9219-z.

Koller, M. *et al.* (2011) 'Linking ecology with economy: Insights into polyhydroxyalkanoate-producing microorganisms', *Engineering in Life Sciences*, 11(3), pp. 222–237. doi: 10.1002/elsc.201000190.

Kondo, T. *et al.* (2012) 'Regulated patterns of bacterial movements based on their secreted cellulose nanofibers interacting interfacially with ordered chitin templates', *Journal of Bioscience and Bioengineering*, 114(1), pp. 113–120. doi: 10.1016/j.jbiosc.2012.02.020.

Kong, M. *et al.* (2010) 'Antimicrobial properties of chitosan and mode of action: A state of the art review', *International Journal of Food Microbiology*, 144(1), pp. 51–63. Available at: http://www.sciencedirect.com.biblioteca.ciad.mx:2048/science/article/pii/S0168160510005167.

Kozicki, M. *et al.* (2016) 'Hydrogels made from chitosan and silver nitrate',

Carbohydrate Polymers, 140, pp. 74–87. doi: 10.1016/j.carbpol.2015.12.017.

Kratochvil, M. J. *et al.* (2016) 'Slippery Liquid-Infused Porous Surfaces that Prevent Bacterial Surface Fouling and Inhibit Virulence Phenotypes in Surrounding Planktonic Cells', *ACS Infectious Diseases*, 2(7), pp. 509–517. doi: 10.1021/acsinfecdis.6b00065.

Kucińska-Lipka, J., Gubanska, I. and Janik, H. (2015) 'Bacterial cellulose in the field of wound healing and regenerative medicine of skin: recent trends and future prospectives', *Polymer Bulletin*, 72(9), pp. 2399–2419. doi: 10.1007/s00289-015-1407-3.

Kuo, C.-H., Teng, H.-Y. and Lee, C.-K. (2015) 'Knock-out of glucose dehydrogenase gene in Gluconacetobacter xylinus for bacterial cellulose production enhancement', *Biotechnology and Bioprocess Engineering*, 20(1), pp. 18–25. doi: 10.1007/s12257-014-0316-x.

Lamboni, L. *et al.* (2016) 'Silk Sericin-Functionalized Bacterial Cellulose as a Potential Wound-Healing Biomaterial', *Biomacromolecules*, 17(9), pp. 3076–3084. doi: 10.1021/acs.biomac.6b00995.

Lavoine, N. *et al.* (2012) 'Microfibrillated cellulose – Its barrier properties and applications in cellulosic materials: A review', *Carbohydrate Polymers*, 90(2), pp. 735–764. doi: 10.1016/j.carbpol.2012.05.026.

Le, H. R. *et al.* (2012) 'Fabrication and mechanical properties of chitosan composite membrane containing hydroxyapatite particles', *Journal of Advanced Ceramics*, 1(1), pp. 66–71. doi: 10.1007/s40145-012-0007-z.

Leaper, D. J. and Edmiston, C. E. (2017) 'World Health Organization: global guidelines for the prevention of surgical site infection', *Journal of Hospital Infection*, 95(2), pp. 135–136. doi: 10.1016/j.jhin.2016.12.016.

Li, J., Wu, Y. and Zhao, L. (2016) 'Antibacterial activity and mechanism of chitosan with ultra high molecular weight', *Carbohydrate Polymers*, 148, pp. 200–

205. doi: 10.1016/j.carbpol.2016.04.025.

Li, S. *et al.* (2018) 'Antibacterial Hydrogels', *Advanced Science*, 5(5), p. 1700527. doi: 10.1002/advs.201700527.

Lin, N. and Dufresne, A. (2014) 'Nanocellulose in biomedicine: Current status and future prospect', *European Polymer Journal*, 59, pp. 302–325. doi: 10.1016/j.eurpolymj.2014.07.025.

Lin, S.-P. *et al.* (2013) 'Biosynthesis, production and applications of bacterial cellulose', *Cellulose*, 20(5), pp. 2191–2219. doi: 10.1007/s10570-013-9994-3.

Lin, Y. K. *et al.* (2011) 'Effects of different extracellular matrices and growth factor immobilization on biodegradability and biocompatibility of macroporous bacterial cellulose', *Journal of Bioactive and Compatible Polymers*, 26(5), pp. 508–518. doi: 10.1177/0883911511415390.

Lindman, B. *et al.* (2017) 'The relevance of structural features of cellulose and its interactions to dissolution, regeneration, gelation and plasticization phenomena', *Physical Chemistry Chemical Physics*, 19(35), pp. 23704–23718. doi: 10.1039/C7CP02409F.

Ling, C. *et al.* (2014) 'Design, Synthesis, and Structure–Activity Relationship Studies of Novel Thioether Pleuromutilin Derivatives as Potent Antibacterial Agents', *Journal of Medicinal Chemistry*, 57(11), pp. 4772–4795. doi: 10.1021/jm500312x.

Liu, J. *et al.* (2016) 'Hemicellulose-reinforced nanocellulose hydrogels for wound healing application', *Cellulose*, 23(5), pp. 3129–3143. doi: 10.1007/s10570-016-1038-3.

Liu, J., Willför, S. and Xu, C. (2015) 'A review of bioactive plant polysaccharides: Biological activities, functionalization, and biomedical applications', *Bioactive Carbohydrates and Dietary Fibre*, 5(1), pp. 31–61. doi: 10.1016/j.bcdf.2014.12.001.

Liu, M. *et al.* (2012) 'Chitosan/halloysite nanotubes bionanocomposites:

Structure, mechanical properties and biocompatibility', *International Journal of Biological Macromolecules*, 51(4), pp. 566–575. doi: 10.1016/j.ijbiomac.2012.06.022.

Liu, Y. *et al.* (2014) 'Antimicrobial cotton containing N-halamine and quaternary ammonium groups by grafting copolymerization', *Applied Surface Science*, 296, pp. 231–236. doi: 10.1016/j.apsusc.2014.01.106.

Liu, Y. *et al.* (2015) 'Superabsorbent Sponge and Membrane Prepared by Polyelectrolyte Complexation of Carboxymethyl Cellulose/Hydroxyethyl Cellulose-Al3+', *BioResources*, 10(4). doi: 10.15376/biores.10.4.6479-6495.

Liu, Y. *et al.* (2016) 'Antibacterial modification of microcrystalline cellulose by grafting copolymerization', *BioResources*, 11(1), pp. 519–529. doi: 10.15376/biores.11.1.519-529.

Lowe, A. B. (2014) 'Thiol–ene "click" reactions and recent applications in polymer and materials synthesis: a first update', *Polym. Chem.*, 5(17), pp. 4820–4870. doi: 10.1039/C4PY00339J.

Lu, Y. *et al.* (2015) 'Self-defensive antibacterial layer-by-layer hydrogel coatings with pH-triggered hydrophobicity', *Biomaterials*, 45, pp. 64–71. doi: 10.1016/j.biomaterials.2014.12.048.

Makvandi, P. *et al.* (2018) 'Antibacterial quaternary ammonium compounds in dental materials: A systematic review', *Dental Materials*, 34(6), pp. 851–867. doi: 10.1016/j.dental.2018.03.014.

Malanovic, N. and Lohner, K. (2016) 'Gram-positive bacterial cell envelopes: The impact on the activity of antimicrobial peptides', *Biochimica et Biophysica Acta (BBA) - Biomembranes*, 1858(5), pp. 936–946. doi: 10.1016/j.bbamem.2015.11.004.

Maneerung, T., Tokura, S. and Rujiravanit, R. (2008) 'Impregnation of silver nanoparticles into bacterial cellulose for antimicrobial wound dressing', *Carbohydrate Polymers*, 72(1), pp. 43–51. doi: 10.1016/j.carbpol.2007.07.025.

Di Martino, A., Sittinger, M. and Risbud, M. V. (2005) 'Chitosan: A versatile

biopolymer for orthopaedic tissue-engineering', *Biomaterials*, 26(30), pp. 5983–5990. doi: 10.1016/j.biomaterials.2005.03.016.

Martins, A. *et al.* (2014) 'Antimicrobial Activity of Chitosan Derivatives Containing N-Quaternized Moieties in Its Backbone: A Review', *International Journal of Molecular Sciences*, 15(11), pp. 20800–20832. doi: 10.3390/ijms151120800.

Mekahlia, S. and Bouzid, B. (2009) 'Chitosan-Copper (II) complex as antibacterial agent: synthesis, characterization and coordinating bond- activity correlation study', *Physics Procedia*, 2(3), pp. 1045–1053. doi: 10.1016/j.phpro.2009.11.061.

Mekkawy, A. *et al.* (2017) 'In vitro and in vivo evaluation of biologically synthesized silver nanoparticles for topical applications: effect of surface coating and loading into hydrogels', *International Journal of Nanomedicine*, Volume 12, pp. 759–777. doi: 10.2147/ijn.s124294.

Mertaniemi, H. *et al.* (2015) 'Human stem cell decorated nanocellulose threads for biomedical applications', *Biomaterials*, 82, pp. 208–220. doi: 10.1016/j.biomaterials.2015.12.020.

Miller, S. I. (2016) 'Antibiotic Resistance and Regulation of the Gram-Negative Bacterial Outer Membrane Barrier by Host Innate Immune Molecules', *mBio*, 7(5). doi: 10.1128/mBio.01541-16.

Milović, N. M. *et al.* (2005) 'Immobilized N-alkylated polyethylenimine avidly kills bacteria by rupturing cell membranes with no resistance developed', *Biotechnology and Bioengineering*, 90(6), pp. 715–722. doi: 10.1002/bit.20454.

Minbiole, K. P. C. *et al.* (2016) 'From antimicrobial activity to mechanism of resistance: the multifaceted role of simple quaternary ammonium compounds in bacterial eradication', *Tetrahedron*, 72(25), pp. 3559–3566. doi: 10.1016/j.tet.2016.01.014.

Mirahmadi, F. *et al.* (2013) 'Enhanced mechanical properties of thermosensitive chitosan hydrogel by silk fibers for cartilage tissue engineering', *Materials Science*

and Engineering: C, 33(8), pp. 4786–4794. doi: 10.1016/j.msec.2013.07.043.

Moghadam, M. Z. *et al.* (2017) 'Formation of porous HPCL/LPCL/HA scaffolds with supercritical CO 2 gas foaming method', *Journal of the Mechanical Behavior of Biomedical Materials*, 69, pp. 115–127. doi: 10.1016/j.jmbbm.2016.12.014.

Mohamad, N. *et al.* (2014) 'Bacterial cellulose/acrylic acid hydrogel synthesized via electron beam irradiation: accelerated burn wound healing in an animal model', *Carbohydrate polymers*, 114, pp. 312–320. Available at: http://ovidsp.ovid.com/ovidweb.cgi?T=JS&PAGE=reference&D=emed13&NEWS=N&AN=25263896.

Mohamed, N. A. and Al-mehbad, N. Y. (2013) 'Novel terephthaloyl thiourea cross-linked chitosan hydrogels as antibacterial and antifungal agents', *International Journal of Biological Macromolecules*, 57, pp. 111–117. doi: 10.1016/j.ijbiomac.2013.03.007.

Mohammadi, A., Hashemi, M. and Masoud Hosseini, S. (2016) 'Effect of chitosan molecular weight as micro and nanoparticles on antibacterial activity against some soft rot pathogenic bacteria', *LWT - Food Science and Technology*, 71, pp. 347–355. doi: 10.1016/j.lwt.2016.04.010.

Moon, R. J. *et al.* (2011) 'Cellulose nanomaterials review: structure, properties and nanocomposites', *Chemical Society Reviews*, 40(7), p. 3941. doi: 10.1039/c0cs00108b.

Moraes, P. R. F. de S. *et al.* (2016) 'Bacterial Cellulose/Collagen Hydrogel for Wound Healing', *Materials Research*, 19(1), pp. 106–116. doi: 10.1590/1980-5373-mr-2015-0249.

Muñoz-Bonilla, A. and Fernández-García, M. (2012) 'Polymeric materials with antimicrobial activity', *Progress in Polymer Science (Oxford)*, 37(2), pp. 281–339. doi: 10.1016/j.progpolymsci.2011.08.005.

Muzzarelli, C. and Muzzarelli, R. A. A. (2002) 'Natural and artificial chitosan–

inorganic composites', *Journal of Inorganic Biochemistry*, 92(2), pp. 89–94. doi: 10.1016/S0162-0134(02)00486-5.

Naessens, M. *et al.* (2005) 'Leuconostoc dextransucrase and dextran: production, properties and applications', *Journal of Chemical Technology & Biotechnology*, 80(8), pp. 845–860. doi: 10.1002/jctb.1322.

Naghili, H. *et al.* (2013) 'Validation of drop plate technique for bacterial enumeration by parametric and nonparametric tests.', *Veterinary research forum : an international quarterly journal*, 4(3), pp. 179–83. Available at: http://www.ncbi.nlm.nih.gov/pubmed/25653794.

Nasrazadani, S. and Hassani, S. (2016) 'Modern analytical techniques in failure analysis of aerospace, chemical, and oil and gas industries', in *Handbook of Materials Failure Analysis with Case Studies from the Oil and Gas Industry*. Elsevier, pp. 39–54. doi: 10.1016/B978-0-08-100117-2.00010-8.

Nayak, S. and Kundu, S. C. (2014) 'Sericin-carboxymethyl cellulose porous matrices as cellular wound dressing material', *Journal of Biomedical Materials Research - Part A*, 102(6), pp. 1928–1940. doi: 10.1002/jbm.a.34865.

Nechyporchuk, O., Belgacem, M. N. and Bras, J. (2016) 'Production of cellulose nanofibrils: A review of recent advances', *Industrial Crops and Products*, 93, pp. 2–25. doi: 10.1016/j.indcrop.2016.02.016.

Newbury, D. E. and Ritchie, N. W. M. (2015) 'Performing elemental microanalysis with high accuracy and high precision by scanning electron microscopy/silicon drift detector energy-dispersive X-ray spectrometry (SEM/SDD-EDS)', *Journal of Materials Science*, 50(2), pp. 493–518. doi: 10.1007/s10853-014-8685-2.

Ng, V. W. L. *et al.* (2014) 'Antimicrobial hydrogels: A new weapon in the arsenal against multidrug-resistant infections', *Advanced Drug Delivery Reviews*, 78, pp. 46–62. doi: 10.1016/j.addr.2014.10.028.

Ng, V. W. L. *et al.* (2014) 'Antimicrobial Polycarbonates: Investigating the Impact of Nitrogen-Containing Heterocycles as Quaternizing Agents', *Macromolecules*, 47(4), pp. 1285–1291. doi: 10.1021/ma402641p.

Nguyen, V. T. *et al.* (2008) 'Characterization of Cellulose Production by a Gluconacetobacter xylinus Strain from Kombucha', *Current Microbiology*, 57(5), pp. 449–453. doi: 10.1007/s00284-008-9228-3.

Nishiyama, Y., Langan, P. and Chanzy, H. (2002) 'Crystal Structure and Hydrogen-Bonding System in Cellulose Iβ from Synchrotron X-ray and Neutron Fiber Diffraction', *Journal of the American Chemical Society*, 124(31), pp. 9074–9082. doi: 10.1021/ja0257319.

Nithyanandan, S. *et al.* (2011) 'Optical switching, photophysical, and electrochemical behaviors of pendant triazole-linked indolylfulgimide polymer', *Journal of Polymer Science Part A: Polymer Chemistry*, 49(5), pp. 1138–1146. doi: 10.1002/pola.24528.

No, H. K. *et al.* (2002) 'Antibacterial activity of chitosans and chitosan oligomers with different molecular weights', *International Journal of Food Microbiology*, 74(1–2), pp. 65–72. doi: 10.1016/S0168-1605(01)00717-6.

Nordli, H. R. *et al.* (2016) 'Producing ultrapure wood cellulose nanofibrils and evaluating the cytotoxicity using human skin cells', *Carbohydrate Polymers*, 150, pp. 65–73. doi: 10.1016/j.carbpol.2016.04.094.

O'Neill, J. (2018) 'Tackling drug-resistant infections globally: final report and recommendations', *Straits Times*, (May). doi: 10.1016/j.jpha.2015.11.005.

O'Sullivan, A. C. (1997) 'Cellulose: the structure slowly unravels', *Cellulose*, 4(C), p. 173.

Ogawa, A. *et al.* (2014) 'Pharmaceutical properties of a low-substituted hydroxypropyl cellulose (L-HPC) hydrogel as a novel external dressing', *International Journal of Pharmaceutics*, 477(1–2), pp. 546–552. doi:

10.1016/j.ijpharm.2014.10.043.

Ogunleye, A. *et al.* (2015) 'Poly-γ-glutamic acid: production, properties and applications', *Microbiology*, 161(1), pp. 1–17. doi: 10.1099/mic.0.081448-0.

Okeke, U. C., Snyder, C. R. and Frukhtbeyn, S. A. (2019) 'Synthesis, Purification and Characterization of Polymerizable Multifunctional Quaternary Ammonium Compounds', *Molecules*, 24(8), p. 1464. doi: 10.3390/molecules24081464.

Olatunji, O. (2016) 'Biomedical Application of Natural Polymers', in *Natural Polymers*. Cham: Springer International Publishing, pp. 93–114. doi: 10.1007/978-3-319-26414-1_4.

Oliva, J. M. *et al.* (2017) 'Solvent-assisted in situ synthesis of cysteamine-capped silver nanoparticles', *Advances in Natural Sciences: Nanoscience and Nanotechnology*, 9(1), p. 015001. doi: 10.1088/2043-6254/aa9de9.

Osredkar, J. (2011) 'Copper and Zinc, Biological Role and Significance of Copper/Zinc Imbalance', *Journal of Clinical Toxicology*, s3(01). doi: 10.4172/2161-0495.S3-001.

Ousey, K. *et al.* (2016) 'The importance of hydration in wound healing: reinvigorating the clinical perspective', *Journal of Wound Care*, 25(3), pp. 122–130. doi: 10.12968/jowc.2016.25.3.122.

Ovington, L. G. (2007) 'Advances in wound dressings', *Clinics in Dermatology*, 25(1), pp. 33–38. doi: 10.1016/j.clindermatol.2006.09.003.

Owens, C. D. and Stoessel, K. (2008) 'Surgical site infections: epidemiology, microbiology and prevention', *Journal of Hospital Infection*, 70, pp. 3–10. doi: 10.1016/S0195-6701(08)60017-1.

Padwa, A. and Murphree, S. S. (2000) 'Three-Membered Ring Systems', in, pp. 57–76. doi: 10.1016/S0959-6380(00)80006-9.

Pandey, M. *et al.* (2017) 'Microwaved bacterial cellulose-based hydrogel

microparticles for the healing of partial thickness burn wounds', *Drug Delivery and Translational Research*, 7(1), pp. 89–99. doi: 10.1007/s13346-016-0341-8.

Peng, Z.-X. *et al.* (2010) 'Adjustment of the antibacterial activity and biocompatibility of hydroxypropyltrimethyl ammonium chloride chitosan by varying the degree of substitution of quaternary ammonium', *Carbohydrate Polymers*, 81(2), pp. 275–283. doi: 10.1016/j.carbpol.2010.02.008.

Percival, N. J. (2002) 'Classification of Wounds and their Management', *Surgery (Oxford)*, 20(5), pp. 114–117. doi: 10.1383/surg.20.5.114.14626.

Petri, D. F. S. (2015) 'Xanthan gum: A versatile biopolymer for biomedical and technological applications', *Journal of Applied Polymer Science*, 132(23), p. n/a-n/a. doi: 10.1002/app.42035.

Philip, S., Keshavarz, T. and Roy, I. (2007) 'Polyhydroxyalkanoates: biodegradable polymers with a range of applications', *Journal of Chemical Technology & Biotechnology*, 82(3), pp. 233–247. doi: 10.1002/jctb.1667.

Picheth, G. F. *et al.* (2017) 'Bacterial cellulose in biomedical applications: A review', *International Journal of Biological Macromolecules*, 104, pp. 97–106. doi: 10.1016/j.ijbiomac.2017.05.171.

Powell, L. C. *et al.* (2015) '3D Bioprinting of Carboxymethylated-Periodate Oxidized Nanocellulose Constructs for Wound Dressing Applications', *BioMed Research International*, 2015, pp. 1–7. doi: 10.1155/2015/925757.

Power, G., Moore, Z. and O'Connor, T. (2017) 'Measurement of pH, exudate composition and temperature in wound healing: a systematic review', *Journal of Wound Care*, 26(7), pp. 381–397. doi: 10.12968/jowc.2017.26.7.381.

Purser, K. (2010) 'Royal United Hospital Bath NHS Trust–Wound dressing guidelines', (September 2009), pp. 1–25.

Qi, L. *et al.* (2004) 'Preparation and antibacterial activity of chitosan nanoparticles', *Carbohydrate Research*, 339(16), pp. 2693–2700. doi:

10.1016/j.carres.2004.09.007.

Qu, J. *et al.* (2011) 'The preparation and characterization of chitosan rods modified with Fe3+ by a chelation mechanism', *Carbohydrate Research*, 346(6), pp. 822–827. doi: 10.1016/j.carres.2011.02.006.

Queen, A. (1967) 'Kinetics of the hydrolysis of acyl chlorides in pure water', *Canadian Journal of Chemistry*, 45(14), pp. 1619–1629. doi: 10.1139/v67-264.

Raafat, D. *et al.* (2008) 'Insights into the mode of action of chitosan as an antibacterial compound', *Applied and Environmental Microbiology*, 74(12), pp. 3764–3773. doi: 10.1128/AEM.00453-08.

Raafat, D. and Sahl, H.-G. (2009) 'Chitosan and its antimicrobial potential - a critical literature survey', *Microbial Biotechnology*, 2(2), pp. 186–201. doi: 10.1111/j.1751-7915.2008.00080.x.

Rabea, E. I. *et al.* (2003) 'Chitosan as Antimicrobial Agent: Applications and Mode of Action', *Biomacromolecules*, 4(6), pp. 1457–1465. doi: 10.1021/bm034130m.

Rabouille, C. and Alberti, S. (2017) 'Cell adaptation upon stress: the emerging role of membrane-less compartments', *Current Opinion in Cell Biology*, 47, pp. 34–42. doi: 10.1016/j.ceb.2017.02.006.

Raffi, M. *et al.* (2010) 'Investigations into the antibacterial behavior of copper nanoparticles against Escherichia coli', *Annals of Microbiology*, 60(1), pp. 75–80. doi: 10.1007/s13213-010-0015-6.

Ramsden, J. J. (2011) 'The Nanoscale', in *Nanotechnology*. Elsevier, pp. 15–34. doi: 10.1016/B978-0-08-096447-8.00002-8.

Rao, K. M. *et al.* (2016) 'Polysaccharides based antibacterial polyelectrolyte hydrogels with silver nanoparticles', *Materials Letters*, 184, pp. 189–192. doi: 10.1016/j.matlet.2016.08.043.

Ravi Kumar, M. N. V. (2000) 'A review of chitin and chitosan applications',

Reactive and Functional Polymers, 46(1), pp. 1–27. doi: 10.1016/S1381-5148(00)00038-9.

Reardon, S. (2014) 'Antibiotic resistance sweeping developing world', *Nature*, 509(7499), pp. 141–142. doi: 10.1038/509141a.

Rehm, B. H. A. (2010) 'Bacterial polymers: biosynthesis, modifications and applications', *Nature Reviews Microbiology*, 8(8), pp. 578–592. doi: 10.1038/nrmicro2354.

Rehm, B. H. A. and Valla, S. (1997) 'Bacterial alginates: biosynthesis and applications', *Applied Microbiology and Biotechnology*, 48(3), pp. 281–288. doi: 10.1007/s002530051051.

Reiniati, I., Hrymak, A. N. and Margaritis, A. (2016) 'Recent developments in the production and applications of bacterial cellulose fibers and nanocrystals', *Critical Reviews in Biotechnology*, 37(4), pp. 510–524. doi: 10.1080/07388551.2016.1189871.

Rensing, C. and McDevitt, S. F. (2013) 'The Copper Metallome in Prokaryotic Cells', in, pp. 417–450. doi: 10.1007/978-94-007-5561-1_12.

Rhazi, M. *et al.* (2002) 'Contribution to the study of the complexation of copper by chitosan and oligomers', *Polymer*, 43(4), pp. 1267–1276. doi: 10.1016/S0032-3861(01)00685-1.

Rivero, S., García, M. A. and Pinotti, A. (2010) 'Crosslinking capacity of tannic acid in plasticized chitosan films', *Carbohydrate Polymers*, 82(2), pp. 270–276. doi: 10.1016/j.carbpol.2010.04.048.

Robson, M. C., Stenberg, B. D. and Heggers, J. P. (1990) 'Wound healing alterations caused by infection.', *Clinics in plastic surgery*, 17(3), pp. 485–92. Available at: http://www.ncbi.nlm.nih.gov/pubmed/2199139.

Roemhild, K. *et al.* (2013) 'Novel bioactive amino-functionalized cellulose nanofibers', *Macromolecular Rapid Communications*, 34(22), pp. 1767–1771. doi:

10.1002/marc.201300588.

Römling, U. (2002) 'Molecular biology of cellulose production in bacteria', *Research in Microbiology*, 153(4), pp. 205–212. doi: 10.1016/S0923-2508(02)01316-5.

Ross, P., Mayer, R. and Benziman, M. (1991) 'Cellulose biosynthesis and function in bacteria.', *Microbiological reviews*, 55(1), pp. 35–58. Available at: http://www.ncbi.nlm.nih.gov/pubmed/2030672.

Roy, N. *et al.* (2010) 'Development and Characterization of Novel Medicated Hydrogels for Wound Dressing', *Soft Materials*, 8(2), pp. 130–148. doi: 10.1080/15394451003756282.

Roy, S. and Das, P. K. (2008) 'Antibacterial hydrogels of amino acid-based cationic amphiphiles', *Biotechnology and Bioengineering*, 100(4), pp. 756–764. doi: 10.1002/bit.21803.

Salajková, M., Berglund, L. A. and Zhou, Q. (2012) 'Hydrophobic cellulose nanocrystals modified with quaternary ammonium salts', *Journal of Materials Chemistry*, 22(37), p. 19798. doi: 10.1039/c2jm34355j.

Salmi, T. *et al.* (2013) 'New modelling approach to liquid–solid reaction kinetics: From ideal particles to real particles', *Chemical Engineering Research and Design*, 91(10), pp. 1876–1889. doi: 10.1016/j.cherd.2013.08.004.

Sasson, Y. (1997) 'Synthesis of quaternary ammonium salts', in *Handbook of Phase Transfer Catalysis*. Dordrecht: Springer Netherlands, pp. 111–134. doi: 10.1007/978-94-009-0023-3_3.

Satarkar, N. S., Biswal, D. and Hilt, J. Z. (2010) 'Hydrogel nanocomposites: a review of applications as remote controlled biomaterials', *Soft Matter*, 6(11), p. 2364. doi: 10.1039/b925218p.

Schlick, S. (1986) 'Binding sites of copper 2+ in chitin and chitosan. An electron spin resonance study', *Macromolecules*, 19(1), pp. 192–195. doi: 10.1021/ma00155a030.

Schotten, C. (1884) 'Ueber die Oxydation des Piperidins', *Berichte der deutschen chemischen Gesellschaft*, 17(2), pp. 2544–2547. doi: 10.1002/cber.188401702178.

Schramm, M. and Hestrin, S. (1954) 'Factors affecting Production of Cellulose at the Air/ Liquid Interface of a Culture of Acetobacter xylinum', *Journal of General Microbiology*, 11(1), pp. 123–129. doi: 10.1099/00221287-11-1-123.

Sen, S., Martin, J. D. and Argyropoulos, D. S. (2013) 'Review of Cellulose Non-Derivatizing Solvent Interactions with Emphasis on Activity in Inorganic Molten Salt Hydrates', *ACS Sustainable Chemistry & Engineering*, 1(8), pp. 858–870. doi: 10.1021/sc400085a.

Shafiq, M. *et al.* (2014) 'Structural, thermal, and antibacterial properties of chitosan/ZnO composites', *Polymer Composites*, 35(1), pp. 79–85. doi: 10.1002/pc.22636.

Shahmohammadi Jebel, F. and Almasi, H. (2016) 'Morphological, physical, antimicrobial and release properties of ZnO nanoparticles-loaded bacterial cellulose films', *Carbohydrate Polymers*, 149, pp. 8–19. doi: 10.1016/j.carbpol.2016.04.089.

Shigematsu, T. *et al.* (2005) 'Cellulose production from glucose using a glucose dehydrogenase gene (gdh)-deficient mutant of Gluconacetobacter xylinus and its use for bioconversion of sweet potato pulp', *Journal of Bioscience and Bioengineering*, 99(4), pp. 415–422. doi: 10.1263/jbb.99.415.

Shih, I., Shen, M. and Van, Y. (2006) 'Microbial synthesis of poly(ε-lysine) and its various applications', *Bioresource Technology*, 97(9), pp. 1148–1159. doi: 10.1016/j.biortech.2004.08.012.

Shindo, D. and Oikawa, T. (2002) *Analytical Electron Microscopy for Materials Science*. Tokyo: Springer Japan. doi: 10.1007/978-4-431-66988-3.

Shoda, M. and Sugano, Y. (2005) 'Recent advances in bacterial cellulose production', *Biotechnology and Bioprocess Engineering*, 10(1), pp. 1–8. doi:

10.1007/BF02931175.

Shukla, K. S. (2014) 'Synthesis and Characterization of Aromatic-Heterocyclic Derivatives of Sulphonamides as Potential Antimicrobial Agents', *Int. J. Pharm. Sci. Nanotech.*, 7, pp. 2393–2398.

Siddhan, P., Sakthivel, K. and Basavaraj, H. (2016) 'Biosynthesis of bacterial cellulose imparting antibacterial property through novel bio-Agents', *Research Journal of Biotechnology*, 11(9), pp. 86–93.

Sievers, M. and Swings, J. (2015) 'Gluconacetobacter', in *Bergey's Manual of Systematics of Archaea and Bacteria*. Chichester, UK: John Wiley & Sons, Ltd, pp. 1–11. doi: 10.1002/9781118960608.gbm00883.

Silhavy, T. J., Kahne, D. and Walker, S. (2010) 'The Bacterial Cell Envelope', *Cold Spring Harbor Perspectives in Biology*, 2(5), pp. a000414–a000414. doi: 10.1101/cshperspect.a000414.

Silva, R. M. *et al.* (2004) 'Preparation and characterisation in simulated body conditions of glutaraldehyde crosslinked chitosan membranes', *Journal of Materials Science: Materials in Medicine*, 15(10), pp. 1105–1112. doi: 10.1023/B:JMSM.0000046392.44911.46.

Simões, D. *et al.* (2018) 'Recent advances on antimicrobial wound dressing: A review', *European Journal of Pharmaceutics and Biopharmaceutics*, 127, pp. 130–141. doi: 10.1016/j.ejpb.2018.02.022.

Simoncic, B. and Tomsic, B. (2010) 'Structures of Novel Antimicrobial Agents for Textiles - A Review', *Textile Research Journal*, 80(16), pp. 1721–1737. doi: 10.1177/0040517510363193.

Singer, A. J. and Clark, R. A. F. (1999) 'Cutaneous Wound Healing', *New England Journal of Medicine*. Edited by F. H. Epstein, 341(10), pp. 738–746. doi: 10.1056/NEJM199909023411006.

Singla, R. *et al.* (2017) 'In vivo diabetic wound healing potential of

nanobiocomposites containing bamboo cellulose nanocrystals impregnated with silver nanoparticles', *International Journal of Biological Macromolecules*, 105, pp. 45–55. doi: 10.1016/j.ijbiomac.2017.06.109.

Siritientong, T. and Aramwit, P. (2015) 'Characteristics of carboxymethyl cellulose/sericin hydrogels and the influence of molecular weight of carboxymethyl cellulose', *Macromolecular Research*, 23(9), pp. 861–866. doi: 10.1007/s13233-015-3116-z.

Smith, M. B. (2010) 'Cd Disconnect Products', in *Organic Synthesis*. Elsevier, pp. 623–779. doi: 10.1016/B978-1-890661-40-3.50008-9.

Smith, T. J., Kennedy, J. E. and Higginbotham, C. L. (2010) 'Rheological and thermal characteristics of a two phase hydrogel system for potential wound healing applications', *Journal of Materials Science*, 45(11), pp. 2884–2891. doi: 10.1007/s10853-010-4278-x.

Son, H.-J. *et al.* (2001) 'Optimization of fermentation conditions for the production of bacterial cellulose by a newly isolated Acetobacter sp.A9 in shaking cultures', *Biotechnology and Applied Biochemistry*, 33(1), p. 1. doi: 10.1042/BA20000065.

Son, H.-J. *et al.* (2003) 'Increased production of bacterial cellulose by Acetobacter sp. V6 in synthetic media under shaking culture conditions', *Bioresource Technology*, 86(3), pp. 215–219. doi: 10.1016/S0960-8524(02)00176-1.

Song, Y. *et al.* (2010) 'Flocculation Properties and Antimicrobial Activities of Quaternized Celluloses Synthesized in NaOH/Urea Aqueous Solution', *Industrial & Engineering Chemistry Research*, 49(3), pp. 1242–1246. doi: 10.1021/ie9015057.

Sood, A., Granick, M. S. and Tomaselli, N. L. (2014) 'Wound Dressings and Comparative Effectiveness Data', *Advances in Wound Care*, 3(8), pp. 511–529. doi: 10.1089/wound.2012.0401.

Soroka, Y. *et al.* (2008) 'Aged keratinocyte phenotyping: Morphology,

biochemical markers and effects of Dead Sea minerals', *Experimental Gerontology*, 43(10), pp. 947–957. doi: 10.1016/j.exger.2008.08.003.

Spinks, G. M. *et al.* (2006) 'Mechanical properties of chitosan/CNT microfibers obtained with improved dispersion', *Sensors and Actuators B: Chemical*, 115(2), pp. 678–684. doi: 10.1016/j.snb.2005.10.047.

Steinbüchel, A. (2001) 'Perspectives for Biotechnological Production and Utilization of Biopolymers: Metabolic Engineering of Polyhydroxyalkanoate Biosynthesis Pathways as a Successful Example', *Macromolecular Bioscience*, 1(1), pp. 1–24. doi: 10.1002/1616-5195(200101)1:1<1::AID-MABI1>3.0.CO;2-B.

Stewart, P. S. and William Costerton, J. (2001) 'Antibiotic resistance of bacteria in biofilms', *The Lancet*, 358(9276), pp. 135–138. doi: 10.1016/S0140-6736(01)05321-1.

Stratton, T. R., Rickus, J. L. and Youngblood, J. P. (2009) 'In Vitro Biocompatibility Studies of Antibacterial Quaternary Polymers', *Biomacromolecules*, 10(9), pp. 2550–2555. doi: 10.1021/bm9005003.

Sun, T. *et al.* (2007) 'Investigation of fibroblast and keratinocyte cell-scaffold interactions using a novel 3D cell culture system', *Journal of Materials Science: Materials in Medicine*, 18(2), pp. 321–328. doi: 10.1007/s10856-006-0696-3.

Svensson, A. *et al.* (2005) 'Bacterial cellulose as a potential scaffold for tissue engineering of cartilage', *Biomaterials*, 26(4), pp. 419–431. doi: 10.1016/j.biomaterials.2004.02.049.

Tan, H. *et al.* (2009) 'Injectable in situ forming biodegradable chitosan-hyaluronic acid based hydrogels for cartilage tissue engineering', *Biomaterials*, 30(13), pp. 2499–2506. doi: 10.1016/j.biomaterials.2008.12.080.

Tan, H. *et al.* (2013) 'Quaternized Chitosan as an Antimicrobial Agent: Antimicrobial Activity, Mechanism of Action and Biomedical Applications in Orthopedics', *International Journal of Molecular Sciences*, 14(1), pp. 1854–1869. doi: 10.3390/ijms14011854.

Tejero, R. *et al.* (2015) 'Antimicrobial polymethacrylates based on quaternized 1,3-thiazole and 1,2,3-triazole side-chain groups', *Polymer Chemistry*, 6(18), pp. 3449–3459. doi: 10.1039/C5PY00288E.

Tenover, F. C. (2006) 'Mechanisms of antimicrobial resistance in bacteria', *American Journal of Infection Control*, 34(5 SUPPL.). doi: 10.1016/j.ajic.2006.05.219.

Thakhiew, W., Devahastin, S. and Soponronnarit, S. (2013) 'Physical and mechanical properties of chitosan films as affected by drying methods and addition of antimicrobial agent', *Journal of Food Engineering*, 119(1), pp. 140–149. doi: 10.1016/j.jfoodeng.2013.05.020.

The PEW charitable trust (2016) 'A scientific roadmap for antibiotic discovery', (June). doi: 10.1111/j.1749-6632.2010.05828.x.

Tian, H. *et al.* (2012) 'Biodegradable synthetic polymers: Preparation, functionalization and biomedical application', *Progress in Polymer Science (Oxford)*, 37(2), pp. 237–280. doi: 10.1016/j.progpolymsci.2011.06.004.

Tiller, J. C. *et al.* (2001) 'Designing surfaces that kill bacteria on contact', *Proceedings of the National Academy of Sciences*, 98(11), pp. 5981–5985. doi: 10.1073/pnas.111143098.

Timofeeva, L. and Kleshcheva, N. (2011) 'Antimicrobial polymers: mechanism of action, factors of activity, and applications', *Applied Microbiology and Biotechnology*, 89(3), pp. 475–492. doi: 10.1007/s00253-010-2920-9.

Tripathi, A. *et al.* (2012) 'Bio-composite scaffolds containing chitosan/nano-hydroxyapatite/nano-copper–zinc for bone tissue engineering', *International Journal of Biological Macromolecules*, 50(1), pp. 294–299. doi: 10.1016/j.ijbiomac.2011.11.013.

Tsuda, M. (1964) 'Schotten-Baumann esterification of poly (vinyl alcohol). I.', *Die Makromolekulare Chemie: Macromolecular Chemistry and Physics*, 72.1, pp. 174–182.

Tu, Y. and Rappel, W.-J. (2018) 'Adaptation in Living Systems', *Annual Review of*

Condensed Matter Physics, 9(1), pp. 183–205. doi: 10.1146/annurev-conmatphys-033117-054046.

Usui, M. L. *et al.* (2008) 'Keratinocyte Migration, Proliferation, and Differentiation in Chronic Ulcers From Patients With Diabetes and Normal Wounds', *Journal of Histochemistry & Cytochemistry*, 56(7), pp. 687–696. doi: 10.1369/jhc.2008.951194.

Vallapa, N. *et al.* (2011) 'Enhancing antibacterial activity of chitosan surface by heterogeneous quaternization', *Carbohydrate Polymers*, 83(2), pp. 868–875. doi: 10.1016/j.carbpol.2010.08.075.

Vandamme, E. J. *et al.* (1998) 'Improved production of bacterial cellulose and its application potential', *Polymer Degradation and Stability*, 59(1–3), pp. 93–99. doi: 10.1016/S0141-3910(97)00185-7.

Vasilev, K., Cook, J. and Griesser, H. J. (2009) 'Antibacterial surfaces for biomedical devices', *Expert Review of Medical Devices*, 6(5), pp. 553–567. doi: 10.1586/erd.09.36.

Veiga, A. S. and Schneider, J. P. (2013) 'Antimicrobial hydrogels for the treatment of infection', *Biopolymers*, 100(6), pp. 637–644. doi: 10.1002/bip.22412.

Wahid, F. *et al.* (2016) 'Synthesis and characterization of antibacterial carboxymethyl Chitosan/ZnO nanocomposite hydrogels', *International Journal of Biological Macromolecules*, 88, pp. 273–279. doi: 10.1016/j.ijbiomac.2016.03.044.

Walsh, C. (2000) 'Molecular mechanisms that confer antibacterial drug resistance', *Nature*, 406(6797), pp. 775–781. doi: 10.1038/35021219.

Walter, M. N. M. *et al.* (2010) 'Mesenchymal stem cell-conditioned medium accelerates skin wound healing: An in vitro study of fibroblast and keratinocyte scratch assays', *Experimental Cell Research*, 316(7), pp. 1271–1281. doi: 10.1016/j.yexcr.2010.02.026.

Wang, K., Loo, L. S. and Goh, K. L. (2016) 'A facile method for processing lignin reinforced chitosan biopolymer microfibres: optimising the fibre mechanical

properties through lignin type and concentration', *Materials Research Express*, 3(3), p. 035301. doi: 10.1088/2053-1591/3/3/035301.

Wang, T. *et al.* (2012) 'Hydrogel sheets of chitosan, honey and gelatin as burn wound dressings', *Carbohydrate Polymers*, 88(1), pp. 75–83. doi: 10.1016/j.carbpol.2011.11.069.

Wang, X. *et al.* (2016) 'Biocomposites of copper-containing mesoporous bioactive glass and nanofibrillated cellulose: Biocompatibility and angiogenic promotion in chronic wound healing application', *Acta Biomaterialia*, 46, pp. 286–298. doi: 10.1016/j.actbio.2016.09.021.

Watanabe, K. *et al.* (1998) 'Structural features and properties of bacterial cellulose produced in agitated culture', *Cellulose*, 5(3), pp. 187–200. doi: 10.1023/A:1009272904582.

Wiener, M. C. and Horanyi, P. S. (2011) 'How hydrophobic molecules traverse the outer membranes of Gram-negative bacteria', *Proceedings of the National Academy of Sciences*, 108(27), pp. 10929–10930. doi: 10.1073/pnas.1106927108.

Winter, G. D. (1962) 'Formation of the Scab and the Rate of Epithelization of Superficial Wounds in the Skin of the Young Domestic Pig', *Nature*, 193(4812), pp. 293–294. doi: 10.1038/193293a0.

Wright, G. D. (2010) 'Q&A: Antibiotic resistance: where does it come from and what can we do about it?', *BMC Biology*, 8(1), p. 123. doi: 10.1186/1741-7007-8-123.

Xi, W. *et al.* (2012) 'Nitrogen-Centered Nucleophile Catalyzed Thiol-Vinylsulfone Addition, Another Thiol-ene "Click" Reaction', *ACS Macro Letters*, 1(7), pp. 811–814. doi: 10.1021/mz3001918.

Xie, Y., Liu, X. and Chen, Q. (2007) 'Synthesis and characterization of water-soluble chitosan derivate and its antibacterial activity', *Carbohydrate Polymers*, 69(1), pp. 142–147. doi: 10.1016/j.carbpol.2006.09.010.

Xue, Y., Xiao, H. and Zhang, Y. (2015) 'Antimicrobial Polymeric Materials with Quaternary Ammonium and Phosphonium Salts', *International Journal of Molecular Sciences*, 16(2), pp. 3626–3655. doi: 10.3390/ijms16023626.

Yadav, P. (2015) 'Biomedical Biopolymers, their Origin and Evolution in Biomedical Sciences: A Systematic Review', *Journal of Clinical and Diagnostic Research*. doi: 10.7860/JCDR/2015/13907.6565.

Yan, C. and Pochan, D. J. (2010) 'Rheological properties of peptide-based hydrogels for biomedical and other applications', *Chemical Society Reviews*, 39(9), p. 3528. doi: 10.1039/b919449p.

Yang, C. H. *et al.* (2015) 'Preparation and characterization of methoxy-poly(ethylene glycol) side chain grafted onto chitosan as a wound dressing film', *Journal of Applied Polymer Science*, 132(31). doi: 10.1002/app.42340.

Yang, G. *et al.* (2012) 'Antimicrobial activity of silver nanoparticle impregnated bacterial cellulose membrane: Effect of fermentation carbon sources of bacterial cellulose', *Carbohydrate Polymers*, 87(1), pp. 839–845. doi: 10.1016/j.carbpol.2011.08.079.

Yu, J. *et al.* (2016) 'Production of Hollow Bacterial Cellulose Microspheres Using Microfluidics to Form an Injectable Porous Scaffold for Wound Healing', *Advanced Healthcare Materials*, 5(23), pp. 2983–2992. doi: 10.1002/adhm.201600898.

Yuan, Y. and Lee, T. R. (2013) 'Contact Angle and Wetting Properties', in, pp. 3–34. doi: 10.1007/978-3-642-34243-1_1.

Zhang, Y. and Zhang, M. (2001) 'Microstructural and mechanical characterization of chitosan scaffolds reinforced by calcium phosphates', *Journal of Non-Crystalline Solids*, 282(2–3), pp. 159–164. doi: 10.1016/S0022-3093(01)00345-3.

Zhao, T. and Sun, G. (2008) 'Hydrophobicity and antimicrobial activities of quaternary pyridinium salts', *Journal of Applied Microbiology*, 104(3), pp. 824–830.

doi: 10.1111/j.1365-2672.2007.03616.x.

Zheng, L. Y. and Zhu, J. F. (2013) 'Study on antimicrobial activity of chitosan with different molecular weights', *Carbohydrate Polymers*, 54(4), pp. 527–530. doi: 10.1016/j.carbpol.2003.07.009.

Zheng, Z. *et al.* (2016) 'Structure–Antibacterial Activity Relationships of Imidazolium-Type Ionic Liquid Monomers, Poly(ionic liquids) and Poly(ionic liquid) Membranes: Effect of Alkyl Chain Length and Cations', *ACS Applied Materials & Interfaces*, 8(20), pp. 12684–12692. doi: 10.1021/acsami.6b03391.

Zhou, L. L. *et al.* (2007) 'Effect of addition of sodium alginate on bacterial cellulose production by Acetobacter xylinum', *Journal of Industrial Microbiology & Biotechnology*, 34(7), pp. 483–489. doi: 10.1007/s10295-007-0218-4.

Zhou, Y. *et al.* (2012) 'Potential of quaternization-functionalized chitosan fiber for wound dressing', *International Journal of Biological Macromolecules*, 52, pp. 327–332. doi: 10.1016/j.ijbiomac.2012.10.012.

Zhou, Z. X. *et al.* (2010) 'Damage of Escherichia coli membrane by bactericidal agent polyhexamethylene guanidine hydrochloride: micrographic evidences', *Journal of Applied Microbiology*, 108(3), pp. 898–907. doi: 10.1111/j.1365-2672.2009.04482.x.

Zubris, D., Minbiole, K. and Wuest, W. (2016) 'Polymeric Quaternary Ammonium Compounds: Versatile Antimicrobial Materials', *Current Topics in Medicinal Chemistry*, 17(3), pp. 305–318. doi: 10.2174/1568026616666160829155805.

Zuidema, J. M. *et al.* (2014) 'A protocol for rheological characterization of hydrogels for tissue engineering strategies', *Journal of Biomedical Materials Research Part B: Applied Biomaterials*, 102(5), pp. 1063–1073. doi: 10.1002/jbm.b.33088.

Zuo, P.-P. *et al.* (2013) 'Fabrication of biocompatible and mechanically reinforced

graphene oxide-chitosan nanocomposite films', *Chemistry Central Journal*, 7(1), p. 39. doi: 10.1186/1752-153X-7-39.